# Bootstrapping some continuous families of conformal field theories

A Dissertation Presented

by

**Connor Classen Behan**

to

The Graduate School

in Partial Fulfillment of the Requirements

for the Degree of

**Doctor of Philosophy**

in

**Physics**

Stony Brook University

August 2019

**Stony Brook University**

The Graduate School

## Connor Classen Behan

We, the dissertation committee for the above candidate for the Doctor of Philosophy degree, hereby recommend acceptance of this dissertation.

Leonardo Rastelli – Dissertation Advisor
Professor, Department of Physics and Astronomy

Peter Van Nieuwenhuizen – Chairperson of Defense
Distinguished Professor, Department of Physics and Astronomy

Martin Roček
Professor, Department of Physics and Astronomy

Dominik Schneble
Professor, Department of Physics and Astronomy

David Simmons-Duffin
Assistant Professor
Walter Burke Institute for Theoretical Physics

This dissertation is accepted by the Graduate School.

Charles Taber
Dean of the Graduate School

Abstract of the Dissertation

# Bootstrapping some continuous families of conformal field theories

by

**Connor Classen Behan**

**Doctor of Philosophy**

in

**Physics**

Stony Brook University

2019

We explore several related bootstrap techniques in conformal field theory (CFT). This sheds light on a number of structures which have resisted previous approaches. First, we develop a procedure for constructing a continuous line of nonlocal CFTs out of a single local CFT. Applying this to the Ising model reveals a way to study its long-range cousin perturbatively in a regime that cannot be accessed by the standard description. This leads to new insights about the counting of states at the long-range to short-range crossover. We show that this infrared duality passes several non-perturbative checks and use it to identify an infinite tower of non-renormalized operators of odd spin. With this information, the long-range Ising model can be located with the numerical bootstrap based on brute-force checks of crossing symmetry and unitarity. Probing numerical results further, we revisit a puzzling feature which is that generalized minimal models are allowed by the 2D bounds despite the fact that they are non-unitary. We prove that this must be the case by combining the exact solution with Euclidean inversion of the operator product expansion. We also prove a similar property of an extremal solution involving a single Virasoro block. Finally, we explore conformal perturbation theory in CFTs that have exactly marginal operators. When

the perturbation is infinitesimal, this leads to a dynamical system for CFT data that can be expressed in closed form when the conformal manifold and space-time manfiold are both 1D. We show that this system abhors level-crossing and comment on other features that it can be used to study.

# Contents

# List of Figures

# List of Tables

# Acknowledgements

The work in this thesis would not have been possible without expert guidance from Leonardo Rastelli. Thank-you for giving me a taste of your visionary ideas and suggesting useful next steps every time I brought you an update. Thank-you also for having high expectations and lighting a fire underneath me whenever there were important calculations to be done. I am grateful to Slava Rychkov for imparting his unmatched physical intuition and being able to spot my calculational errors immediately. Thank-you to Bernardo Zan for turning our collaboration into a powerhouse. I also thank Andreas Stergiou for collaborating on ongoing work which has made a brief appearance here.

I am grateful to all the professors in my circle who put up with the teaching components of their jobs. Peter Van Nieuwenhuizen, in particular, was a formidable instructor for string theory, field theory, group theory and supersymmetry / supergravity. These were taught at a level that would be difficult to find on another campus. Thanks also to Martin Roček for organizing interesting seminars every Friday. To my fellow bootstrappers in and around the department, it was a privilege to be able to have so many interesting discussions. Thank-you Matthijs Hogervorst, Zohar Komargodski, Madalena Lemos, Pedro Liendo, Dalimil Mazáč, Wolfger Peelaers, Konstantinos Roumpedakis and Xinan Zhou.

Workshops have been essential for staying up to date with this field. I appreciate the work done by the scientific and administrative organizers at the Galileo Galilei Institute, Yale University, Perimeter Institute, Princeton University, International Centre for Theoretical Physics (São Paulo), International Centre for Theoretical Sciences (Bangalore) and California Institute of Technology who hosted bootstrap themed meetings in 2016, 2016, 2016, 2017, 2017, 2018 and 2018 respectively. Several friends who were also on the PhD journey were regulars at these events. It was a pleasure to chat about physics and other things with Nima Afkhami-Jeddi, Soner Albayrak, Antonio Antunes, Shai Chester, Minjae Cho, Scott Collier, Lucia Cordova, Luca Illesiu, Denis Karateev, Apratim Kaviraj, Petr Kravchuk, Ho Tat Lam, Andrea Manenti, David Meltzer, Marten Reehorst, Daniel Rutter, Adar Sharon, Joao Silva, Emilio Trevisani and anyone else I forgot to mention.

The first three years of this degree were supported by the Natural Sciences and Engineering Research Council of Canada (CGS03-460190-2014). The most intensive numerical calculations described here were performed on the SeaWulf cluster of the Institute for Advanced Computational Science which was itself funded by the National Science Foundation.

Some of the other calculations were performed on a smaller cluster at Stony Brook maintained by Chi Ming Hung.

# Chapter 1

# Introduction

With the possible exception of gravity, all of our theoretical understanding of fundamental physics is based on *quantum field theories* (QFTs) — continuous quantum mechanical systems (with infinitely many degrees of freedom) that obey the special theory of relativity. The study of quantum field theories (which is called *quantum field theory*) became a pillar of modern physics in 1973 with the discovery of asymptotic freedom [1, 2]. This is the statement that our overall framework is powerful enough to yield renormalizable theories that are UV complete, *i.e.* microscopically well defined even when their dynamics are probed at an arbitrarily high energy scale. Any QFT we observe that does not already have this property (at least in the idealized picture) must be an effective low energy description of some yet to be determined UV complete theory. So far, the most all-encompassing theory yet proposed that has withstood significant experimental testing is the Standard Model.

While this insight is conceptually important, it is far from practical. Exact results in quantum field theory have always been few and far between. Rather than beginning with some microscopic theory like the Standard Model and attempting to map out all of its effective phenomena in a top-down manner, we should develop methods that directly exploit whatever special structures might be present in a particular part of this landscape. The standard recipie of perturbative quantum field theory is inadequate for this purpose. Apart from lacking mathematical rigor and being limited to the weak coupling regime, this approach assumes that all observables may be built out of finitely many fundamental fields that are described by a Lagrangian. Even when this is the case, a cumbersome expansion in Feynman diagrams leaves something to be desired as important symmetries only reappear at the end of the calculation after a conspiracy of cancelling terms [3].

This thesis will make use of an alternative viewpoint known as the *bootstrap philosophy* whose history is richly varied. The bootstrap began in the early 1960s with the proposal that the principal observable of massive QFT, the S-matrix, should be self-consistently determined from the basic requirements of analyticity, crossing symmetry and unitarity [4]. At the time, this was a competitor to the idea of perturbing a free theory using Feynman diagrams. While perturbative QFT was ultimately found to be the superior choice for modelling scattering

experiments, the bootstrap arguably left an equally large imprint on physics in that it led to the development of string theory.

Instead of the S-matrix bootstrap, which is undoubtedly still relevant [5–8], this work will focus on a slightly newer offshoot that applies to theories with an especially large amount of symmetry [9, 10]. These are the *conformal field theories* (CFTs) which are invariant under all spacetime transformations that preserve angle. CFTs play a privileged role in bottom-up studies of the landscape due to a powerful organizing principle: a general theory at a given scale may be reached by deforming another theory that has no dependence on scale. Scale invariance is necessary for conformal invariance and, under fairly mild assumptions, it turns out to be sufficient as well [11]. For a time, the conformal bootstrap was best known for providing an exact solution for infinitely many CFTs in two dimensions [12]. By now, the technique has expanded its reach into high-precision numerical and asymptotic results for CFTs in higher dimensions, along with general theorems that transcend any particular theory [13–15]. The breakthrough that led to this revival came in 2008 with an efficient algorithm for rigorously bounding the allowed spectral data [16].

## 1.1 Outline

We begin by reviewing essential aspects of the conformal bootstrap in chapter 2. We will focus on the numerical bootstrap and present some results that give an overall sense of how restrictive the bounds can be. This reveals that the bounds harbor lines of CFTs that are often very different from the theories that have attracted attention in the past. The first example we explore is the generalized minimal model line which is non-unitary and only appears due to the special properties of two dimensions. A more serious example to consider comes about from violating locality. Nonlocal CFTs, which exist in any dimension, are able to overwhelm a bootstrap search since any local CFT can be regarded as a special point on a nonlocal line.

Chapter 3 proves a few new results about the generalized minimal models. It also includes some results about fermionic theories that violate unitarity. Chapter 4 is all about the long-range Ising model. This nonlocal theory has a simple lattice description where interactions are allowed to take place between all sites, not just the nearest neighbours. When the decay of this interaction is sufficiently slow, mean-field theory becomes exact enabling a field-theoretic treatment of the critical point that goes back to 1972. When the decay of the interaction is fast, however, we expect the physics of the short-range Ising model to be reproduced. Taking this seriously leads to a second field theory for exploring the critical point. The first is weakly coupled if and only if the second is strongly coupled. We use this duality to make new predictions about long-range Ising critical exponents and initiate the numerical bootstrap for this model.

The most widely studied CFTs that occur in familes are conformal manifolds, discussed in chapter 5. These include one or more exactly marginal operators — a very special condition

which has prevented us from finding any examples without enhanced symmetry. We develop a bootstrap-like constraint on conformal manifolds which does not depend on the usual step of assuming superconformal invariance. We further explore how CFT observables are allowed to depend on the coupling and arrive at a system of coupled nonlinear evolution equations. These allow us to make some general statements, particularly in one dimension, before we conclude in chapter 6.

# Chapter 2

# A taste of bootstrap methods

The conformal bootstrap [9, 10] has joined holography [17] as one of the most important tools for understanding strongly coupled conformal field theories (CFTs) in higher dimensions. In addition to the [16] breakthrough, which revived the numerical prospects for conformal [18–30] and superconformal [31–35] theories, there are also incarnations of the bootstrap which use small kinematic parameters to obtain analytic results. These are shown schematically in Figure 2.1.

These methods are all based on imposing crossing symmetry for a four-point function of local operators. Crossing symmetry is the statement that we must find a unique answer after inserting a complete set of states into $\langle \mathcal{O}_1(x_1)\mathcal{O}_2(x_2)\mathcal{O}_3(x_3)\mathcal{O}_4(x_4)\rangle$ even though there are $\binom{4}{2}$ possible ways of doing this. Equivalently, we may take the *s-channel* expansion that separates $\mathcal{O}_1(x_1)\mathcal{O}_2(x_2)$ from $\mathcal{O}_3(x_3)\mathcal{O}_4(x_4)$ and demand that it be invariant under a simultaneous permutation of labels on quantum numbers and spacetime points.

As we will see in more detail later, kinematics only constrain this correlator up to an arbitrary function of the two invariants

$$u \equiv \frac{x_{12}^2 x_{34}^2}{x_{13}^2 x_{24}^2} \equiv z\bar{z} \ , \ v \equiv \frac{x_{14}^2 x_{23}^2}{x_{13}^2 x_{24}^2} = (1-z)(1-\bar{z}) \tag{2.1}$$

where we have introduced the convenient parameters $(z, \bar{z})$. Their physical interpretation can be made clear if use use conformal covariance to move our four points to $x_1 = 0$, $x_2 = (x, t, 0, \dots)$, $x_3 = (1, 0, 0, \dots)$ and $x_4 = \infty$. In this case, satisfying 2.1 with the Euclidean norm means that

$$z = x + it \ , \bar{z} = x - it \ . \tag{2.2}$$

The answer for the Minkowskian norm is simply given by a Wick rotation

$$z = x + t \ , \bar{z} = x - t \ . \tag{2.3}$$

While $(x, t)$ can take arbitrary values in (2.3), Figure 2.1 would become more complicated

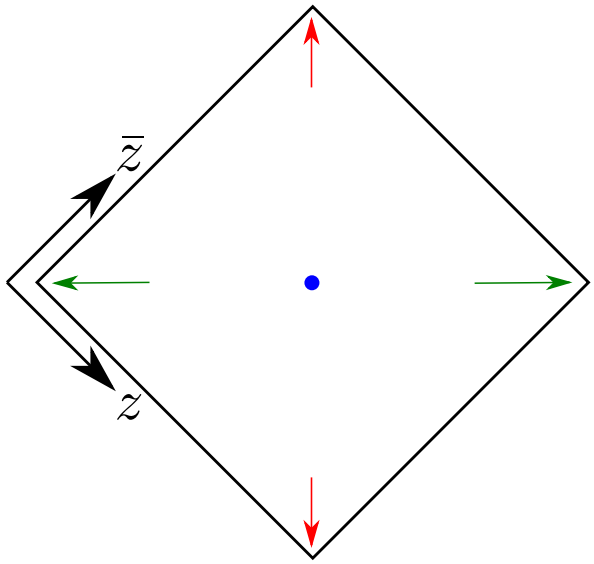


Figure 2.1: Important limits for the cross-ratios starting from $0 < z, \bar{z} < 1$. The numerical bootstrap is usually conducted with reference to the blue point $(z, \bar{z}) = \left(\frac{1}{2}, \frac{1}{2}\right)$, even though it works for any Euclidean configuration. The red arrows denote the lightcone limit in which the operator product expansion (OPE) becomes an expansion in twist. This leads to a universal structure in the large spin sector of a CFT [36–39]. The green arrows denote the deep Euclidean limit which controls the sector with large scaling dimension. The leading estimates in [40, 41] have recently been improved through the use of compelx tauberian theorems [42, 43]. Not shown in the figure is the so called Regge limit which involves the second sheet and provides an analogue of high energy scattering [44–48].

for $z \notin (0,1)$ or $\bar{z} \notin (0,1)$. This is because, outside the diamond, $\mathcal{O}_2$ is no longer spacelike separated from the fixed operators $\mathcal{O}_1$, $\mathcal{O}_3$ and $\mathcal{O}_4$. Its position can be reached by more than one analytic continuation leading to a multivalued correlator. This reflects the possibility of having multiple operator orderings in Minkowskian signature. Even though Euclidean correlators do not have branch cuts, it should be noted that this is not manifest in the OPE. Indeed, the s-channel expansion cannot be done for $1 < z < \infty$ as this configuration prevents us from finding a sphere that separates $(x_1, x_2)$ from $(x_3, x_4)$.

This thesis, which has a heavy emphasis on numerics, will also derive some analytic bootstrap results in 2D. This review will summarize some results from the vast literature on $d = 2$ CFT and explain which ones continue to have an analogue in $d > 2$.

## 2.1 CFT basics

A fundamental result in theoretical physics is the Coleman-Mandula theorem which states that any $d > 2$ QFT with a mass gap must be free if it includes higher spin currents [49]. The basic reason for this is that, in 2-to-2 scattering, tensorial conservation laws force the outgoing momenta $(p_1', p_2')$ to be a permutation of the incoming momenta $(p_1, p_2)$. If there are multiple spatial directions, we must have analyticity in the scattering angle which singles out the free theory. If there is only one spatial direction — and therefore no scattering angle — non-trivial permutations are allowed which give rise to a rich landscape of integrable theories.

There are only a few known extensions of the Poncaré algebra which allow non-integrable QFTs to exist. We will focus on the conformal algebra, which evades the Coleman-Mandula theorem by not having a mass gap.[1] Although such a setup still leads to a trivial S-matrix, this no longer implies that the theory is free. Instead, scattering is forbidden for a more fundamental reason — there is no linear combination of states which becomes asymptotic to the single-particle states of a free theory. As a result, the more interesting observables in conformal field theory are correlation functions of local operators, such as those described above. It is these objects that diagnose whether or not a CFT is free. A variation of the Coleman-Mandula theorem, which classifies the symmetries compatible with interacting CFT correlators, was recently proven in [50].

### 2.1.1 Simple examples

The simplest possible starting point is the free massless scalar in $d$ dimensions.

$$S = \int \mathrm{d}^d x \frac{1}{2} \partial_\mu \phi \partial^\mu \phi \tag{2.4}$$

To describe the translation symmetry, we will write

$$\begin{aligned} x'_\mu &= x_\mu + a_\mu \ , \ \phi'(x') = \phi(x) \\ T_{\mu\nu} &= \partial_\mu \phi \partial_\nu \phi - \frac{1}{2} \delta_{\mu\nu} (\partial\phi)^2 - \frac{1}{6} \left( \partial_\mu \partial_\nu - \delta_{\mu\nu} \partial^2 \right) \phi^2 \ . \end{aligned} \tag{2.5}$$

This stress-energy tensor includes the part that follows from the Noether procedure but also a manifestly conserved operator acting on $\phi^2$. This is the well known improvement term which cancels the trace of the first part. Our ability to make $T_{\mu\nu}$ traceless is of course a consequence of the fact that $\phi$ is massless. The rotation currents — as with the other currents of interest to us — will be expressed in terms of $T_{\mu\nu}$ using the fact that an infinitesimal rotation is

[1] The other famous extension is the *Super* Poincaré algebra whose additional charges are Grassman-odd. It is of course very fruitful to study theories that posess both supersymmetry and conformal symmetry.

simply an infinitesimal translation with a parameter that is linear in $x$.

$$\begin{aligned} x'_\mu &= \Lambda_\mu{}^\nu x_\nu \ , \ \phi'(x') = \phi(x) \\ \mathcal{M}_{\mu\nu\rho} &= x_\mu T_{\nu\rho} - x_\nu T_{\mu\rho} \end{aligned} \tag{2.6}$$

Another transformation we can consider (again due to the lack of a mass in (2.4)) is the global rescaling of all co-ordinates. This time, the field will not be in the singlet representation as it was for (2.5) and (2.6).

$$\begin{aligned} x'_\mu &= \lambda x_\mu \ , \ \phi'(x') = \lambda^{\frac{d-2}{2}} \phi(x) \\ \mathcal{D}_\mu &= x^\nu T_{\mu\nu} \end{aligned} \tag{2.7}$$

The last transformation of interest to us might be slightly harder to notice as it is nonlinear. However, it is easily checked that

$$\begin{aligned} x'_\mu &= \frac{x_\mu - b_\mu x^2}{1 - 2b\cdot x + b^2 x^2} \ , \ \phi'(x') = \left(\frac{1}{1 - 2b\cdot x + b^2 x^2}\right)^{\frac{d-2}{2}} \phi(x) \\ \mathcal{K}_{\mu\nu} &= 2x_\mu x^\rho T_{\rho\nu} - x^2 T_{\mu\nu} \ , \end{aligned} \tag{2.8}$$

which we call the *special conformal transformation*, is a symmetry as well. With explicit expressions for the currents in hand, the corresponding charges are easily obtained through

$$\begin{aligned} P_\mu &= \int \mathrm{d}^{d-1}x T_{0\mu} \quad , \quad M_{\mu\nu} = \int \mathrm{d}^{d-1}x \mathcal{M}_{0\mu\nu} \\ D &= \int \mathrm{d}^{d-1}x \mathcal{D}_0 \quad , \quad K_\mu = \int \mathrm{d}^{d-1}x \mathcal{K}_{0\mu} \ . \end{aligned} \tag{2.9}$$

After repeatedly invoking the canonical commutation relations, we arrive at the following algebra of conserved charges.

$$\begin{aligned} [D, P_\mu] &= iP_\mu \\ [D, K_\mu] &= -iK_\mu \\ [K_\mu, P_\nu] &= 2i(\delta_{\mu\nu} D - M_{\mu\nu}) \\ [K_\rho, M_{\mu\nu}] &= i(\delta_{\rho\mu} K_\nu - \delta_{\rho\nu} K_\mu) \\ [P_\rho, M_{\mu\nu}] &= i(\delta_{\rho\mu} P_\nu - \delta_{\rho\nu} P_\mu) \\ [M_{\mu\nu}, M_{\rho\sigma}] &= \delta_{\mu\rho} M_{\nu\sigma} - \delta_{\nu\rho} M_{\mu\sigma} \\ &\quad -\delta_{\mu\sigma} M_{\nu\rho} + \delta_{\nu\sigma} M_{\mu\rho} \end{aligned} \tag{2.10}$$

The algebra (2.10), known as the *conformal algebra*, would hardly be worth discussing if it were only applicable to free theories. Rather, the conformal algebra has a simple geometric

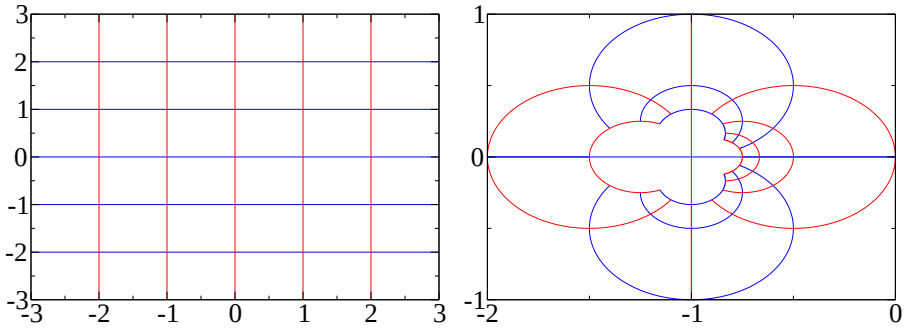


(a) Before (b) After

Figure 2.2: A set of grid lines and its image under the map $e^{ib^\mu K_\mu}$ where $b_\mu = (0, 1)$. Clearly, the lines continue to meet at right angles.

meaning which makes it imperative that we find other QFTs where it is realized. It is easily checked that (2.10) is isomorphic to $SO(d+1,1)$. The transformations generated by $P_\mu$, $M_{\mu\nu}$, $D$ and $K_\mu$ are precisely those which preserve the flat metric up to a local rescaling, *i.e.* they preserve the angle between two vectors. This can be seen in the solutions to the conformal Killing equation

$$\partial_\mu \epsilon_\nu + \partial_\nu \epsilon_\mu = \Omega(x)\delta_{\mu\nu} \tag{2.11}$$

which is a condition on the vector field $\epsilon^\mu \partial_\mu$ by which $x$ is translated. After showing that the most general solution is

$$\epsilon^\mu = \delta a^\mu + \delta\Lambda^{\mu\nu}x_\nu + \delta\lambda x^\mu + \delta b^\nu \left(2x^\mu x_\nu - x^2\delta_{\mu\nu}\right) \ , \tag{2.12}$$

we immediately recognize the results in (2.5), (2.6), (2.7) and (2.8).[2]

To find conformal theories, it is usually enough to search for scale invariance. This is because $T^\mu_\mu = 0$ automatically ensures that $T_{\mu\nu}\epsilon^\nu$ is conserved for any conformal Killing vector. The only way to have scale invariance without a traceless stress-energy tensor is

$$T^\mu_\mu = \partial_\mu V^\mu \ , \ V^\mu \neq \partial_\nu L^{\mu\nu} \ . \tag{2.13}$$

In this case, the dilation current (2.7) is modified to $x^\nu T_{\mu\nu} - V_\mu$ [51]. This scenario is implausible since it requires the scaling dimension $V_\mu$ to have exactly the conserved current value $d-1$ despite the fact that $V_\mu$ is not conserved.[3]

According to the above logic, one may reach a new CFT by taking an old CFT and

[2]In two dimensions, (2.12) only describes the solutions that have a globally defined inverse. The others are most easily constructed in complex notation, which turns (2.11) into the Cauchy-Riemann equations.

[3]It is also worth noting that only non-unitary theories can achieve conformal invariance without $T^\mu_\mu = 0$. This is because $V_\mu$ saturates the unitarity bound while being a descendant. One such example is the biharmonic scalar [52].

deforming it by a relevant operator which modifies the low-energy dynamics. The relevant operator should be added with a finely tuned coupling so that we sit at an infrared fixed-point of the renormalization group flow. This thesis will explore some of these flows using conformal perturbation theory — the (conceptually simple but technically challenging) framework for perturbing around a solved CFT that is not necessarily free. There are two ways to ensure that such a flow is perturbative in the first place. One is to choose an operator whose scaling dimension is very close to $d$. In the prototypical example, which deforms (2.4) by $\lambda\phi^4$, this is done by setting the spacetime dimension to $d = 4 - \varepsilon$, resulting in an $O(\varepsilon)$ zero of the one-loop beta function. We will call this CFT either the Wilson-Fisher fixed-point or the critical Ising model, to highlight its connection to the second-order phase transition of

$$H = -J \sum_{\langle i,j \rangle} \sigma_i \sigma_j \ . \tag{2.14}$$

It is also possible to derive RG flows that are neither gapped nor free in the IR by starting from operators that are classically marginal. This requires two-loop effects to cancel one-loop effects in the beta function. The celebrated example of this comes from a 4D gauge theory with massless matter [53, 54]. Taking gauge group $SU(N_c)$ with $N_f$ fundamental fermions and no scalars, we wil write

$$\begin{aligned} \beta(g) &= \beta_0 \frac{g^3}{16\pi^2} + \beta_1 \frac{g^5}{(16\pi^2)^2} + \dots \\ \beta_0 &= -\frac{11}{3} N_c + \frac{2}{3} N_f \\ \beta_1 &= -\frac{34}{3} N_c^2 + \left( \frac{10}{3} N_c + 2 \frac{N_c^2 - 1}{N_c} \right) N_f \end{aligned} \tag{2.15}$$

for definiteness. This has a zero given by the Caswell-Banks-Zaks fixed-point:

$$\frac{g_*^2}{16\pi^2} = -\frac{\beta_0}{\beta_1} \approx \frac{11 N_c - 2 N_f}{16 N_c N_f - 34 N_c^2} \ . \tag{2.16}$$

Here, we have taken $N_c$ to be large since $N_c \sim N_f \gg 1$ is the condition for having a small coupling anyway. As QFTs are either conformal or not conformal, it is perfectly legitimate to ask how small $N_c$ and $N_f$ can be before this fixed-point ceases to exist. At the time of writing, there is significant hope that this question can be answered with bootstrap methods.

While the problem of finding the conformal window typically refers to Yang-Mills theory, there are several ways to mod out by the global symmetry of a CFT in order to produce a closed subsector. Sometimes this retains the notion of "gauge charge" through the introduction of Wilson lines. Unlike the above examples — free theories and their deformations — this procedure could easily face obstructions on curved manifolds. Hence, we will limit our discussion to the best understood example — a 2D CFT with a discrete abelian global

symmetry. To make its thermal partition function finite, we must compactify both the space and time directions but the distinction between the two is arbitrary. The direction along which we quantize may be parameterized by a number $\tau$ with positive imaginary part. We therefore write

$$Z(\tau,\bar{\tau}) = \mathrm{Tr}\left[e^{-\Im\tau H + i\Re\tau P}\right] \ . \tag{2.17}$$

This partition function should be invariant under the transformation that exchanges time and space. In other words, consistency on the torus requires $Z(\tau,\bar{\tau}) = Z\left(-\frac{1}{\tau},-\frac{1}{\bar{\tau}}\right)$. This is one of the modular transformations which should supplement crossing symmetry of all four-point functions. Clearly, a well defined theory can easily lose modular invariance if certain (non-singlet) states are removed from the trace (2.17). Gauging should therefore bring in *twisted sectors* to ensure that this does not happen. The sum over these sectors can be represented schematically as

$$Z(\tau,\bar{\tau}) = \frac{1}{|G|}\sum_{g,h\in G} \begin{matrix} g & \square \\ h & \end{matrix} \ . \tag{2.18}$$

This notation means that an arbitrary state $|\psi\rangle$ is taken to $g|\psi\rangle$ around the first cycle and $h|\psi\rangle$ around the second cycle [55]. What we have just described is the *orbifold* procedure. Its name comes from the fact that it can be used to relate two nonlinear sigma models — one with target space $M$ and the other with target space $M/G$. A simple and useful example of an orbifold theory is the free boson on $\mathbb{S}^1/\mathbb{Z}_2$, *i.e.* with the $\mathbb{Z}_2$ global symmetry modded out. In this case, a second $\mathbb{Z}_2$ symmetry emerges which distinguishes states in the twisted sector from those in the untwisted sector. An orbifold of this symmetry yields the free boson on $\mathbb{S}^1$ again. The phenomenon of recovering the original theory by gauging twice happens in higher dimensions as well if one considers higher form symmetries.

### 2.1.2 Examples without locality

Our list of viable theories can be extended greatly if we allow those with various forms of nonlocality. This does not require us to take the drastic step of eschewing local operators altogether. Topological QFTs, describing only extended objects, are certainly interesting objects to study but this thesis will be more concerned with the following definitions of locality.

1. A local QFT should have a stress-energy tensor in its spectrum of local operators.

2. A local QFT should have conserved currents for all continuous symmetries in its spectrum of local operators. This is clearly stronger than definition 1.

3. A local QFT should be consistent on orientable (possibly spin) manifolds with nontrivial topology. This is certainly not weaker than definition 2 since we will see many

examples of 2D CFTs posessing conserved currents that are not consistent on $\mathbb{S}^1 \times \mathbb{S}^1$. The opposite phenomenon — violating Noether's theorem while preserving modular invariance — seems unlikely but we do not have a proof.

To reflect on the importance of a stress-energy tensor, $\frac{\mathrm{d}E}{\mathrm{d}t} = 0$ is a very weak condition — it allows energy to move from one place to another at arbitrary speeds. A more desirable conservation law takes the form of a continuity equation where, within some ball $B$, the non-conservation $\frac{\mathrm{d}E_B}{\mathrm{d}t}$ is controlled entirely by the physics at $\partial B$. As such, one would like to be able to calculate it by inserting some $T^{0\mu}$ into the $\int_{\partial B} \mathrm{d}S_\mu \ldots$ surface integral. If there is no operator that does the job (or if the only such operator is itself the integral of a local quantity) then predictions about how energy will enter and leave $B$ require information that comes from an infinite distance away.

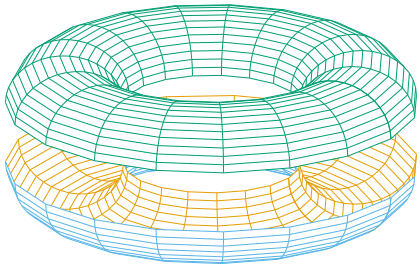

Figure 2.3: A torus in two halves, which are topologically equivalent to cylinders. If the same theory were defined on both halves, losing consistency after they are glued together would be a type of nonlocal behaviour.

The last definition, which is that local theories should not "know" about non-trivial topology, appears to be very strong. In two-dimensional CFT, where this condition is also required for defining perturbative string theory, a useful theorem was proven in [56]. It states that consistency on arbitrary Riemann surfaces is guaranteed once four-point functions obey crossing symmetry on the plane and one-point functions obey modular covariance on the torus. Deriving a similar theorem in higher dimensions appears to be much more difficult. Looking at Figure 2.3, a torus is cut into two halves, which are both conformally flat. If a CFT were to pick up an anomaly upon gluing these two halves together, its local operators would contain information about what happens after we traverse a full cycle.

Let us list a few examples of CFTs which are nonlocal in all three senses of the word.

- Even though free theory two-point functions are supposed to look like $\langle \phi(x)\phi(0)\rangle = \frac{1}{|x|^{d-2}}$, we may define a new theory by considering $\langle \phi(x)\phi(0)\rangle = \frac{1}{|x|^{2\Delta_\phi}}$ for general $\Delta_\phi$ with the stipulation that higher-point correlators are defined by Wick's theorem and composite operators are defined by point-splitting. The resulting solution to crossing symmetry, with no stress-energy tensor, is called the *generalized free theory*.

- Given any CFT, it is possible to artificially set various co-ordinates to zero so that correlators live on a defect and still exhibit conformal covariance. Even when this is done by starting with a local theory, there is no reason to expect locality to be visible after this restriction. For instance, in the codimension one case, the stress-energy tensor has divergence $-\partial_\perp T^{\perp\nu}$ and dimension $d+1$ from the defect point of view. As we will see in chapter 4, the generalized free theory is a special case of this construction in which the bulk harbors a regular free theory. Something very special happens when an $\mathbb{R}^2 \subset \mathbb{R}^4$ is singled out for a local superconformal theory. If there is at least $\mathcal{N}=2$ supersymmetry, we may define a nilpotent supercharge that allows us to recover locality (along with other features helpful for the bootstrap) after passing to its cohomology [57].

- Given any of the nonlocal CFTs above, it is again possible to identify relevant operators and use them to flow to new infrared fixed-points. In this case, it is usually much easier to find some flow that is weakly coupled. The generalized free scalar is just one example of a theory which has a parameter (other than $d$) which allows operators to be brought arbitrarily close to marginality.

- Another deformation procedure involves taking a CFT (local or not) and adding an operator that is nonlocal. We will see an example of this in chapter 4 which is actually equivalent to one of the deformations above. In other words, a nonlocal theory deformed by a local operator becomes a local theory deformed by a nonlocal operator once one of the fields is integrated out.

Lastly, we should note that even though tensor product theories can be local according to the above definition, they always have multiple stress-energy tensors if they have one.

### 2.1.3 The Ward identity

One thing the stress-energy tensor allows us to do is derive the four basic infinitesimal transformations which would have to be taken as assumptions for defining a nonlocal CFT.

$$\begin{aligned}
[P_\mu, \mathcal{O}(x)] &= \partial_\mu \mathcal{O}(x) \\
[M_{\mu\nu}, \mathcal{O}(x)] &= (x_\nu \partial_\mu - x_\mu \partial_\nu + S_{\mu\nu})\mathcal{O}(x) \\
[D, \mathcal{O}(x)] &= (x^\mu \partial_\mu + \Delta)\mathcal{O}(x) \\
[K_\mu, \mathcal{O}(x)] &= (2x_\mu x^\nu \partial_\nu - x^2 \partial_\mu + 2\Delta x_\mu - 2x^\nu S_{\mu\nu})\mathcal{O}(x)
\end{aligned} \tag{2.19}$$

In (2.19), we have assumed that the "spin parts" of the transformation laws are given by

$$\begin{aligned}
[M_\mu \nu, \mathcal{O}(0)] &= S_{\mu\nu}\mathcal{O}(0) \\
[D, \mathcal{O}(0)] &= \Delta \mathcal{O}(0) \\
[K_\mu, \mathcal{O}(0)] &= 0
\end{aligned} \tag{2.20}$$

where the matrix $S_{\mu\nu}$ acts on Lorentz indices of $\mathcal{O}$ which have been suppressed. The first two lines indicate that we have chosen to work with operators that are in well defined representations with respect to dilations and rotations. That this is possible reflects the fact that $D$ and $M_{\mu\nu}$ commute in (2.10). The fact that angular momentum and scaling dimension are the *only* eigenvalues appearing in (2.19) reflects the fact that $D$ and $M_{\mu\nu}$ generate the maximally compact subgroup of the conformal group. The third line of (2.20) requires more explanation since there is no way to make it hold for every operator in a theory. For instance, starting from any operator in the kernel of $K_\mu$, it is clear that powers of $P_\mu$ will take us out of the kernel. However, through repeated differentiation, (2.19) implicitly defines the transformation law for all such operators obtained in this way. This is enough for theories with spectra that are bounded from below since $K_\mu$ acts as a lowering operator for scaling dimension. Clearly, all unitary CFTs are included in this class. The operators annihilated by $K_\mu$, which have the lowest scaling dimension for a given multiplet, are called *primary operators* while all others are called *descendant operators*. In this thesis, we will not encounter any CFTs that include local operators other than primaries and descendants. However, we mention in passing that some theories (particularly logarithmic CFTs [58]) have this as one of their defining properties.

The transformation laws (2.19) are known as conformal Ward identities. Writing an ansatz for a correlation function that enjoys the right conformal covariance properties formally amounts to imposing (2.19) as a differential equation. A Ward identity, which appears in any QFT with a stress-energy tensor, is

$$\partial_\mu \left\langle T^{\mu\nu}(x)\mathcal{O}_1(x_1)\dots\mathcal{O}_n(x_n)\right\rangle = -\sum_{i=1}^{n}\delta(x-x_i)\partial_i^\nu \left\langle \mathcal{O}_1(x_1)\dots\mathcal{O}_n(x_n)\right\rangle \ . \tag{2.21}$$

Clearly, there can only be one normalization of $T^{\mu\nu}$ for which (2.21) holds as written. This is called the *central charge* of the theory and denoted by $C_T$. For other currents with a similar Ward identity, there are flavour central charges denoted by $C_J$. In most bootstrap studies, these exhaust the list of special normalizations since unit normalization is the preferred choice in the absence of another governing principle. The main quantities that can be fixed from this Ward identity are the three-point couplings $\lambda_{12T}$ involving the stress-energy tensor. Something immediately clear is that this should vanish unless $\mathcal{O}_1$ and $\mathcal{O}_2$ are the same. By differentiating an ansatz for $\langle T^{\mu\nu}(x)\mathcal{O}_1(x_1)\mathcal{O}_2(x_2)\rangle$ on the left-hand side of (2.21), the undetermined coefficients can be read off from the known two-point functions on the right-hand side.

A nice application of the conformal Ward identities is to show that the stress-energy tensor is necessarily primary. For other operators studied using the bootstrap philosophy, we have a completely arbitrary choice. When asking if a generic $\mathcal{O}$ is a primary or descendant, the answer is that it is whatever it needs to be for constraints like crossing symmetry to hold. Following an argument in [14], we may write an infinitesimal change in $T^{\mu\nu}$ that satisfies

symmetry, conservation and tracelessness once the conformal Killing equation is imposed.

$$\delta T^{\mu\nu} = \epsilon^\rho \partial_\rho T^{\mu\nu} + \partial_\rho \epsilon^\rho T^{\mu\nu} - \partial_\rho \epsilon^\mu T^{\rho\nu} + \partial^\nu \epsilon_\rho T^{\rho\mu} \tag{2.22}$$

We have required the right-hand side to be linear in $\epsilon$ and dependent only upon operators that are universal, *i.e.* $T^{\mu\nu}$ itself. Since there are no arbitrary coefficients left, this expression can be matched against (2.19). We find precisely the result for a conformal primary after using the fact that

$$S_{\mu\nu} T_{\rho\sigma} = \delta_{\mu\rho} T_{\nu\sigma} - \delta_{\nu\sigma} T_{\mu\rho} \ . \tag{2.23}$$

There are two caveats to (2.22) that we want to mention. The first is that in $d = 2$, primality of $T^{\mu\nu}$ can be violated by the term $2\partial_\mu \partial_\nu \partial_\rho \epsilon^\rho - \partial^2 \partial_\mu \epsilon_\nu - \partial^2 \partial_\nu \epsilon_\mu$. This leads us to conclude that the algebra of conformal transformations is now centrally extended. The second is that $T^{\mu\nu}$ is also not a primary under an algebra that includes supercharges in addition to momentum generators. To demonstrate this most convincingly, we should clarify the sense in which conservation is being demanded for (2.22). Instead of demanding that $\partial_\mu \delta T^{\mu\nu}$ be identically zero (even though this happens to hold for (2.10)), we should allow it to also be some other null quantity. In a Lagrangian QFT, this is reminiscent of certain conservation laws only holding on-shell. Consider the following combination of 3D supercurrents which is symmetric and traceless with $\Delta = d$.

$$T_{\mu\nu} = Q_\alpha (\gamma_\mu)^\alpha{}_\beta J^\beta_\nu + Q_\alpha (\gamma_\nu)^\alpha{}_\beta J^\beta_\mu \tag{2.24}$$

If we can show that it is conserved as well, we must conclude that it is a valid stress-energy tensor leading to additional terms in the variation (2.22). It is clear that we cannot do this by taking a naive divergence. However, the weak form of conservation that we need is for the descendant given by the divergence to also be a primary. Abusing notation slightly,

$$\begin{aligned}
K_\rho \partial^\mu T_{\mu\nu} &= -2d T_{\mu\nu} + 2i M_\rho{}^\mu T_{\mu\nu} \\
&= -2d T_{\mu\nu} + 2i \left[ -\frac{i}{2} Q_\gamma (\gamma_\rho{}^\mu)^\gamma{}_\alpha + Q_\alpha M_\rho{}^\mu \right] \left[ (\gamma_\mu)^\alpha{}_\beta J^\beta_\nu + (\gamma_\nu)^\alpha{}_\beta J^\beta_\mu \right] \\
&= -2d T_{\mu\nu} + (d+1) Q_\gamma (\gamma_\rho)^\gamma{}_\beta J^\beta_\nu - Q_\gamma (\gamma_\nu)^\gamma{}_\beta J^\beta_\rho \\
&\quad + 2i Q_\alpha (\gamma_\mu)^\alpha{}_\beta M_\rho{}^\mu J^\beta_\nu + 2i Q_\alpha (\gamma_\nu)^\alpha{}_\beta M_\rho{}^\mu J^\beta_\mu \\
&= -2d T_{\mu\nu} + (d+1) Q_\gamma (\gamma_\rho)^\gamma{}_\beta J^\beta_\nu - Q_\gamma (\gamma_\nu)^\gamma{}_\beta J^\beta_\rho \\
&\quad - 2 Q_\alpha (\gamma_\mu)^\alpha{}_\beta \left[ \delta_{\rho\nu} J^{\mu\beta} - \delta^\mu_\nu J^\beta_\rho + \frac{1}{2} (\gamma_\rho{}^\mu)^\beta{}_\gamma J^\gamma_\nu \right] \\
&\quad - 2 Q_\alpha (\gamma_\nu)^\alpha{}_\beta \left[ (1-d) J^\beta_\rho + \frac{1}{2} (\gamma_\rho{}^\mu)^\beta{}_\gamma J^\gamma_\mu \right] \\
&= 0 \ .
\end{aligned} \tag{2.25}$$

Note that we have used $i\varepsilon_{\mu\rho\sigma}J^\mu = \gamma_\sigma J_\rho - \gamma_\rho J_\sigma$ twice. Understanding how conserved currents arrange themselves into multiplets is a fundamental part of the superconformal bootstrap.

| $d$ | Superalgebras |
|---|---|
| 3 | $\mathfrak{osp}(\mathcal{N}\|4)$ |
| 4 | $\mathfrak{su}(2,2\|\mathcal{N})$ |
| 5 | $\mathfrak{f}_2(4)$ |
| 6 | $\mathfrak{osp}(8^*\|\mathcal{N})$ |

Table 2.1: The possibile choices for a superconformal algebra in $d \geq 3$. The many additions to this list for $d < 3$ will be discussed momentarily. The value of $\mathcal{N}$ is usually chosen so that the number of Poincaré supercharges is at most 16. A larger number would lead to higher spin currents and therefore free theories. Setting $\mathcal{N} = 0$ returns a real form of $\mathfrak{so}(d+2)$ or possibly a double cover.

The above computation has been done with the 3D $\mathcal{N} = 1$ superconformal algebra. Its fermionic part is

$$\begin{aligned} \{Q_\alpha, Q_\beta\} &= P_\mu(\gamma^\mu C)_{\alpha\beta} \\ \{S_\alpha, S_\beta\} &= K_\mu(\gamma^\mu C)_{\alpha\beta} \\ \{Q_\alpha, S_\beta\} &= \frac{1}{4}M_{\mu\nu}(\gamma^{\mu\nu}C)_{\alpha\beta} + DC_{\alpha\beta} \end{aligned} \tag{2.26}$$

while the mixed part

$$\begin{aligned} [M_{\mu\nu}, Q_\alpha] &= \frac{i}{2}Q_\beta(\gamma_{\mu\nu})^\beta{}_\alpha \\ [M_{\mu\nu}, S_\alpha] &= \frac{i}{2}S_\beta(\gamma_{\mu\nu})^\beta{}_\alpha \\ [D, Q_\alpha] &= \frac{i}{2}Q_\alpha \\ [D, S_\alpha] &= -\frac{i}{2}S_\alpha \\ [P_\mu, S_\alpha] &= iQ_\beta(\gamma_\mu)^\beta{}_\alpha \\ [K_\mu, Q_\alpha] &= -iS_\beta(\gamma_\mu)^\beta{}_\alpha \end{aligned} \tag{2.27}$$

is what we have directly used. This algebra can be derived geometrically using conformal Killing spinors as in [59]. The various ways to have a superconformal algebra, shown in Table 2.1 for at least three dimensions, were classified in [60]. The notation makes it clear what the maximal bosonic subalgebra is — the $\mathcal{N}$-dependent R-symmetry is on one side of the bar and the $d$-dependent conformal symmetry is on the other.

### 2.1.4 Radial quantization

The conformal Ward identities allow us to show that two-point functions have a single tensor structure.

$$\langle \mathcal{O}^{\mu_1\cdots\mu_\ell}(x_1)\mathcal{O}^{\nu_1\cdots\nu_\ell}(x_2)\rangle = \frac{H_{12}^{\mu_1\nu_1}\dots H_{12}^{\mu_\ell\nu_\ell} - \text{traces}}{|x_{12}|^{2(\Delta+\ell)}} \tag{2.28}$$

Three-point functions also have a single tensor structure if they include at most one spinning operator.

$$\langle \phi_1(x_1)\phi_2(x_2)\mathcal{O}^{\mu_1\cdots\mu_\ell}(x_3)\rangle = \frac{\lambda_{12\mathcal{O}} V_3^{\mu_1}\dots V_3^{\mu_\ell} - \text{traces}}{|x_{12}|^{\Delta_1+\Delta_2-\Delta-\ell}|x_{13}|^{\Delta+\ell+\Delta_{12}}|x_{23}|^{\Delta+\ell-\Delta_{12}}} \tag{2.29}$$

Here, we have defined

$$\begin{aligned} H_{12}^{\mu\nu} &= x_{12}^2\delta^{\mu\nu} - 2x_{12}^\mu x_{12}^\nu \\ V_3^\mu &= \frac{x_{13}^\mu x_{23}^2 - x_{23}^\mu x_{13}^2}{x_{12}^2}\,. \end{aligned} \tag{2.30}$$

In chapter 4, we will express these correlators more efficiently by lifting them from $\mathbb{R}^d$ to $\mathbb{R}^{d+1,1}$ where the conformal group acts linearly. This also goes hand-in-hand with an index-free formalism that automatically accounts for the subtraction of traces. Here, we would like to point out that an $(n+1)$-point function may be written as a sum of $n$-point functions once all the three-point couplings are known. As a result, four-point functions of scalars are in principle determined by (2.28) and (2.29).

The standard derivation of this employs a quantization scheme in which states are created by local operators at the origin. Clearly $\mathcal{O}(0)\,|0\rangle$ represents some state in the Hilbert space of a QFT. A stronger statement, unique to CFTs, is that *every* state may be created this way after taking linear combinations. Let us trade the radial direction for cylinder time with $t = \log r$. Under this Weyl transformation, the dilation operator on $\mathbb{R}^d$ maps to the Hamiltonian on $\mathbb{S}^{d-1}\times\mathbb{R}$. In this framework, called *radial quantization*, a state on the cylinder determined by data in the infinite past may be thought of as originating from a single point on the plane. Although not the most formal derivation, we can see how this works by decomposing a correlator that involves a non-vacuum state.

$$\langle 0|\dots\mathcal{O}_0(r)\,|\Psi\rangle = \int [D\varphi]\,\langle 0|\dots\mathcal{O}_0(r_0)\left(\frac{r}{r_0}\right)^D|\varphi\rangle\,\Psi[\varphi,r_0] \tag{2.31}$$

The path integral we have written imagines that there are some "field configurations" $\{\varphi\}$. The wavefunctional assigning a weight to each one lives on the radius $r_0$ slice since our operators are in the Heisenberg picture. If $|\Psi\rangle$ is an eigenstate of $D$, taking $r_0\to 0$ is well defined which turns the wavefunctional into a purely local object. We are then free to use the basic quantum mechanical fact that an operator can be defined by its matrix elements.

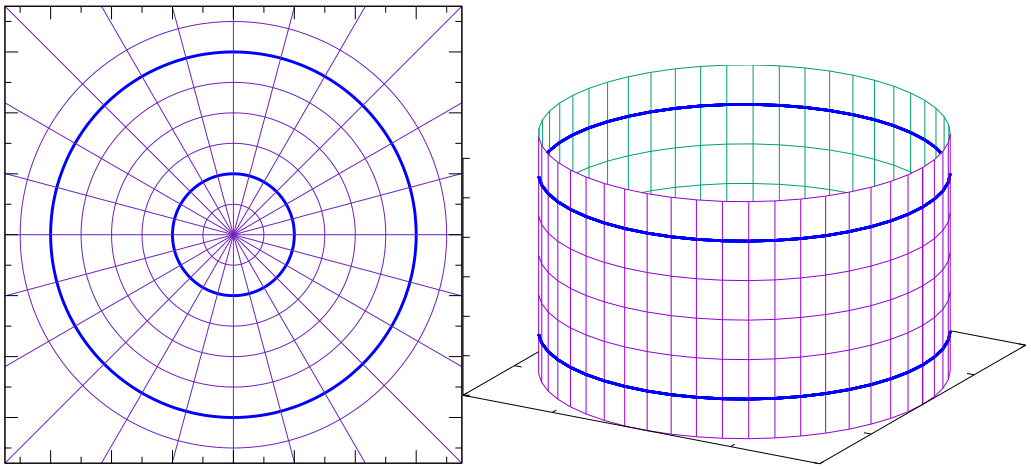

(a) Plane (b) Cylinder

Figure 2.4: The plane and the cylinder showing a mapping between circles at fixed $r$ and fixed $t$. States on the right live on these circles while local operators on the left live at points. We learn two interesting things from the fact that $D = r\partial_r$ maps to $H = \partial_t$. The first is that the spectrum of scaling dimensions must be bounded from below in a unitary theory. The second is a general expectation that $D$ (unlike the plane Hamiltonian) should have a discrete spectrum.

This allows us to write (2.31) as

$$\int [D\varphi] \langle 0| \dots \mathcal{O}_0(r) |\varphi\rangle \langle\varphi| \mathcal{O}(0) |0\rangle = \langle 0| \dots \mathcal{O}_0(r)\mathcal{O}(0) |0\rangle \ . \tag{2.32}$$

Once we believe that states created by local operators span the full Hilbert space, a state like $\mathcal{O}_1(x_1)\mathcal{O}_2(x_2) |0\rangle$ can be written as a convergent sum. This leads to the operator product expansion

$$\phi_1(x)\phi_2(0) = \sum_{\mathcal{O}} \frac{\lambda_{12\mathcal{O}}}{|x|^{\Delta_1+\Delta_2-\Delta}} C_{\mu_1\dots\mu_\ell}(x,\partial)\mathcal{O}^{\mu_1\cdots\mu_\ell}(0) \tag{2.33}$$

where we have distinguished between primaries and descendants. Note that our $\lambda_{12\mathcal{O}}$ in (2.33) is clearly the same one that appears in (2.29). Since $x \mapsto -x$ produces a factor of $(-1)^\ell$, only an even-spin operators can appear if $\phi_1$ and $\phi_2$ are identical. Moreover, the operators are symmetric as $x^{\mu_1} \cdots x^{\mu_\ell}$ vanishes against any operator with an antisymmetric part.[4]

[4] A more general OPE will have external indices that do not need to be saturated. In this case, the Young tableaux for exchanged operators are allowed to contain additional rows.

### 2.1.5 The power of the OPE

The OPE allows one to expand the unknown part of

$$\langle\phi(x_1)\phi(x_2)\phi(x_3)\phi(x_4)\rangle = \frac{g(u,v)}{|x_{12}|^{2\Delta_\phi}|x_{34}|^{2\Delta_\phi}} \tag{2.34}$$

into a sum of kinematically determined special functions called conformal blocks. By relabelling points, the s-channel block $g_{\mathcal{O}}(u,v)$ turns into the t-channel block after swapping the arguments and multiplying by an overall factor. This leads to the simplest crossing equation

$$\begin{aligned}&\sum_{\mathcal{O}} \lambda^2_{\phi\phi\mathcal{O}} F^-_{\mathcal{O}}(u,v) = 0\\ &F^-_{\mathcal{O}}(u,v) \equiv v^{\Delta_\phi} g_{\mathcal{O}}(u,v) - u^{\Delta_\phi} g_{\mathcal{O}}(v,u)\ .\end{aligned} \tag{2.35}$$

The power of (2.35) is that some choices for quantum numbers and OPE coefficients make it impossible to solve. To demonstrate this, [16] explored the properties of the 4D blocks

$$\begin{aligned}&g_{\Delta,\ell}(z,\bar{z}) = \left(-\frac{1}{2}\right)^{\ell} \frac{z\bar{z}}{z-\bar{z}}\\ &\left[z^{\frac{\Delta+\ell}{2}}\bar{z}^{\frac{\Delta-\ell-2}{2}}\,{}_2F_1\left(\begin{matrix}\frac{\Delta+\ell}{2},\frac{\Delta+\ell}{2}\\ \Delta+\ell\end{matrix};z\right){}_2F_1\left(\begin{matrix}\frac{\Delta-\ell-2}{2},\frac{\Delta-\ell-2}{2}\\ \Delta-\ell-2\end{matrix};\bar{z}\right) - (z\leftrightarrow\bar{z})\right]\end{aligned} \tag{2.36}$$

near $\Delta_\phi = 1$. Along the diagonal $z = \bar{z}$, the convolved blocks in (2.35) are concave up at $z = \frac{1}{2}$ for $\ell > 0$. By contrast, $F^-_{\Delta,0}(z,z)$ is concave down at the same point until $\Delta \approx 3.61$. This reveals a crude bound which states that 4D CFTs with a dimension one scalar must have a scalar in their OPE with dimension 3.61 or less. In this case, the bound is obtained by applying the second derivative to (2.35). By applying another differential operator, in addition to the second derivative, [16] strengthened this bound to $\Delta < 1$. The point is that the $\phi^2$ and $T_{\mu\nu}$ blocks, $F^-_{2,0}$ and $F^-_{4,2}$, lie on the boundary of the convex hull of the $\alpha\left[F^-_{\Delta,\ell}(z,\bar{z})\right]$ vectors. Therefore, omitting either one causes the identity operator to violate the sum rule (2.35). More generally, it useful to consider all derivatives as a basis for functionals.

$$\alpha = \sum_{m\leq n} a_{m,n}\partial_z\partial_{\bar{z}}\Big|_{z=\bar{z}=\frac{1}{2}} \tag{2.37}$$

Cutting off this sum at an arbitrary order and searching for a functional that is positive above a certain gap can be done efficiently with linear or semidefinite programming. With more than a handful of derivatives, it quickly becomes impossible to visualize the sum rule vectors — hence the common statement that the numerical bootstrap is a "black-box" or "oracle" that spits out mysterious bounds. It is worth noting that recent work has increased the number of components that one may use when performing this optimization by hand.

This is due to non-trivial geometric properties shared by conformal blocks along the diagonal [61, 62].

Computing conformal blocks is equivalent to inserting a complete set of descendants for a given primary — we write this here in one dimension since the higher-dimensional case is much less practical.

$$\sum_{n=0}^{\infty} \frac{\langle \phi(x_1)\phi(x_2)\partial^n \mathcal{O}(0)\rangle \langle \partial^n \mathcal{O}(\infty)\phi(x_3)\phi(x_4)\rangle}{\langle \mathcal{O}(\infty)\mathcal{O}(0)\rangle} = \frac{g_\Delta(u,v)}{|x_{12}|^{2\Delta_\phi}|x_{34}|^{2\Delta_\phi}} \tag{2.38}$$

The operators $C(x,\partial)$, which resum the contributions of descendants in the OPE, have only been computed in full generality very recently [63, 64]. For many years, these OPE blocks [65] were only known for certain small values of the spin, *e.g.*

$$\begin{aligned} C_\mu(x,\partial) \;=\; & B\left(\frac{\Delta+\Delta_{12}+1}{2}, \frac{\Delta-\Delta_{12}+1}{2}\right)^{-1} \int_0^1 \mathrm{d}\alpha \alpha^{\frac{\Delta+\Delta_{12}-1}{2}} (1-\alpha)^{\frac{\Delta-\Delta_{12}-1}{2}} e^{\alpha x\cdot\partial} \\ & \frac{1}{(\Delta-\frac{d-2}{2})_n} \sum_{n=0}^{\infty} \frac{1}{n!} \left(-\frac{1}{4}\alpha(1-\alpha)x^2\partial^2\right)^n \\ & \left[x_\mu + \frac{(\Delta+\Delta_{12}+1-d)\alpha - (\Delta-\Delta_{12}+1-d)(1-\alpha)}{4(\Delta-d+1)(\Delta-\frac{d-2}{2}+n)} x^2\partial_\mu\right] \end{aligned} \tag{2.39}$$

for $\ell = 1$ [66]. Several modern methods for computing the blocks are based on the conformal Casimir which gives the same eigenvalue to all operators in a given multiplet. Expressions (2.57) and (2.58), which we will use later on, come from the formula

$$C_2 = \frac{1}{2} M_{\mu\nu} M^{\mu\nu} - \frac{1}{2}\left(P_\mu K^\mu - K_\mu P^\mu\right) - D^2 \,. \tag{2.40}$$

To derive (2.40), it is helpful to recognize that time reversal on the cylinder corresponds to inversion on the plane. This explains why we have written conjugate states as created by $\mathcal{O}(\infty)$ rather than $\mathcal{O}(0)$. Applying these conjugation properties to the stress-energy tensor, we may read off the following rules for conformal generators in radial quantization.

$$\begin{aligned} M_{\mu\nu}^\dagger = -M_{\mu\nu} \quad &, \quad D^\dagger = D \\ P_\mu^\dagger = K_\mu \quad &, \quad K_\mu^\dagger = P_\mu \end{aligned} \tag{2.41}$$

An immediate application of (2.41) is to compute the norm of the states $P_\mu |\mathcal{O}^{\mu_1\cdots\mu_\ell}\rangle$. We may also compute the norm of $P_\mu P^\mu |\mathcal{O}\rangle$ where $\mathcal{O}$ is a scalar primary. Demanding that these

norms are non-negative, we derive

$$\Delta \geq \begin{cases} \ell + d - 2 & \ell > 0 \\ \frac{d-2}{2} & \ell = 0 \end{cases} \tag{2.42}$$

which are known as the unitarity bounds. Saturation of (2.42) implies a vanishing norm and, in a unitary theory, this requires the state itself to be zero. We therefore reinterpret equations of motion as *shortening conditions* for a conformal multiplet. A scalar primary of dimension $\frac{d-2}{2}$ must have a vanishing Laplacian and is therefore free. A spinning primary of dimension $\ell + d - 2$ must have a vanishing divergence and is therefore a current. The bootstrap has motivated a systematic understanding of unitarity bounds and shortening conditions, especially in the superconformal case [67].

Conformal blocks have become useful in several contexts, leading to a growing interest in how to compute them. We close this section by mentioning some alternative approaches that this thesis will not be able to review in depth.

- As with correlation functions in more general QFTs, there is a long history of using momentum space. This leads to an interesting conservation of difficulty in (2.19). The order of the differential operator encoding the action of $P_\mu$ decreases by one while the corresponding order for $K_\mu$ increases by one. Momentum space can sometimes be awkward in CFTs because the Fourier transform of the three-point function (2.29) does not have a closed form expression. On the other hand, a conformal block in momentum space is immediately computable as a product of two of these three-point functions [68]. Going back to position space produces a convolution which is known as the shadow integral.

- The Casimir equation satisfied by the blocks has recently been mapped to the Schrödinger equation for a famous integrable system known as the Calgero-Sutherland model [69]. Treating conformal blocks as Calgero-Sutherland wavefunctions has led to a number of new relations involving shifts in the internal and external parameters. It has also led to some new analytic bootstrap approaches in defect CFT [70, 71].

- Although the correlators of several theories at large 't Hooft coupling may be computed holographically in AdS, the Witten diagram expansion does not require one to compute individual conformal blocks. The holographic dual of a block was found to be *geodesic* Witten diagram where vertices are no longer integrated over all of space [72]. Instead, they are integrated along geodesics which connect pairs of operators corresponding to the OPE channel of interest. There is also an analogous treatment for the larger conformal blocks that exist in $d = 2$ [73]. This machinery leads to explicit linear combinations of s-channel blocks that compute a full tree-level Witten diagram, be it a contact diagram or an s-channel exchange. Expanding the other exchange Witten

diagrams into s-channel blocks again is a much more difficult problem which is related to studies of the crossing kernel [74, 75].

## 2.2 The numerical bootstrap

The previous section has advocated a technique based on computing conformal blocks and searching for functionals that act on them with nice positivity properties. Several codes have been written to aid in such tasks. The first widely released example was `JuliBoots` [76], a conformal bootstrap package based around a linear program solver. Shortly afterward, the solver `SDPB` [77] was released, giving the community access to the semidefinite programming methods pioneered in [24, 32, 78]. The frontend that will be used most in this thesis (which includes several functions for computing blocks) is `PyCFTBoot` [79]. There is also the `cboot` + `autoboot` combination [80, 81] which significantly reduces the work needed to formulate crossing equations.[5] In this section, we review the ideas used in the packages above.

Before beginning, we will emphasize that numerical bounds produced by these programs are rigorous up to tiny errors in how well the conformal blocks are known. In other words, only $k_{\text{max}}$, in the truncation parameters that we call $(k_{\text{max}}, \ell_{\text{max}}, m_{\text{max}}, n_{\text{max}})$, leads to errors that might be hard to bound uniformly. Increasing the number of derivatives only leads to stronger bounds because any functional computed at smaller $(m, n)$ still has the right properties for $(m_{\text{max}}, n_{\text{max}})$ once zeros are appended. Also, demanding positivity on sufficiently many values of $\ell$ appears to guarantee positivity on all values of $\ell$ — even those that were not part of the optimization [77].

### 2.2.1 Conformal blocks

Unlike with two or three point functions, conformal kinematics only determine the four point function up to an arbitrary dependence on two variables. Specifically for scalars,

$$\langle \phi_1(x_1)\phi_2(x_2)\phi_3(x_3)\phi_4(x_4)\rangle = \left(\frac{|x_{24}|}{|x_{14}|}\right)^{\Delta_{12}} \left(\frac{|x_{14}|}{|x_{13}|}\right)^{\Delta_{34}} \frac{g(u,v)}{|x_{12}|^{\Delta_1+\Delta_2}|x_{34}|^{\Delta_3+\Delta_4}}\,, \tag{2.43}$$

where $u = \frac{x_{12}^2 x_{34}^2}{x_{13}^2 x_{24}^2}$ and $v = \frac{x_{14}^2 x_{23}^2}{x_{13}^2 x_{24}^2}$. As explained in the seminal works [66, 83] on (global) conformal blocks, $g(u,v)$ may be expanded in a convergent series with each term coming from a primary operator in the theory. This is done by way of the OPE (2.33). Using this in the (12)(34) channels for example produces $g(u,v) = \sum_{\mathcal{O}} \lambda_{12\mathcal{O}}\lambda_{34\mathcal{O}} g_{\mathcal{O}}^{\Delta_{12},\Delta_{34}}(u,v)$ where each function depends on the spatial dimension $d$ or equivalently on $\nu = \frac{d-2}{2}$. The subscript $\mathcal{O}$ is often written as $(\Delta, \ell)$ since all primary operators that couple to scalars transform in some spin-$\ell$ representation of $SO(d)$. Crossing symmetry is the statement that all three choices for

[5] Recent work on semidefinite programming algorithms has led to the interesting proposal of implementing a program like `SDPB` on quantum computers [82].

| First | Second | Crossing point |
|---|---|---|
| $u = \lvert z\rvert^2$ | $v = \lvert 1-z\rvert^2$ | $(u_*, v_*) = \left(\frac{1}{4}, \frac{1}{4}\right)$ |
| $a = z + \bar{z}$ | $b = (z-\bar{z})^2$ | $(a_*, b_*) = (1, 0)$ |
| $\rho = \frac{z}{(1+\sqrt{1-z})^2}$ | $\bar{\rho} = \frac{\bar{z}}{(1+\sqrt{1-\bar{z}})^2}$ | $(\rho_*, \bar{\rho}_*) = (3-2\sqrt{2}, 3-2\sqrt{2})$ |
| $r = \lvert\rho\rvert$ | $\eta = \frac{\rho+\bar{\rho}}{2\lvert\rho\rvert}$ | $(r_*, \eta_*) = (3-2\sqrt{2}, 1)$ |

Table 2.2: Useful variables for four point conformal blocks in terms of $z$ and $\bar{z}$.

the OPE channels must agree. Our discussion above omitted numerically efficient methods for computing conformal blocks so we rectify that now.

Rather than the cross-ratios $u$ and $v$, conformal blocks are most often considered as functions of $z$ and $\bar{z}$, defined by using conformal transformations to send $x_1$, $x_3$ and $x_4$ to 0, 1 and $\infty$ respectively. The blocks are analytic for $0 < z, \bar{z} < 1$ and most bootstrap studies focus on the crossing symmetric point $(z_*, \bar{z}_*) = (\frac{1}{2}, \frac{1}{2})$. Table 2.2 shows the co-ordinates that are encountered most often. As observed in [24, 84], a block may be expanded in powers of $r$ where each term corresponds to a new descendant in the multiplet of $\mathcal{O}$. As the scaling dimension $\Delta$ is varried, coefficients in the sum diverge at certain non-unitary values. When they do, the residue is proportional to a conformal block itself.[6] This motivated [24] to develop the recurrence relations

$$\begin{aligned} h^{\Delta_{12},\Delta_{34}}_{\Delta,\ell}(r,\eta) &\equiv r^{-\Delta} g^{\Delta_{12},\Delta_{34}}_{\Delta,\ell}(r,\eta) \\ h^{\Delta_{12},\Delta_{34}}_{\Delta,\ell}(r,\eta) &= h^{\Delta_{12},\Delta_{34}}_{\infty,\ell}(r,\eta) + \sum_i \frac{c_i^{\Delta_{12},\Delta_{34}}(\ell) r^{n_i}}{\Delta - \Delta_i(\ell)} h^{\Delta_{12},\Delta_{34}}_{\Delta_i(\ell)+n_i,\ell_i}(r,\eta)\,. \end{aligned} \tag{2.44}$$

The leading term is given by [78]

$$h^{\Delta_{12},\Delta_{34}}_{\infty,\ell}(r,\eta) = \frac{\ell!}{(2\nu)_\ell} \frac{(-1)^\ell C^\nu_\ell(\eta)}{(1-r^2)^\nu (1+r^2+2r\eta)^{\frac{1}{2}(1+\Delta_{12}-\Delta_{34})} (1+r^2-2r\eta)^{\frac{1}{2}(1-\Delta_{12}+\Delta_{34})}}\,. \tag{2.45}$$

Table 2.3 describes the data needed to construct the poles and residues in (2.44). These

[6] Because of this, one conformal block can mimic the appearance of another if a certain pole in $\Delta$ is not ruled out by the gaps being imposed [85, 86]. This *fake primary effect* can even occur in the unitary bootstrap since the poles in Table 2.3 (and the appropriate spinning generalization) are not all strictly below the unitarity bound. Poles sitting precisely at the unitarity bound are present in a system that includes mixed correlators and / or spinning correlators. As a result, bounds that happen to reach certain integer values experience a jump — they switch from bounding the lightest operator in a given irrep to bounding the second lightest since operators at these fixed integer dimensions are already secretly present.

| $n_i$ | $\Delta_i(\ell)$ | $\ell_i$ | $c_i^{\Delta_{12},\Delta_{34}}(\ell)$ |
|---|---|---|---|
| $k$ | $1-\ell-k$ | $\ell+k$ | $c_1^{\Delta_{12},\Delta_{34}}(\ell,k)$ |
| $2k$ | $1+\nu-k$ | $\ell$ | $c_2^{\Delta_{12},\Delta_{34}}(\ell,k)$ |
| $k$ | $1+\ell+2\nu-k$ | $\ell-k$ | $c_3^{\Delta_{12},\Delta_{34}}(\ell,k)$ |

Table 2.3: The three types of poles in $\Delta$ for the meromorphic conformal blocks. Two of them have infinitely many elements labelled by the integer $k>0$. The third type requires $0<k\leq\ell$.

were noticed empirically in [78] but most of them were later proven in [87]. We must use

$$\begin{aligned}
c_1^{\Delta_{12},\Delta_{34}}(\ell,k) &= -\frac{k(-4)^k}{(k!)^2}\frac{(\ell+2\nu)_k}{(\ell+\nu)_k}\left(\frac{1}{2}(1-k+\Delta_{12})\right)_k\left(\frac{1}{2}(1-k+\Delta_{34})\right)_k \\
c_2^{\Delta_{12},\Delta_{34}}(\ell,k) &= \frac{k(\nu+1)_{k-1}(-\nu)_{k+1}}{(k!)^2}\frac{\ell+\nu-k}{\ell+\nu+k}\left(\frac{\ell+\nu-k+1}{2}\right)_k^{-2}\left(\frac{\ell+\nu-k}{2}\right)_k^{-2} \\
&\quad \left(\frac{1}{2}(1-k+\ell-\Delta_{12}+\nu)\right)_k\left(\frac{1}{2}(1-k+\ell+\Delta_{12}+\nu)\right)_k \\
&\quad \left(\frac{1}{2}(1-k+\ell-\Delta_{34}+\nu)\right)_k\left(\frac{1}{2}(1-k+\ell+\Delta_{34}+\nu)\right)_k \qquad (2.46) \\
c_3^{\Delta_{12},\Delta_{34}}(\ell,k) &= -\frac{k(-4)^k}{(k!)^2}\frac{(\ell+1-k)_k}{(\ell+\nu+1-k)_k}\left(\frac{1}{2}(1-k+\Delta_{12})\right)_k\left(\frac{1}{2}(1-k+\Delta_{34})\right)_k
\end{aligned}$$

to fill in the last column. One fact that can be seen from (2.46) is that $c_1^{0,0}(\ell,k)$ and $c_3^{0,0}(\ell,k)$ are only non-zero when $k$ is even. This means that when the external scalars are identical, blocks of even and odd spin do not show up in each other's recurrence relations. Consequently, adjusting the overall normalization of $h^{0,0}_{\Delta,\ell}(r,\eta)$ by $(-1)^\ell$ is equivalent to simply removing the factor of $(-1)^\ell$ from (2.45). Indeed, for many studies involving identical scalars, it was not present. The generalization to non-zero dimension differences shows us that more drastic changes would be needed if we still wanted to cancel the $(-1)^\ell$ in (2.45).

For spins up to some $\ell_{\text{max}}$, we need to know several derivatives of $h^{\Delta_{12},\Delta_{34}}_{\Delta,\ell}$ evaluated at $(r_*,\eta_*)=(3-2\sqrt{2},1)$. If we evaluated (2.44) for powers of $r$ up to $k_{\text{max}}$ and differentiated after, we would suffer a large performance hit. This is because there would be many appearances of (2.45)'s non-polynomial contributions all multiplied by different powers of $r$. A better strategy is to compute all derivatives at the same time via matrix multiplication [25]. To this end, we define the vector $\mathbf{h}_{\infty,\ell}$ with all desired derivatives of (2.45) already evaluated at the crossing point. They are grouped into "chunks" of $\partial_r$ powers for a given number of

$\partial_\eta$ powers. For example, a computation going up to third order would set

$$\mathbf{h}_{\infty,\ell} = \left[1 \ \frac{\partial}{\partial r} \ \frac{\partial^2}{\partial r^2} \ \frac{\partial^3}{\partial r^3} \ \frac{\partial}{\partial \eta} \ \frac{\partial^2}{\partial \eta \partial r} \ \frac{\partial^3}{\partial \eta \partial r^2} \ \frac{\partial^2}{\partial \eta^2} \ \frac{\partial^3}{\partial \eta^2 \partial r} \ \frac{\partial^3}{\partial \eta^3}\right]^{\mathrm{T}} h_{\infty,\ell} \ . \tag{2.47}$$

Seeing what happens when we differentiate $r^{n_i} h_{\Delta,\ell}$ several times, the matrix telling us what linear combination of derivatives to take is

$$\mathbf{R}^{n_i} = \begin{bmatrix} r_*^{n_i} & 0 & 0 & \dots \\ n_i r_*^{n_i-1} & r_*^{n_i} & 0 & \dots \\ n_i(n_i-1) r_*^{n_i-2} & 2n_i r_*^{n_i-1} & r_*^{n_i} & \dots \\ \vdots & \vdots & \vdots & \ddots \end{bmatrix} = \begin{bmatrix} r_* & 0 & 0 & \dots \\ 1 & r_* & 0 & \dots \\ 0 & 2 & r_* & \dots \\ \vdots & \vdots & \vdots & \ddots \end{bmatrix}^{n_i} . \tag{2.48}$$

This is the matrix acting on a single chunk. Since $\eta$ is unaffected, the full $\mathbf{R}$ is the tensor product of (2.48) with the identity. There is a problem with simply writing

$$\mathbf{h}_{\Delta,\ell} = \mathbf{h}_{\infty,\ell} + \sum_i \frac{c_i(\ell)\mathbf{R}^{n_i}}{\Delta - \Delta_i(\ell)} \mathbf{h}_{\Delta_i(\ell)+n_i,\ell_i} \tag{2.49}$$

and repeating this calculation every time a new block appears. It is most easily seen if we compare the number of matrix multiplications involved to the number of unique $\mathbf{h}_{\Delta_i+n_i,\ell_i}$ terms introduced by the recursion. Looking at (2.46), we see a residue $c_2(\ell,k)$ which may vanish sometimes and a residue $c_3(\ell,k)$ which only exists for certain spins. Therefore, the best case scenario (only using $c_1(\ell,k)$) tells us that the number of matrix multiplications # satisfies

$$\begin{aligned} \#(0) &= 1 \\ \#(k_{\max}) &> \sum_{k=0}^{k_{\max}-1} \#(k) \ . \end{aligned} \tag{2.50}$$

This is the same relation satisfied by the partition function which counts the number of ways to write an integer as the sum of smaller ones. The well known asymptotics of this function [88], tell us that duplicated matrix multiplications will abound by many orders of magnitude with this naive method. Instead, we should again follow [25] and predicts which residues will be needed ahead of time. This is simply a matter of letting the spin take values $\ell \leq \ell_{\max} + k_{\max}$ for a table whose final entires describe spins up to $\ell_{\max}$. For each value of $\ell$, we let the index $i$ run over all admissible poles in Table 2.3 and define the residue vectors

$\mathbf{d}_{\ell,i}$. All of these are initialized to $\mathbf{h}_{\infty,\ell_i}$. It is then straightforward to iterate

$$\mathbf{d}_{\ell,i} = c_i(\ell)\mathbf{R}^{n_i}\left[\mathbf{h}_{\infty,\ell_i} + \sum_j \frac{\mathbf{d}_{\ell_i,j}}{\Delta_i(\ell) + n_i - \Delta_j(\ell_i)}\right] \tag{2.51}$$

and stop once enough powers of $\mathbf{R}$ are introduced. Rather than updating the residues right away, we consider all $\mathbf{d}_{\ell,i}$ on the right-hand side to be the "old values" and replace them with the "new values" once everything on the left-hand side has been calculated. These go into the expression

$$\mathbf{h}_{\Delta,\ell} = \mathbf{h}_{\infty,\ell} + \sum_i \frac{\mathbf{d}_{\ell,i}}{\Delta - \Delta_i(\ell)}\,. \tag{2.52}$$

It is clear that the entries in $\mathbf{h}_{\Delta,\ell}$ are rational functions of $\Delta$. They all have different numerators and the same denominator. Instead of computing (2.52) as written and taking extra time to extract the numerator and denominator, it is convenient to store them separately from the start. The leading term of (2.52) is multiplied by $\prod_j(\Delta - \Delta_j(\ell))$ and the $i^{\text{th}}$ term of it is multiplied by $\prod_{j\neq i}(\Delta - \Delta_j(\ell))$.

There is a modification to (2.52) that can be used to produce polynomials of smaller degree. Described in [24], it slightly increases the time needed to generate a conformal block table but it can greatly decrease the running time of `SDPB`. The idea is to split the set of poles $\mathcal{P}$ into "large and small" types and use the poles of $\mathcal{P}_>$ to approximate those in $\mathcal{P}_<$. As our crieterion, we check whether the maximum component of $\mathbf{d}_{\ell,i}$ is above or below some cutoff $\theta$. For $\Delta_i \in \mathcal{P}_<$, we attempt to choose the $a_{i,k}$ coefficients optimally in

$$\frac{1}{\Delta - \Delta_i} \approx \sum_{\Delta_k \in \mathcal{P}_>} \frac{a_{i,k}}{\Delta - \Delta_k}\,. \tag{2.53}$$

Following the choice in [24], we demand that the first $|\mathcal{P}_>|/2$ derivatives of (2.53) hold exactly at $\Delta = \Delta_{\text{unitary}} + \theta$ and $\Delta = \theta^{-1}$. If $|\mathcal{P}_>|$ is odd, the last of these derivatives will only hold at one of the points. Once the $a_{i,k}$ are determined by this invertible linear system, they can be incorporated into (2.52). Whenever it needs to multiply by $\prod_{\Delta_j\neq\Delta_i}(\Delta - \Delta_j)$ and $\Delta_i \in \mathcal{P}_<$, it instead multiplies by $\sum_{\Delta_k\in\mathcal{P}_>} a_{i,k}\prod_{\Delta_j\in\mathcal{P}_>\setminus\{\Delta_k\}}(\Delta - \Delta_j)$.

After the (2.52) computation with the optional degree reduction step, one must obtain a vector $\mathbf{g}_{\Delta,\ell}$ of true conformal block derivatives from its meromorphic version $\mathbf{h}_{\Delta,\ell}$. This is done by restoring the $r_*^\Delta$ singularity with another matrix. Specifically,

$$\mathbf{g}_{\Delta,\ell} = r_*^\Delta \mathbf{S}\mathbf{h}_{\Delta,\ell}\,. \tag{2.54}$$

It is easy to see that $r_*^\Delta\mathbf{S}$ must be the same matrix as $\mathbf{R}^{n_i}$ in (2.48) with $n_i$ replaced by $\Delta$. There is no need to build up $\mathbf{S}$ by repeatedly multiplying some simpler matrix by itself. Its $(i,j)$ element is immediately known to be $\frac{\Delta\ldots(\Delta-j)}{r_*^j}\binom{i}{j}$. Elements of the conformal block vector

continue to be rational functions. However, if all numerators in $\mathbf{h}_{\Delta,\ell}$ have the same degree, those in $\mathbf{g}_{\Delta,\ell}$ will have a degree that increases with the order of the derivative. Looking at these numerators, the end result is something of the form

$$\frac{\partial^{m+n}}{\partial\eta^m\partial r^n}g_{\Delta,\ell}^{\Delta_{12},\Delta_{34}}(r_*,\eta_*)=\chi_\ell(\Delta)P_\ell^{\Delta_{12},\Delta_{34};mn}(\Delta) \tag{2.55}$$

which is a polynomial times the positive function $\chi_\ell(\Delta)=r_*^\Delta\prod_j(\Delta-\Delta_j(\ell))^{-1}$. This is precisely the form required for a task that involves semidefinite programming.

Going from the (12)(34) to the (14)(23) channel switches $u\leftrightarrow v$ and modifies the prefactor in the four point function (2.65). Crossing equations are obtained by setting the differences of these four point functions to zero. The simplest crossing equation with no global symmetry is $v^{\frac{\Delta_2+\Delta_3}{2}}g_{1234}(u,v)-u^{\frac{\Delta_1+\Delta_2}{2}}g_{3214}(v,u)=0$ [78]. As a result, functions of the form

$$F_{\pm,\Delta,\ell}(u,v)=v^{\Delta_\phi}g_{\Delta,\ell}^{\Delta_{12},\Delta_{34}}(u,v)\pm u^{\Delta_\phi}g_{\Delta,\ell}^{\Delta_{12},\Delta_{34}}(v,u)\ , \tag{2.56}$$

are the natural objects to consider once conformal blocks are known. These have come to be called convolved conformal blocks [76]. In principle, convolved conformal blocks and their derivatives could be calculated directly from the (2.55) result with its $r$ and $\eta$ variables. However, the simple $u\leftrightarrow v$ transformation is represented by $r$ and $\eta$ in a much more complicated way. When the second half of (2.56) involves a new function $g_{\Delta,\ell}^{\Delta_{12},\Delta_{34}}(\tilde{r}(r,\eta),\tilde{\eta}(r,\eta))$, much of the work that goes into the $\frac{\partial^{m+n}}{\partial\eta^m\partial r^n}F_{\pm,\Delta,\ell}(r_*,\eta_*)$ calculation will be spent differentiating $\tilde{r}$ and $\tilde{\eta}$. This extra work during the convolution step can be eliminated if we instead add extra work during the conformal block step to convert (2.55) to $(z,\bar{z})$ or $(a,b)$ variables. At first glance, it might seem that the benefit of this choice is purely organizational — it allows the fast and slow calculations to be conceptually separate. As we now discuss however, there is another recurrence relation which gives us a much stronger incentive to change variables. This is used by the program `PyCFTBoot`.

Conformal blocks are eigenfunctions of the quadratic Casimir [83]:

$$\left[D_z+D_{\bar{z}}+2\nu\frac{z\bar{z}}{z-\bar{z}}\left((1-z)\frac{\mathrm{d}}{\mathrm{d}z}-(1-\bar{z})\frac{\mathrm{d}}{\mathrm{d}\bar{z}}\right)\right]g_{\Delta,\ell}^{\Delta_{12},\Delta_{34}}=c_2g_{\Delta,\ell}^{\Delta_{12},\Delta_{34}}\ . \tag{2.57}$$

Here, the definitions

$$\begin{aligned}D_z&=(1-z)z^2\frac{\mathrm{d}^2}{\mathrm{d}z^2}+\left(\frac{1}{2}\Delta_{12}-\frac{1}{2}\Delta_{34}-1\right)\frac{\mathrm{d}}{\mathrm{d}z}+\frac{1}{4}\Delta_{12}\Delta_{34}z\\ c_2&=\frac{1}{2}\left[\ell(\ell+2\nu)+\Delta(\Delta-2-2\nu)\right]\ ,\end{aligned} \tag{2.58}$$

are standard. The existence of a linear differential equation satisfied by the blocks suggests the possibility of building up high order derivatives from lower ones. We may pretend for

a minute that $g_{\Delta,\ell}$, $\frac{\partial g_{\Delta,\ell}}{\partial z}$ and $\frac{\partial^2 g_{\Delta,\ell}}{\partial z \partial \bar{z}}$ are all known at $\left(\frac{1}{2},\frac{1}{2}\right)$. The content of (3.15) is then to tell us what $\frac{\partial^2 g_{\Delta,\ell}}{\partial z^2}$ is at the same point. We could attempt to continue this pattern by differentiating (3.15) with respect to $z$ but then $\frac{\partial^3 g_{\Delta,\ell}}{\partial z^3}$ would not be the only unknown derivative anymore. The presence of new unknowns like $\frac{\partial^3 g_{\Delta,\ell}}{\partial \bar{z}^2 \partial z}$ forces us to use something more clever.

Such cleverness was found by [89] in which the quadratic and quartic Casimirs of the conformal group are used together. This reveals an ordinary differential equation satisfied by the blocks on the $z = \bar{z}$ diagonal. In terms of the $a$ co-ordinate, this new equation (which clearly keeps new derivatives under control) is

$$\begin{aligned} &D_a^{(4,3)} g_{\Delta,\ell}^{\Delta_{12},\Delta_{34}} = 0 \\ &D_a^{(4,3)} \equiv \left(\frac{a}{2}-1\right)^3 a^4 \frac{\mathrm{d}^4}{\mathrm{d}a^4} + p_3 \left(\frac{a}{2}-1\right)^2 a^3 \frac{\mathrm{d}^3}{\mathrm{d}a^3} + p_2 \left(\frac{a}{2}-1\right) a^2 \frac{\mathrm{d}^2}{\mathrm{d}a^2} + p_1 a \frac{\mathrm{d}}{\mathrm{d}a} + p_0 \,. \end{aligned} \tag{2.59}$$

The polynomials $p_0, \ldots, p_3$ used by `PyCFTBoot` are the ones in [89] except with a slight change: they are written with $\frac{a}{2}$ in place of $z$ and multiplied by 8 to force as many coefficients as possible to still be integers. Differentiating (2.59), a fifth derivative of $g_{\Delta,\ell}^{\Delta_{12},\Delta_{34}}$ becomes the highest order term. However, the lowest order term continues to be a zeroth derivative. Because $p_0(a)$ has degree 3, our equation only stops having non-derivative terms once it goes up to $\frac{\mathrm{d}^8 g_{\Delta,\ell}}{\mathrm{d}a^8}$. This means that the $m^{\text{th}}$ diagonal derivative is calculated from the $\min(m,7)$ lower ones using a handful of simple polynomials. One only needs $m$ to be at least 4 in order to start this process. Because of this, vectors in the slow original recursion (2.51) only need to fit four $\partial_r$ powers. Once the $a$ derivatives are known, more recurrence relations determine the $b$ derivatives. Defining $S = -\frac{1}{2}(\Delta_{12} - \Delta_{34})$ and $P = -\frac{1}{2}\Delta_{12}\Delta_{34}$, we use

$$\begin{aligned} &2(1-2n-2\nu)\frac{\partial^{m+n} g_{\Delta,\ell}}{\partial a^m \partial b^n} = \\ &2m(1-2n-2\nu)\left[-\frac{\partial^{m+n-1} g_{\Delta,\ell}}{\partial a^{m-1}\partial b^n} + (m-1)\frac{\partial^{m+n-2} g_{\Delta,\ell}}{\partial a^{m-2}\partial b^n} + (m-1)(m-2)\frac{\partial^{m+n-3} g_{\Delta,\ell}}{\partial a^{m-3}\partial b^n}\right] \\ &+\frac{\partial^{m+n+1} g_{\Delta,\ell}}{\partial a^{m+2}\partial b^{n-1}} - (6-m-4n+2\nu+2S)\frac{\partial^{m+n} g_{\Delta,\ell}}{\partial a^{m+1}\partial b^{n-1}} \\ &-\big[4c_2 + m^2 + 8mn - 5m + 4n^2 - 2n - 2 \\ &-4\nu(1-m-n) + 4S(m+2n-2) + 2P\big]\frac{\partial^{m+n-1} g_{\Delta,\ell}}{\partial a^m \partial b^{n-1}} \\ &-m\big[m^2 + 12mn - 13m + 12n^2 - 34n + 22 \\ &-2\nu(2n-m-1) + 2S(m+4n-5) + 2P\big]\frac{\partial^{m+n-2} g_{\Delta,\ell}}{\partial a^{m-1}\partial b^{n-1}} \\ &+(1-n)\left[\frac{\partial^{m+n} g_{\Delta,\ell}}{\partial a^{m+2}\partial b^{n-2}} - (6-3m-4n+2\nu-2S)\frac{\partial^{m+n-1} g_{\Delta,\ell}}{\partial a^{m+1}\partial b^{n-2}}\right] . \end{aligned} \tag{2.60}$$

This is the transverse derivative recursion found in [23] generalized to unequal external dimensions with the different definition of $c_2$ taken into account. It follows from going back to the original Casimir PDE (3.15) in the $(a, b)$ co-ordinates. The same coefficients can also be found in recent versions of the [76] source code. The form of (2.60) tells us the shape that will be taken by a lattice of derivatives we compute this way. When we make $m$ as high as possible for a given $n$, the right-hand side shows that 2 must be added to reach the highest possible $m$ for $n-1$. This leads to the triangle

$$\begin{aligned} n &\in \{0, \ldots, n_{\max}\} \\ m &\in \{0, \ldots, 2(n_{\max} - n) + m_{\max}\} , \end{aligned} \tag{2.61}$$

depending on two user-defined parameters. As found in [90], a high $n_{\max}$ is more important than a high $m_{\max}$. An obvious point worth remembering is that (2.59) and (2.60) are only satisfied by exact conformal blocks, not their rational approximations. As a result, these recursions are only valid for computing derivatives if $k_{\max}$ is sufficiently large.

Returning to the task of convolution, we need to compute derivatives of

$$F_{\pm,\Delta,\ell}(a,b) = \left(\frac{(2-a)^2 - b}{4}\right)^{\Delta_\phi} g_{\Delta,\ell}^{\Delta_{12},\Delta_{34}}(a,b) \pm \left(\frac{a^2-b}{4}\right)^{\Delta_\phi} g_{\Delta,\ell}^{\Delta_{12},\Delta_{34}}(2-a,b) , \tag{2.62}$$

at $(a_*, b_*) = (1, 0)$. We may immediately see that only one of the two terms in (4.155) needs to be differentiated. If the number of $a$ derivatives is even (odd), the other term will contribute equally (oppositely) for $F_{+,\Delta,\ell}$ and oppositely (equally) for $F_{-,\Delta,\ell}$. We therefore reduce one vector of derivatives to another vector of derivatives having roughly half the size. As in the unconvolved case, its components have the positive-times polynomial form. Knowing that $\Delta_\phi$ will eventually be determined by the external dimensions $\Delta_i, \Delta_j, \Delta_k, \Delta_l$, we write

$$\frac{\partial^{m+n}}{\partial a^m \partial b^n} F_{\pm,\Delta,\ell}^{ij;kl}(a_*, b_*) = \chi_\ell(\Delta) P_{\pm,\ell}^{ij;kl;mn}(\Delta) . \tag{2.63}$$

The linear combinations we need to take in order to compute these polynomials are known in closed form. For the following calculation, it is easiest to take all of the $b$ derivatives first

and then set $b = 0$. This allows us to treat all terms as being linear in $a$.

$$\begin{aligned}
\frac{\partial^{m+n}}{\partial a^m \partial b^n}\left(\frac{(2-a)^2-b}{4}\right)^{\Delta_\phi} g_{\Delta,\ell} &= \sum_{i=0}^{m}\sum_{j=0}^{n}\binom{m}{i}\binom{n}{j}\frac{\partial^{i+j}}{\partial a^i \partial b^j}\left(\frac{(2-a)^2-b}{4}\right)^{\Delta_\phi}\frac{\partial^{m+n-i-j} g_{\Delta,\ell}}{\partial a^{m-i}\partial b^{n-j}} \\
&\to \sum_{i=0}^{m}\sum_{j=0}^{n}\binom{m}{i}\binom{n}{j}\left(\frac{1}{4}\right)^j (-\Delta_\phi)_j \qquad (2.64) \\
&\frac{\partial^i}{\partial a^i}\left(1-\frac{a}{2}\right)^{2\Delta_\phi-2j}\frac{\partial^{m+n-i-j} g_{\Delta,\ell}}{\partial a^{m-i}\partial b^{n-j}} \\
&= \sum_{i=0}^{m}\sum_{j=0}^{n}\binom{m}{i}\binom{n}{j}\left(\frac{1}{4}\right)^j\left(\frac{1}{2}\right)^i (-\Delta_\phi)_j\,(2j-2\Delta_\phi)_i \\
&\left(1-\frac{a}{2}\right)^{2\Delta_\phi-2j-i}\frac{\partial^{m+n-i-j} g_{\Delta,\ell}}{\partial a^{m-i}\partial b^{n-j}} \\
&\to \sum_{i=0}^{m}\sum_{j=0}^{n}\binom{m}{i}\binom{n}{j}\left(\frac{1}{4}\right)^{\Delta_\phi}(-\Delta_\phi)_j\,(2j-2\Delta_\phi)_i\frac{\partial^{m+n-i-j} g_{\Delta,\ell}}{\partial a^{m-i}\partial b^{n-j}}
\end{aligned}$$

We may summarize by saying that the input parameters $d, k_{\max}, \ell_{\max}, m_{\max}, n_{\max}, \Delta_{12}, \Delta_{34}$ are used to prepare a conformal bootstrap environment.

Significant work has been invested into generalizing the above methods to correlators that involve external spin. It is always possible, though sometimes tedious, to construct the necessary blocks by acting with weight-shifting operators that change internal and external representations [91]. More direct methods, based on recursions, are in development with [92, 93] being the state of the art.

### 2.2.2 Semidefinite programming

Semidefinite programming has appeared in all efficient implementations of the non-identical numerical bootstrap, *i.e.* demanding that crossing symmetry and unitarity hold for the four-point function:

$$\langle\phi_i(x_1)\phi_j(x_2)\phi_k(x_3)\phi_l(x_4)\rangle = \left(\frac{|x_{24}|}{|x_{14}|}\right)^{\Delta_{ij}}\left(\frac{|x_{14}|}{|x_{13}|}\right)^{\Delta_{kl}}\frac{\sum_{\mathcal{O}}\lambda_{ij\mathcal{O}}\lambda_{kl\mathcal{O}}g_{\mathcal{O}}^{\Delta_{ij},\Delta_{kl}}(u,v)}{|x_{12}|^{\Delta_i+\Delta_j}|x_{34}|^{\Delta_k+\Delta_l}}\,. \qquad (2.65)$$

The conformal blocks $g_{\mathcal{O}}^{\Delta_{ij},\Delta_{kl}}(u,v)$ are functions of the cross-ratios $u = \frac{x_{12}^2 x_{34}^2}{x_{13}^2 x_{24}^2}$ and $v = \frac{x_{14}^2 x_{23}^2}{x_{13}^2 x_{24}^2}$. Invariance under $(1,i) \leftrightarrow (3,k)$, which relates two channels of crossing symmetry, leads to

the following sum rule [78].

$$\sum_{\mathcal{O}} \left[\lambda_{ij\mathcal{O}}\lambda_{kl\mathcal{O}}F^{ij;kl}_{\mp,\mathcal{O}}(u,v) \pm \lambda_{kj\mathcal{O}}\lambda_{il\mathcal{O}}F^{kj;il}_{\mp,\mathcal{O}}(u,v)\right] = 0 \tag{2.66}$$
$$F^{ij;kl}_{\pm,\mathcal{O}} \equiv v^{\frac{\Delta_k+\Delta_j}{2}} g^{\Delta_{ij},\Delta_{kl}}_{\mathcal{O}}(u,v) \pm u^{\frac{\Delta_k+\Delta_j}{2}} g^{\Delta_{ij},\Delta_{kl}}_{\mathcal{O}}(v,u)$$

To apply this rule, we choose an odd scalar $\sigma$ and an even scalar $\epsilon$ and let our external operators run over all admissible combinations of these. Using $\lambda_{\sigma\epsilon\mathcal{O}} = (-1)^\ell \lambda_{\epsilon\sigma\mathcal{O}}$, this yields

$$\sum_{\mathcal{O},2|\ell} \left(\lambda_{\sigma\sigma\mathcal{O}}\ \lambda_{\epsilon\epsilon\mathcal{O}}\right) V_{+,\Delta,\ell} \begin{pmatrix} \lambda_{\sigma\sigma\mathcal{O}} \\ \lambda_{\epsilon\epsilon\mathcal{O}} \end{pmatrix} + \sum_{\mathcal{O}} \lambda^2_{\sigma\epsilon\mathcal{O}} V_{-,\Delta,\ell} = 0 \tag{2.67}$$

where

$$V_{+,\Delta,\ell} = \begin{bmatrix} \begin{pmatrix} F^{\sigma\sigma;\sigma\sigma}_{-,\Delta,\ell} & 0 \\ 0 & 0 \end{pmatrix} \\ \begin{pmatrix} 0 & 0 \\ 0 & F^{\epsilon\epsilon;\epsilon\epsilon}_{-,\Delta,\ell} \end{pmatrix} \\ \begin{pmatrix} 0 & 0 \\ 0 & 0 \end{pmatrix} \\ \begin{pmatrix} 0 & \frac{1}{2}F^{\sigma\sigma;\epsilon\epsilon}_{-,\Delta,\ell} \\ \frac{1}{2}F^{\sigma\sigma;\epsilon\epsilon}_{-,\Delta,\ell} & 0 \end{pmatrix} \\ \begin{pmatrix} 0 & \frac{1}{2}F^{\sigma\sigma;\epsilon\epsilon}_{+,\Delta,\ell} \\ \frac{1}{2}F^{\sigma\sigma;\epsilon\epsilon}_{+,\Delta,\ell} & 0 \end{pmatrix} \end{bmatrix}, \quad V_{-,\Delta,\ell} = \begin{bmatrix} 0 \\ 0 \\ F^{\sigma\epsilon;\sigma\epsilon}_{-,\Delta,\ell} \\ (-1)^\ell F^{\epsilon\sigma;\sigma\epsilon}_{-,\Delta,\ell} \\ -(-1)^\ell F^{\epsilon\sigma;\sigma\epsilon}_{+,\Delta,\ell} \end{bmatrix}. \tag{2.68}$$

In ruling out solutions to (2.67), which is a set of five functional equations, we must approximate each row as a finite-dimensional vector. The standard way to do this is to expand around the point $(z,\bar{z}) = \left(\frac{1}{2},\frac{1}{2}\right)$. We may either take derivatives with respect to $z$ and $\bar{z}$ directly, or the diagonal / off-diagonal variables $a = z+\bar{z}, b = (z-\bar{z})^2$ [90]. We choose $(a,b)$ and control the order of our derivatives $\frac{\partial^{m+n} g_{\Delta,\ell}}{\partial a^m \partial b^n}$ with two parameters $m_{\text{max}}$ and $n_{\text{max}}$:

$$\begin{aligned} n &\in \{0,\ldots,n_{\text{max}}\} \\ m &\in \{0,\ldots,2(n_{\text{max}}-n)+m_{\text{max}}\}\,. \end{aligned} \tag{2.69}$$

Since half of the derivatives vanish when our conformal blocks are added or subtracted, the resulting number of components is

$$N = \lfloor (n_{\text{max}}+1)(m_{\text{max}}+n_{\text{max}}+1)/2 \rfloor\,. \tag{2.70}$$

There are two additional parameters needed to turn (2.67) into a concrete bootstrapping problem. One is a cutoff on the number of spins, which we call $\ell_{\text{max}}$. The other is the

accuracy parameter for a single conformal block, which we call $k_{\text{max}}$. This controls how many poles from the triple series

$$\begin{array}{ll} \Delta_1(\ell) = 1 - \ell - k & k = 1, 2, \dots \\ \Delta_2(\ell) = \frac{d}{2} - k & k = 1, 2, \dots \\ \Delta_3(\ell) = d - 1 + \ell - k & k = 1, 2, \dots, \ell \end{array} \tag{2.71}$$

appear in the function

$$\begin{aligned} \chi_\ell(\Delta) &= \frac{r_*^\Delta}{\Pi_i(\Delta - \Delta_i(\ell))} \\ r_* &\equiv 3 - 2\sqrt{2}\,. \end{aligned} \tag{2.72}$$

As explained previously, and in [78, 84, 89], there are algorithms for explicitly constructing each conformal block derivative as a rational approximation:

$$\frac{\partial^{m+n}}{\partial a^m \partial b^n} F^{ij;kl}_{\pm,\Delta,\ell}(a = 1, b = 0) = \chi_\ell(\Delta) P^{ij;kl;mn}_{\pm,\ell}(\Delta)\,. \tag{2.73}$$

Here, $P^{ij;kl;mn}_{\pm,\ell}$ is a polynomial with the same degree as $\chi_\ell$ for $m = n = 0$. Its degree goes up by one whenever the derivative order is increased. The task of inputting $(k_{\text{max}}, \ell_{\text{max}}, m_{\text{max}}, n_{\text{max}})$ and computing a table suitable for approximating (2.67) is typically accomplished with a frontend to `SDPB`.

With the truncations described above, problems of this form are tractable with semidefinite programming [77]. In the dual formulation, one wishes to find a linear functional $\mathbf{y}$ which sends each term of (2.67) to a positive-definite matrix, thereby certifying that no solution to crossing symmetry exists. For illustrative purposes, we consider a single correlator problem which allows us to drop the $ij;kl$ and $\pm$ labels on $P^{ij;kl;mn}_{\pm,\ell}$. We will also drop $mn$ through our understanding that $\mathbf{P}_\ell$ is a vector with components $P^i_\ell$. If we single out the contribution of the identity operator as $\mathbf{n}$, we arrive at the polynomial matrix program (PMP) where we include an objective $\mathbf{b}$ for generality.

$$\begin{aligned} &\text{maximize } \mathbf{b}^{\mathrm{T}}\mathbf{y} \text{ over } \mathbf{n}^{\mathrm{T}}\mathbf{y} = 1 \\ &\text{such that } \mathbf{P}_\ell(\Delta)^{\mathrm{T}}\mathbf{y} \geq 0 \text{ for all } \ell \leq \ell_{\text{max}}, \Delta \geq \Delta_{\text{min}} \end{aligned} \tag{2.74}$$

After all, the crossing equation

$$\sum_{k,\ell} \lambda^2_{k,\ell} \mathbf{P}_\ell(\Delta_k) = \mathbf{n} \tag{2.75}$$

becomes a contradiction when $\mathbf{y}$ solving the above conditions is applied to both sides. If we

reshuffle each vector according to

$$\begin{aligned}\tilde{P}^0_\ell &= \frac{1}{n^0}P^0_\ell \\ \tilde{P}^i_\ell &= P^i_\ell - \frac{n^i}{n^0}P^0_\ell\,,\end{aligned} \tag{2.76}$$

dotting $\mathbf{P}_\ell$ with a functional whose action on $\mathbf{n}$ is 1 becomes the same as dotting $\tilde{\mathbf{P}}_\ell$ with a functional whose leading component is 1. This is precisely the choice to work with crossing equations projectively as (2.75) becomes

$$\sum_{k,\ell}\lambda^2_{k,\ell}\begin{bmatrix}\tilde{P}^0_\ell(\Delta_k)\\ \tilde{P}^i_\ell(\Delta_k)\end{bmatrix} = \begin{bmatrix}1\\0\end{bmatrix} \tag{2.77}$$

after reshuffling both sides. Any spectrum satisfying the bottom row can automatically be made to satisfy the top row through a rescaling. From now on, we will denote the polynomial vector in the bottom row of (2.77) by $\mathbf{P}_\ell$ to rewrite the PMP.

$$\begin{aligned}&\text{maximize } \mathbf{b}^{\mathrm{T}}\mathbf{y}\\ &\text{such that } P^0_\ell(x) + \mathbf{P}_\ell(x)^{\mathrm{T}}\mathbf{y} \geq 0 \text{ for all } \ell \leq \ell_{\max}, x \geq 0\end{aligned} \tag{2.78}$$

Here, $x = \Delta - \Delta_{\min}$. To solve this type of problem efficiently, we use the program `SDPB` [77]. Because we will see an alternative choice shortly, we briefly review the process by which `SDPB` translates (2.78) into a semidefinite program (SDP).

Positivity of $P^0_\ell(x) + \mathbf{P}_\ell(x)^{\mathrm{T}}\mathbf{y}$ on the half-line is equivalent to the requirement that it be equal to

$$\mathrm{Tr}\left(\begin{bmatrix}\mathbf{q}_\ell(x)\mathbf{q}^{\mathrm{T}}_\ell(x) & 0\\ 0 & x\mathbf{q}_\ell(x)\mathbf{q}^{\mathrm{T}}_\ell(x)\end{bmatrix}Y_\ell\right) \tag{2.79}$$

where $Y_\ell$ is positive-definite and $\mathbf{q}_\ell$ is a vector of orthogonal polynomials. We have abused notation slightly since the maximum power of $x$ that (2.79) needs to express may be even or odd. Because of this, the first $\mathbf{q}_\ell$ might have one more component than the second $\mathbf{q}_\ell$. It is sufficient to demand this equality on a set of sample points which we denote $x_k$. It is also possible to combine all $Y_{(k,\ell)}$ into a single matrix $Y$. Making the identifications

$$\begin{aligned}A_{(k,\ell)} &= \mathrm{diag}\left(0,\ldots,0,\begin{bmatrix}\mathbf{q}_\ell(x_k)\mathbf{q}^{\mathrm{T}}_\ell(x_k) & 0\\ 0 & x_k\mathbf{q}_\ell(x_k)\mathbf{q}^{\mathrm{T}}_\ell(x_k)\end{bmatrix},0,\ldots,0\right)\\ B_{(k,\ell),i} &= -P^i_\ell(x_k)\\ c_{(k,\ell)} &= P^0_\ell(x_k)\\ C &= 0\,,\end{aligned} \tag{2.80}$$

(2.78) becomes

$$\begin{aligned} &\text{maximize } \mathrm{Tr}(CY) + \mathbf{b}^{\mathrm{T}}\mathbf{y} \text{ over } Y \succeq 0 \\ &\text{such that } \mathrm{Tr}(A_* Y) + B\mathbf{y} = \mathbf{c}. \end{aligned} \tag{2.81}$$

In the numerical bootstrap, (2.81) and the primal problem corresponding to it are typically solved together, in order to see which one becomes feasible first [77].

### 2.2.3 The extremal functional method

It was shown in [90] that solutions to crossing symmetry may be built by locating the zeros of $\mathbf{y}$. This functional may be found either by ruling out CFTs just outside the allowed region or by maximizing an OPE coefficient just inside it. Ideally, elements of the spin-$\ell$ spectrum are dimensions $\Delta_k$ such that

$$\det\left(\mathbf{y}^{\mathrm{T}}\begin{bmatrix} (\mathbf{P}_\ell(\Delta_k))_{0,0} & \cdots & (\mathbf{P}_\ell(\Delta_k))_{0,n} \\ \vdots & \ddots & \vdots \\ (\mathbf{P}_\ell(\Delta_k))_{n,0} & \cdots & (\mathbf{P}_\ell(\Delta_k))_{n,n} \end{bmatrix}\right) = 0 \tag{2.82}$$

where $\mathbf{P}_\ell$ is one of the polynomial vectors appearing in (2.73). On the other hand, we have to worry about numerical errors.

Since $\mathbf{y}$ is defined by its positivity on a continuum of conformal blocks, all but one scaling dimension satisfying (2.82) will be second-order. The unique zero where the functional changes sign is the maximal allowed value of the gap. In other words, a functional that has not converged perfectly will not just have zeros in the wrong places. It will give rise to a polynomial that never reaches zero for real $\Delta$. Such a functional (which provides a valid bootstrap bound, but not the best one possible) forces us to relax the condition (2.82).

There are two approaches, both based on the `spectrum.py` script [94], which make it easy to account for this. The first is to run the script as written after spending several iterations to bring the primal and dual solutions close together. A highly converged functional is needed since `spectrum.py` assumes that the would-be zeros are close to the local minima of (2.82) which uses only the polynomial numerator. The second is to modify the script to use a non-polynomial function minimizer, allowing us to multiply (2.82) by the prefactor $\chi_\ell$ from (2.73). The advantage is that when $\mathbf{y}$ acts on a full convolved block, the local minima are closer to the physical $\Delta_k$. As a result, punishing `SDPB` parameters are no longer required. We have typically used the first approach and specified

```
--precision=660
--dualityGapThreshold=1e-75
```

as the non-default parameters. The rest of the script obtains high precision OPE coefficients

directly from the primal solution.[7]

The systematic use of the non-identical extremal functional method in [94] has revealed a surprising fact about generic interacting CFTs — they are still quite similar to free CFTs! To explain further, free (or holographic) CFTs start with a single-twist primary $\phi$ and define double-twist primaries (like $\phi^2$) as the ones that appear in $\phi \times \phi$. Quadruple-twist primaries (like $\phi^4$) certainly exist, just not in $\phi \times \phi$. One has to look at a double-twist OPE such as $\phi^2 \times \phi^2$ in order to find them. Even though OPE coefficients like $\lambda_{\phi\phi\phi^4}$, that are allowed by selection rules, clearly turn on in a generic interacting CFT, the results from the 3D Ising model suggest that the hierarchy among them is maintained [94]. This leads to OPE coefficients that are small enough that the numerical bootstrap cannot see them.[8] Several operators that $\langle\sigma\sigma\sigma\sigma\rangle$ alone cannot see become visible once $\langle\epsilon\epsilon\epsilon\epsilon\rangle$ is considered. It is also likely that many more operators (which technically appear in $\sigma \times \sigma$ and $\epsilon \times \epsilon$) would need an even larger correlator system to become numerically detectable. We have emphasized that this is the case for *generic* interacting CFTs because there are some 2D CFTs with a higher spin symmetry that do not run into this problem [90]. The similarity with the genericity assumption in the analytic bootstrap is almost certainly not a coincidence [36, 37]. CFTs with infinitely many minimal-twist operators are special while CFTs posessing a twist gap take on a mean-field spectral density at large spin. The suppressed effect of multi-twist operators in the numerical bootstrap can be interpreted as the statement that these asymptotic results continue to be a good approximation at small dimension and spin [38, 39].

These considerations become especially important when one attempts to find multi-twist operators through an older method which minimizes the error in a set of crossing equations with known scaling dimensions.[9] This method, which uses the dual solution for everything, was examined in [98] as a potential way to learn about multi-correlator OPE coefficients from a single correlator. Again, it was found to be ineffective for theories without a higher spin symmetry. Let us summarize the results below.

Once a set of $Z$ stable operators has been found, we may consider a truncated crossing equation of the form

$$\sum_{k=1}^{Z} a_k \mathbf{F}_k = \mathbf{n} \ . \tag{2.83}$$

[7] For an implementation with linear programming, see [95]. The semidefinite programming version first appeared in [35] which uses opposite conventions for what the primal and dual problems are.

[8] Comparisons to [96] have been suggested as this might depend on the algorithm to a certain extent.

[9] An analogous approach to the severely truncated bootstrap — fitting operator dimensions and OPE coefficients at the same time — was recently explored in [97].

When studying a single correlator involving $\mathbb{Z}_2$-even operators, we make the identifications

$$\begin{aligned} a_k &= \lambda^2_{\phi\phi\mathcal{O}_k} \\ \mathbf{F}_k &= \mathbf{F}^{\phi\phi;\phi\phi}_{-,\Delta_k,\ell_k} \\ \mathbf{n} &= -\mathbf{F}^{\phi\phi;\phi\phi}_{-,0,0} \ . \end{aligned} \tag{2.84}$$

The point is that $\phi$ may denote $\sigma$, $\epsilon$ or indeed any scalar whose self-OPE is well approximated by the $Z$ operators in our set. We regard (2.83) as a set of $N > Z$ linear equations with $N$ given by (2.70). A naive approach is to remove rows corresponding to high derivatives bringing the number of equations down to $Z$. This often leads to $a_k$ coefficients that are negative, even when we use dimensions that are accurate to four digits. To overcome this, we follow [90] and leave one extra equation so that $N = Z + 1$. With this overdetermined system, we will not be able to find $a_k$ that satisfy (2.83) exactly. Rather, we find the $a_k$ that minimize the distance between the left and right sides of (2.83). In this fit, the constraint $a_k \geq 0$ may be specified by hand. If our norm for this is the 1-norm, it is convenient to introduce a vector of positive entries $\mathbf{t}$ such that

$$\begin{aligned} -\mathbf{t} \leq \mathbf{n} - \sum_{k=1}^{Z} a_k \mathbf{F}_k \leq \mathbf{t} \\ \left\| \mathbf{n} - \sum_{k=1}^{Z} a_k \mathbf{F}_k \right\| \leq \sum_{k=1}^{Z+1} t_k \ . \end{aligned} \tag{2.85}$$

We may now concatenate $\mathbf{t}$ and $\mathbf{a}$ into a vector $\mathbf{y}$ and recognize that the norm (2.85) is $\mathbf{b}^{\mathrm{T}}\mathbf{y}$ with the objective $\mathbf{b}^{\mathrm{T}} = [1, \ldots, 1, 0, \ldots, 0]$. Under the identifications

$$\begin{aligned} B &= \begin{bmatrix} -I_{Z+1} & \mathbf{F}_1 & \ldots & \mathbf{F}_Z \\ -I_{Z+1} & -\mathbf{F}_1 & \ldots & -\mathbf{F}_Z \end{bmatrix} \\ \mathbf{c} &= \begin{bmatrix} \mathbf{n} \\ -\mathbf{n} \end{bmatrix} , \end{aligned} \tag{2.86}$$

this becomes the linear program (LP):

$$\begin{aligned} &\text{minimize } \mathbf{b}^{\mathrm{T}}\mathbf{y} \text{ over } \mathbf{y} \geq 0 \\ &\text{such that } B\mathbf{y} \leq \mathbf{c}. \end{aligned} \tag{2.87}$$

It is amusing to point out that a reader using `SDPB` may continue to use it for solving (2.87) because every linear program is also a semidefinite program. To do this, the $(2Z+2)\times(2Z+1)$ and $(2Z+2)\times 1$ matrices $B$ and $\mathbf{c}$ must be enlarged to $(4Z+3)\times(2Z+1)$ and $(4Z+3)\times 1$ so that they encode component-wise positivity of $\mathbf{y}$ in addition to (2.85). The next necessary

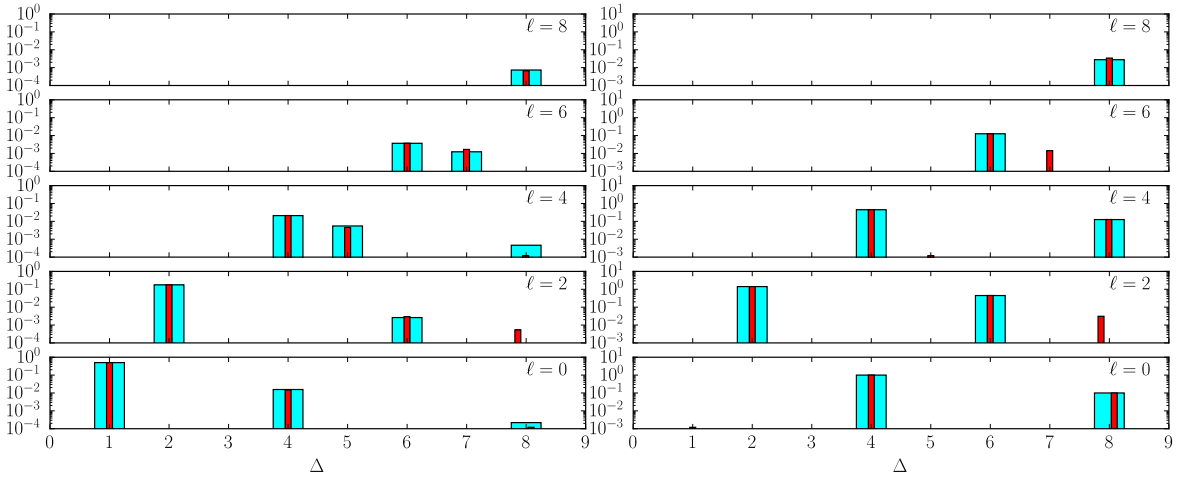


(a) $|\lambda_{\sigma\sigma\mathcal{O}}|$ comparison (b) $|\lambda_{\epsilon\epsilon\mathcal{O}}|$ comparison

Figure 2.5: OPE coefficients in the 2D Ising model for operators with $\Delta \leq 8$. Wide blue bars show exact values and narrow red bars show estimates from the fit used in [90].

step is replacing $\mathbf{b}$ with $-\mathbf{b}$ (and prepending an arbitrary number) as `SDPB`'s objective is maximized instead of minimized. Finally, the orthogonal polynomials should all be 1. With this choice, constraint matrices in (2.81) simply pull off a diagonal component of $Y$ and $\mathbf{c} - B\mathbf{y} = \mathrm{Tr}(A_* Y)$ reads $\mathbf{c} - B\mathbf{y} \geq 0$. In any case, whether (2.87) is solved as an LP or SDP, it is clear that the returned $\mathbf{y}$ will give us the OPE coefficients $\lambda^2_{\phi\phi\mathcal{O}_k}$.

To verify that this gives reliable values for $a_k$ in two dimensions, we have compared exact and approximate results in the Ising model where $\epsilon \times \epsilon$ operators are also in $\sigma \times \sigma$. Starting with $\Delta_\phi = \Delta_\sigma$, the $\lambda^2_{\sigma\sigma\mathcal{O}}$ coefficients are very close to the ones found in [90]. Changing the external dimension to $\Delta_\phi = \Delta_\epsilon$, the same algorithm produces accurate $\lambda^2_{\epsilon\epsilon\mathcal{O}}$ coefficients as well. These are shown in Figure 2.5.

Turning to three dimensions, exact Ising CFT data are not available, but the tables in [94] have negligible error for our purposes. Despite all the progress in isolating this model, it appears that several spin-$\ell$ operators are still missing from these spectra: the ones that do not fall into $[\sigma\sigma]_n$, $[\epsilon\epsilon]_n$ and $[\sigma\epsilon]_n$ twist families. As evidence of this, Figure 2.6 shows that OPE coefficients fit with the dual method differ greatly from the ones returned by `spectrum.py`. To guess where the first missing operator appears, we can take the naive view that twist families exist all the way down to $\ell = 0$. Constructing one out of an irrelevant operator $\Phi$, we have $\Delta \approx 2\Delta_\Phi + 2n + \ell > 2d$. Four-point functions approximated by bootstrap data have already proven useful for conformal perturbation theory and measuring non-Gaussianity [99, 100]. As it is significantly affected by the incompleteness of the spectrum above $\Delta_* \approx 2d$, a fit to the crossing equations must be a less forgiving problem.

Although we have not done so yet, it should also be possible to fit mixed OPE coefficients

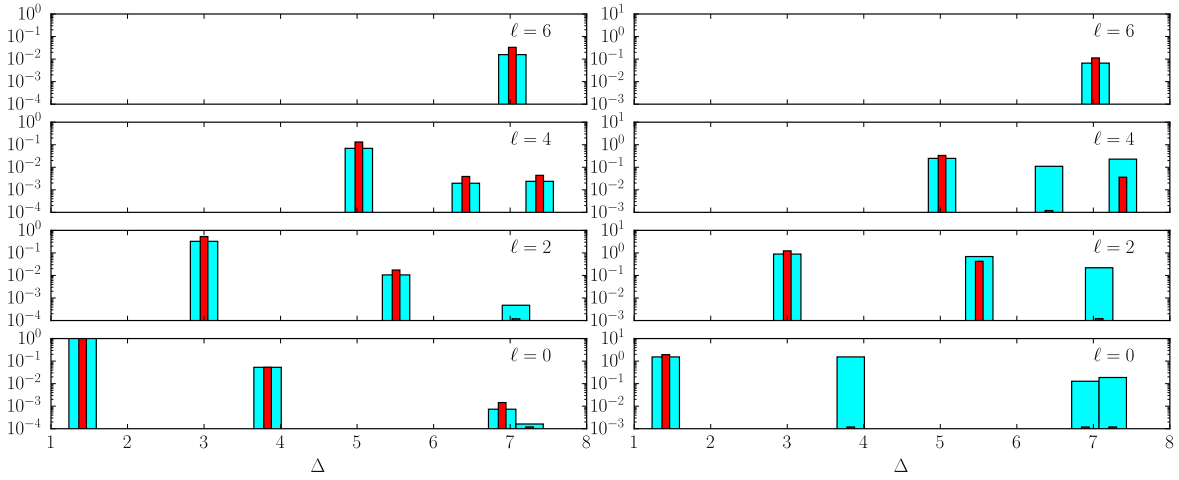


(a) $|\lambda_{\sigma\sigma\mathcal{O}}|$ comparison (b) $|\lambda_{\epsilon\epsilon\mathcal{O}}|$ comparison

Figure 2.6: The analogue of Figure 2.5 for the 3D Ising model. In the fit, we have used the $\mathbb{Z}_2$-even operator dimensions from [94]. This is already a longer list than anything that is likely to come from a one-correlator bootstrap. Due to a remaining bias in the spectrum, there is strong disagreement between the primal and dual methods.

in a 2D theory. The last two rows of (2.67) would lead to coupled quadratic equations which rapidly become impractical to solve as our system grows. Therefore, we will focus on the third row. If only the identity has been singled out, this is a homogenous equation and its parameters are ambiguous up to a rescaling. This is why it helps to find OPE coefficients in a prescribed order. As long as $\lambda_{\phi\phi\phi^2}$ has been found from the $\phi \times \phi$ fit described above, permutation symmetry of this coefficient may be used to make our equation inhomogeneous. In this case, it takes the form of (2.83) but now with

$$\begin{aligned} a_k &= \lambda^2_{\phi\phi^2\mathcal{O}_k} \\ \mathbf{F}_k &= \mathbf{F}^{\phi\phi^2;\phi\phi^2}_{-,\Delta_k,\ell_k} \\ \mathbf{n} &= -\lambda^2_{\phi\phi^2\phi}\mathbf{F}^{\phi\phi^2;\phi\phi^2}_{-,\Delta_\phi,0} \ . \end{aligned} \tag{2.88}$$

Essentially, $\phi$ plays the same role that the identity operator played before.

## 2.3 One and two dimensions

To complete Table 2.1, we should consider a superalgebra, or a pair of two superalgebras, from the following list: $\mathfrak{osp}(\mathcal{N}|2)$, $\mathfrak{su}(\mathcal{N}|1,1)$, $\mathfrak{osp}(4^*|2\mathcal{N})$, $\mathfrak{g}(3)$, $\mathfrak{f}_0(4)$ and $\mathfrak{d}_0(1,2,\alpha)$. These enable the construction of superconformal quantum mechanics in one dimension. Such theories are

nonlocal (by our favourite definition) since a traceless stress-energy tensor with a single component must be identically zero. Two-dimensional CFTs all have a supergroup given by $G \times \bar{G}$, associated to $\mathfrak{g}$ and $\bar{\mathfrak{g}}$ in the above list, but the appropriate conformal algebra is allowed to be much larger.

This is most easily seen by using complex co-ordinates $z = x + iy$ and $\bar{z} = x - iy$. In this notation, the Euclidean line element becomes

$$ds^2 = dx^2 + dy^2 = dz d\bar{z} \ . \tag{2.89}$$

It is clear that any holomorphic reparameterization of $z$, combined with any anti-holomorphic reparameterization of $\bar{z}$, will leave (2.89) invariant up to an overall factor. We therefore find a conformal algebra with Killing vectors $z^{n+1}\partial$ and $\bar{z}^{n+1}\bar{\partial}$ generated by $z^{n+1}T$ and $\bar{z}^{n+1}\bar{T}$ respectively. These operators, defined by

$$T = \frac{1}{4}\left(T_{11} - 2iT_{12} - T_{22}\right) \ , \ \bar{T} = \frac{1}{4}\left(T_{11} + 2iT_{12} - T_{22}\right) \ , \tag{2.90}$$

are the two independent components of $T_{\mu\nu}$ once symmetry and tracelessness are imposed. Conservation implies that $\bar{\partial}T = \partial\bar{T} = 0$, which also follows from the algebra. Holomorphic and anti-holomorphic weights, which dictate an operator's transformation properties, are defined by

$$h = \frac{\Delta + \ell}{2} \ , \ \bar{h} = \frac{\Delta - \ell}{2} \ , \tag{2.91}$$

and it is easy to see that one is always zero for $T$ and $\bar{T}$. Note that the spin $\ell$ is the only Cartan of the rotation group in two dimensions. The algebra generated by these vector fields (called the Witt algebra) centrally extends to

$$\begin{aligned} [L_m, L_n] &= (m-n)L_{m+n} + \frac{c}{12}m(m-1)(m+1)\delta_{m+n,0} \\ \left[\bar{L}_m, \bar{L}_n\right] &= (m-n)\bar{L}_{m+n} + \frac{c}{12}m(m-1)(m+1)\delta_{m+n,0} \end{aligned} \tag{2.92}$$

which will be all-important in this section. Known as the *Virasoro algebra*, (2.92) determines how infinitesimal transformations rescaling (2.89) are able to act on correlation functions. It appears as an enhancement of any $\mathfrak{sl}(2) \times \mathfrak{sl}(2)$ theory with a stress-energy tensor unless the strictly finite conformal invariance is achieved through the strange mechanism in (2.13).

The operator equations $\bar{\partial}J = \partial\bar{J} = 0$ can appear again for higher spin currents in this context since the conformal Coleman-Mandula theorem does not apply for $d = 2$. Even in purely Virasoro-symmetric CFTs, there are infinitely many conserved currents built from polynomials in $T$ and their derivatives. These have $\bar{h} = 0$ by definition, while $h$ must be an integer to allow single-valuedness of correlation functions. The OPE of such operators was

explicitly found to be

$$J_i(z)J_j(0) = \frac{\delta_{ij}}{z^{h_i+h_j}} + \sum_k \sum_{n=0}^{\infty} \frac{\lambda_{ijk}}{n!} \frac{(h_i - h_j + h_k)_n}{(2h_k)_n} \frac{\partial^n J_k(0)}{z^{h_i+h_j-h_k-n}} \tag{2.93}$$

in [101]. Currents of arbitrarily high spin *not* generated by $T$ are allowed in 2D CFT as well. An algebra generated by such currents is called a W-algebra to distinguish it from a Lie algebra. Generic examples differ from (2.92) in that charges appear nonlinearly in commutation relations. Although no complete classification is available, several W-algebra families, along with sporadic examples, have been found since the work of [102].

### 2.3.1 Exactly solvable theories

Rewriting general CFT results in the complex notation appropriate for this section is a straightforward exercise. Two-point functions and three-point functions become

$$\begin{aligned} \langle \mathcal{O}(z_1,\bar{z}_1)\mathcal{O}(z_2,\bar{z}_2)\rangle &= \frac{1}{z_{12}^{2h}\bar{z}_{12}^{2\bar{h}}} \\ \langle \mathcal{O}_1(z_1,\bar{z}_1)\mathcal{O}_2(z_2,\bar{z}_2)\mathcal{O}_3(z_3,\bar{z}_3)\rangle &= \frac{\lambda_{123}}{z_{12}^{h_1+h_2-h_3} z_{13}^{h_1+h_3-h_2} z_{23}^{h_2+h_3-h_1} \bar{z}_{12}^{\bar{h}_1+\bar{h}_2-\bar{h}_3} \bar{z}_{13}^{\bar{h}_1+\bar{h}_3-\bar{h}_2} \bar{z}_{23}^{\bar{h}_2+\bar{h}_3-\bar{h}_1}} \end{aligned} \tag{2.94}$$

which look somewhat more compact than (2.28) and (2.29). Also, we stress that (2.94) represents the most general three-point function of conformal primaries this time. There is a further notion of *Virasoro primary* which describes an operator annihilated by all Virasoro generators with a positive subscript. Our ability to construct a sensible theory by acting on these operators with $L_{-|n|}, \bar{L}_{-|n|}$ follows from the same unitarity logic as before. A powerful fact about the Virasoro algebra is that correlators of descendants may be obtained from the corresponding correlators of primaries, even when the charges being used to descend are more complicated than total derivatives.[10]

To see how this works, we should derive the singular OPE between the stress-energy tensor and a primary from

$$\delta\mathcal{O}(w,\bar{w}) = \frac{1}{2\pi i}\oint_w \left[\mathrm{d}z\epsilon(z)T(z)\mathcal{O}(w,\bar{w}) + \mathrm{d}\bar{z}\bar{\epsilon}(\bar{z})\bar{T}(\bar{z})\mathcal{O}(w,\bar{w})\right] \tag{2.95}$$

where the Killing vector this time is an arbitrary holomorphic vector field. To have consis-

[10] Having a larger algebra of spacetime charges generally increases the amount of information that can be extracted from a correlation function of primaries. However, there are sometimes descendant correlators that are not determined by the primaries of a higher W-algebra.

tency with the finite conformal transformation

$$\mathcal{O}'(z'\bar{z}') = \left(\frac{\partial z'}{\partial z}\right)^{h} \left(\frac{\partial \bar{z}'}{\partial \bar{z}}\right)^{\bar{h}} \mathcal{O}(z,\bar{z}) \ , \tag{2.96}$$

it must be the case that

$$\begin{aligned} T(z)\mathcal{O}(0) &= \frac{h\mathcal{O}(0)}{z^2} + \frac{\partial\mathcal{O}(0)}{z} \\ \bar{T}(\bar{z})\mathcal{O}(0) &= \frac{\bar{h}\mathcal{O}(0)}{\bar{z}^2} + \frac{\bar{\partial}\mathcal{O}(0)}{\bar{z}} \end{aligned} \tag{2.97}$$

up to regular terms. The other OPE we need is

$$\begin{aligned} T(z)T(0) &= \frac{c/2}{z^4} + \frac{2T(0)}{z^2} + \frac{\partial T(0)}{z} \\ \bar{T}(\bar{z})\bar{T}(0) &= \frac{\bar{c}/2}{\bar{z}^4} + \frac{2\bar{T}(0)}{\bar{z}^2} + \frac{\bar{\partial}\bar{T}(0)}{\bar{z}} \end{aligned} \tag{2.98}$$

which is more singular than (2.97) because the stress-energy tensor is not a Virasoro primary. It is in fact given by $T = L_{-2}I$. Nevertheless, (2.98) is easy to verify since it reproduces the commutation relations (2.92) once the charges are written as explicit modes

$$L_n = \oint \frac{\mathrm{d}z}{2\pi i} z^{n+1} T(z) \ , \quad \bar{L}_n = \oint \frac{\mathrm{d}\bar{z}}{2\pi i} \bar{z}^{n+1} \bar{T}(\bar{z}) \ . \tag{2.99}$$

Insertion of (2.99) into a correlation function with one descendant, for instance, yields the expression

$$\begin{aligned} &\left\langle L_{-m_1} \dots L_{-m_j} \mathcal{O}(z,\bar{z}) \mathcal{O}_1(z_1,\bar{z}_1) \dots \mathcal{O}_k(z_k,\bar{z}_k) \right\rangle = \frac{1}{(2\pi i)^j} \oint \frac{\mathrm{d}w_1}{w^{m_1-1}} \cdots \oint \frac{\mathrm{d}w_j}{w^{m_j-1}} \\ &\langle T(w_1) \dots T(w_j) \mathcal{O}(z,\bar{z}) \mathcal{O}_k(z_1,\bar{z}_1) \dots \mathcal{O}_k(z_k,\bar{z}_k) \rangle \end{aligned} \tag{2.100}$$

which can be computed by iterating (2.97) and (2.98). There is a very convenient property of these chiral OPEs when used inside contour integrals (which is sometimes confusingly referred to as a properties of OPEs in general). It is that the universal singular terms we have been able to deduce are enough to evaluate (2.100) through the residue theorem.

The other indispensable information about the Virasoro algebra is its representation theory. This is rich enough to reveal infinitely many interacting CFTs built solely from primary fields that have null descendants. The extension of (2.41) to the Virasoro case is simply $L_n^\dagger = L_{-n}$. As such, we should demand that representations have a positive

semidefinite Gram matrix for unitarity.

$$M = \begin{bmatrix} \langle h|h\rangle & 0 & 0 & 0 & \dots \\ 0 & \langle h|L_1L_{-1}|h\rangle & 0 & 0 & \dots \\ 0 & 0 & \langle h|L_1^2L_{-1}^2|h\rangle & \langle h|L_2L_{-1}^2|h\rangle & \dots \\ 0 & 0 & \langle h|L_1^2L_{-2}|h\,\rangle & \langle h|L_2L_{-2}|h\rangle & \dots \\ \vdots & \vdots & \vdots & \vdots & \ddots \end{bmatrix} \tag{2.101}$$

$$= \begin{bmatrix} 1 & 0 & 0 & 0 & \dots \\ 0 & 2h & 0 & 0 & \dots \\ 0 & 0 & 4h(1+2h) & 6h & \dots \\ 0 & 0 & 6h & 4h+\frac{c}{2} & \dots \\ \vdots & \vdots & \vdots & \vdots & \ddots \end{bmatrix}$$

Te determinant of the level-$l$ block, found by Kac in [103], is

$$\begin{aligned} \det M_l &= \alpha_l \prod_{rs\le l} [h - h_{r,s}(c)]^{p(l-rs)} \\ \alpha_l &= \prod_{rs\le l} [(2r)^s s!]^{p(l-rs)-p(l-rs-r)} \end{aligned} \tag{2.102}$$

where $p(n)$ is the number theoretic partition function. Its appearance is clear once we know that a state with weight $h_{r,s}(c)$ is null at level $rs$. The non-trivial part of the Kac determinant is the formula for the roots, which has the parameterization

$$c = 1 - \frac{6}{m(m+1)}\ ,\ h_{r,s} = \frac{[(m+1)r - ms]^2 - 1}{4m(m+1)}\ . \tag{2.103}$$

We will not prove (2.103) in this thesis but a singular vector expression used in (3.7) plays a role in the proof. By plotting (2.103) in the $(c,h)$ plane, we find that the curves where $\det M_l$ can change sign are all in the $c<1$ half-space. Representations on the other side are clearly unitary as the Gram matrix is diagonally dominant in the $c\to\infty$ limit. A detailed analysis in [104, 105] showed that all but countably many points with $c<1$ have at least one $p(l)\times p(l)$ block with a negative determinat. The only way to construct a unitary representation in this half-space is to choose a point where two $\det M_l = 0$ curves intersect ($m\in\mathbb{N}$), leading to states that are not just null at level $rs$ but null at level $(m-r)(m+1-s)$ as well.[11] Some work generalizing this to the W-algebra case was recently done in [106].

Let us consider a correlator with three primaries — one with a level-2 null, one with a

[11] These are in fact the *first intersections*. There are other points where the curves for two levels intersect that do not lead to unitary representations. This is because there is a third level for which these points lie strictly to the left.

level-$rs$ null and one that is to be determined. If we construct the linear combination of $L_{-1}^2$ and $L_{-2}$ that must annihilate this three-point function, we find only two possibilities for what the third weight must be.

$$\phi_{1,2} \times \phi_{r,s} = \phi_{r,s-1} + \phi_{r,s+1} \quad , \quad \phi_{2,1} \times \phi_{r,s} = \phi_{r-1,s} + \phi_{r+1,s} \tag{2.104}$$

Iterating (2.104) does not lead to primaries with arbitrarily large Kac indices because we have chosen to take $m \in \mathbb{N}$ (we relax this assumption in chapter 3). Once an index becomes large enough, the corresponding weight becomes equal to one we have already seen up to an integer multiple of $rs$ or $(m-r)(m+1-s)$. In other words, we get a closed OPE given by the ansatz

$$\phi_{r,s} \times \phi_{r',s'} = \sum_{k=0}^{\min\left(\left\lfloor \frac{r+r'-|r-r'|-2}{2} \right\rfloor, \left\lfloor \frac{2m-3-r-r'-|r-r'|}{2} \right\rfloor\right)} \sum_{l=0}^{\min\left(\left\lfloor \frac{s+s'-|s-s'|-2}{2} \right\rfloor, \left\lfloor \frac{2m-s-s'-|s-s'|}{2} \right\rfloor\right)} \phi_{|r-r'|+2k+1,|s-s'|+2l+1} \tag{2.105}$$

having only finitely many Virasoro primaries. Theories that can be constructed from finitely many primaries are referred to either as rational CFTs or minimal models for a particular chiral algebra.[12] In this case, the theories obeying (2.105) will be *Virasoro minimal models*. One way to get a consistent torus partition function (2.17) in a minimal model is to let every primary have equal weights $h$ and $\bar{h}$. These so-called diagonal minimal models for $m = 3, 4, 5, \ldots$ are properly called the Ising model, tricritical Ising model, tetracritical Ising model, *etc*. Many of them admit orbifolds that take us to a non-diagonal minimal model. The most famous example is an orbifold of the tetracritical Ising model called the 3-state Potts model. These models are solved by the bootstrap because the four-point functions

$$\langle \phi_{r_1,s_1}(0) \phi_{r_2,s_2}(z,\bar{z}) \phi_{r_3,s_3}(1) \phi_{r_4,s_4}(\infty) \rangle \tag{2.106}$$

may be expanded into finitely many Virasoro blocks. These blocks do not have to be computed with a tedious OPE sum because there is always a differential operator annihilating (2.106). Once the appropriate differential operator is constructed with the Virasoro Ward identity, the Virasoro blocks in question form a basis of solutions where each one has a different leading behaviour. This is usually illustrated with differential operators that happen to be second-order leading to hypergeomeric solutions. The constraint of crossing symmetry

[12] We do not know why the parlance developed in this way. It would be just as correct to say that minimal CFTs are rational models for a particular chiral algebra.

pins down their coefficients after using relations like

$$\begin{aligned} {}_2F_1(a,b,c;z) &= \frac{\Gamma(c)\Gamma(c-a-b)}{\Gamma(c-a)\Gamma(c-b)}{}_2F_1\left(\begin{array}{c} a,b \\ a+b-c+1 \end{array};1-z\right) \\ &+ \frac{\Gamma(c)\Gamma(a+b-c)}{\Gamma(a)\Gamma(b)}(1-z)^{c-a-b}{}_2F_1\left(\begin{array}{c} c-a,c-b \\ c-a-b+1 \end{array};1-z\right) \end{aligned} \tag{2.107}$$

which describe the branching of a direct channel block into crossed channel blocks. A more systematic approach needs to be developed when the Virasoro Ward identity is not second-order. The solutions are usually not generalized hypergeometric functions, and even when they are, analogues of (2.107) require the Meijer G-function. Instead, there is an elegant integral representation called the Coulomb gas formalism, reviewed *e.g* in [85]. Contour deformations make the crossing kernel transparent, leading to explicit expressions for the minimal model OPE coefficients [107–109]. We will have more to say about these ideas in chapter 3.

Our introduction would not be complete without a discussion of the free boson in two dimensions. This is a $c = 1$ CFT with a spectrum that is either discrete or continuous depending on whether we take the target space to be compact: $X \sim X+2\pi R$. Understanding this theory is actually important for the minimal model problem as well since the Coulomb gas formalism expresses (2.106) as a free boson correlator in the presence of a background charge. A strange thing about the free boson theory is that it is only a CFT in the usual sense once operators that generate logarithmic singularities are removed. This means that we disregard powers of $X(z)$ and $\bar{X}(\bar{z})$ when constructing primaries. Instead, we should use the derivatives $i\partial X(z)$ and $i\bar{\partial}\bar{Z}(\bar{z})$ along with exponentials

$$V_{k,\bar{k}}(z,\bar{z}) = e^{ikX(z)}e^{i\bar{k}\bar{X}(\bar{z})} \ . \tag{2.108}$$

We should in fact regard (2.108) as the *only* primaries once we recognize that the symmetry of the free boson enhances beyond the Virasoro algebra. The single derivatives of $X$ and $\bar{X}$ are generators of this new symmetry, $\mathfrak{u}(1) \times \mathfrak{u}(1)$, and descendants of the identity with respect to it. The momenta in (2.108) belong to the lattice

$$\Gamma = \left\{ \left( \frac{n}{R} + \frac{mR}{2}, \frac{n}{R} - \frac{mR}{2} \right) \,\middle|\, m,n \in \mathbb{Z} \right\} \tag{2.109}$$

which is invariant under $R \mapsto \frac{2}{R}$ — the origin of T-duality in string theory. Generically, the free boson as one discrete symmetry which can be gauged, leading to two continuous families of free CFTs labelled by the radius. The picture, along with three special orbifolds of the $R = \sqrt{2}$ theory, is often referred to as the $c = 1$ moduli space. However, it is more correct to refer to it as the space of two-dimensional CFTs that have a $\mathfrak{u}(1) \times \mathfrak{u}(1)$ symmetry [110].

### 2.3.2 Fun with twist fields

The most complicated $c = 1$ CFT is the $\mathbb{S}_1/\mathbb{Z}_2$ orbifold theory. This is the compact free boson with $X \sim -X$ identified. A twist field of dimension $\left(\frac{1}{16}, \frac{1}{16}\right)$ appears for every fixed point of the symmetry being modded out — in this case, there are twists around $X = 0$ and $X = \pi$.

$$\begin{array}{ll} X(e^{2\pi i}z, \bar{z})\sigma_0(0) = -X(z, \bar{z})\sigma_0(0) & X(e^{2\pi i}z, \bar{z})\sigma_1(0) = [2\pi R - X(z, \bar{z})]\sigma_1(0) \\ X(z, e^{2\pi i}\bar{z})\sigma_0(0) = -X(z, \bar{z})\sigma_0(0) & X(z, e^{2\pi i}\bar{z})\sigma_1(0) = [2\pi R - X(z, \bar{z})]\sigma_1(0) \end{array}$$

While three-point functions involving twist fields once again follow from the trick of expanding a four-point function, there are several subtleties in this calculation.

When a correlation function has four twist fields, these create two branch cuts which are responsible for the multi-valuedness of local operators in the $z$ plane. Alternatively, we may turn this into a partition function on the two-sheeted cover where the operators are single valued functions of a parameter $\tau$ or $q \equiv e^{2\pi i\tau}$. The standard map from $z$ to $\tau$ is

$$z = \left[\frac{\vartheta_2(\tau)}{\vartheta_3(\tau)}\right]^4 \quad \Leftrightarrow \quad \tau = i\frac{K(1-z)}{K(z)} \tag{2.110}$$

and one can actually write nice expressions for the theta functions individually [111].

$$\begin{aligned} \vartheta_2(\tau)^2 &= \frac{2}{\pi}K(z)\sqrt{z} \\ \vartheta_3(\tau)^2 &= \frac{2}{\pi}K(z) \\ \vartheta_4(\tau)^2 &= \frac{2}{\pi}K(z)\sqrt{1-z} \end{aligned} \tag{2.111}$$

The statement of crossing symmetry for $\langle\sigma(0)\sigma(z, \bar{z})\sigma(1)\sigma(\infty)\rangle$ is the usual functional equation. This is equivalent to modular invariance as shown by the standard identities:

$$\begin{aligned} \vartheta_2\left(-\frac{1}{\tau}\right) &= \sqrt{-i\tau}\vartheta_4(\tau)\ ,\ \vartheta_2(\tau+1) = e^{\frac{\pi i}{4}}\vartheta_2(\tau) \\ \vartheta_3\left(-\frac{1}{\tau}\right) &= \sqrt{-i\tau}\vartheta_3(\tau)\ ,\ \vartheta_3(\tau+1) = \vartheta_4(\tau) \\ \vartheta_4\left(-\frac{1}{\tau}\right) &= \sqrt{-i\tau}\vartheta_2(\tau)\ ,\ \vartheta_4(\tau+1) = \vartheta_3(\tau)\ . \end{aligned} \tag{2.112}$$

We will show a curious fact that many of these four-point functions are "solvable by radicals" at $R^2 = 2^M$.

Without loss of generality, we may assume that the last twist field is always $\sigma_0$. This is due to an invariance under the $D_4$ group generated by $\sigma_0 \leftrightarrow \sigma_1$ and $\sigma_0 \leftrightarrow -\sigma_0$. The

four-point function in question was found to be

$$\begin{aligned}\langle\sigma_s(0)\sigma_{r+s}(z,\bar{z})\sigma_r(1)\sigma_0(\infty)\rangle &= Z_\infty(\tau,\bar{\tau})Z_R(\tau,\bar{\tau}) \\ Z_\infty(\tau,\bar{\tau}) &= \frac{1}{\sqrt{\Im\tau}|\eta(\tau)|^2}\left|\frac{\vartheta_3(\tau)^2}{4\vartheta_2(\tau)\vartheta_4(\tau)}\right|^{\frac{1}{3}} \\ Z_R(\tau,\bar{\tau}) &= \sum_{m,m'\in\mathbb{Z}}\exp\left[-\frac{\pi R^2}{\Im\tau}\left|m'+m\tau+\frac{1}{2}(s+r\tau)\right|^2\right] \end{aligned} \tag{2.113}$$

in [112]. Under $\tau \leftrightarrow -\frac{1}{\tau}$, the sum reshuffles according to $(m,m') \leftrightarrow (m',-m)$. Therefore, both pieces are separately modular invariant. We can force the weights $h,\bar{h} = \frac{1}{2}\left(\frac{n}{R} \pm \frac{mR}{2}\right)^2$ to show up if we perform a Poisson resummation in $m'$.

$$\begin{aligned}\langle\sigma_s(0)\sigma_{r+s}(z,\bar{z})\sigma_r(1)\sigma_0(\infty)\rangle &= \frac{1}{|\eta(\tau)|^2}\left|\frac{\vartheta_3(\tau)^2}{4\vartheta_2(\tau)\vartheta_4(\tau)}\right|^{\frac{1}{3}}\sum_{\substack{n\in\mathbb{Z}\\ m\in 2\mathbb{Z}+r}}(-1)^{ns}q^{\frac{1}{4}\left(\frac{n}{R}+\frac{mR}{2}\right)^2}\bar{q}^{\frac{1}{4}\left(\frac{n}{R}-\frac{mR}{2}\right)^2} \\ q &\equiv e^{2\pi i\tau} \quad , \quad \bar{q}\equiv e^{-2\pi i\bar{\tau}}\end{aligned} \tag{2.114}$$

The right-hand side of (2.114) is given in [112] but as a formula for $\langle\sigma_r(0)\sigma_{r+s}(z,\bar{z})\sigma_s(1)\sigma_0(\infty)\rangle$ with $z = [\vartheta_3(\tau)/\vartheta_4(\tau)]^4$. The $r \leftrightarrow s$ switch does not seem to compensate the redefinition of $z$. Nevertheless, we believe (2.114) is correct for two reasons. The first is that the square of the non-compact four-point function

$$Z_\infty(z,\bar{z})^2 = \frac{\pi^2}{2|z(1-z)|^{\frac{1}{2}}}\frac{1}{K(1-z)K(\bar{z})+K(z)K(1-\bar{z})} \tag{2.115}$$

is precisely the *complex* boson expression which was calculated in [113] by a different method. The second is that [114] exactly writes (2.114), saying that it comes from tracking down strange conventions in the original sources and imposing (2.110) instead.

One more point, not made clear in [112], is that $R \leftrightarrow \frac{2}{R}$, despite being a duality of the theory, does not leave $Z_R(\tau,\bar{\tau})$ invariant. This is because a relabelling of operators occurs. For $R \in (0,\sqrt{2})$, the formula (2.114) describes the four-point functions of $\sigma_0$ and $\sigma_1$ as we defined them above. For $R \in (\sqrt{2},\infty)$, it describes the four-point functions of new twist operators defined by

$$\sigma_+ = \frac{\sigma_0+\sigma_1}{\sqrt{2}} \quad , \quad \sigma_- = \frac{\sigma_0-\sigma_1}{\sqrt{2}} \ . \tag{2.116}$$

Although we will see that this is true explicitly, [115] has an argument which explains this phenomenon in a neighbourhood of $R=\sqrt{2}$. Consider the primaries

$$V^+_{m,n} = \cos\left(\frac{n+m}{\sqrt{2}}X+\frac{n-m}{\sqrt{2}}\bar{X}\right) \quad , \quad V^-_{m,n} = \sin\left(\frac{n+m}{\sqrt{2}}X+\frac{n-m}{\sqrt{2}}\bar{X}\right) \ . \tag{2.117}$$

If the definition of a vertex operator is extended to allow half-integers, these can be given weight $(h,\bar{h}) = \left(\frac{1}{16},\frac{1}{16}\right)$ by choosing $(m,n) = \left(\frac{1}{2},0\right)$. Next we demand that the marginal operator traversing the orbifold line acquire a sign under T-duality. This says that one of the chiral components of the scalar field must shift:

$$\begin{array}{c} J_1\bar{J}_1 = \cos(\sqrt{2}X)\cos(\sqrt{2}\bar{X}) \\ X \mapsto X \end{array} \quad \mapsto \quad \begin{array}{c} -\cos(\sqrt{2}X)\cos(\sqrt{2}\bar{X}) = -J_1\bar{J}_1 \\ \bar{X} \mapsto \bar{X} + \frac{\pi}{\sqrt{2}} \end{array}$$

Performing this shift, we see that $V^+_{\frac{1}{2},0}$ and $V^-_{\frac{1}{2},0}$ are mapped to linear combinations of themselves that are precisely given by (2.116). We may summarize this discussion by writing the list in Table 2.4.

| $R < \sqrt{2}$ | | $R > \sqrt{2}$ |
|---|---|---|
| $\langle\sigma_0\sigma_0\sigma_0\sigma_0\rangle$ | $\frac{1}{\lvert\vartheta_2\vartheta_4\rvert}\sum_{m,n} q^{\frac{1}{4}\left(\frac{n}{R}+mR\right)^2}\bar{q}^{\frac{1}{4}\left(\frac{n}{R}-mR\right)^2}$ | $\langle\sigma_+\sigma_+\sigma_+\sigma_+\rangle$ |
| $\langle\sigma_+\sigma_+\sigma_+\sigma_+\rangle$ | $\frac{1}{\lvert\vartheta_2\vartheta_4\rvert}\sum_{m,n} q^{\frac{1}{4}\left(\frac{2m}{R}+\frac{nR}{2}\right)^2}\bar{q}^{\frac{1}{4}\left(\frac{2m}{R}-\frac{nR}{2}\right)^2}$ | $\langle\sigma_0\sigma_0\sigma_0\sigma_0\rangle$ |
| $\langle\sigma_1\sigma_1\sigma_0\sigma_0\rangle$ | $\frac{1}{\lvert\vartheta_2\vartheta_4\rvert}\sum_{m,n} (-1)^n q^{\frac{1}{4}\left(\frac{n}{R}+mR\right)^2}\bar{q}^{\frac{1}{4}\left(\frac{n}{R}-mR\right)^2}$ | $\langle\sigma_-\sigma_-\sigma_+\sigma_+\rangle$ |
| $\langle\sigma_-\sigma_-\sigma_+\sigma_+\rangle$ | $\frac{1}{\lvert\vartheta_2\vartheta_4\rvert}\sum_{m,n} (-1)^n q^{\frac{1}{4}\left(\frac{2m}{R}+\frac{nR}{2}\right)^2}\bar{q}^{\frac{1}{4}\left(\frac{2m}{R}-\frac{nR}{2}\right)^2}$ | $\langle\sigma_1\sigma_1\sigma_0\sigma_0\rangle$ |
| $\langle\sigma_0\sigma_1\sigma_1\sigma_0\rangle$ | $\frac{1}{\lvert\vartheta_2\vartheta_4\rvert}\sum_{m,n} q^{\frac{1}{4}\left(\frac{n}{R}+mR+\frac{R}{2}\right)^2}\bar{q}^{\frac{1}{4}\left(\frac{n}{R}-mR-\frac{R}{2}\right)^2}$ | $\langle\sigma_+\sigma_-\sigma_-\sigma_+\rangle$ |
| $\langle\sigma_+\sigma_-\sigma_-\sigma_+\rangle$ | $\frac{1}{\lvert\vartheta_2\vartheta_4\rvert}\sum_{m,n} q^{\frac{1}{4}\left(\frac{2m}{R}+\frac{nR}{2}+\frac{1}{R}\right)^2}\bar{q}^{\frac{1}{4}\left(\frac{2m}{R}-\frac{nR}{2}+\frac{1}{R}\right)^2}$ | $\langle\sigma_0\sigma_1\sigma_1\sigma_0\rangle$ |
| $\langle\sigma_1\sigma_0\sigma_1\sigma_0\rangle$ | $\frac{1}{\lvert\vartheta_2\vartheta_4\rvert}\sum_{m,n} (-1)^n q^{\frac{1}{4}\left(\frac{n}{R}+mR+\frac{R}{2}\right)^2}\bar{q}^{\frac{1}{4}\left(\frac{n}{R}-mR-\frac{R}{2}\right)^2}$ | $\langle\sigma_-\sigma_+\sigma_-\sigma_+\rangle$ |
| $\langle\sigma_-\sigma_+\sigma_-\sigma_+\rangle$ | $\frac{1}{\lvert\vartheta_2\vartheta_4\rvert}\sum_{m,n} (-1)^n q^{\frac{1}{4}\left(\frac{2m}{R}+\frac{nR}{2}+\frac{1}{R}\right)^2}\bar{q}^{\frac{1}{4}\left(\frac{2m}{R}-\frac{nR}{2}+\frac{1}{R}\right)^2}$ | $\langle\sigma_1\sigma_0\sigma_1\sigma_0\rangle$ |

Table 2.4: While (2.114) is a four-point function of twist fields on either side of $R = \sqrt{2}$, the interpretation of those twist fields changes on either side. This table lists the four inequivalent correlators in the two different bases.

For some values of $R$, simple expressions can be obtained by evaluating these sums in terms of theta functions. This is done in the Appendix A. Looking at just the first two rows, we can produce Table 2.5 where blue represents a sum computed in Appendix A and red represents a sum that looks too hard. Staring at Table 2.5, every sum appearing on the left-hand side for radius $R$ also appears on the right-hand side for radius $\frac{1}{R}$ which represents a different theory. One might therefore imagine an algorithm which starts from the blue sums and composes the maps $R \mapsto \frac{1}{R}$ and $R \mapsto \frac{2}{R}$ to generate closed-form expressions at all powers of 2. In the rest of this section, we will comment on this hope and explain how the results in Appendix A verify known dualities.

| $R^2$ | $\langle\sigma_0\sigma_0\sigma_0\sigma_0\rangle$ | $\langle\sigma_+\sigma_+\sigma_+\sigma_+\rangle$ |
|---|---|---|
| 32 | $\frac{1}{\lvert\vartheta_2\vartheta_4\rvert}\sum_{m,n} q^{2\left(m+\frac{n}{8}\right)^2}\bar{q}^{2\left(m-\frac{n}{8}\right)^2}$ | $\frac{1}{\lvert\vartheta_2\vartheta_4\rvert}\sum_{m,n} q^{8\left(m+\frac{n}{32}\right)^2}\bar{q}^{8\left(m-\frac{n}{32}\right)^2}$ |
| 16 | $\frac{1}{\lvert\vartheta_2\vartheta_4\rvert}\sum_{m,n} q^{\left(m+\frac{n}{4}\right)^2}\bar{q}^{\left(m-\frac{n}{4}\right)^2}$ | $\frac{1}{\lvert\vartheta_2\vartheta_4\rvert}\sum_{m,n} q^{4\left(m+\frac{n}{16}\right)^2}\bar{q}^{4\left(m-\frac{n}{16}\right)^2}$ |
| 8 | $\frac{1}{\lvert\vartheta_2\vartheta_4\rvert}\sum_{m,n} q^{\frac{1}{2}\left(m+\frac{n}{2}\right)^2}\bar{q}^{\frac{1}{2}\left(m-\frac{n}{2}\right)^2}$ | $\frac{1}{\lvert\vartheta_2\vartheta_4\rvert}\sum_{m,n} q^{2\left(m+\frac{n}{8}\right)^2}\bar{q}^{2\left(m-\frac{n}{8}\right)^2}$ |
| 4 | $\frac{1}{\lvert\vartheta_2\vartheta_4\rvert}\sum_{m,n} q^{\frac{1}{4}(m+n)^2}\bar{q}^{\frac{1}{4}(m-n)^2}$ | $\frac{1}{\lvert\vartheta_2\vartheta_4\rvert}\sum_{m,n} q^{\left(m+\frac{n}{4}\right)^2}\bar{q}^{\left(m-\frac{n}{4}\right)^2}$ |
| 2 | $\frac{1}{\lvert\vartheta_2\vartheta_4\rvert}\sum_{m,n} q^{\frac{1}{8}(m+2n)^2}\bar{q}^{\frac{1}{8}(m-2n)^2} = \frac{1}{\lvert\vartheta_2\vartheta_4\rvert}\sum_{m,n} q^{\frac{1}{2}\left(m+\frac{n}{2}\right)^2}\bar{q}^{\frac{1}{2}\left(m-\frac{n}{2}\right)^2}$ | |
| 1 | $\frac{1}{\lvert\vartheta_2\vartheta_4\rvert}\sum_{m,n} q^{\frac{1}{4}(m+n)^2}\bar{q}^{\frac{1}{4}(m-n)^2}$ | $\frac{1}{\lvert\vartheta_2\vartheta_4\rvert}\sum_{m,n} q^{\left(m+\frac{n}{4}\right)^2}\bar{q}^{\left(m-\frac{n}{4}\right)^2}$ |
| $\frac{1}{2}$ | $\frac{1}{\lvert\vartheta_2\vartheta_4\rvert}\sum_{m,n} q^{\frac{1}{2}\left(m+\frac{n}{2}\right)^2}\bar{q}^{\frac{1}{2}\left(m-\frac{n}{2}\right)^2}$ | $\frac{1}{\lvert\vartheta_2\vartheta_4\rvert}\sum_{m,n} q^{2\left(m+\frac{n}{8}\right)^2}\bar{q}^{2\left(m-\frac{n}{8}\right)^2}$ |
| $\frac{1}{4}$ | $\frac{1}{\lvert\vartheta_2\vartheta_4\rvert}\sum_{m,n} q^{\left(m+\frac{n}{4}\right)^2}\bar{q}^{\left(m-\frac{n}{4}\right)^2}$ | $\frac{1}{\lvert\vartheta_2\vartheta_4\rvert}\sum_{m,n} q^{4\left(m+\frac{n}{16}\right)^2}\bar{q}^{4\left(m-\frac{n}{16}\right)^2}$ |
| $\frac{1}{8}$ | $\frac{1}{\lvert\vartheta_2\vartheta_4\rvert}\sum_{m,n} q^{2\left(m+\frac{n}{8}\right)^2}\bar{q}^{2\left(m-\frac{n}{8}\right)^2}$ | $\frac{1}{\lvert\vartheta_2\vartheta_4\rvert}\sum_{m,n} q^{8\left(m+\frac{n}{32}\right)^2}\bar{q}^{8\left(m-\frac{n}{32}\right)^2}$ |

Table 2.5: The first two rows of Table 2.4 with some powers of 2 plugged in for $R^2$. The fact that some red sums can be obtained from blue sums indicates that, between the two bases, difficulty is not always conserved.

Using (A.2) and (A.3), we find two of the four-point functions at $R = \sqrt{2}$.

$$\begin{aligned}
\langle\sigma_0(0)\sigma_0(z,\bar{z})\sigma_0(1)\sigma_0(\infty)\rangle &= \frac{|\vartheta_2(\tau)|^2+|\vartheta_3(\tau)|^2+|\vartheta_4(\tau)|^2}{2|\vartheta_2(\tau)\vartheta_4(\tau)|} \\
&= \frac{1}{2|z(1-z)|^{\frac{1}{4}}}\left(|z|^{\frac{1}{2}}+1+|1-z|^{\frac{1}{2}}\right) \\
\langle\sigma_0(0)\sigma_1(z,\bar{z})\sigma_1(1)\sigma_0(\infty)\rangle &= \frac{|\vartheta_2(\tau)|^2+|\vartheta_3(\tau)|^2-|\vartheta_4(\tau)|^2}{2|\vartheta_2(\tau)\vartheta_4(\tau)|} \\
&= \frac{1}{2|z(1-z)|^{\frac{1}{4}}}\left(|z|^{\frac{1}{2}}+1-|1-z|^{\frac{1}{2}}\right)
\end{aligned} \tag{2.118}$$

Two partners of the second line come from (A.4) and (A.5)

$$\begin{aligned}
\langle\sigma_1(0)\sigma_1(z,\bar{z})\sigma_0(1)\sigma_0(\infty)\rangle &= \frac{-|\vartheta_2(\tau)|^2+|\vartheta_3(\tau)|^2+|\vartheta_4(\tau)|^2}{2|\vartheta_2(\tau)\vartheta_4(\tau)|} \\
&= \frac{1}{2|z(1-z)|^{\frac{1}{4}}}\left(-|z|^{\frac{1}{2}}+1+|1-z|^{\frac{1}{2}}\right) \\
\langle\sigma_1(0)\sigma_0(z,\bar{z})\sigma_1(1)\sigma_0(\infty)\rangle &= \frac{|\vartheta_2(\tau)|^2-|\vartheta_3(\tau)|^2+|\vartheta_4(\tau)|^2}{2|\vartheta_2(\tau)\vartheta_4(\tau)|} \\
&= \frac{1}{2|z(1-z)|^{\frac{1}{4}}}\left(|z|^{\frac{1}{2}}-1+|1-z|^{\frac{1}{2}}\right)
\end{aligned} \tag{2.119}$$

which could have just been guessed from crossing symmetry. It so happens that the correlators just found are exactly equal to $\langle\sigma_+\sigma_+\sigma_+\sigma_+\rangle$, $\langle\sigma_+\sigma_-\sigma_-\sigma_+\rangle$, $\langle\sigma_-\sigma_-\sigma_+\sigma_+\rangle$ and $\langle\sigma_-\sigma_+\sigma_-\sigma_+\rangle$ in that order. We can arrive at these same functions of $z$ if we take correlation functions of vertex operators which exist in the circle theory at $R=2\sqrt{2}$. Specifically, we make the following identifications:

$$\sigma_0=\sqrt{2}\cos\left(\frac{1}{2\sqrt{2}}(X+\bar{X})\right) \quad , \quad \sigma_1=\sqrt{2}\sin\left(\frac{1}{2\sqrt{2}}(X+\bar{X})\right) \ . \tag{2.120}$$

This is an operator-level check of the relation $Z_{\rm Orb}(R=\sqrt{2})=Z_{\rm Circ}(R=2\sqrt{2})$. Although it will not be relevant for us, we note that this partition function can be written in terms of finitely many characters. This is clearly true for all powers of 2 (since they are rational) but the special thing about $R^2=2$ is that it is not divisible by 4. The arguments in [114] therefore tell us that we will need to take *complex* linear combinations of $\sigma_0$ and $\sigma_1$ in order to construct the diagonal modular invariant.

Treating $R=2$ next, we have (A.6) which looks like an Ising four-point function.

$$\begin{aligned}
\langle\sigma_0(0)\sigma_0(z,\bar{z})\sigma_0(1)\sigma_0(\infty)\rangle &= \frac{|\vartheta_3(\tau)^2+\vartheta_4(\tau)^2|+|\vartheta_3(\tau)^2-\vartheta_4(\tau)^2|}{2|\vartheta_2(\tau)\vartheta_4(\tau)|} \\
&= \frac{|1+\sqrt{1-z}|+|1-\sqrt{1-z}|}{2|z(1-z)|^{\frac{1}{4}}}
\end{aligned} \tag{2.121}$$

We also have (A.7), (A.8) and (A.9) which all look like two-point functions.

$$\begin{aligned}
\langle\sigma_0(0)\sigma_1(z,\bar{z})\sigma_1(1)\sigma_0(\infty)\rangle &= \left|\frac{\vartheta_3(\tau)}{\vartheta_4(\tau)}\right| = \frac{1}{|1-z|^{\frac{1}{4}}} \\
\langle\sigma_1(0)\sigma_1(z,\bar{z})\sigma_0(1)\sigma_0(\infty)\rangle &= \left|\frac{\vartheta_3(\tau)}{\vartheta_2(\tau)}\right| = \frac{1}{|z|^{\frac{1}{4}}} \\
\langle\sigma_1(0)\sigma_0(z,\bar{z})\sigma_1(1)\sigma_0(\infty)\rangle &= 1
\end{aligned} \tag{2.122}$$

This is perfectly consistent with the statement that orbifold twist fields become decoupled Ising spin fields in the duality $Z_{\rm Orb}(R=2) = Z^2_{\rm Ising}$. The correlators above are enough to deduce

$$\begin{aligned}
\langle\sigma_+(0)\sigma_+(z,\bar z)\sigma_+(1)\sigma_+(\infty)\rangle &= \frac{|1+\sqrt{1-z}|+|1-\sqrt{1-z}|}{4|z(1-z)|^{\frac14}} + \frac12\left(\frac{1}{|1-z|^{\frac14}}+1+\frac{1}{|z|^{\frac14}}\right)\\
\langle\sigma_+(0)\sigma_-(z,\bar z)\sigma_-(1)\sigma_+(\infty)\rangle &= \frac{|1+\sqrt{1-z}|+|1-\sqrt{1-z}|}{4|z(1-z)|^{\frac14}} + \frac12\left(\frac{1}{|1-z|^{\frac14}}-1-\frac{1}{|z|^{\frac14}}\right)\\
\langle\sigma_-(0)\sigma_-(z,\bar z)\sigma_+(1)\sigma_+(\infty)\rangle &= \frac{|1+\sqrt{1-z}|+|1-\sqrt{1-z}|}{4|z(1-z)|^{\frac14}} + \frac12\left(-\frac{1}{|1-z|^{\frac14}}-1+\frac{1}{|z|^{\frac14}}\right)\\
\langle\sigma_-(0)\sigma_+(z,\bar z)\sigma_-(1)\sigma_+(\infty)\rangle &= \frac{|1+\sqrt{1-z}|+|1-\sqrt{1-z}|}{4|z(1-z)|^{\frac14}} + \frac12\left(-\frac{1}{|1-z|^{\frac14}}+1-\frac{1}{|z|^{\frac14}}\right)
\end{aligned}$$

when we take sums and differences of $\sigma_0, \sigma_1$. Since these are also the results of (A.10), (A.11), (A.12) and (A.13), we confirm that (2.116) is indeed the relabelling induced by $R \leftrightarrow \frac{2}{R}$.

At $R = 2\sqrt{2}$, which corresponds to the 4-state Potts model, four correlation functions are computed in Appendix A. For (A.14), (A.15) and (A.16), we find:

$$\begin{aligned}
\langle\sigma_0(0)\sigma_0(z,\bar z)\sigma_0(1)\sigma_0(\infty)\rangle &= \frac{|\vartheta_2(\tau)|^2+|\vartheta_3(\tau)|^2+|\vartheta_4(\tau)|^2}{2|\vartheta_2(\tau)\vartheta_4(\tau)|}\\
&= \frac{1}{2|z(1-z)|^{\frac14}}\left(|z|^{\frac12}+1+|1-z|^{\frac12}\right)\\
\langle\sigma_0(0)\sigma_1(z,\bar z)\sigma_1(1)\sigma_0(\infty)\rangle &= \frac{|\vartheta_2(\tau)\vartheta_3(\tau)[\vartheta_3(\tau)^2+\vartheta_2(\tau)^2]|^{\frac12}+|\vartheta_2(\tau)\vartheta_3(\tau)[\vartheta_3(\tau)^2-\vartheta_2(\tau)^2]|^{\frac12}}{\sqrt{2}|\vartheta_2(\tau)\vartheta_4(\tau)|}\\
&= \frac{|z^{\frac14}(1+\sqrt{z})|^{\frac12}+|z^{\frac14}(1-\sqrt{z})|^{\frac12}}{\sqrt{2}|z(1-z)|^{\frac14}}\\
\langle\sigma_1(0)\sigma_1(z,\bar z)\sigma_0(1)\sigma_0(\infty)\rangle &= \frac{|\vartheta_3(\tau)\vartheta_4(\tau)[\vartheta_3(\tau)^2+\vartheta_4(\tau)^2]|^{\frac12}+|\vartheta_3(\tau)\vartheta_4(\tau)[\vartheta_3(\tau)^2-\vartheta_4(\tau)^2]|^{\frac12}}{\sqrt{2}|\vartheta_2(\tau)\vartheta_4(\tau)|}\\
&= \frac{|(1-z)^{\frac14}(1+\sqrt{1-z})|^{\frac12}+|(1-z)^{\frac14}(1-\sqrt{1-z})|^{\frac12}}{\sqrt{2}|z(1-z)|^{\frac14}}\,. \qquad (2.123)
\end{aligned}$$

The sum for (A.17) looks a bit harder but it evaluates to

$$\begin{aligned}\langle\sigma_1(0)\sigma_0(z,\bar{z})\sigma_1(1)\sigma_0(\infty)\rangle &= \frac{|\vartheta_2(\tau)\vartheta_4(\tau)[\vartheta_2(\tau)^2+\vartheta_4(\tau)^2]|^{\frac{1}{2}}+|\vartheta_2(\tau)\vartheta_4(\tau)[\vartheta_2(\tau)^2-\vartheta_4(\tau)^2]|^{\frac{1}{2}}}{\sqrt{2}|\vartheta_2(\tau)\vartheta_4(\tau)|}\\ &= \frac{|\sqrt{z}+\sqrt{1-z}|^{\frac{1}{2}}+|\sqrt{z}-\sqrt{1-z}|^{\frac{1}{2}}}{\sqrt{2}|z(1-z)|^{\frac{1}{8}}}\,. \end{aligned} \tag{2.124}$$

Their images under $R\leftrightarrow\frac{2}{R}$ cannot be computed directly with the techniques in these notes. However, we may use the fact that these complicated expressions have to be related to the simpler expressions through the linear combination (2.116). This allows us to predict entirely non-obvious mathematical identities like

$$\begin{aligned}\sum_{m,n} q^{2\left(m+\frac{n}{8}\right)^2}\bar{q}^{2\left(m-\frac{n}{8}\right)^2} &= \frac{1}{4}\left(|\vartheta_2(\tau)|^2+|\vartheta_3(\tau)|^2+|\vartheta_4(\tau)|^2\right)\\ &+\frac{1}{2\sqrt{2}}\Big[\left|\vartheta_2(\tau)\vartheta_3(\tau)[\vartheta_3(\tau)^2+\vartheta_2(\tau)^2]\right|^{\frac{1}{2}}+\left|\vartheta_2(\tau)\vartheta_3(\tau)[\vartheta_3(\tau)^2-\vartheta_2(\tau)^2]\right|^{\frac{1}{2}}\\ &+\left|\vartheta_3(\tau)\vartheta_4(\tau)[\vartheta_3(\tau)^2+\vartheta_4(\tau)^2]\right|^{\frac{1}{2}}+\left|\vartheta_3(\tau)\vartheta_4(\tau)[\vartheta_3(\tau)^2-\vartheta_4(\tau)^2]\right|^{\frac{1}{2}}\\ &+\left|\vartheta_2(\tau)\vartheta_4(\tau)[\vartheta_2(\tau)^2+\vartheta_4(\tau)^2]\right|^{\frac{1}{2}}+\left|\vartheta_2(\tau)\vartheta_4(\tau)[\vartheta_2(\tau)^2-\vartheta_4(\tau)^2]\right|^{\frac{1}{2}}\Big]\end{aligned} \tag{2.125}$$

which we have checked numerically. We would now like to see if we can continue this cascade of inferring increasingly complicated expressions on physical grounds. The sum we deduced in (2.125), which gives $\langle\sigma_+\sigma_+\sigma_+\sigma_+\rangle$ at $R^2=8$, is also the sum that gives $\langle\sigma_0\sigma_0\sigma_0\sigma_0\rangle$ at $R^2=32$. However, there seems to be no relation between the other correlators at these two radii, due to the fact that the sums do not treat the two indices symmetrically. To convert (2.125) into an expression for a mixed correlator of $\sigma_+$ and $\sigma_-$ at $R=2\sqrt{2}$, we introduce $(-1)^n$ or increment $m$ by $\frac{1}{2}$. Conversely, we make a mixed correlator of $\sigma_0$ and $\sigma_1$ at $R=4\sqrt{2}$ by introducing $(-1)^m$ or incrementing $n$ by $\frac{1}{2}$. It therefore appears that $\langle\sigma_0\sigma_0\sigma_0\sigma_0\rangle$ is the only twist-field four-point function we can compute at this radius. We need at least one more in order to start learning about what they are at $R=8\sqrt{2}$ and so on. Most authors resort to defining new theta functions at these radii but it would be nice to find some way around this.

### 2.3.3 Analytic bootstrap functionals

While the bootstrap is applicable to general CFTs, integrable or not, we have seen that many two-dimensional examples do not need a numerical treatment. They have already been exactly solved through the power of chiral symmetry. There is also a sense in which numerics can be obviated in one dimension but the principle underlying this result is very

different. In [116–118], functionals certifying the non-existence of CFTs above a certain gap were constructed analytically. This allowed the authors to prove certain numerical bounds that had previously been seen in [119]. These functionals are specified by their action on

$$F_{\Delta}^{\pm}(z) = \frac{G_{\Delta}(z)}{z^{2\Delta_\phi}} \pm \frac{G_{\Delta}(1-z)}{(1-z)^{2\Delta_\phi}} \tag{2.126}$$

where $z = \frac{z_{12}z_{34}}{z_{13}z_{24}}$ and

$$G_{\Delta}(z) = {}_2F_1(\Delta, \Delta, 2\Delta; z) \tag{2.127}$$

is the $\mathfrak{sl}(2)$ block. We have seen that $F_{\Delta}^{-}$ occurs in single correlator bootstrap problems. We can also see $F_{\Delta}^{+}$ without external dimension differences if we consider operators that transform non-trivially under an internal symmetry.

The functionals we discuss will all have the "cut-touching" form

$$\begin{aligned} \omega[\mathcal{F}(z)] &= \frac{1}{2\pi i}\int_1^{\infty} h(z)\text{Disc}[\mathcal{F}(z)]\mathrm{d}z \\ \text{Disc}[\mathcal{F}(z)] &= \lim_{\epsilon\to 0^+}\left[\mathcal{F}(z+i\epsilon) - \mathcal{F}(z-i\epsilon)\right] . \end{aligned} \tag{2.128}$$

When $\mathcal{F}(z)$ is a convolved conformal block, (2.128) can be written as (the analytic continuation of)

$$\omega[\mathcal{F}(z)] = \int_1^{\infty} z^{2\Delta_\phi-2} g\left(\frac{z-1}{z}\right)\frac{\hat{G}_{\Delta}(1-z)}{(z-1)^{2\Delta_\phi}}\mathrm{d}z - \Re\left[e^{-i\pi(\Delta-2\Delta_\phi)}\int_1^{\infty} f(z)\frac{\hat{G}_{\Delta}(1-z)}{(z-1)^{2\Delta_\phi}}\mathrm{d}z\right] \tag{2.129}$$

where

$$\hat{G}_{\Delta}(z) = (-z)^{\Delta}{}_2F_1(\Delta, \Delta; 2\Delta; z) . \tag{2.130}$$

The precise relation between the various kernels depends on whether the convolved block is $F_{\Delta}^{-}(z)$ or $F_{\Delta}^{+}(z)$ as shown in Table 2.6. The conjugation condition in the last line follows immediately from taking $h(z)$ to be real for $z \in (1, \infty)$.

| $\mathcal{F}(z) = F_{\Delta}^{-}(z)$ | $\mathcal{F}(z) = F_{\Delta}^{+}(z)$ |
|---|---|
| $g(z) = -\frac{\text{Disc}[h(z)]}{2\pi i}$ | $g(z) = -\frac{\text{Disc}[h(z)]}{2\pi i}$ |
| $f(z) = \frac{h(z)-h(1-z)}{\pi i}$ | $f(z) = -\frac{h(z)+h(1-z)}{\pi i}$ |
| $f(z) = \overline{f(1-\bar{z})}$ | $f(z) = -\overline{f(1-\bar{z})}$ |

Table 2.6: Definitions of the (2.129) kernels in terms of $h(z)$ in (2.128). These reality properties are essential for finding a direct relation between $f(z)$ and $g(z)$.

The proof of this comes from writing

$$\omega[F^{\pm}_{\Delta}(z)] = -\frac{1}{2\pi i}\int_{-\infty}^{0} h(1-z)\text{Disc}\left[\frac{G_{\Delta}(1-z)}{(1-z)^{2\Delta_\phi}}\right]\mathrm{d}z \pm \frac{1}{2\pi i}\int_{1}^{\infty} h(z)\text{Disc}\left[\frac{G_{\Delta}(1-z)}{(1-z)^{2\Delta_\phi}}\right]\mathrm{d}z \tag{2.131}$$

and rotating so that all integration contours are $z \in (1,\infty)$. This yields

$$\begin{aligned}\omega[F^{\pm}_{\Delta}(z)] &= \int_{1}^{\infty} z^{2\Delta_\phi-2} g\left(\frac{z-1}{z}\right)\frac{\hat{G}_{\Delta}(1-z)}{(z-1)^{2\Delta_\phi}}\mathrm{d}z \\ &+ \frac{1}{2\pi i}\int_{1}^{\infty}\left[e^{-i\pi(\Delta-2\Delta_\phi)}h(1-z-i\epsilon) - e^{i\pi(\Delta-2\Delta_\phi)}h(1-z+i\epsilon)\right]\frac{\hat{G}_{\Delta}(1-z)}{(z-1)^{2\Delta_\phi}}\mathrm{d}z \\ &\pm \frac{1}{2\pi i}\int_{1}^{\infty} h(z)\text{Disc}\left[\frac{G_{\Delta}(1-z)}{(1-z)^{2\Delta_\phi}}\right]\mathrm{d}z \end{aligned} \tag{2.132}$$

where $g(z)$ is defined as in the table. One may try to simplify this further by writing

$$\begin{aligned} h(1-z-i\epsilon) &= h(z+i\epsilon) - \pi i f(z+i\epsilon) \\ h(1-z+i\epsilon) &= h(z-i\epsilon) + \pi i \overline{f(z+i\epsilon)}\,. \end{aligned} \tag{2.133}$$

For the lower sign, this causes all integrals containing $h(z)$ to cancel in (2.132), leaving (2.129). Conversely, if we are interested in the upper sign, the way to make all $h(z)$ terms cancel is to perform

$$\begin{aligned} h(1-z-i\epsilon) &= -h(z+i\epsilon) - \pi i f(z+i\epsilon) \\ h(1-z+i\epsilon) &= -h(z-i\epsilon) + \pi i \overline{f(z+i\epsilon)}\,. \end{aligned} \tag{2.134}$$

It is easy to see that (2.133) and (2.134) pick out the definitions for $f(z)$ in the left and right columns of the table respectively.

Once we are confident about how $f(z)$ and $g(z)$ are defined, we may write down the so-called gluing condition. This is one of two necesssary ingredients in solving for useful functionals. By referring to the table, we find the following.

$$\Re f(z) = \begin{cases} -g(z) - g(1-z) & \mathcal{F} = F^{-} \\ +g(z) - g(1-z) & \mathcal{F} = F^{+} \end{cases} \tag{2.135}$$

The action of any one of these functionals has infinitely many local minima. For bootstrap applications, it helps to set things up so that these local minima are also zeros. This gives us some hope of finding extremal functionals that pick out theories with equal spacing between their operators – the generalized free fermion and the generalized free boson. The simplest way forward is to make the choice $f(z) = \pm z^{2\Delta_\phi-2} g\left(\frac{z-1}{z}\right)$ so that (2.129) becomes

proportional to either $\sin^2\left[\frac{\pi}{2}(\Delta-2\Delta_\phi)\right]$ or $\cos^2\left[\frac{\pi}{2}(\Delta-2\Delta_\phi)\right]$. These are called extremality conditions. Notice that for one of them, the zeros are at

$$\Delta=\Delta_n^{(\psi)}\equiv 2\Delta_\phi+2n+1\ , \tag{2.136}$$

while for the other one, the zeros are at

$$\Delta=\Delta_n^{(\phi)}\equiv 2\Delta_\phi+2n\ . \tag{2.137}$$

This is nice because (2.136) is the spectrum of the generalized free fermion while (2.137) is the spectrum of the generalized free boson. The right extremality condition is controlled by whether we want a functional that picks out a bosonic or fermionic spectrum. The right gluing condition to use is controlled by whether we want functionals to do this on $F_\Delta^-$ or $F_\Delta^+$. We summarize the coupled functional equations that must be solved in each case in Table 2.7.

| | Fermion | Boson |
|---|---|---|
| $\mathcal{F}(z)=F_\Delta^-(z)$ | $\Re f(z)=-g(z)-g(1-z)$<br>$f(z)=-z^{2\Delta_\phi-2}g\left(\frac{z-1}{z}\right)$ | $\Re f(z)=-g(z)-g(1-z)$<br>$f(z)=z^{2\Delta_\phi-2}g\left(\frac{z-1}{z}\right)$ |
| $\mathcal{F}(z)=F_\Delta^+(z)$ | $\Re f(z)=g(z)-g(1-z)$<br>$f(z)=-z^{2\Delta_\phi-2}g\left(\frac{z-1}{z}\right)$ | $\Re f(z)=g(z)-g(1-z)$<br>$f(z)=z^{2\Delta_\phi-2}g\left(\frac{z-1}{z}\right)$ |

Table 2.7: Functional equations to solve for two types of blocks and two types of spectra. Functionals in the top line can (and have been) used to prove numerical bootstrap bounds rigorously. Functionals in the bottom line might be useful in 1D bounds that impose global symmetry.

When solutions to these equations are found, the most singular power-law, as $z\to 0$, will tell us when one of the seemingly second-order zeros is really first-order. The functional is finite on either side of this zero since the integral is interpreted as an analytic continuation. It is quite useful to find the linear combination of solutions with the *smallest* first-order zero. This tells us the bound on the gap if the functional is such that summation over a physical spectrum can be swapped with the integration [120]. Other solutions in the basis have been especially useful in other problems [118]. To actually find solutions, one general method has been published so far [117].

1. Go to Mellin space.
2. Solve everything for some small integer or half-integer values of $\Delta_\phi$.
3. Conjecture a general formula based on this (which would be harder in position space).
4. Compute the inverse Mellin transform.

5. Show that the resulting expression is indeed a solution.

Instead of demonstrating this method, we will focus on $\Delta_\phi = 1$ for which two of the four cells in Table 2.7 can be solved by guesswork. Defining $p_n(x) = P_{n-1}(1-2x)$, we may check that

$$\begin{aligned} g_n^{(\phi,-)}(z) &= -\frac{2\Gamma(2n+2)^2}{\pi^2\Gamma(4n+3)}\left[p_{2n+2}(z) + p_{2n+2}\left(\frac{1}{z}\right)\right] \\ g_n^{(\psi,+)}(z) &= -\frac{2\Gamma(2n+3)^2}{\pi^2\Gamma(4n+5)}\left[p_{2n+3}(z) - p_{2n+3}\left(\frac{1}{z}\right)\right] \end{aligned} \tag{2.138}$$

yields the orthogonality relations

$$\begin{aligned} \omega_m^{(\phi,-)}\left[F^-_{\Delta_n^{(\phi)}}(z)\right] = 0 \quad &, \quad \omega_m'^{(\phi,-)}\left[F^-_{\Delta_n^{(\phi)}}(z)\right] = \delta_{mn} \\ \omega_m^{(\psi,+)}\left[F^+_{\Delta_n^{(\psi)}}(z)\right] = 0 \quad &, \quad \omega_m'^{(\psi,+)}\left[F^+_{\Delta_n^{(\psi)}}(z)\right] = \delta_{mn} \end{aligned} \tag{2.139}$$

which will be useful at the end of this thesis. It is worth noting that other integer values of $\Delta_\phi$ exhibit the same pattern — bosonic "$-$" functionals and fermionic "$+$" functionals are easy. At half-integer values, the opposite is true — we get nice expressions for bosonic "$+$" functionals and fermionic "$-$" functionals.

Since (non-convolved) 2D blocks are, in a sense, products of 1D blocks, it seems reasonable to expect some mileage from the analytic functional approach in two dimensions. In particular, it is possible to find a different family of functionals that satisfies

$$\omega_m\left[z^{-\Delta_\phi}G_{\Delta_n^{(\phi)}}(z)\right] = \delta_{mn}\ ,\ \omega_m\left[(1-z)^{-\Delta_\phi}G_{\Delta_n^{(\phi)}}(1-z)\right] = 0 \tag{2.140}$$

instead of (2.139). This allows one to show that the generalized free boson scaling dimensions uniquely fix the OPE coefficients to take on their generalized free boson values as well. It would be interesting to explore other 2D applications of 1D extremal functionals.

# Chapter 3

# Analytic continuation and unitarity

As soon as one has a proper algorithm for conformal blocks, an immediate consequence is that she can run the numerical bootstrap in a fractional number of dimensions [79, 121–124]. In Figure 3.1, we show some of the resulting low resolution islands around the Ising models in $3 < d < 4$. This is curious in view of the now standard fact that fractional dimensions abhor

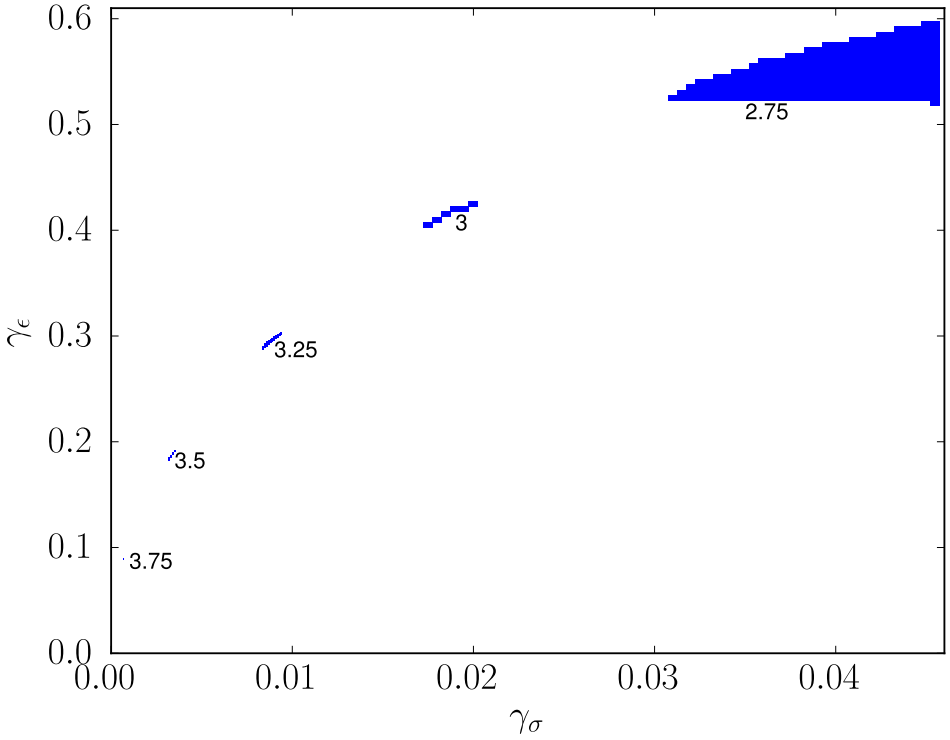


Figure 3.1: Allowed regions carved out by crossing symmetry and unitarity in a $\mathbb{Z}_2$-symmetric system of correlators involving $\sigma$ and $\epsilon$. Each value of $d$ exhibits good agreement with the perturbative critical exponents of the Wilson-Fisher fixed-point.

unitarity. Consider a local operator $\mathcal{O}^{[i_1\cdots i_n]}$ whose indices furnish a non-trivial representation of $SO(d)$ or some other global symmetry. We have used $[\dots]$ to denote anti-symmetrization. If the indices are taken to run over a finite set $\{1,\dots,m\}$, these operators are null for $n > m$. However, this restriction disappears as soon as we let $m$ vary continuously. Analyticity then dictates that $\left\langle \mathcal{O}^{[i_1\cdots i_n]}(\infty)\mathcal{O}^{[j_1\cdots j_n]}(0)\right\rangle$, as a function of $m$, have zeros at all integers from 0 to $n-1$. Without an infinite amount of fine-tuning, we expect some of these zeros to be first order, leading to negative norms in the theories that interpolate between those of greatest physical interest. This was shown to be the case for the Wilson-Fisher fixed-point in [125]. The essential operator to consider was

$$\delta^{[\mu_1}_{[\nu_1}\delta^{\mu_2}_{\nu_2}\delta^{\mu_3}_{\nu_3}\delta^{\mu_4}_{\nu_4}\delta^{\mu_5]}_{\nu_5]}\partial_{\mu_1}\partial^{\nu_1}\phi\partial_{\mu_2}\partial^{\nu_2}\phi\partial_{\mu_3}\partial^{\nu_3}\phi\partial_{\mu_4}\partial^{\nu_4}\phi\partial_{\mu_5}\partial^{\nu_5}\phi \tag{3.1}$$

which is not primary but has a negative norm below $d = 4$.

The fact that Wilson-Fisher fixed-points belong to the allowed region in Figure 3.1 is usually attributed to the black-box nature of the numerics — norms are still positive for operators of a reasonably low dimension so it is unclear how difficult it will be to exclude these theories. There are several other analytic continuation procedures available if we wish to see more examples of unitarity violation. One choice is to continue $d$ in a fixed-point that may be reached from a theory of free fermions. The end of this chapter presents a host of surprising phenomena that can be seen in a fermionic version of [125]. Before returning to this issue, it is worth analyzing a continuation that can be done in *fixed* dimension. It is interesting focus on $d = 2$ and varry the parameter $m$ that labels the well known minimal models $\mathcal{M}(m+1,m)$. Thanks to Virasoro symmetry, the unitarity violation can be investigated non-perturbatively allowing us to arrive at an interesting conclusion: the points corresponding to non-unitary values of $m$ in the simplest numerical plots will never disappear.

We begin by discussing the Virasoro algebra for central charge $c$

$$[L_m, L_n] = (m-n)L_{m+n} + \frac{c}{12}m(m-1)(m+1)\delta_{m+n,0}\ , \tag{3.2}$$

which is ubiquitous for CFTs in two dimensions. The power of this infinite-dimensional symmetry was perhaps most famously demonstrated in [12] with the discovery of the minimal models. In addition to providing an exact solution, representation theory of the Virasoro algebra enabled [104, 105, 126, 127] to show that these models are the only unitary CFTs in two dimensions with $c < 1$. However, one can also see hints of the special role played by minimal models in a numerical bootstrap which uses only the global conformal transformations — two copies of $\mathfrak{sl}(2)$. Exclusion plots, based on crossing symmetry and unitarity, are shown in Figure 3.2 where a straight line containing the minimal models is clearly visible. Specifically, the upper bound

$$\Delta_\epsilon = \frac{1}{3}(8\Delta_\sigma + 2)\ , \tag{3.3}$$

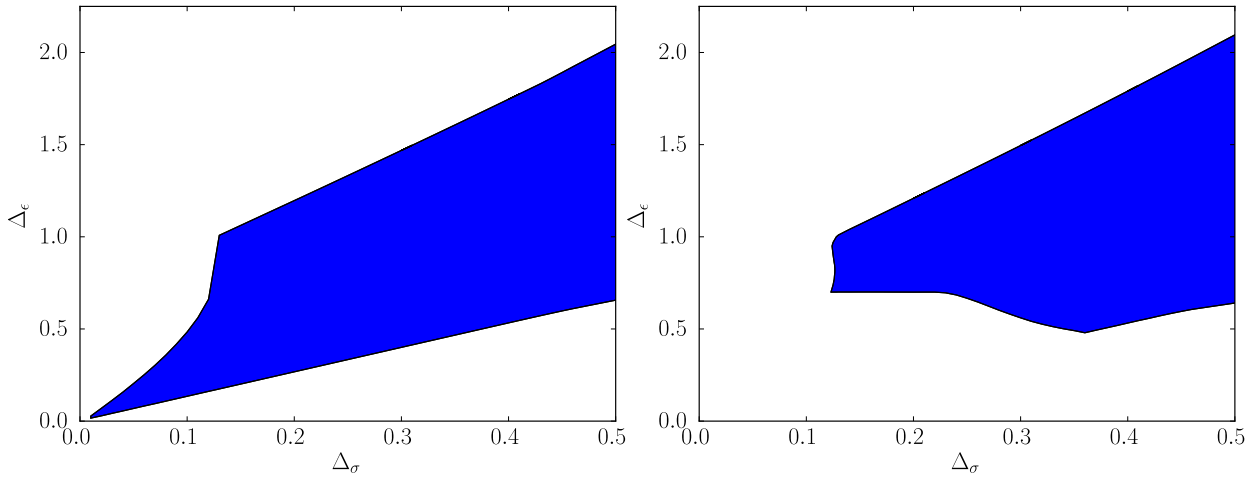


(a) One correlator (b) Three correlators

Figure 3.2: Allowed regions for the dimensions of $\sigma$ and $\epsilon$ — the $\mathbb{Z}_2$-odd scalar of smallest dimension and the $\mathbb{Z}_2$-even scalar of smallest dimension respectively. The left plot follows from the constraints of crossing symmetry and unitarity on the four-point function $\langle\sigma\sigma\sigma\sigma\rangle$. The right plot comes from the same constraints on $\langle\sigma\sigma\sigma\sigma\rangle$, $\langle\sigma\sigma\epsilon\epsilon\rangle$ and $\langle\epsilon\epsilon\epsilon\epsilon\rangle$. In both cases, all OPEs are restricted to contain only one relevant scalar.

is realized by the generalized minimal model four-point function $\langle\sigma\sigma\sigma\sigma\rangle$ if we identify $\sigma \equiv \phi_{1,2}$ and $\epsilon \equiv \phi_{1,3}$.[1] The authors of [128] observed squared OPE coefficients of quasiprimaries in this correlator that were all positive. If this conjecture is correct, we must conclude that in an arbitrary $\mathcal{M}(m+1,m)$ theory, the non-unitarity is mild enough that it cannot be diagnosed from the correlator of four $\sigma$ operators. Note that the kink present at the Ising point, $(\Delta_\sigma, \Delta_\epsilon) = \left(\frac{1}{8}, 1\right)$ is robust than the analogous kink in the three-dimensional case [77, 78, 129]. It does not sharpen into an island when three correlators are used to restrict the number of relevant operators.

Studying the $\frac{1}{8} \leq \Delta_\sigma \leq \frac{1}{2}$ part of the bound as in [128], we will put the one-correlator upper bound on a more rigorous footing and explain why the three-correlator upper bound is unchanged. Our results are summarized in Table 3.1 which shows that for $3 < m < 4$, $\langle\sigma\sigma\sigma\sigma\rangle$ is a *unitary subsector* meaning that other correlators are necessary for seeing the negative norms manifest themselves in the squared OPE coefficients.[2] It appears that the generalized minimal models with $m > 4$ have larger unitary subsectors that include the other two four-point functions. The last line shows a surprising tension with Figure 3.2. Despite

[1] This notation differs from the statistical physics literature in which it is natural to regard $\phi_{2,2}$ as the spin-field.

[2] Looking ahead, the decompositions (3.37) and (3.40) are essential for the positivity proof. We have learned that they were previously obtained, through a slightly different method, in unpublished work by Mikhail Isachenkov and Volker Schomerus.

| Correlator | $3 < m < 4$ | $4 < m < \infty$ |
|---|---|---|
| $\langle\sigma\sigma\sigma\sigma\rangle$ | All coefficients $\geq 0$ | All coefficients $\geq 0$ |
| $\langle\sigma\sigma\epsilon\epsilon\rangle$ | One checked coefficient $< 0$ | All checked coefficients $\geq 0$ |
| $\langle\epsilon\epsilon\epsilon\epsilon\rangle$ | Infinitely many coefficients $< 0$ | All checked coefficients $\geq 0$ |

Table 3.1: The status of three-correlator $\mathfrak{sl}(2)$ block coefficients in the generalized minimal models. Statements about $\langle\sigma\sigma\sigma\sigma\rangle$ apply rigorously to the full set of coefficients. For the other two correlators, we have manually decomposed them up to order 15.

the fact that $\langle\epsilon\epsilon\epsilon\epsilon\rangle$ displays significant unitarity violation for $m < 4$, the line (3.3) in the three-correlator exclusion plot is uninterrupted. The numerics are telling us that there is a partial solution to crossing, other than $\mathcal{M}(m+1, m)$, which fills in this region. Using the properties of minimal models, we will show that the existence of this solution can be concluded from a *simpler* numerical setup. It would be nice to eventually find a fully analytic construction.

## 3.1 Generalized minimal models

In order to have a unitary 2D CFT with $c < 1$, it is necessary that all primary operators have conformal weights equal to Kac's formula $h_{r,s}(c)$ for some $(r, s)$. The Kac table of degenerate weights is given by

$$\begin{aligned} c &= 1 - \frac{6}{m(m+1)} \qquad m > 2 \\ h_{r,s} &= \frac{[(m+1)r - ms]^2 - 1}{4m(m+1)} \quad r, s \in \mathbb{Z}_{>0} \,. \end{aligned} \tag{3.4}$$

Each of these Verma modules has a null state at level $rs$. In the operator product expansion (OPE) of primary operators $\phi_{r,s}$ and $\phi_{r',s'}$, the new conformal families that appear are captured in the fusion rule

$$\phi_{r,s} \times \phi_{r',s'} = \sum_{k=0}^{\left\lfloor \frac{r+r'-|r-r'|-2}{2} \right\rfloor} \sum_{l=0}^{\left\lfloor \frac{s+s'-|s-s'|-2}{2} \right\rfloor} \phi_{|r-r'|+2k+1,|s-s'|+2l+1} \,. \tag{3.5}$$

For generic values of $m$, this leads to an infinite discrete spectrum. All OPEs are finite, but as we raise the values of $r$ and $s$, these sums become arbitrarily long. A special situation occurs when $m$ is an integer. This precisely describes a central charge for which $h_{r,s}(c) = h_{m-r,m+1-s}(c)$. The Kac table for these doubly degenerate weights can be shown to truncate, allowing us to consider only $0 < r < m$ and $0 < s < m+1$. This leads to a finite number

of primary operators and, as it turns out, a unitary theory. This theory, called a (unitary) minimal model, is often denoted $\mathcal{M}(m+1,m)$. Since Figure 3.2 only shows a kink for $m=3$, it is evident that non-integer values of $m$ are still important for the bootstrap. This is the subject of the current section — the generic $\mathcal{M}(m+1,m)$, found to be a solvable consistent theory and referred to as a *generalized minimal model* in [130, 131].[3] It obeys the 2D CFT axioms of associativity and Virasoro symmetry but not unitary [132].

The first null descendant of $|h_{r,s}\rangle$, dual to a degenerate operator in a generalized minimal model, will be denoted by $|\chi_{r,s}\rangle$ which is also called a singular vector. Four-point functions may be calculated once the necessary singular vectors are known. For the correlators of interest to us, the rules for converting $\chi_{r,s}$ to a differential operator may be summarized by

$$\begin{aligned} L_{-n} \mapsto \mathcal{L}_{-n} &= \sum_{i\neq 1} \frac{h_i(n-1)}{(z_i-z_1)^n} - \frac{\partial_i}{(z_i-z_1)^{n-1}} \\ L_{-1} \mapsto \mathcal{L}_{-1} &= \partial_1 \,. \end{aligned} \tag{3.6}$$

After applying the Ward identities in this way, we use the fact that this operator must annihilate any correlation function involving $\phi_{r,s}$ in the first position. The resulting equation, known as a BPZ differential equation [12], has $rs$ linearly independent solutions representing the exchanged multiplets. One may read off their dimensions by looking at the $O(z^h)$ behaviour as $z\to 0$. While expressions for singular vectors are generally non-trivial, with some appearing only recently [133–135], the ones we need are relatively simple:

$$\begin{aligned} |\chi_{1,s}\rangle &= \sum_{p_1+\cdots+p_k=s} \frac{(-t)^{s-k}[(s-1)!]^2}{\prod_{i=1}^{k-1}(p_1+\cdots+p_i)(s-p_1-\cdots-p_i)} L_{-p1}\ldots L_{-p_k}|h_{1,s}\rangle \\ t &\equiv \frac{m}{m+1} \,. \end{aligned} \tag{3.7}$$

It is clear that we may confine ourselves to the border of the Kac table when studying correlators of $\sigma\equiv\phi_{1,2}$ and $\epsilon\equiv\phi_{1,3}$. The set of operators $\phi_{1,s}$ which closes under fusion is called the Verlinde subalgebra. We will continue to parametrize the generalized minimal model by $\Delta_\sigma$ — the horizontal axis of Figure 3.2. For convenience, Table 3.2 summarizes the OPEs that are important for the simplest mixed correlator system.

Before deriving the results in Table 3.1 for the upper bound (3.3), it is instructive to consider the lower bound

$$\Delta_\epsilon = \frac{4}{3}\Delta_\sigma \,, \tag{3.8}$$

which appears on the left side of Figure 3.2. This gives us a more straightforward opportunity to use the techniques in [136, 137]. The explicit solution for $\langle\sigma\sigma\sigma\sigma\rangle$ along this line was found

[3] This should not be confused with *non-unitary minimal model*, which describes a non-unitary $c<1$ theory with finitely many primaries. This discrete set is denoted $\mathcal{M}(p,q)$ with $p$ and $q$ relatively prime.

| Fusion rules | Weights |
|---|---|
| $\phi_{1,2} \times \phi_{1,2} = \phi_{1,1} + \phi_{1,3}$ | $h_{1,1} = 0$ |
| $\phi_{1,2} \times \phi_{1,3} = \phi_{1,2} + \phi_{1,4}$ | $h_{1,2} = \frac{\Delta_\sigma}{2}$ |
| $\phi_{1,3} \times \phi_{1,3} = \phi_{1,1} + \phi_{1,3} + \phi_{1,5}$ | $h_{1,3} = \frac{4\Delta_\sigma+1}{3} \equiv \frac{\Delta_\epsilon}{2}$ |
| | $h_{1,4} = \frac{5\Delta_\sigma+2}{2}$ |
| | $h_{1,5} = 4\Delta_\sigma + 2$ |

Table 3.2: Operators that can appear in $\langle\sigma\sigma\sigma\sigma\rangle$, $\langle\sigma\sigma\epsilon\epsilon\rangle$, $\langle\epsilon\epsilon\epsilon\epsilon\rangle$ and their holomorphic weights. The fusion rules would shorten *e.g.* in the Ising model $m = 3$ and tricritical Ising model $m = 4$, but we are interested in $\mathcal{M}(m+1, m)$ for real $m$.

in [85], which focused on its special role in the non-unitary (severe truncation) bootstrap of [138–140].[4] This solution exhibits Virasoro symmetry with a central charge given by

$$c = 1 + 16\Delta_\sigma \tag{3.9}$$

but no Virasoro identity block. To find an analytic explanation for why this four-point function appears in the unitary bootstrap, one must be able to show that this vacuum decoupling is the only sign of non-unitarity that appears at the level of a single correlator. In other words, one must be able to repeat the logic of [128] and find positive squared OPE coefficients for all of the quasiprimaries that do appear. These will be seen as very large coefficients by the numerics because the algorithm used for Figure 3.2 fixes $\lambda_{\sigma\sigma I} = 1$. This is indeed what we find from the extremal functional method of [90].

### 3.1.1 The lower line: A warm-up

The four-point function along the line (3.8) consists of a single Virasoro block $V(h_i, h, c; z)$. It was found in [85] via the Coulomb gas formalism which writes the central charge as $c = 1 - 24\alpha_0^2$ and places a background charge of $2\alpha_0$ at infinity. This allows a number of four-point functions to be realized as correlators of vertex operators with additional insertions of screening charges. The simplest of these is a correlator of four scalars that all have charge $\frac{\alpha_0}{2}$. Since the neutrality condition for this is satisfied without any screening charges, one finds the manifestly crossing symmetric

$$\begin{aligned}\langle\sigma(0)\sigma(z,\bar{z})\sigma(1)\sigma(\infty)\rangle &= V\left(-\frac{3}{4}\alpha_0^2, -\alpha_0^2, 1-24\alpha_0^2; z\right) V\left(-\frac{3}{4}\alpha_0^2, -\alpha_0^2, 1-24\alpha_0^2; \bar{z}\right) \\ &= |z(1-z)|^{\alpha_0^2}\,,\end{aligned} \tag{3.10}$$

[4]The fact that it also appears in the unitary bootstrap has not received much attention. In [14], it was mentioned that the lower bound at $\Delta_\sigma = \frac{1}{8}$ was somewhat close to $\Delta_\epsilon = \frac{1}{6}$. Interestingly, the region below the bound coincides with the region where standard OPE maximization techniques cannot constrain the central charge [141].

where we have used $h = \alpha(\alpha - 2\alpha_0)$. Expressing (3.10) in terms of $\Delta_\sigma$,

$$\begin{aligned} \langle \sigma(0)\sigma(z,\bar{z})\sigma(1)\sigma(\infty)\rangle &= \frac{g(z)g(\bar{z})}{|z|^{2\Delta_\sigma}} \\ g(z) &= z^{\frac{2}{3}\Delta_\sigma}(1-z)^{-\frac{1}{3}\Delta_\sigma} \ . \end{aligned} \tag{3.11}$$

Our task now is to expand $g(z)$ into $\mathfrak{sl}(2)$ blocks:

$$\begin{aligned} g(z) &= \sum_{n=0}^{\infty} c_n K_{\frac{2}{3}\Delta_\sigma+n}(z) \\ K_h(z) &\equiv z^h {}_2F_1(h,h;2h;z) \ . \end{aligned} \tag{3.12}$$

This is guaranteed to be an expansion in even integers due to the Bose symmetry of the $\sigma \times \sigma$ OPE. To proceed by the brute-force approach, we expand the hypergeometric function and switch the order of two sums.

$$\begin{aligned} g(z) &= \sum_{n=0}^{\infty}\sum_{m=0}^{\infty} c_n \frac{\left(\frac{2}{3}\Delta_\sigma + n\right)_m^2}{\left(\frac{4}{3}\Delta_\sigma + 2n\right)_m} \frac{z^{\frac{2}{3}\Delta_\sigma+n+m}}{m!} \\ &= \sum_{k=0}^{\infty}\sum_{n=0}^{k} c_n \frac{\left(\frac{2}{3}\Delta_\sigma + n\right)_{k-n}^2}{\left(\frac{4}{3}\Delta_\sigma + 2n\right)_{k-n}} \frac{z^{\frac{2}{3}\Delta_\sigma+k}}{(k-n)!} \end{aligned} \tag{3.13}$$

We may now compare the inner finite sums to the Taylor coefficients of (3.11), given by $b_k = \frac{(\frac{1}{3}\Delta_\sigma)_k}{k!}$. Since the lower triangular system for $c_n$ yields to back-substitution,

$$c_{2k} = b_{2k} - \sum_{n=0}^{k-1} c_{2n} \frac{\left(\frac{2}{3}\Delta_\sigma + 2n\right)_{2(k-n)}^2}{\left(\frac{4}{3}\Delta_\sigma + 4n\right)_{2(k-n)}} \frac{1}{(2k-2n)!} \ . \tag{3.14}$$

Rather than using this recursive procedure, we will now review a method for computing the $c_n$ directly. The blocks, defined in (3.12), are eigenfunctions of the conformal Casimir

$$\begin{aligned} DK_h(z) &= h(h-1)K_h(z) \\ D &= z^2(1-z)\frac{\partial^2}{\partial z^2} - z^2\frac{\partial}{\partial z} \ . \end{aligned} \tag{3.15}$$

It is well known that $D$ is self-adjoint on $[0,1]$ with respect to the measure $z^{-2}$. The authors of [136] used this fact to develop the Sturm-Liouville theory of this operator and construct

the orthogonal eigenfunctions

$$\Psi_h(z) = \frac{\Gamma(1-2h)}{\Gamma(1-h)^2} K_h(z) + (h \leftrightarrow 1-h) \ . \tag{3.16}$$

It is convenient to set $h = \frac{1}{2} + \alpha$ in which case (3.16) becomes a function $\Psi_\alpha(z)$ which is even in $\alpha$. In order for it to have a finite norm, $\alpha$ cannot be real. We must go to imaginary dimension space and take $\alpha \in i\mathbb{R}$.[5] The result is that to any four-point function $f(z)$, we may associate a density $\hat{f}(\alpha) = \hat{f}(-\alpha)$ via the invertible transform

$$\begin{aligned} f(z) &= \frac{1}{2\pi i} \int_{-i\infty}^{i\infty} \hat{f}(\alpha) \Psi_\alpha(z) \frac{\mathrm{d}\alpha}{N(\alpha)} \\ N(\alpha) &\equiv \frac{\Gamma(\alpha)\Gamma(-\alpha)}{2\pi\Gamma(\frac{1}{2}+\alpha)\Gamma(\frac{1}{2}-\alpha)} \ . \end{aligned} \tag{3.17}$$

It is now clear that OPE coefficients may be read off from the residues of $\hat{f}(\alpha)$ whenever its poles are on the real axis. A formula that [136, 137] derived using this method is

$$z^p (1-z)^{-q} = \sum_{n=0}^{\infty} \frac{(p)_n^2}{(2p+n-1)_n n!} {}_3F_2 \left( \begin{matrix} -n, 2p+n-1, p-q \\ p, p \end{matrix} ; 1 \right) K_{p+n}(z) \ . \tag{3.18}$$

We will use this in the current analysis and the next one.

Specializing (3.18) to the four-point function (3.11), we immediately find

$$c_n = \frac{\left(\frac{2}{3}\Delta_\sigma\right)_n^2}{\left(\frac{4}{3}\Delta_\sigma + n - 1\right)_n n!} {}_3F_2 \left( \begin{matrix} -n, \frac{4}{3}\Delta_\sigma + n - 1, \frac{1}{3}\Delta_\sigma \\ \frac{2}{3}\Delta_\sigma, \frac{2}{3}\Delta_\sigma \end{matrix} ; 1 \right) \ . \tag{3.19}$$

There are two ways to assess the positivity of (3.19). The first is to recall the definition of a continuous Hahn polynomial [142].

$$\tilde{P}_n(a,b,c,d;x) = {}_3F_2 \left( \begin{matrix} -n, n+a+b+c+d-1, a+x \\ a+c, a+d \end{matrix} ; 1 \right) \tag{3.20}$$

Clearly,

$$c_n = \frac{\left(\frac{2}{3}\Delta_\sigma\right)_n^2}{\left(\frac{4}{3}\Delta_\sigma + n - 1\right)_n n!} \tilde{P}_n \left( \frac{2}{3}\Delta_\sigma, \frac{2}{3}\Delta_\sigma, 0, 0; -\frac{1}{3}\Delta_\sigma \right) \ , \tag{3.21}$$

is a valid rewriting of (3.19).[6] Suppressing their parameters, the polynomials $\tilde{P}_n(a,b,c,d;x)$

[5] There is another name for this space as evidenced by the title of [136].

[6] In the notation of [143], we would write $c_n = \frac{2^{-n}}{n!} Q_{n,0}^{\frac{4}{3}\Delta_\sigma + n}\left(-\frac{1}{3}\Delta_\sigma\right)$.

satisfy the following recurrence relation:

$$\begin{aligned}(x+a)\tilde{P}_n(x) &= A_n\tilde{P}_{n+1}(x) - (A_n+B_n)\tilde{P}_n(x) + B_n\tilde{P}_{n-1}(x)\\ A_n &\equiv -\frac{(n+a+b+c+d-1)(n+a+c)(n+a+d)}{(2n+a+b+c+d-1)(2n+a+b+c+d)}\\ B_n &\equiv \frac{n(n+b+c-1)(n+b+d-1)}{(2n+a+b+c+d-2)(2n+a+b+c+d-1)}\,.\end{aligned} \tag{3.22}$$

For our parameters, we may easily check that $A_n+B_n+a+x=0$. It then follows by induction that all $c_{2k+1}$ vanish. Once we know this, (3.22) is effectively a two-term recursion. Seeing a positive constant of proportionality in

$$\begin{aligned}\tilde{P}_{2k}\left(-\frac{1}{3}\Delta_\sigma\right) &= -\frac{B_{2k-1}}{A_{2k-1}}\tilde{P}_{2k-2}\left(-\frac{1}{3}\Delta_\sigma\right)\\ &= \frac{3(2k-1)(\Delta_\sigma+3k-3)}{(2\Delta_\sigma+3k-3)(2\Delta_\sigma+6k-3)}\tilde{P}_{2k-2}\left(-\frac{1}{3}\Delta_\sigma\right)\,,\end{aligned} \tag{3.23}$$

we conclude that the sequence $c_{2k}$ decays to zero monotonically from above. It is therefore imperative that the bootstrap single out a region that includes (3.8). To derive this without referring to continuous Hahn polynomials, one may instead express $c_n$ in terms of gamma functions. This is possible because Watson's theorem [144],

$${}_3F_2\left(\begin{matrix}a,b,c\\ \frac{a+b+1}{2},2c\end{matrix};1\right) = \frac{\Gamma(\frac{1}{2})\Gamma(\frac{1+a+b}{2})\Gamma(\frac{1}{2}+c)\Gamma(\frac{1-a-b}{2}+c)}{\Gamma(\frac{1+a}{2})\Gamma(\frac{1+b}{2})\Gamma(\frac{1-a}{2}+c)\Gamma(\frac{1-b}{2}+c)} \tag{3.24}$$

applies whenever $p=2q$ in (3.18). Although $\Re(a+b-2c)<1$ is usually needed for convergence, we may drop this requirement for a hypergeometric function that terminates.

This analysis does not explain why (3.8) saturates the lower bound in the one-correlator result of Figure 3.2. However, it is encouraging that bounds of this form in one dimension have been proven in [116]. The Coulomb gas formalism does not yield an obvious way to solve for the correlators $\langle\sigma\sigma\epsilon\epsilon\rangle$, $\langle\epsilon\epsilon\epsilon\epsilon\rangle$ or even to verify that they exist. Because the three-correlator plot in Figure 3.2 excludes this line, any theory to which $\langle\sigma\sigma\sigma\sigma\rangle$ could extend would have to be highly non-unitary.

In this section, we have seen two methods for proving that global block coefficients in (3.11) are positive. One uses Watson's theorem and the other uses a recurrence relation for orthogonal polynomials. We will need both of these methods when we prove positivity in the generalized minimal models. Before moving on, there is an interesting way to check our results in a spacetime with Minkowski signature. Even though (3.11) is not strictly a correlation function in a unitary theory, it is still bounded in the Regge limit. Its $\mathfrak{sl}(2)$ block expansion should therefore be calculable with the conformal Froissart-Gribov formula [39]

which in our case reads

$$\begin{aligned} c(\Delta,\ell) &= \kappa_{\Delta+\ell}\int_0^1\int_0^1 K_{\frac{\Delta+\ell}{2}}(z)K_{\frac{\ell-\Delta+2}{2}}(\bar{z})\text{dDisc}[|z|^{2\Delta_\sigma}\langle\sigma(0)\sigma(z,\bar{z})\sigma(1)\sigma(\infty)\rangle]\frac{\mathrm{d}z}{z^2}\frac{\mathrm{d}\bar{z}}{\bar{z}^2} \\ \kappa_\beta &\equiv \frac{\Gamma(\frac{\beta}{2})^4}{2\pi^2\Gamma(\beta-1)\Gamma(\beta)}\,. \end{aligned} \tag{3.25}$$

To define the double-discontinuity, we must treat $z,\bar{z}$ as independent variables and rotate around the $\bar{z}=1$ branch point. Since this can be done in two ways, we subtract the average from our four-point function to find

$$\text{dDisc}\left[g(z)g(\bar{z})\right] = 2\sin^2\left(\frac{\pi\Delta_\sigma}{3}\right)(z\bar{z})^{\frac{2}{3}\Delta_\sigma}[(1-z)(1-\bar{z})]^{-\frac{1}{3}\Delta_\sigma}\,. \tag{3.26}$$

Performing the factored integrals yields a spectral density given by

$$\begin{aligned} \frac{c(\Delta,\ell)\Gamma(1-\frac{1}{3}\Delta_\sigma)^{-2}}{2\sin^2\left(\frac{\pi\Delta_\sigma}{3}\right)\kappa_{\Delta+\ell}} &= \frac{\Gamma(\frac{2}{3}\Delta_\sigma+\frac{\ell-\Delta}{2})}{\Gamma(\frac{1}{3}\Delta_\sigma+\frac{\ell-\Delta+2}{2})}{}_3F_2\left(\begin{matrix}\frac{\ell-\Delta+2}{2},\frac{\ell-\Delta+2}{2},\frac{2}{3}\Delta_\sigma+\frac{\ell-\Delta}{2}\\ \ell-\Delta+2,\frac{1}{3}\Delta_\sigma+\frac{\ell-\Delta+2}{2}\end{matrix};1\right) \\ &\quad \frac{\Gamma(\frac{2}{3}\Delta_\sigma+\frac{\Delta+\ell-2}{2})}{\Gamma(\frac{1}{3}\Delta_\sigma+\frac{\Delta+\ell}{2})}{}_3F_2\left(\begin{matrix}\frac{\Delta+\ell}{2},\frac{\Delta+\ell}{2},\frac{2}{3}\Delta_\sigma+\frac{\Delta+\ell-2}{2}\\ \Delta+\ell,\frac{1}{3}\Delta_\sigma+\frac{\Delta+\ell}{2}\end{matrix};1\right) \end{aligned} \tag{3.27}$$

with poles at $\Delta-\ell=\frac{4}{3}\Delta_\sigma+2n$. As none of these are integers, the correct prescription for finding OPE coefficients is to simply take the residue [39].

$$\begin{aligned} -\text{Res}\left(c(\Delta,\ell),n\right) &= \frac{(-1)^n}{n!}\frac{8\sin^2\left(\frac{\pi\Delta_\sigma}{3}\right)\kappa_{\frac{4}{3}\Delta_\sigma+2\ell+2n}\Gamma(1-\frac{1}{3}\Delta_\sigma)^2\Gamma(\frac{4}{3}\Delta_\sigma+n+\ell-1)}{\Gamma(\Delta_\sigma+\ell+n)\Gamma(1-\frac{1}{3}\Delta_\sigma-n)} \\ &\quad {}_3F_2\left(\begin{matrix}\frac{4}{3}\Delta_\sigma+\ell+n-1,\frac{2}{3}\Delta_\sigma+\ell+n,\frac{2}{3}\Delta_\sigma+\ell+n\\ \Delta_\sigma+\ell+n,\frac{4}{3}\Delta_\sigma+2\ell+2n\end{matrix};1\right) \\ &\quad {}_3F_2\left(\begin{matrix}-n,1-n-\frac{2}{3}\Delta_\sigma,1-n-\frac{2}{3}\Delta_\sigma\\ 1-n-\frac{1}{3}\Delta_\sigma,2-2n-\frac{4}{3}\Delta_\sigma\end{matrix};1\right) \end{aligned} \tag{3.28}$$

Although it is not obvious, we have checked that (3.28) is equal to $c_n c_{n+\ell}$ by using Watson's theorem twice.

### 3.1.2 The upper line with one correlator

We will now derive new expressions for the squared OPE coefficients in $\langle\sigma\sigma\sigma\sigma\rangle$ along (3.3). Positivity, as predicted by [128], will then follow from methods analogous to those in the last

section. Since this correlator solves a second-order BPZ equation, we may write it as

$$\langle\sigma(z_1,\bar{z}_1)\sigma(z_2,\bar{z}_2)\sigma(z_3,\bar{z}_3)\sigma(z_4,\bar{z}_4)\rangle = \frac{G(z,\bar{z})}{|z_{12}z_{34}|^{2\Delta_\sigma}}$$
$$G(z,\bar{z}) = G^{\sigma\sigma\sigma\sigma}_{(1,1)}(z)G^{\sigma\sigma\sigma\sigma}_{(1,1)}(\bar{z}) + C^{(1,3)}_{(1,2)(1,2)}G^{\sigma\sigma\sigma\sigma}_{(1,3)}(z)G^{\sigma\sigma\sigma\sigma}_{(1,3)}(\bar{z}) \ , \tag{3.29}$$

where the functions of $z$ are Virasoro blocks.[7] The specific operator, read off from (3.7), is

$$\frac{3}{2(\Delta_\sigma+1)}\mathcal{L}_{-1}^2 - \mathcal{L}_{-2} \ . \tag{3.30}$$

Acting on (3.29) with (3.30), we arrive at a PDE in terms of $(z_1,z_2,z_3,z_4)$. To reduce it to an ODE, we map these points to $(0,z,1,\infty)$ by a global conformal transformation:

$$\frac{3}{2}z(z-1)^2\frac{\partial^2 G}{\partial z^2} + (z-1)[(2-\Delta_\sigma)z + 2\Delta_\sigma - 1]\frac{\partial G}{\partial z} - \frac{1}{2}\Delta_\sigma(\Delta_\sigma+1)zG = 0 \ . \tag{3.31}$$

Well known solutions, which have the expected asymptotic behaviour, are

$$\begin{aligned} G^{\sigma\sigma\sigma\sigma}_{(1,1)}(z) &= (1-z)^{-\Delta_\sigma}{}_2F_1\left(-2\Delta_\sigma, \frac{1-2\Delta_\sigma}{3}; \frac{2-4\Delta_\sigma}{3}; z\right) \\ G^{\sigma\sigma\sigma\sigma}_{(1,3)}(z) &= z^{\frac{1+4\Delta_\sigma}{3}}(1-z)^{-\Delta_\sigma}{}_2F_1\left(\frac{1-2\Delta_\sigma}{3}, \frac{2+2\Delta_\sigma}{3}; \frac{4+4\Delta_\sigma}{3}; z\right) \ . \end{aligned} \tag{3.32}$$

First, let us look at the identity block. After a quadratic transformation, the hypergeometric function becomes a series in $\frac{z^2}{4z-4}$. This makes the formula (3.18) applicable if we set $p=2n$ and $q=n$.

$$G^{\sigma\sigma\sigma\sigma}_{(1,1)}(z) = {}_2F_1\left(-\Delta_\sigma, \frac{1+\Delta_\sigma}{3}; \frac{5-4\Delta_\sigma}{6}; \frac{1}{4}\frac{z^2}{z-1}\right) \tag{3.33}$$
$$= \sum_{n=0}^{\infty}\left(-\frac{1}{4}\right)^n \frac{(-\Delta_\sigma)_n\left(\frac{1+\Delta_\sigma}{3}\right)_n}{\left(\frac{5-4\Delta_\sigma}{6}\right)_n n!}\sum_{m=0}^{\infty}\frac{(2n)_m^2}{(4n+m-1)_m m!}{}_3F_2\left(\begin{matrix}-m, 4n+m-1, n\\ 2n, 2n\end{matrix};1\right)K_{2n+m}(z)$$

Exchanging the two sums, we find

$$c_{2k} = \sum_{n=0}^{k}\left(-\frac{1}{4}\right)^n \frac{(-\Delta_\sigma)_n\left(\frac{1+\Delta_\sigma}{3}\right)_n}{\left(\frac{5-4\Delta_\sigma}{6}\right)_n n!}\frac{(2n)_{2k-2n}^2}{(2n+2k-1)_{2k-2n}(2k-2n)!}{}_3F_2\left(\begin{matrix}2n-2k, 2n+2k-1, n\\ 2n, 2n\end{matrix};1\right) \tag{3.34}$$

[7] For the moment, we will be concerned with the global OPE coefficients contained within each one. The overall coefficients $C^{(r_3,s_3)}_{(r_1,s_1)(r_2,s_2)}$ are the generalized minimal model structure constants that were obtained with the Coulomb gas formalism in [107–109].

for the non-vanishing global block coefficients.[8] Since $p = 2q$, this hypergeometric is in a form that can be treated with Watson's theorem. When we apply this to the $c_{2k}$, one pole in the numerator cancels another in the denominator.[9]

$$
\begin{aligned}
{}_3F_2\left(\begin{array}{c} 2n-2k, 2n+2k-1, n \\ 2n, 2n \end{array};1\right) &= \frac{(-1)^{n+k}\Gamma(\frac{1}{2})\Gamma(n+\frac{1}{2})\Gamma(2n)}{\Gamma(n)\Gamma(n-k+\frac{1}{2})\Gamma(2n+2k-1)}\frac{(k-1)!}{(n-1)!} \\
&= \frac{(-1)^{n+k}\Gamma(2n)^2}{\Gamma(2n+2k-1)}\frac{\Gamma(n+k-\frac{1}{2})\Gamma(\frac{1}{2})}{\Gamma(n-k+\frac{1}{2})\Gamma(k+\frac{1}{2})}\lim_{\delta\to 0}\frac{2^{2k-1}(k-1)!}{[\Gamma(\delta)(\delta)_n]^2}
\end{aligned}
\tag{3.35}
$$

Above, we can easily see three gamma functions that will cancel when we multiply by $\frac{(2n)^2_{2k-2n}}{(2n+2k-1)_{2k-2n}(2k-2n)!}$. We have also written $\frac{1}{\Gamma(n)^2}$ in a limiting form for later convenience. After substituting (3.35), one must use the identities

$$
\Gamma(x+n) = \Gamma(x)(x)_n \quad , \quad \Gamma(x-n) = (-1)^n\frac{\Gamma(x)}{(1-x)_n} \tag{3.36}
$$

until each term of (3.34) only depends on $n$ through the Pochhammer symbol. This leads to

$$
\begin{aligned}
c_{2k} &= \binom{4k-2}{2k-1}^{-1}\lim_{\delta\to 0}\frac{1}{k(2k-1)\Gamma(\delta)^2}{}_4F_3\left(\begin{array}{c} -k, k-\frac{1}{2}, -\Delta_\sigma, \frac{1+\Delta_\sigma}{3} \\ \delta, \delta, \frac{5-4\Delta_\sigma}{6} \end{array};1\right) \\
&= \binom{4k-2}{2k-1}^{-1}\frac{\Delta_\sigma(1+\Delta_\sigma)}{5-4\Delta_\sigma}{}_4F_3\left(\begin{array}{c} 1-k, k+\frac{1}{2}, 1-\Delta_\sigma, \frac{4+\Delta_\sigma}{3} \\ 1, 2, \frac{11-4\Delta_\sigma}{6} \end{array};1\right) .
\end{aligned}
\tag{3.37}
$$

The $\epsilon$ block can be analyzed in the same way. Doing so will in fact be easier since we will not have to pass to the $\delta \to 0$ limit. Starting from

$$
G^{\sigma\sigma\sigma\sigma}_{(1,3)}(z) = z^{\frac{1+4\Delta_\sigma}{3}}(1-z)^{-\frac{1+4\Delta_\sigma}{6}}{}_2F_1\left(\frac{1+2\Delta_\sigma}{2}, \frac{1-2\Delta_\sigma}{6}; \frac{7+4\Delta_\sigma}{6}; \frac{1}{4}\frac{z^2}{z-1}\right) , \tag{3.38}
$$

we may use (3.18) with $p = \frac{1+4\Delta_\sigma}{3} + 2n$ and $q = \frac{1+4\Delta_\sigma}{6} + n$. This leads to

$$
\begin{aligned}
c_{2k} &= \sum_{n=0}^{k}\left(-\frac{1}{4}\right)^n\frac{\left(\frac{1+2\Delta_\sigma}{6}\right)_n\left(\frac{1+2\Delta_\sigma}{2}\right)_n}{\left(\frac{7+4\Delta_\sigma}{6}\right)_n n!}\frac{\left(\frac{1+4\Delta_\sigma}{3}+2n\right)^2_{2k-2n}}{\left(\frac{2+8\Delta_\sigma}{3}+2n+2k-1\right)_{2k-2n}(2k-2n)!} \\
&\quad {}_3F_2\left(\begin{array}{c} 2n-2k, \frac{2+8\Delta_\sigma}{3}+2n+2k-1, \frac{1+4\Delta_\sigma}{6}+n \\ \frac{1+4\Delta_\sigma}{3}+2n, \frac{1+4\Delta_\sigma}{3}+2n \end{array};1\right)
\end{aligned}
\tag{3.39}
$$

[8] We derived this by applying a quadratic transformation to (3.32) which makes the Bose symmetry manifest. By leaving the function in its original form, or by applying Euler / Pfaff transformations, we can derive other sums that are non-trivially equivalent to (3.34).

[9] Because we have not allowed for other poles, our expression for $c_{2k}$ will not be correct for $k = 0$. There is no need to treat this case separately as it is already clear that $c_0 = 1$.

which again allows us to use Watson's theorem. Employing (3.36) to perform the sum, we arrive at

$$c_{2k} = \frac{1}{4^k k!}\frac{\left(\frac{1+4\Delta_\sigma}{6}\right)_k^2}{\left(\frac{1+4\Delta_\sigma}{3}+k-\frac{1}{2}\right)_k}{}_4F_3\left(\begin{matrix}-k, \frac{1+4\Delta_\sigma}{3}+k-\frac{1}{2}, \Delta_\sigma+\frac{1}{2}, \frac{1-2\Delta_\sigma}{6} \\ \frac{1+4\Delta_\sigma}{6}, \frac{1+4\Delta_\sigma}{6}, \frac{7+4\Delta_\sigma}{6}\end{matrix};1\right) . \tag{3.40}$$

A useful observation about the hypergeometric functions in (3.37) and (3.40) is that they both have a parameter excess of 1. This means that they are Wilson polynomials [142].[10]

$$P_n(a,b,c,d;x) = {}_4F_3\left(\begin{matrix}-n, n+a+b+c+d-1, a+x, a-x \\ a+b, a+c, a+d\end{matrix};1\right) \tag{3.41}$$

Invoking this notation, our results are

$$\begin{aligned} c_{2n}^{\sigma\sigma(1,1)\sigma\sigma} &= \binom{4n-2}{2n-1}^{-1}\frac{\Delta_\sigma(1+\Delta_\sigma)}{5-4\Delta_\sigma}P_{n-1}\left(\frac{7-2\Delta_\sigma}{6}, \frac{4-2\Delta_\sigma}{6}, -\frac{1-2\Delta_\sigma}{6}, \frac{5+2\Delta_\sigma}{6}; \frac{1+4\Delta_\sigma}{6}\right) \\ c_{2n}^{\sigma\sigma(1,3)\sigma\sigma} &= \frac{1}{4^n n!}\frac{\left(\frac{1+4\Delta_\sigma}{6}\right)_n^2}{\left(\frac{1+4\Delta_\sigma}{3}+n-\frac{1}{2}\right)_n}P_n\left(\frac{2+2\Delta_\sigma}{3}, \frac{1}{2}, -\frac{1}{2}, -\frac{1}{2}; \frac{1+4\Delta_\sigma}{6}\right) . \end{aligned} \tag{3.42}$$

As with continuous Hahn polynomials, there is a recurrence relation that the Wilson polynomials satisfy.

$$\begin{aligned} (x^2-a^2)P_n(x) &= A_nP_{n+1}(x) - (A_n+B_n)P_n(x) + B_nP_{n-1}(x) \\ A_n &\equiv \frac{(n+a+b+c+d-1)(n+a+b)(n+a+c)(n+a+d)}{(2n+a+b+c+d-1)(2n+a+b+c+d)} \\ B_n &\equiv \frac{n(n+b+c-1)(n+b+d-1)(n+c+d-1)}{(2n+a+b+c+d-2)(2n+a+b+c+d-1)} \end{aligned} \tag{3.43}$$

In Appendix B, we use this recursion to solve for the asymptotic behaviour of Wilson polynomials and prove that the ones in (3.42) are positive.

### 3.1.3 The upper line with three correlators

Given our success at explaining the one-correlator results, the next logical step is to find the global block decompositions applicable to three correlators. We will start with $\langle\epsilon\epsilon\epsilon\epsilon\rangle$. Although this is another four-point function of identical scalars, the main difference compared to $\langle\sigma\sigma\sigma\sigma\rangle$ is the lack of a closed-form Virasoro block. Because a generic $\epsilon$ only has a null descendant at level 3, we will have to work with a third-order BPZ equation which does

[10] Note that we are using the normalization in [145]. There is another common normalization that makes the Wilson polynomial symmetric in $(a,b,c,d)$.

not have simple solutions analogous to (3.32). This makes the formula (3.14) important for finding low-lying OPE coefficients. The singular vector that must annihilate

$$\langle \epsilon(z_1,\bar{z}_1)\epsilon(z_2,\bar{z}_2)\epsilon(z_3,\bar{z}_3)\epsilon(z_4,\bar{z}_4)\rangle = \frac{G(z,\bar{z})}{|z_{12}z_{34}|^{2\Delta_\epsilon}} \tag{3.44}$$
$$G(z,\bar{z}) = G^{\epsilon\epsilon\epsilon\epsilon}_{(1,1)}(z)G^{\epsilon\epsilon\epsilon\epsilon}_{(1,1)}(\bar{z}) + C^{(1,3)}_{(1,3)(1,3)}G^{\epsilon\epsilon\epsilon\epsilon}_{(1,3)}(z)G^{\epsilon\epsilon\epsilon\epsilon}_{(1,3)}(\bar{z}) + C^{(1,5)}_{(1,3)(1,3)}G^{\epsilon\epsilon\epsilon\epsilon}_{(1,5)}(z)G^{\epsilon\epsilon\epsilon\epsilon}_{(1,5)}(\bar{z})$$

has four terms that can be read off from (3.7). The Virasoro commutation relations reduce it to the three term expression

$$\frac{4}{\Delta_\epsilon(\Delta_\epsilon+2)}\mathcal{L}_{-1}^3 - \frac{4}{\Delta_\epsilon}\mathcal{L}_{-2}\mathcal{L}_{-1} + \mathcal{L}_{-3}\ . \tag{3.45}$$

The null state condition that follows from (3.44) and (3.45) is

$$\begin{aligned}
&4z^2(z-1)^3\frac{\partial^3 G}{\partial z^3} + 4z(z-1)^2[(4-\Delta_\epsilon)z + 2\Delta_\epsilon - 2]\frac{\partial^2 G}{\partial z^2} \\
&-(z-1)[(\Delta_\epsilon^2 + 10\Delta_\epsilon - 8)z^2 + (3\Delta_\epsilon^2 - 14\Delta_\epsilon + 8)z - 3\Delta_\epsilon(\Delta_\epsilon - 2)]\frac{\partial G}{\partial z} \\
&+\Delta_\epsilon^2(\Delta_\epsilon+2)z(z-2)G = 0\ .
\end{aligned} \tag{3.46}$$

To approximate the Virasoro blocks that solve this, it will be helpful to use the Frobenius method.[11] Inserting the ansatz $G(z) = \sum_{k=-\infty}^{\infty} b_k z^{r+k}$, we may reindex the sum so that all terms carry the same power of $z$. This gives a recurrence relation for the coefficients.

$$\begin{aligned}
&[-4(k+r)(k+r-1) + 8(\Delta_\epsilon - 1)(k+r) + 3\Delta_\epsilon(2-\Delta_\epsilon)](k+r+1)b_{k+1} \\
&+2[6(k+r-1)(k+r-2) + 2(8-5\Delta_\epsilon)(k+r-1) + 3\Delta_\epsilon^2 - 10\Delta_\epsilon + 4](k+r)b_k \\
&-2\left[6(k+r-1)(k+r-2)(k+r-3) - 4(2\Delta_\epsilon - 5)(k+r-1)(k+r-2)\right. \\
&\left.+(\Delta_\epsilon^2 - 12\Delta_\epsilon + 8)(k+r-1) + \Delta_\epsilon^2(\Delta_\epsilon+2)\right] b_{k-1} \\
&+\left[4(k+r-2)(k+r-3)(k+r-4) + 4(4-\Delta_\epsilon)(k+r-2)(k+r-3)\right. \\
&\left.-(\Delta_\epsilon^2 + 10\Delta_\epsilon - 8)(k+r-2) + \Delta_\epsilon^2(\Delta_\epsilon+2)\right] b_{k-2} = 0
\end{aligned} \tag{3.47}$$

We will set $b_0 = 1$ and $b_k = 0$ for all $k < 0$. The values of $r$ that make this consistent (called roots of the indicial equation) are $h_{1,1}$, $h_{1,3}$ and $h_{1,5}$ as expected. We find them by demanding that $b_0$ drop out of (3.47) when $k = -1$. For each value of $r$, it is straightforward to iterate (3.47) and then feed the results into (3.14). Some of the OPE coefficients that follow from this are written in Table 3.3. Due to the appearance of the upper bound (3.3)

[11] Even though they describe exchanged weights of $h_{1,1}$ and $h_{1,3}$, we cannot reuse either of the expressions in (3.32). Unlike global blocks which only see dimension differences, Virasoro blocks depend on the external weights individually [146].

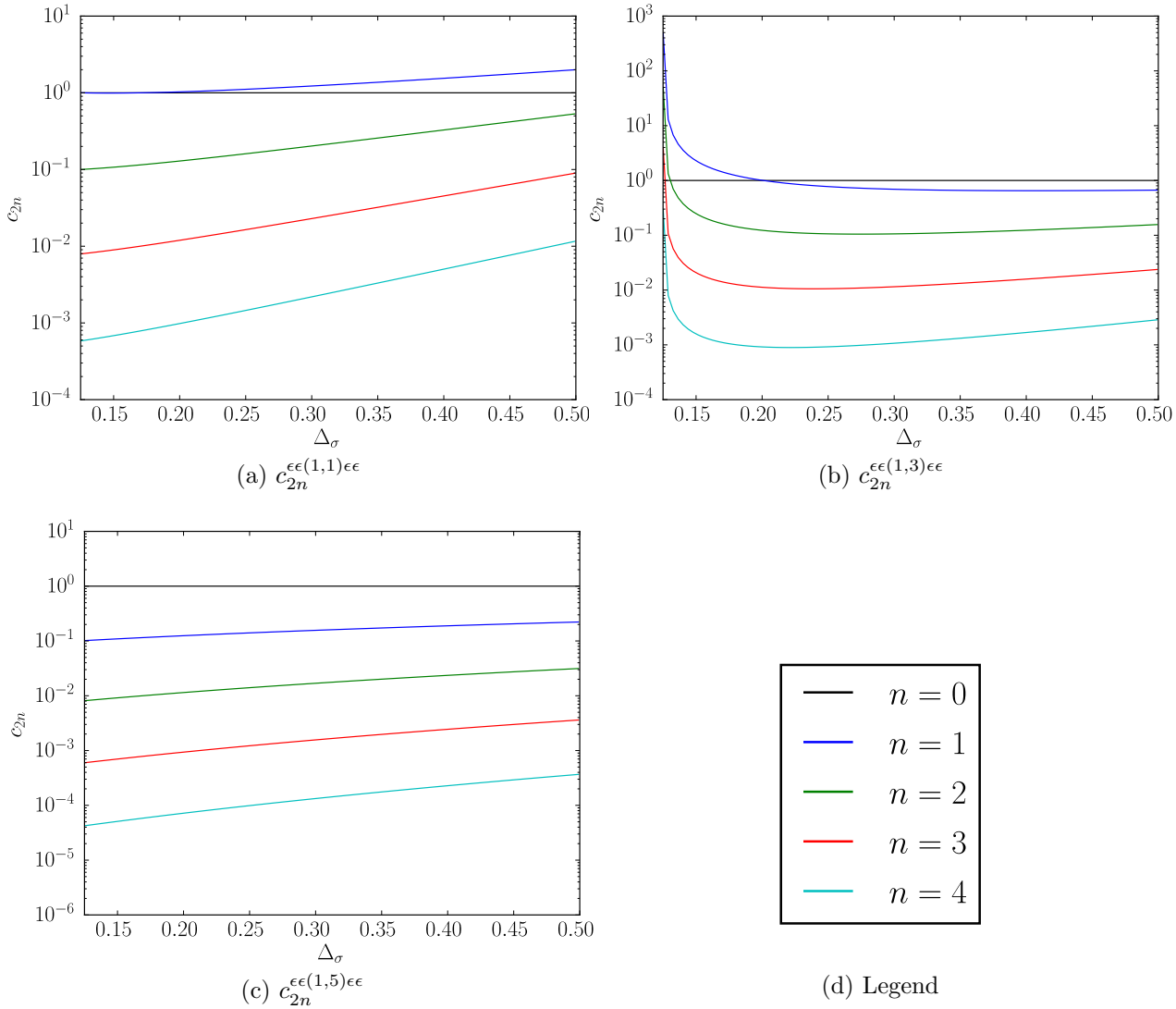


(a) $c_{2n}^{\epsilon\epsilon(1,1)\epsilon\epsilon}$ (b) $c_{2n}^{\epsilon\epsilon(1,3)\epsilon\epsilon}$

(c) $c_{2n}^{\epsilon\epsilon(1,5)\epsilon\epsilon}$ (d) Legend

Figure 3.3: Log-scale plots of $c_{2n}^{\epsilon\epsilon(1,s)\epsilon\epsilon}$ showing that the first five are all positive on the interval $\frac{1}{8} \leq \Delta_\sigma \leq \frac{1}{2}$.

in the three-correlator bootstrap, we expect the coefficients to be positive when $1 \leq \Delta_\epsilon \leq 2$, at least up to some high order. Figure 3.3 shows that this is indeed the case.

We should also be able to find positive squared OPE coefficients in the mixed correlator.

| $n$ | $c_{2n}^{\epsilon\epsilon(1,1)\epsilon\epsilon}$ |
|---|---|
| 0 | 1 |
| 1 | $-\frac{\Delta_\epsilon^2(\Delta_\epsilon+2)}{(\Delta_\epsilon-4)(3\Delta_\epsilon-2)}$ |
| 2 | $\frac{\Delta_\epsilon^2(\Delta_\epsilon+2)^2[5\Delta_\epsilon+2]}{30(\Delta_\epsilon-8)(\Delta_\epsilon-4)(3\Delta_\epsilon-2)}$ |
| $n$ | $c_{2n}^{\epsilon\epsilon(3,1)\epsilon\epsilon}$ |
| 0 | 1 |
| 1 | $\frac{\Delta_\epsilon^2(\Delta_\epsilon+2)[5\Delta_\epsilon+2]}{16(\Delta_\epsilon-1)(\Delta_\epsilon+1)(\Delta_\epsilon+4)}$ |
| 2 | $\frac{\Delta_\epsilon^2(\Delta_\epsilon+2)[25\Delta_\epsilon^5+167\Delta_\epsilon^4-66\Delta_\epsilon^3-1904\Delta_\epsilon^2-2752\Delta_\epsilon-384]}{512(\Delta_\epsilon-3)(\Delta_\epsilon-1)(\Delta_\epsilon+3)(\Delta_\epsilon+4)(\Delta_\epsilon+5)(\Delta_\epsilon+8)}$ |
| $n$ | $c_{2n}^{\epsilon\epsilon(5,1)\epsilon\epsilon}$ |
| 0 | 1 |
| 1 | $\frac{\Delta_\epsilon(\Delta_\epsilon+2)[7\Delta_\epsilon+6]}{48(\Delta_\epsilon+1)(\Delta_\epsilon+3)}$ |
| 2 | $\frac{\Delta_\epsilon(\Delta_\epsilon+2)[441\Delta_\epsilon^5+5121\Delta_\epsilon^4+20732\Delta_\epsilon^3+37796\Delta_\epsilon^2+31056\Delta_\epsilon+8640]}{1536(\Delta_\epsilon+3)(\Delta_\epsilon+5)(3\Delta_\epsilon+5)(3\Delta_\epsilon+7)(3\Delta_\epsilon+10)}$ |

Table 3.3: The first three global block coefficients in the $(1,1)$, $(1,3)$ and $(1,5)$ contributions found by taking the $\epsilon \times \epsilon$ OPE twice.

The four-point function

$$\langle\sigma(z_1,\bar{z}_1)\epsilon(z_2,\bar{z}_2)\sigma(z_3,\bar{z}_3)\epsilon(z_4,\bar{z}_4)\rangle = \left(\frac{|z_{24}|}{|z_{13}|}\right)^{\Delta_{\sigma\epsilon}} \frac{G(z,\bar{z})}{|z_{12}|^{\Delta_\sigma+\Delta_\epsilon}|z_{34}|^{\Delta_\sigma+\Delta_\epsilon}}$$
$$G(z,\bar{z}) = C^{(1,2)}_{(1,2)(1,3)} G^{\sigma\epsilon\sigma\epsilon}_{(1,2)}(z) G^{\sigma\epsilon\sigma\epsilon}_{(1,2)}(\bar{z}) + C^{(1,4)}_{(1,2)(1,3)} G^{\sigma\epsilon\sigma\epsilon}_{(1,4)}(z) G^{\sigma\epsilon\sigma\epsilon}_{(1,4)}(\bar{z}) \tag{3.48}$$

satisfies second-order and third-order BPZ equations.

For simplicity, we will consider the second-order equation

$$\frac{3}{2}z^2(z-1)^2\frac{\partial^2 G}{\partial z^2} + \frac{1}{2}z(z-1)[(2-7\Delta_\sigma)z+9\Delta_\sigma]\frac{\partial G}{\partial z}$$
$$+\frac{1}{24}[3\Delta_\sigma(11\Delta_\sigma+2)z^2 - 2(5\Delta_\sigma+2)(11\Delta_\sigma+2)z + 9\Delta_\sigma(5\Delta_\sigma+2)]G = 0 \tag{3.49}$$

which has the recurrence relation

$$\begin{aligned} &9[4(k+r+1)(k+r) - 12\Delta_\sigma(k+r+1) + \Delta_\sigma(5\Delta_\sigma+2)]b_{k+1} \\ &-2[36(k+r)(k+r-1) - 12(8\Delta_\sigma-1)(k+r) + (5\Delta_\sigma+2)(11\Delta_\sigma+2)]b_k \\ &+3[12(k+r-1)(k+r-2) + 4(2-7\Delta_\sigma)(k+r-1) + \Delta_\sigma(11\Delta_\sigma+2)]b_{k-1} = 0\ . \end{aligned} \tag{3.50}$$

It is easily seen that $r \in \{h_{1,2}, h_{1,4}\}$ is the solution of the indicial equation for (3.50). Because the product $\sigma \times \epsilon$ no longer has Bose symmetry, the procedure by which we extract the conformal block expansion this time is somewhat different. We must include dimension

differences in the hypergeometric function and sum over all integers whether even or odd.

$$\begin{aligned} G(z) &= \sum_{n=0}^{\infty}(-1)^n c_n z^{r+n}{}_2F_1\left(r+n-\frac{1}{2}\Delta_{\sigma\epsilon}, r+n+\frac{1}{2}\Delta_{\sigma\epsilon}; 2(r+n); z\right) \\ &= \sum_{n=0}^{\infty}\sum_{m=0}^{\infty}(-1)^n c_n \frac{\left(r+n-\frac{1}{2}\Delta_{\sigma\epsilon}\right)_m \left(r+n+\frac{1}{2}\Delta_{\sigma\epsilon}\right)_m}{(2r+2n)_m}\frac{z^{r+n+m}}{m!} \\ &= \sum_{k=0}^{\infty}\sum_{n=0}^{k}(-1)^n c_n \frac{\left(r+n-\frac{1}{2}\Delta_{\sigma\epsilon}\right)_{k-n} \left(r+n+\frac{1}{2}\Delta_{\sigma\epsilon}\right)_{k-n}}{(2r+2n)_{k-n}}\frac{z^{r+k}}{(k-n)!} \end{aligned} \tag{3.51}$$

The lower triangular system from this leads to the recursion

$$(-1)^k c_k = b_k - \sum_{n=0}^{k-1}(-1)^n c_n \frac{\left(r+n-\frac{1}{2}\Delta_{\sigma\epsilon}\right)_{k-n} \left(r+n+\frac{1}{2}\Delta_{\sigma\epsilon}\right)_{k-n}}{(2r+2n)_{k-n}(k-n)!} \ . \tag{3.52}$$

Some low-lying global block coefficients found with (3.52) are listed in Table 3.4. While all of them are non-negative above the tricritical Ising value $\Delta_\sigma = \frac{1}{5}$, there is actually one that takes on negative values for $\frac{1}{8} < \Delta_\sigma < \frac{1}{5}$ as shown in Figure 3.4. We may explain this by noticing that $\phi_{1,4}$ is also $\phi_{3,1}$ in the minimal model $\mathcal{M}(5,4)$. This field has exactly one quasiprimary descendant at level 3. The presence of a null state is therefore enough to conclude that $c_3^{\sigma\epsilon(1,4)\sigma\epsilon} = 0$.

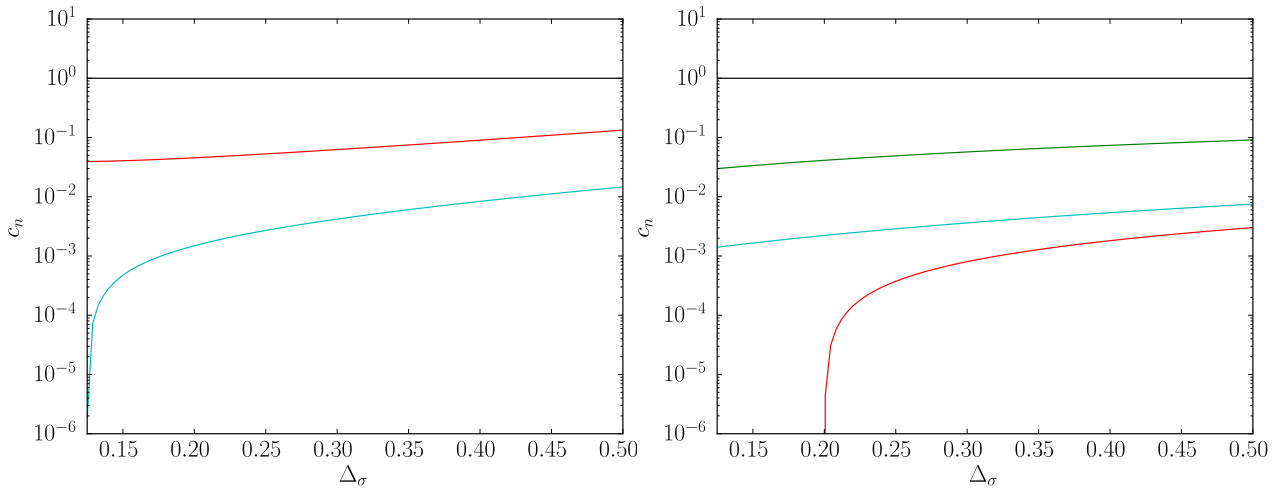


(a) $c_n^{\sigma\epsilon(1,2)\sigma\epsilon}$ (b) $c_n^{\sigma\epsilon(1,4)\sigma\epsilon}$

Figure 3.4: Log-scale plots of the $c_n^{\sigma\epsilon(1,s)\sigma\epsilon}$ that are non-zero. The legend is the same as that of Figure 3.3.

| $n$ | $c_n^{\sigma\epsilon(1,2)\sigma\epsilon}$ |
|---|---|
| 0 | 1 |
| 1 | 0 |
| 2 | 0 |
| 3 | $-\frac{(\Delta_\sigma+1)(4\Delta_\sigma+1)^2}{729\Delta_\sigma(\Delta_\sigma-1)(\Delta_\sigma+2)}(5\Delta_\sigma+2)$ |
| 4 | $-\frac{4(\Delta_\sigma+1)^2(4\Delta_\sigma+1)^2}{729\Delta_\sigma(\Delta_\sigma+3)(\Delta_\sigma+6)(2\Delta_\sigma-3)}(8\Delta_\sigma-1)$ |
| $n$ | $c_n^{\sigma\epsilon(1,4)\sigma\epsilon}$ |
| 0 | 1 |
| 1 | 0 |
| 2 | $\frac{\Delta_\sigma+1}{9(2\Delta_\sigma+3)(5\Delta_\sigma+3)}(2\Delta_\sigma+1)(10\Delta_\sigma+1)$ |
| 3 | $\frac{4(\Delta_\sigma+1)(5\Delta_\sigma+2)}{729(\Delta_\sigma+2)(5\Delta_\sigma+4)(5\Delta_\sigma+6)}(5\Delta_\sigma-1)(7\Delta_\sigma+4)$ |
| 4 | $\frac{(\Delta_\sigma+1)^2(5\Delta_\sigma+2)}{81(5\Delta_\sigma+7)(5\Delta_\sigma+8)}(10\Delta_\sigma+1)$ |

Table 3.4: The first five global block coefficients in the $(1,2)$ and $(1,4)$ contributions found by taking the $\sigma\times\epsilon$ OPE twice.

Alternatively, we can take the OPE in the other channel by permuting operator positions in (3.48). This yields the global block coefficients in Table 3.5 which are related to the $\lambda_{\sigma\sigma\mathcal{O}}\lambda_{\epsilon\epsilon\mathcal{O}}$ CFT data. There is no reason for these numbers to be positive, but we expect

$$c_{2n}^{\sigma\sigma(1,s)\sigma\sigma}c_{2n}^{\epsilon\epsilon(1,s)\epsilon\epsilon}\geq\left(c_{2n}^{\sigma\sigma(1,s)\epsilon\epsilon}\right)^2 \tag{3.53}$$

to be obeyed.[12] When $\sigma\times\sigma$ and $\epsilon\times\epsilon$ share a set of operators $\mathcal{S}$ with the same quantum numbers, the left-hand side is a product of sums. The right-hand side is a sum of products and therefore smaller by the arithmetic-geometric mean inequality. A departure from (3.53) would be a violation of unitarity since the matrix

$$\sum_{\mathcal{O}\in\mathcal{S}}\begin{bmatrix}\lambda_{\sigma\sigma\mathcal{O}}\\ \lambda_{\epsilon\epsilon\mathcal{O}}\end{bmatrix}\begin{bmatrix}\lambda_{\sigma\sigma\mathcal{O}} & \lambda_{\epsilon\epsilon\mathcal{O}}\end{bmatrix}=\begin{bmatrix}c_{2n}^{\sigma\sigma(1,s)\sigma\sigma} & c_{2n}^{\sigma\sigma(1,s)\epsilon\epsilon}\\ c_{2n}^{\sigma\sigma(1,s)\epsilon\epsilon} & c_{2n}^{\epsilon\epsilon(1,s)\epsilon\epsilon}\end{bmatrix} \tag{3.54}$$

would not be positive-definite.

### 3.1.4 Virasoro block coefficients

Our analysis so far has been focused on $c_{2n}^{\sigma\sigma(1,s)\sigma\sigma}$, $c_{2n}^{\epsilon\epsilon(1,s)\epsilon\epsilon}$ and $c_n^{\sigma\epsilon(1,s)\sigma\epsilon}$, which encode the decomposition of a Virasoro block into $\mathfrak{sl}(2)$ blocks. With the sole exception of $c_3^{\sigma\epsilon(1,4)\sigma\epsilon}$,

[12] For another quick check of our results, $\Delta_\epsilon^2 c_0^{\sigma\sigma(1,1)\sigma\sigma}c_2^{\sigma\sigma(1,1)\sigma\sigma}=\Delta_\sigma^2 c_0^{\epsilon\epsilon(1,1)\epsilon\epsilon}c_2^{\epsilon\epsilon(1,1)\epsilon\epsilon}$ holds as it must by the Ward identity.

| $n$ | $c_{2n}^{\sigma\sigma(1,1)\epsilon\epsilon}$ |
|---|---|
| 0 | 1 |
| 1 | $\frac{(\Delta_\sigma+1)(4\Delta_\sigma+1)}{3(5-4\Delta_\sigma)}$ |
| 2 | $\frac{2(\Delta_\sigma+1)^2(4\Delta_\sigma+1)[5\Delta_\sigma+2]}{45(5-4\Delta_\sigma)(11-4\Delta_\sigma)}$ |
| $n$ | $c_{2n}^{\sigma\sigma(1,3)\epsilon\epsilon}$ |
| 0 | 1 |
| 1 | $\frac{2(\Delta_\sigma+1)(4\Delta_\sigma+1)[5\Delta_\sigma+2]}{3(7+4\Delta_\sigma)(5+8\Delta_\sigma)}$ |
| 2 | $\frac{(\Delta_\sigma+1)^2(4\Delta_\sigma+1)[400\Delta_\sigma^3+1548\Delta_\sigma^2+1644\Delta_\sigma+361]}{18(7+4\Delta_\sigma)(13+4\Delta_\sigma)(11+8\Delta_\sigma)(17+8\Delta_\sigma)}$ |

Table 3.5: The first three global block coefficients in the $(1,1)$ and $(1,3)$ contributions found by taking the $\sigma \times \sigma$ and $\epsilon \times \epsilon$ OPEs.

which we could imagine to have a small effect, we have found that these coefficients are non-negative when $\frac{1}{8} \leq \Delta_\sigma \leq \frac{1}{2}$. However, this is only meaningful if the same property holds for the structure constants that unite holomorphic and anti-holomorphic halves of a four-point function. A single $C^{(r_3,s_3)}_{(r_1,s_1)(r_2,s_2)} < 0$ for instance would give rise to an infintie number of negative contributions in $\langle \phi_{r_1,s_1}\phi_{r_2,s_2}\phi_{r_1,s_1}\phi_{r_2,s_2}\rangle$, severely complicating the interpretation of Figure 3.2.

In a given correlation function, the Virasoro block coefficients that appear must be compatible with crossing symmetry and single-valuedness. By briefly reviewing the method of [107–109], we will show that this condition is enough to fix them uniquely. For definiteness, consider the $\langle\epsilon\epsilon\epsilon\epsilon\rangle$ correlator in the generalized minimal model with central charge $\frac{13}{21}$. The holomorphic part of this function comes from the kernel of the operator (3.45), which is three-dimensional. Solving (3.47) has given us a basis for this kernel in which each function vanishes at $z = 0$. We could equally well have chosen any of the regular singular points 0, 1 and $\infty$, corresponding to the $s$, $t$ and $u$ channels for Virasoro blocks. When going from $z = 0$ to $z = 1$, there is a special matrix $F$ called the *crossing matrix* (or *fusion matrix*) that accomplishes $G^a(z) = F^a{}_b G^b(1-z)$. It is a special case of the *crossing kernel* which applies to theories with a continuous spectrum.[13] Since it represents a change of basis, the expression for $F$ is unique. In this case, it is given by

$$F = \begin{bmatrix} 0.7422 & 0.3124 & -0.1563 \\ 2.3762 & -1.8795 & 1.4405 \\ 1.8760 & -2.2733 & 2.1372 \end{bmatrix}, \tag{3.55}$$

[13]Several interchangeable terms have proliferated over the years. When replacing the $z \mapsto 1-z$ map with $z \mapsto \frac{1}{z}$, the words *crossing* and *fusion* become *exchange* and *braiding*. Outside the CFT context, one says that a linear ODE has a *monodromy matrix* or *connection matrix*. For ODEs that have less structure than a BPZ equation, finding this matrix is often a difficult problem.

which was obtained in [147] via the Coulomb gas formalism. Later reviews are [85, 148]. In the following, we will use $G^1$, $G^2$ and $G^3$ to denote $G^{\epsilon\epsilon\epsilon\epsilon}_{(1,1)}$, $G^{\epsilon\epsilon\epsilon\epsilon}_{(1,3)}$ and $G^{\epsilon\epsilon\epsilon\epsilon}_{(1,5)}$ respectively.

The constraints from (3.55) are best phrased in terms of a metric on the space of conformal blocks; $G(z,\bar{z}) = W_{ab}G^a(z)G^b(\bar{z})$. We have three conditions that $W_{ab}$ must satisfy:

1. $W_{11} = 1$
2. $W_{cd} = W_{ab}F^a{}_c F^b{}_d$
3. $W_{ab} = 0$ for $a \neq b$

The first of these is an obvious consequence of having unit-normalized operators. The second comes from writing $G(1-z,1-\bar{z}) = W_{ab}G^a(1-z)G^b(1-\bar{z})$ in terms of s-channel blocks and setting it equal to $G(z,\bar{z})$. The third ensures that the four-point function has trivial monodromy under $z \mapsto e^{2\pi i}z$, $\bar{z} \mapsto e^{-2\pi i}\bar{z}$. This would appear to rule out a non-diagonal metric since we only find $h_{r,s}$ weights that differ by integers at special values of $m$.[14] See however [149]. We build solutions out of the left eigenvectors of $F$,

$$v^1 = \begin{bmatrix} 0.9537 \\ -0.1157 \\ 0.2776 \end{bmatrix}, \; v^2 = \begin{bmatrix} 0.9805 \\ 0.1758 \\ -0.0879 \end{bmatrix}, \; v^3 = \begin{bmatrix} 0.5938 \\ -0.7196 \\ 0.3600 \end{bmatrix}, \tag{3.56}$$

which have eigenvalues of 1, 1 and $-1$ respectively. Clearly $F^2 = 1$, which follows from $z \leftrightarrow 1-z$ being an involution, requires all eigenvalues to be $\pm 1$. The following form is invariant under two multiplications by $F$:

$$W_{ab} = c_{11}v^1_a v^1_b + c_{12}v^1_a v^2_b + c_{21}v^2_a v^1_b + c_{22}v^2_a v^2_b + c_{33}v^3_a v^3_b \; . \tag{3.57}$$

There are six off-diagonal components of $W$ that need to vanish. If we set $c_{21} = c_{12}$, (3.57) becomes manifestly symmetric and we can use three more parameters, $c_{11}$, $c_{12}$ and $c_{22}$, to make $W$ diagonal. As the single remaining parameter, $c_{33}$ is used to rescale $W$ so that its leading component is 1.

We may summarize this discussion by stating that there is no freedom in the three-correlator bootstrap equations once the Virasoro blocks involving $\sigma$ and $\epsilon$ are specified. Knowledge of these blocks fully determines $\langle\sigma\sigma\sigma\sigma\rangle$, $\langle\sigma\sigma\epsilon\epsilon\rangle$ and $\langle\epsilon\epsilon\epsilon\epsilon\rangle$, whether or not we demand consistency conditions for other correlators. This means that the generalized minimal model structure constants are the only valid choices for the coefficients in (3.29), (3.44)

[14] It is well known that this happens in discrete minimal models. Some of the non-diagonal theories so constructed also satisfy the stronger requirement of modular invariance.

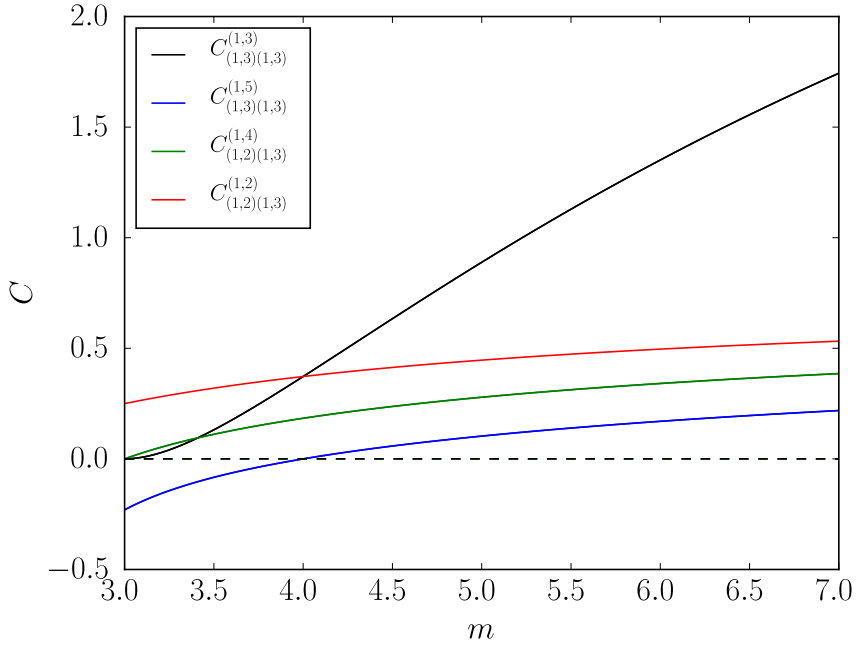


Figure 3.5: Low-lying squared OPE coefficients for Virasoro primaries in the generalized minimal models. Between the Ising model at $m = 3$ ($\Delta_\sigma = \frac{1}{8}$) and the tricritical Ising model at $m = 4$ ($\Delta_\sigma = \frac{1}{5}$), there is one that becomes negative.

and (3.48). Defining $\gamma(x) = \Gamma(x)/\Gamma(1-x)$ and $t = \frac{m}{m+1}$, the expressions we need are

$$\begin{aligned}
C^{(1,3)}_{(1,3)(1,3)} &= \gamma(t)^3\gamma(4t-1)^2\gamma(1-2t)^3\gamma(2-2t)\gamma(2-3t) \\
C^{(1,5)}_{(1,3)(1,3)} &= \gamma(t)\gamma(2t)\gamma(4t-1)\gamma(5t-1)\gamma(1-3t)\gamma(1-4t)\gamma(2-2t)\gamma(2-3t) \\
C^{(1,4)}_{(1,2)(1,3)} &= \gamma(t)\gamma(4t-1)\gamma(1-3t)\gamma(2-2t) \\
C^{(1,2)}_{(1,2)(1,3)} &= C^{(1,3)}_{(1,2)(1,2)} = \gamma(t)\gamma(3t-1)\gamma(1-2t)\gamma(2-2t)\ .
\end{aligned} \tag{3.58}$$

The last coefficient in (3.58) is clearly the one that was rederived in [128]. Plotting these in Figure 3.5, we see that $C^{(1,5)}_{(1,3)(1,3)} < 0$ for the generalized minimal models between $\mathcal{M}(4,3)$ and $\mathcal{M}(5,4)$. This reveals a problem with our strategy for proving that the allowed region in Figure 3.2 must be large enough to include (3.3). Constructing the generalized minimal model solution to crossing symmetry only accomplishes this in the one-correlator case. We must therefore conclude that there is at least one other way to extend the unitary subsector $\langle\sigma\sigma\sigma\sigma\rangle$ into a consistent three-correlator system. This solution to crossing should have positive squared OPE coefficients wherever it exists, not just in $\frac{1}{5} \leq \Delta_\sigma \leq \frac{1}{2}$. As the solution might be very different from the theories discussed above, it is worth using the numerical bootstrap to see what else can be learned about it.

## 3.2 Lessons for the bootstrap

We saw in the last section that above central charge $\frac{7}{10}$, the generalized minimal models exhibit the restricted notion of unitarity that allows them to appear in Figure 3.2. On the other hand, for $\frac{1}{2} < c < \frac{7}{10}$, they are highly non-unitary at the level of three correlators; the global coefficient $c_3^{\sigma\epsilon(1,4)\sigma\epsilon}$ and the Virasoro coefficient $C^{(1,5)}_{(1,3)(1,3)}$ both become negative in this region. Working around this problem, the machinery of the bootstrap has filled in this region with another solution whose $\sigma \times \sigma$ OPE agrees with that of a generalized minimal model. In this section, we will give an intuitive argument for why this should be possible. Beyond this, we will discuss two issues related to the replacement solution.

This first is whether it can be found uniquely. A technique called the extremal functional method is often used to extract a unique solution to crossing symmetry and unitarity whenever a dimension gap or OPE coefficient is extremized [90, 94, 95, 150–153]. Based on this, we might expect to find a single line of exotic solutions that smoothly joins the $\mathcal{M}(m+1,m)$ line at $\Delta_\sigma = \frac{1}{5}$. We will actually find the opposite — a boundary of Figure 3.2 that has many possible choices for the local CFT data outside $\sigma \times \sigma$. To reconcile this with the standard lore about extremality, one has to remember that the bootstrap equations take on a more intricate form when there are multiple correlators.

The second is the prospect of excluding the above solution with further numerics. One reason for doing this with global conformal blocks is simply the technical challenge posed by Virasoro conformal blocks. There has indeed been recent progress in using the full Virasoro symmetry to carve out $c > 1$ CFTs [154]. However, tractable four-point functions with extended supersymmetry appear to be limited to those of BPS operators [155, 156]. Global blocks were therefore a necessary ingredient of [157], a program which aims to constrain the space of superconformal theories using external operators in long multiplets. There has also been recent interest in conformal theories that have no locality and therefore no Virasoro algebra [158–160]. These provide a different motivation for shrinking the regions in Figure 3.2.

### 3.2.1 Reduction to one correlator

The well known bootstrap constraints for three correlators with $\mathbb{Z}_2$ symmetry take the form of five crossing equations. The vector of equations has one component for $\langle\sigma\sigma\sigma\sigma\rangle$, one component for $\langle\epsilon\epsilon\epsilon\epsilon\rangle$ and three components for $\langle\sigma\sigma\epsilon\epsilon\rangle$. Given a generic solution to crossing, it is easy to see that four (three) sum rules will break when an even (odd) operator is removed from the theory. However, there is a pleasing non-generic property that holds for generalized minimal models; $\epsilon \times \epsilon$ contains more operators than $\sigma \times \sigma$. Because of this, only one crossing equation is disturbed when we remove the $\phi_{1,5}$ conformal family. This is the source of almost all unitarity violation in the system built from $\phi_{1,2}$ and $\phi_{1,3}$. Since negativity of $c_3^{\sigma\epsilon(1,4)\sigma\epsilon}$ only affects spinning operators with $\Delta > \frac{45}{8}$, it is possible that the numerics are largely insensitive

to it [161]. Assuming that problems with the mixed correlator are negligible, we will focus on

$$\sum_{\mathcal{O}} \lambda^2_{\epsilon\epsilon\mathcal{O}} F^{\epsilon\epsilon;\epsilon\epsilon}_{-,\mathcal{O}}(u,v) = 0$$
$$F^{\epsilon\epsilon;\epsilon\epsilon}_{-,\Delta,\ell}(u,v) \equiv v^{\Delta_\epsilon} g^{0,0}_{\Delta,\ell}(u,v) - u^{\Delta_\epsilon} g^{0,0}_{\Delta,\ell}(v,u) \tag{3.59}$$

as the single condition that needs to be restored. Once a solution to (3.59) is found, one can incorporate it into the three-correlator problem by choosing $\lambda_{\sigma\sigma\mathcal{O}} = 0$ for new operators.[15]

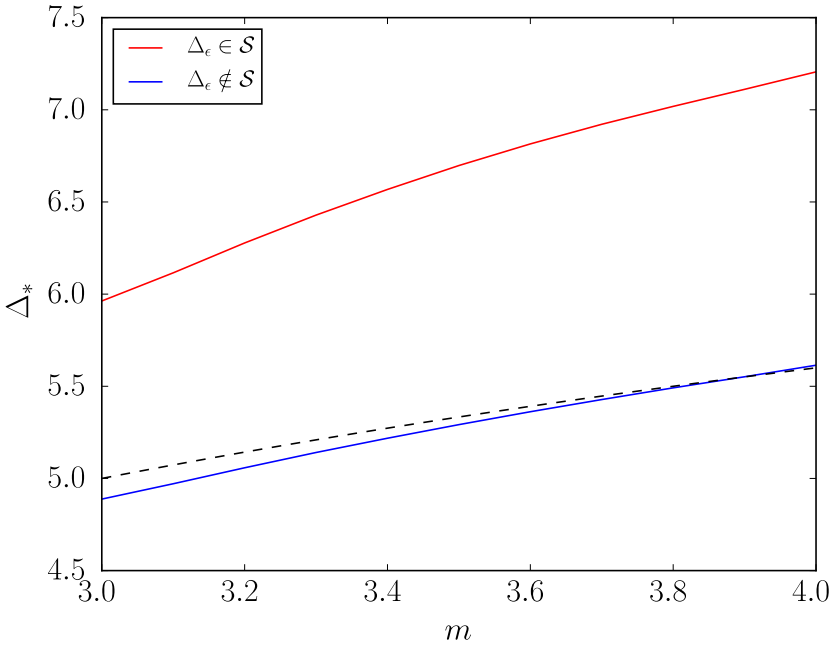


Figure 3.6: Dimension bounds for irrelevant operators in (3.60). The dotted line shows the dimension of the primary scalar $\phi_{1,5}$ whose multiplet needs to be replaced for $3 < m < 4$.

Checking the solvability of (3.59) for real $\lambda_{\epsilon\epsilon\mathcal{O}}$ is the simplest numerical bootstrap prob-

[15] We are using four crossing equations to derive (3.3) analytically and then claiming that the fifth crossing equation can be satisfied for free. This is different from what happens in three dimensions. We have checked that the island in [78] merges with the rest of the allowed region once the fifth crossing equation is dropped.

lem. Emphasizing the contributions of operators that are already present, we may write

$$\begin{aligned}
\sum_{\mathcal{O}} \lambda^2_{\epsilon\epsilon\mathcal{O}} F^{\epsilon\epsilon;\epsilon\epsilon}_{-,\mathcal{O}}(u,v) &= -F_{1,1}(u,v) - C^{(1,3)}_{(1,3)(1,3)} F_{1,3}(u,v) \\
F_{1,1}(u,v) &\equiv \sum_{n,\bar{n}} c_n^{\epsilon\epsilon(1,1)\epsilon\epsilon} c_{\bar{n}}^{\epsilon\epsilon(1,1)\epsilon\epsilon} F^{\epsilon\epsilon;\epsilon\epsilon}_{-,n+\bar{n},|n-\bar{n}|}(u,v) \\
F_{1,3}(u,v) &\equiv \sum_{n,\bar{n}} c_n^{\epsilon\epsilon(1,3)\epsilon\epsilon} c_{\bar{n}}^{\epsilon\epsilon(1,3)\epsilon\epsilon} F^{\epsilon\epsilon;\epsilon\epsilon}_{-,\Delta_\epsilon+n+\bar{n},|n-\bar{n}|}(u,v) \ .
\end{aligned} \tag{3.60}$$

Keeping operators with $\Delta \leq 30$, we have used the results of the last section to approximate the right-hand side of (3.60). In the sum over operators, there will be a continuum of irrelevant scalars not in $\phi_{1,1} \cup \phi_{1,3}$ which begins at some gap $\Delta_* > 2$. If this is the only set of scalars on the left-hand side of (3.60), we are dealing with the set $\mathcal{S} = \{\Delta > \Delta_*\}$. Alternatively, we could allow the dimension $\Delta_\epsilon$ to appear again and enlarge it to $\mathcal{S} = \{\Delta > \Delta_*\} \cup \{\Delta = \Delta_\epsilon\}$. The second choice is the one applicable to Figure 3.2. However, in Figure 3.6, we consider the first choice as well. This is because it is possible to rederive Figure 3.2 under the requirement that $\epsilon$ is non-degenerate [129]. As numerical accuracy is improved, we expect the blue line to precisely meet the dotted line at $m = 4$.[16]

In Figure 3.6, the red curve tells us that (3.3) is admissible whenever we treat $(\Delta_\sigma, \Delta_\epsilon)$ as allowed dimensions and perform a two-parameter scan. The blue curve tells us that (3.3) will still be admissible when we fix $\epsilon$ as a single operator at angle $\theta = \arctan\left(\frac{\lambda_{\sigma\sigma\epsilon}}{\lambda_{\epsilon\epsilon\epsilon}}\right)$ and scan over $(\Delta_\sigma, \Delta_\epsilon, \theta)$. Finally, one may contemplate the effect of imposing $\theta = \frac{\pi}{2}$ which is one consequence of Kramers-Wannier duality in the Ising model. Although this question cannot be answered with Figure 3.6, we have found that (3.3) persists yet again. In all three cases, (3.3) is not just an allowed line — it is the *maximal* allowed line. From this, we must conclude that many solutions to crossing, labelled by values of $\Delta_*$ between the red and blue lines, lie along the bound on the left side of Figure 3.2. This signals the presence of a flat direction, *e.g.* a bound in $(\Delta_\sigma, \Delta_\epsilon, \theta)$ space which is independent of $\theta$. A flat direction in the modular bootstrap was previously seen in [162]. The main argument for unique extremal functionals comes from [150], in which the multi-correlator bootstrap equations were augmented with angles for each operator in OPE space. To extract a spectrum in this formulation, one would have to look for zeros of these functionals on the entire $(\Delta, \theta)$ plane. We suspect that the flat direction here corresponds to a zero being achieved on a codimension-one locus.

Because the generalized minimal model line (3.3) is allowed by the bootstrap, there are several lines in the interior of Figure 3.2 that must be allowed as well. These can be constructed through one or more tensor products. If we multiply two generalized minimal models for instance, the only non-trivial operator whose dimension lies to the left of $\Delta_\sigma = \frac{1}{2}$

[16] Varying the spatial dimension provides one indication that numerical errors have a large effect. Evaluating conformal blocks at $d = 2.01$ instead of $d = 2$ results in a much smaller bound on $\Delta_*$.

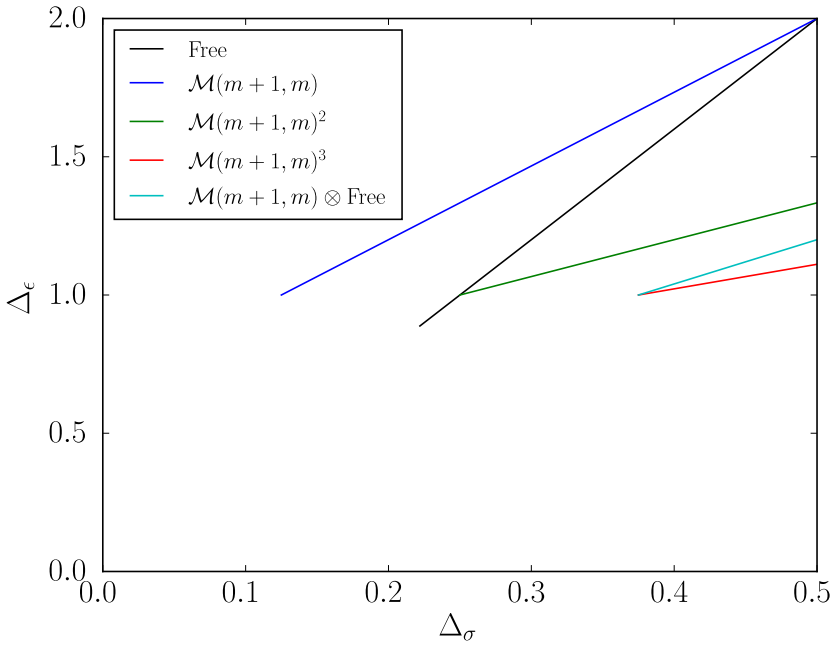


Figure 3.7: Tensor product theories that are allowed in both sides of Figure 3.2. Since we must have $\Delta_\epsilon \geq 1$, all other tensor products involving the free field vertex operators necessarily lie to the right.

is $\sigma \otimes \sigma$. Writing its OPE schematically,

$$(\sigma \otimes \sigma) \times (\sigma \otimes \sigma) = (I \otimes I) + (I \otimes \epsilon) + (\epsilon \otimes I) + (\epsilon \otimes \epsilon) + \dots \tag{3.61}$$

includes two relevant operators. In order for these to have the same scaling dimension, the $\mathcal{M}(m+1,m) \otimes \mathcal{M}(m'+1,m')$ product must have $m = m'$. Expanding the search to include free theories and generalized free theories, it is a simple exercise to check that the lines in Figure 3.7 all have one relevant $\mathbb{Z}_2$-odd scaling dimension and one relevant $\mathbb{Z}_2$-even scaling dimension.

Evidently, it is not possible to isolate particular minimal models in a three-correlator bootstrap by specifying the number of relevant operators. One has to consider more stringent assumptions or add more correlators. The former approach was discussed already in [163], where it was found that the one-correlator Ising kink sharpens considerably when scalars are restricted to lie in $\mathcal{S} = \{\Delta > 3\} \cup \{\Delta = \Delta_\epsilon\}$. This kink becomes an island when a similar restriction is made for a three-correlator system. Following [164], it is likely that one can obtain this island from a single correlator by imposing large gaps in the spin-0 and spin-2 sectors.

A more ambitious goal is to produce islands under minimal assumptions by introducing a third external scalar. Taking this external scalar to be odd, plots along the lines of

| Coefficients | Signs |
|---|---|
| $C^{(1,3)}_{(1,4)(1,4)}$ | Positive |
| $C^{(1,5)}_{(1,4)(1,4)}$ | Negative for $m < 4$ |
| $C^{(1,7)}_{(1,4)(1,4)}$ | Negative for $m < 6$ |
| $C^{(1,6)}_{(1,3)(1,4)}$ | Negative for $m < 5$ |
| $C^{(1,5)}_{(1,2)(1,4)}$ | Negative for $m < 4$ |

Table 3.6: Virasoro block coefficients (other than the ones in Figure 3.5) appearing in four-point functions made from $\sigma$, $\epsilon$ and $\sigma'$. Only one is non-negative for all $m \geq 3$.

Figure 3.5 offer some preliminary insight.[17] Regions where all $C^{(r_3,s_3)}_{(r_1,s_1)(r_2,s_2)} > 0$ are likely to survive, but as Table 3.6 shows, there can be several negative structure constants with more than three correlators. We have seen that the negative constant $C^{(1,5)}_{(1,3)(1,3)}$ in the three-correlator system was innocuous because it did not appear in any mixed correlators. It is therefore encouraging that the coefficients $C^{(1,5)}_{(1,2)(1,4)}$ and $C^{(1,6)}_{(1,3)(1,4)}$, which have first-order zeros, participate in $\langle\sigma\sigma\sigma'\sigma'\rangle$ and $\langle\epsilon\epsilon\sigma'\sigma'\rangle$ respectively. Lest we become too encouraged, it is important to note that $\Delta_{\sigma'}$ is defined as the starting point for a continuum of irrelevant operators. This represents a fundamental difference as compared to the one-correlator and three-correlator analysis. It remains to be seen whether we can still derive strong bounds from a scan over two isolated scaling dimensions and one non-isolated scaling dimension.

### 3.2.2 Supersymmetric minimal models

So far, we have been concerned with finding the necessary correlators to single out theories that are minimal with respect to the Virasoro algebra. However, the unitary representations of the $\mathcal{N} = 1$ super-Virasoro algebra also admit a discrete series for central charges below that of the free field. In analogy with $\mathcal{M}(m+1, m)$, we can continue them to $\mathcal{SM}(m+2, m)$ where non-integer $m$ breaks unitarity but preserves crossing symmetry. Studying these solved theories offers another route toward understanding the systematics of the bootstrap. It could also be interesting to compare results for the tricritical Ising model since this is the lowest model of $\mathcal{SM}(m+2, m)$ but the second lowest model of $\mathcal{M}(m+1, m)$.

[17] The lightest $\mathbb{Z}_2$-odd scalar after $\sigma$ is $\sigma' \equiv \phi_{1,4}$. The lightest $\mathbb{Z}_2$-even scalar after $\epsilon$ is $\epsilon' \equiv [L_{-2}\bar{L}_{-2}, \phi_{1,1}]$. We have made the choice in which all operator fusions are between Virasoro primaries.

The super-Virasoro graded commutation relations

$$\begin{aligned}
[L_m, L_n] &= (m-n)L_{m+n} + \frac{c}{12}m(m-1)(m+1)\delta_{m+n,0} \\
[L_m, G_r] &= \left(\frac{m}{2} - r\right) G_{m+r} \\
\{G_r, G_s\} &= 2L_{r+s} + \frac{c}{3}\left(r - \frac{1}{2}\right)\left(r + \frac{1}{2}\right)\delta_{r+s,0}
\end{aligned} \tag{3.62}$$

actually describe two algebras since fermions do not have to be periodic in radial quantization. When the indices on $G_r$ are integers, (3.62) is the Ramond superalgebra, otherwise it is the Neveu-Schwarz superalgebra. The super-Virasoro minimal models, which contain representations of each, have a Kac formula given by

$$\begin{aligned}
c &= \frac{3}{2} - \frac{12}{m(m+2)} && m > 2 \\
h_{r,s} &= \frac{[(m+2)r - ms]^2 - 4}{8m(m+2)} + \frac{1}{32}[1 - (-1)^{r-s}] && r, s \in \mathbb{Z}_{>0}\ .
\end{aligned} \tag{3.63}$$

If $r - s$ is even (odd), this is a Neveu-Schwarz (Ramond) degenerate weight [165]. In either case, it is degenerate at level $rs/2$. It is clear by inspection that $G_{\pm\frac{1}{2}}$ generate a subalgebra of (3.62) that is independent of $c$. For integer indices, on the other hand, no global subalgebra exists. A numerical bootstrap approach is therefore most readily accessible for the Neveu-Schwarz sectors of $\mathcal{N} = (1,1)$ theories.

In the global algebra, which is $\mathfrak{osp}(2|1)$, primary operators may be written as superfields; $\Phi(z,\theta) = \phi(z) + \theta\psi(z)$. The superspace distance, which enters in correlation functions, is $Z_{ij} \equiv z_i - z_j - \theta_i\theta_j$. Even though cross-ratios in $\mathbb{R}^d$ all involve at least four points, invariant combinations in superspace may be built using three points as well. The quantity

$$\eta = \frac{\theta_1 Z_{23} + \theta_2 Z_{31} + \theta_3 Z_{12} + \theta_1\theta_2\theta_3}{\sqrt{Z_{12}Z_{23}Z_{31}}} \tag{3.64}$$

is invariant under $\mathfrak{osp}(2|1)$ [166]. As a result, the three-point function depends on more than just an OPE coefficient. The general expression for the chiral half is

$$\langle \Phi_1(z_1,\theta_1)\Phi_2(z_2,\theta_2)\Phi_3(z_3,\theta_3)\rangle = \frac{\lambda_{123}(1+\zeta\eta)}{Z_{12}^{h_1+h_2-h_3}Z_{23}^{h_2+h_3-h_1}Z_{31}^{h_3+h_1-h_2}} \tag{3.65}$$

where $\zeta$ is an arbitrary Grassman number. Until recently, such extra parameters were eliminated by restricting the superconformal bootstrap to correlators of BPS operators [31, 167]. We may indeed impose shortening conditions on (3.65), but due to the small amount of supersymmetry, this would require us to give up a lot. To be annihilated by a supercharge,

each external operator would have to be the identity in at least one of the $\mathfrak{osp}(2|1)$ factors. It is therefore preferable to leave (3.65) in its most general form and use superconformal blocks that include unknown coefficients reflecting the presence of $\zeta$.

The authors of [157] computed some of the necessary blocks and introduced a framework that still allows the bootstrap to proceed. Their idea is to consider an entire multiplet at once, with the external correlators involving all combinations of a primary and its super-descendants. When this is carried out for $\mathcal{N} = (1,1)$, the allowed regions will have to include all points corresponding to the $\mathcal{SM}(m+2,m)$. The strongest statement we can make from this is that the line

$$\Delta_\epsilon = \frac{8}{3}\Delta_\sigma \tag{3.66}$$

must be inside the bound for $\Delta_\sigma < \frac{1}{8}$. This comes from choosing the Neveu-Schwarz fields $\sigma \equiv \phi_{2,2}$ and $\epsilon \equiv \phi_{3,3}$. Right at $\Delta_\sigma = \frac{1}{8}$, we find ourselves in the $c = 1$ model where $\phi_{3,3} = \phi_{1,3}$ and the entire level-$\frac{3}{2}$ subspace decouples. To see this, we may check that

$$|\chi\rangle = \left[G_{-\frac{3}{2}} - \frac{2}{2h+1}L_{-1}G_{-\frac{1}{2}}\right]|h\rangle \tag{3.67}$$

is the unique quasiprimary state. Computing the norm and setting $h \mapsto h_{3,3}$, we find

$$\begin{aligned}\langle\chi|\chi\rangle &= \frac{2(2ch+c+6h^2-9h)}{3(2h+1)} \\ &\mapsto \frac{(m-4)(m+6)}{m^2+2m+8}\end{aligned} \tag{3.68}$$

with a first-order zero. This is the behaviour that we saw for $m = 3$ in the bosonic case, but now it occurs for $m = 4$. The tricritical Ising model, which has no $\phi_{3,3}$ operator, lives at the point $(\Delta_\sigma, \Delta_\epsilon) = \left(\frac{1}{10}, \frac{1}{10}\right)$.

The above calculation shows that a global block coefficient in the supersymmetric generalized minimal model line becomes negative for $m < 4$. If we are to see an associated kink, this line must saturate the bound on operator dimensions from the long multiplet bootstrap. This brings us to a crucial difference between $\mathcal{M}(m+1,m)$ and the Neveu-Schwarz sector of $\mathcal{SM}(m+2,m)$. In the former case, we saw the correct saturation with (3.3). The same cannot hold for (3.66) because it is strictly below the line for vertex operators. Writing a CFT vertex operator as $e^{iq\phi(z)}$ and an SCFT vertex operator as $e^{iq\Phi(z,\theta)}$, the two important properties are $\Delta \propto q^2$ and additivity of $q$. These lead to $\Delta_\epsilon = 4\Delta_\sigma$ which is allowed by the one-correlator region of Figure 3.2. Due to the restriction on the number of relevant operators, the three-correlator region omits this line until $\Delta_\sigma = \frac{2}{9}$. It is therefore clear that treating four copies of the same multiplet with the methods of [157] is not enough. If our goal is to see a minimal model kink, the $\mathcal{N} = (1,1)$ bootstrap will require multiple correlators at the superspace level. Since each of these must separately expand to a mixed correlator

system, the resulting problem is likely to be numerically intensive.

## 3.3 Evanescent deformations in fermionic theories

While unitary subsectors of generalized minimal models have only been appreciated recently, they share some features with older problems related to dimensional regularization. In particular, methods for treating fermions in general dimension have been the subject of considerable effort. For this discussion, we will focus on *evanescent operators* or those that exist in fractional but not integer $d$. We previously saw that perturbative scalar CFTs lose unitarity because of the evanescent operator (3.1), built out of five fields and ten derivatives. This story becomes richer when we have gamma matrices that allow us to anti-symmetrize Lorentz indices without increasing conformal dimension. This leads to an infinite degeneracy of evanescent operators

$$\mathcal{O}_n = \left(\bar{\psi}_i \Gamma^{(n)}_{\mu_1\ldots\mu_n} \psi^i\right)\left(\bar{\psi}_j \Gamma^{\mu_1\ldots\mu_n}_{(n)} \psi^j\right) \tag{3.69}$$

before any derivatives are included. These indeed lead to negative norms as well [168]. Moreover, their spectrum can become continuous at the fixed-point [169] — something that is thought to be forbidden in unitary theories above $d = 2$. Since the $\mathcal{O}_n$ have a classical scaling dimension of $2(d-1)$, they can become arbitrarily weakly irrelevant as $d \to 2$. Our goal is to focus on this regime in which the tower of evanescent operators affects the search for a perturbative fixed-point itself and not just the subsequent analysis.

### 3.3.1 Basics of the generalized Thirring model

It will be helpful to review some widely studied 2D theories that are candidates for analytic continuation. The generalized Thirring model is defined by the action

$$S = \int \bar{\psi}\partial\!\!\!/\psi - \frac{1}{2} g_{\mathrm{S}} \left(\bar{\psi}\psi\right)^2 - \frac{1}{2} g_{\mathrm{V}} \left(\bar{\psi}\gamma^\mu\psi\right)^2 - \frac{1}{2} g_{\mathrm{P}} \left(\bar{\psi}\gamma_5\psi\right)^2 \mathrm{d}^2x \ . \tag{3.70}$$

The symmetry of (3.70) is generically $U(N)$ but it may enhance for certain values of the couplings. These can be identified by using the 2D Fierz identities

$$\begin{bmatrix} \delta^\alpha_\beta\delta^\gamma_\delta \\ (\gamma^\mu)^\alpha{}_\beta(\gamma_\mu)^\gamma{}_\delta \\ (\gamma_5)^\alpha{}_\beta(\gamma_5)^\gamma{}_\delta \end{bmatrix} = \begin{bmatrix} \frac{1}{2} & \frac{1}{2} & -\frac{1}{2} \\ 1 & 0 & -1 \\ \frac{1}{2} & -\frac{1}{2} & \frac{1}{2} \end{bmatrix} \begin{bmatrix} \delta^\alpha_\delta\delta^\gamma_\beta \\ (\gamma^\mu)^\alpha{}_\delta(\gamma_\mu)^\gamma{}_\beta \\ (\gamma_5)^\alpha{}_\delta(\gamma_5)^\gamma{}_\beta \end{bmatrix} \tag{3.71}$$

and demanding that (3.70) take the form of a current-current interaction.

1. In the $SU(N)$ Thirring model, $(g_{\mathrm{S}}, g_{\mathrm{V}}, g_{\mathrm{P}}) = \left(g, \frac{1}{N}g, -g\right)$. This can be seen by starting from $\left(\bar{\psi}_i\gamma^\mu(T_a)^i{}_j\psi^j\right)\left(\bar{\psi}_k\gamma_\mu(T^a)^k{}_l\psi^l\right)$ and applying the completeness relation $(T_a)^i{}_j(T^a)^k{}_l = \frac{1}{2}\left(\delta^i_l\delta^k_j - \frac{1}{N}\delta^i_j\delta^k_l\right)$.

2. In the $SO(2N)$ Thirring model, $(g_{\rm S}, g_{\rm V}, g_{\rm P}) = (g, 0, 0)$. This time, we start from $(\psi^i C_+ \gamma^\mu (T_a)_{ij} \psi^j) \left(\psi^k C_+ \gamma_\mu (T^a)_{kl} \psi^l\right)$ where the $\psi$ fields are Majorana fermions. As long as we have an even number of them, $(T_a)_{ij}(T^a)_{kl} = 2\left(\delta_{il}\delta_{jk} - \delta_{ik}\delta_{jl}\right)$ can be used to express the interaction in Dirac notation. This is also known as the Gross-Neveu model [170].

3. In the $Sp(2N)$ Thirring model, $(g_{\rm S}, g_{\rm V}, g_{\rm P}) = (0, 0, g)$. While the charge conjugation matrix $C_+$ used above only permits a Majorana condition, we may invoke its anti-symmetric cousin $C_-$ to define symplectic Majorana fermions. In terms of these fields, the interaction is $\left(\psi\Omega_i C_- \gamma^\mu (T_a)^i{}_j \psi^j\right) \left(\psi\Omega_k C_- \gamma_\mu (T^a)^k{}_l \psi^l\right)$ and the completeness of generators is $(T_a)^i{}_j (T^a)^k{}_l = 2\left(\delta^i_l \delta^j_k - \Omega^{ik}\Omega_{jl}\right)$.

4. Thirring models for exceptional Lie groups would appear if we extended (3.70) to include invariant tensors built from more than two indices.

This same structure is borne out by the renormalization of (3.70). Using $d = 2+\varepsilon$ to regulate divergences, [171, 172] obtained the following beta functions.

$$\begin{aligned}
\beta_{\rm S} &= \varepsilon g_{\rm S} - \frac{1}{\pi}\left[(N-1)g_{\rm S}^2 - g_{\rm S}g_{\rm P} - 2g_{\rm V}(g_{\rm S}+g_{\rm P})\right] \\
\beta_{\rm P} &= \varepsilon g_{\rm P} + \frac{1}{\pi}\left[(N-1)g_{\rm P}^2 - g_{\rm S}g_{\rm P} + 2g_{\rm V}(g_{\rm S}+g_{\rm P})\right] \\
\beta_{\rm V} &= \varepsilon g_{\rm V} + \frac{1}{\pi} g_{\rm S} g_{\rm P}
\end{aligned} \tag{3.72}$$

These vanish for

$$(g_{\rm S}^*, g_{\rm V}^*, g_{\rm P}^*) \in \left\{ \left(\frac{\pi\varepsilon}{N}, \frac{\pi\varepsilon}{N^2}, -\frac{\pi\varepsilon}{N}\right), \left(\frac{\pi\varepsilon}{N-1}, 0, 0\right), \left(0, 0, \frac{\pi\varepsilon}{1-N}\right) \right\} \tag{3.73}$$

in direct correspondence with the models above. Nevertheless, it would be wrong to refer to these as UV fixed-points as we have not yet said anything about the couplings of higher $\mathcal{O}_n$ deformations which are necessarily present for $d = 2+\varepsilon$. Hence, we will consider the generalized Thirring model for finite $\varepsilon$,

$$S = \int \bar{\psi}\partial\!\!\!/\psi - \frac{1}{2}\sum_{n=0}^{\infty} g_n \mathcal{O}_n \mathrm{d}^{2+\varepsilon}x \tag{3.74}$$

where $g_{\rm S} = g_0$, $g_{\rm V} = g_1$ and $g_{\rm P} = -2g_2$. It appears that very little is known about the critical properties of (3.74) at finite $N$. The one discussion we are aware of comes from a remarkable series of papers [173–176] which defined the Gross-Neveu CFT as the fixed-point closest to the $g_0$ axis. Their result of $g_0^* = O(\varepsilon)$ and $g_3^*, g_4^* = O(\varepsilon^3)$, for the lowest order couplings, has been extended in [177].

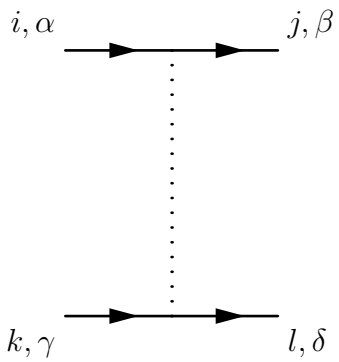


Figure 3.8: The diagram for a vertex which contracts fermion lines with $g_n \delta^i_j \delta^k_l \left(\Gamma^{(n)}_A\right)^{\alpha}_{\ \beta} \left(\Gamma^{(n)}_A\right)^{\gamma}_{\ \delta}$. Loop diagrams will of course introduce divergences which lead to a running of $g_n$.

We will use a common diagrammatic representation (Figure 3.8) in which a dotted line separates the pairs of fermions that are contracted. Clearly, at higher orders, the number of dotted lines will be one more than the number of loops. It will be convenient to work with the redefined couplings $u_n = g_n/4\pi$ and leave $\mathrm{Tr}(\mathbf{1})$ unevaluated for now.

The diagrams contributing to the one-loop beta function are shown in Figure 3.9. They have the same momentum integrals, namely

$$\int \frac{\not{p} \otimes (\not{k} - \not{p})}{p^2 (k-p)^2} \frac{\mathrm{d}^d p}{(2\pi)^d} = \frac{1}{4\pi\varepsilon} \gamma^\mu \otimes \gamma_\mu + O(1) \ , \tag{3.75}$$

but different $\Gamma$ structures. The expressions for them are

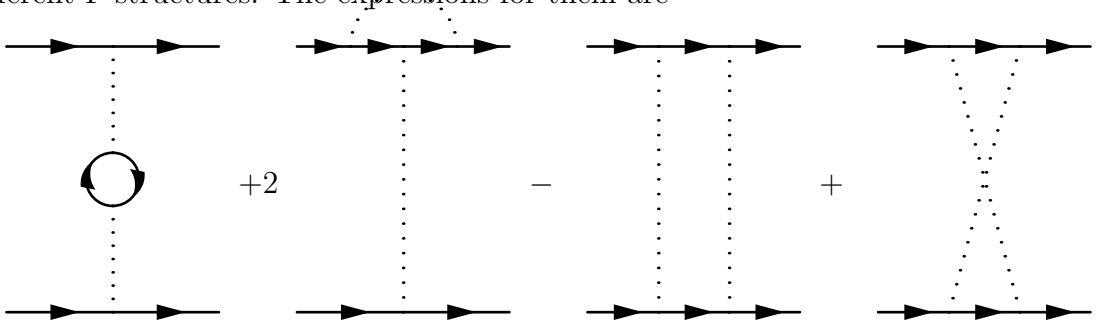


Figure 3.9: The one-loop correction to Figure 3.8. The two vertices in each diagram above should be summed over all $g_n$.

$$
\begin{aligned}
\Gamma_A^{(m)} \otimes \Gamma_B^{(n)} \mathrm{Tr}\left(\gamma^\mu \Gamma_A^{(m)} \gamma_\mu \Gamma_B^{(n)}\right) &= A_n(\varepsilon)\delta_{mn}\mathrm{Tr}(\mathbf{1})\Gamma_B^{(n)} \otimes \Gamma_B^{(n)} \\
\left(\Gamma_A^{(m)} \gamma^\mu \Gamma_B^{(n)} \gamma_\mu \Gamma_A^{(m)}\right) \otimes \Gamma_B^{(n)} &= B_n^m(\varepsilon)\Gamma_B^{(n)} \otimes \Gamma_B^{(n)} \\
\left(\Gamma_A^{(m)} \gamma^\mu \Gamma_B^{(n)}\right) \otimes \left(\Gamma_A^{(m)} \gamma_\mu \Gamma_B^{(n)}\right) &= \sum_{p=0}^{\infty} L_p^{mn}(\varepsilon)\Gamma_C^{(p)} \otimes \Gamma_C^{(p)} \\
\left(\Gamma_A^{(m)} \gamma^\mu \Gamma_B^{(n)}\right) \otimes \left(\Gamma_B^{(n)} \gamma_\mu \Gamma_A^{(m)}\right) &= \sum_{p=0}^{\infty} R_p^{mn}(\varepsilon)\Gamma_C^{(p)} \otimes \Gamma_C^{(p)}
\end{aligned}
\tag{3.76}
$$

respectively. Clearly, the potential for physical couplings to generate evanescent couplings comes solely from the last two diagrams. The appendix explains how to find the multivariate generating functions associated with (3.76). More conveniently, the coefficients in this case are simple enough to be found in closed form [174].

$$
\begin{aligned}
A_n(\varepsilon) &= (-1)^{n+\binom{n}{2}}(d-2n)n! \\
B_n^m(\varepsilon) &= (-1)^{n+mn+\binom{m}{2}}(d-2n)\partial_x^m\left[(1+x)^{d-n}(1-x)^n\right]\Big|_{x=0} \\
&= (-1)^{m+n+mn+\binom{m}{2}}(d-2n)\frac{\Gamma(m+n-d)}{\Gamma(n-d)}{}_2F_1\left(\begin{array}{c} -m,-n \\ d+1-m-n \end{array};-1\right) \\
R_p^{mn}(\varepsilon) &= \frac{(-1)^{q+\binom{m}{2}+\binom{n}{2}+\binom{p}{2}}}{p!}\partial_1^m\partial_2\partial_3^n\left[(1-x_1x_2-x_1x_3-x_2x_3)^{d-p}(x_1+x_2+x_3-x_1x_2x_3)^p\right]\Big|_{x=0} \\
&= \frac{m!n!}{q!}\frac{\Gamma(d-p+1)}{\Gamma(d-p-q+2)}\frac{q(p+1)(d-p-q+1)+(d-p+1)(m-q+1)(n-q+1)}{(m-q+1)!(n-q+1)!} \\
L_p^{mn}(\varepsilon) &= (-1)^{mn+m+n+q}R_p^{mn}(\varepsilon)
\end{aligned}
\tag{3.77}
$$

In the last line, we have defined the integer $q$ such that $p = m+n+1-2q$. Adding these contributions gives

$$
T_p^{mn}(\varepsilon) = -N\mathrm{Tr}(\mathbf{1})\delta_{pm}\delta_{pn}A_p(\varepsilon) + \delta_{pm}B_p^n(\varepsilon) + \delta_{pn}B_p^m(\varepsilon) - L_p^{mn}(\varepsilon) + R_p^{mn}(\varepsilon)\,, \tag{3.78}
$$

which is the object that appears naturally in the Green's function given by Figures 3.8 and 3.9. The $\overline{\mathrm{MS}}$-renormalized four-point Green's function is

$$
\begin{aligned}
G_{\mathrm{R}}(k) &= \mu^{-\varepsilon}\sum_p \Gamma_C^{(p)} \otimes \Gamma_C^{(p)}\left[u_p + \frac{1}{\varepsilon}\sum_{m,n} u_m u_n\left(\left|\frac{k}{\mu}\right|^\varepsilon T_p^{mn}(\varepsilon) - T_p^{mn}(0)\right)\right] + \ldots \\
&= \mu^{-\varepsilon}\sum_p \Gamma_C^{(p)} \otimes \Gamma_C^{(p)}\left[u_p + \sum_{m,n} u_m u_n\left(\log\left|\frac{k}{\mu}\right| T_p^{mn}(0) + T_p^{mn\prime}(0)\right)\right] + \ldots
\end{aligned}
\tag{3.79}
$$

where we have written the counterterm in red. Its form allows us to conclude that the infinite system of couplings runs according to

$$\beta_p^{(1)} = \varepsilon u_p + 2\sum_{m,n} u_m u_n T_p^{mn}(0) \ . \tag{3.80}$$

### 3.3.2 The projection scheme

Any attempt to use (3.80) must confront the fact that it describes an RG flow in an infinite-dimensional space. Before we delve into this, notice that the first three beta functions have the form

$$T_0^{mn}(0), T_1^{mn}(0), T_2^{mn}(0) = \left[\begin{array}{ccc|cc} * & * & * & 0 & \dots \\ * & * & * & 0 & \dots \\ * & * & * & 0 & \dots \\ \hline 0 & 0 & 0 & 0 & \dots \\ \vdots & \vdots & \vdots & \vdots & \ddots \end{array}\right] \tag{3.81}$$

while higher $T_p^{mn}(0)$ have non-zero entries both inside and outside the $3 \times 3$ physical block. In other words, evanescent couplings only induce other evanescent couplings while physical couplings induce both. This allows one to at least begin the epsilon expansion since anomalous dimensions are particularly nice at one loop. The bilinear $\bar{\psi}\Gamma_A^{(m)}\psi$ is only corrected by $u_m$ which means that physical one-loop anomalous dimensions only depend on $(u_0, u_1, u_2)$. Hence, it is possible obtain something that looks like a CFT at $O(\varepsilon)$ by solving for the projection $(u_0^*, u_1^*, u_2^*)$ and imagining that the other couplings have been tuned to whatever the necessary values are such that the true fixed-point is reached [178]. We are mainly interested in the special cases that allow non-trivial fixed-points to be explored beyond the leading order. However, we now explain the orthogonal approach of extending (3.80) order-by-order for arbitrary couplings when $\varepsilon$ is a regulator for a purely two-dimensional theory.

The idea is to choose a scheme such that (3.79)'s dependence on all $u_p$ is repackaged in terms of just three new coupling constants $(u_0', u_1', u_2')$. These will differ from $(u_0, u_1, u_2)$ by a finite renormalization. A non-unique choice for this redefinition is

$$u_p' = \begin{cases} u_p + \sum_{m,n} u_m u_n T_p^{mn\prime}(0) & p \leq 2 \\ u_p & p > 2 \end{cases} \ . \tag{3.82}$$

Nice properties can be seen after inserting this into (3.79). To the given order,

$$\begin{aligned} G_{\rm R}(k) &= \mu^{-\varepsilon}\sum_{p\leq 2}\Gamma_C^{(p)}\otimes\Gamma_C^{(p)}\left[u'_p+\sum_{m,n\leq 2}u'_m u'_n\log\left|\frac{k}{\mu}\right|T_p^{mn}(0)\right] \\ &+ \mu^{-\varepsilon}\sum_{p>2}\Gamma_C^{(p)}\otimes\Gamma_C^{(p)}\left[u'_p+\sum_{m,n}u'_m u'_n\left(\log\left|\frac{k}{\mu}\right|T_p^{mn}(0)+T_p^{mn\prime}(0)\right)\right]+\dots\ . \end{aligned} \tag{3.83}$$

The new scheme and the rule (3.81) have ensured that the first line only involves a finite sum. The second line drops out in two dimensions by the vanishing of the higher $\Gamma$ structures themselves. It is clear from the above that the definition of $u'_p$ could have been given extra terms depending on $(u_0,u_1,u_2)$ without changing this decoupling. An explanation for the ambiguity is given in [174] which also presents a few useful modifications of (3.82). Going back to (3.80), the three physical beta functions stay restricted to the physical block if we take $\varepsilon\to 0$:

$$\beta_p^{(1)\prime}=\begin{cases}\beta_p^{(1)}\big|_{u=u'}-\varepsilon\sum_{m,n}u'_m u'_n T_p^{mn\prime}(0) & p\leq 2\\ \beta_p^{(1)}\big|_{u=u'} & p>2\end{cases}\ . \tag{3.84}$$

A more impressive statement is that two-loop quantities of interest, which depend on all couplings in $\overline{\rm MS}$, become functions of the physical block in this limit as well. For instance,

$$\begin{aligned} \beta_0^{(2)\prime}&=4[N{\rm Tr}(\mathbf{1})-2]u_0^3+8N{\rm Tr}(\mathbf{1})[u_0u_1^2+2u_0u_2^2-2u_1^2u_2]-16u_0^2u_1+16u_0^2u_2+64u_1u_2^2+O(\varepsilon)\\ \beta_1^{(2)\prime}&=4[N{\rm Tr}(\mathbf{1})-2][u_0^2u_1+4u_1u_2^2-4u_0u_1u_2]+16u_0^2u_2+32u_0u_2^2+O(\varepsilon)\\ \beta_2^{(2)\prime}&=16[N{\rm Tr}(\mathbf{1})-2]u_2^3+4N{\rm Tr}(\mathbf{1})[u_0^2u_2+2u_1^2u_2-u_0u_1^2]+16u_0u_2^2+8u_0^2u_1-32u_1u_2^2+O(\varepsilon)\end{aligned} \tag{3.85}$$

in the unmodified (3.82). These beta functions are due to [172] while the result was generalized to anomalous dimensions in [174]. The latter requires a corresponding redefinition $Z'_{\mathcal{O}}$ of the counterterm in

$$\gamma_{\mathcal{O}}=\frac{{\rm d}\log Z_{\mathcal{O}}}{{\rm d}\log\mu}=\sum_p\beta_p\frac{\partial\log Z_{\mathcal{O}}}{\partial u_p}\ . \tag{3.86}$$

Two comments are in order. First, a scheme that removes evanescent couplings from $\gamma_{\mathcal{O}}$ at $\varepsilon=0$ cannot possibly remove them at finite $\varepsilon$. Indeed, by (3.86), $\gamma'_{\mathcal{O}}$ contains a leftover $\varepsilon\sum_p u'_p\frac{\partial}{\partial u_p}\left(1-\frac{Z'_{\mathcal{O}}}{Z_{\mathcal{O}}}\right)$ from the classical scaling which cannot be ignored. Second, a function like $\beta_3$ which depends on infinitely many couplings in one scheme will still depend on infinitely many couplings in another scheme. To actually remove a one-loop appearance of some $u_p$, we would have to shift by an $O\left(\frac{1}{\varepsilon}\right)$ amount which is an illegal operation.

Mixing between physical and evanescent four-fermi composites occurs in many theories whether or not these operators are nearly marginal. An analogous scheme to the one just described has been used in the $d=4-\varepsilon$ context since [179, 180]. Again, infinite sums are

only removed from anomalous dimensions if $\varepsilon \to 0$ is taken at the end of the calculation. The terms in $\gamma'_{\mathcal{O}}$, where coupling constants appear beside explicit factors of $\varepsilon$, are important for applications to three-dimensional physics. They are also important for verifying that anomalous dimensions are scheme-independent at the fixed-point [181]. Therefore, the results we are after might as well be obtained in $\overline{\text{MS}}$.

### 3.3.3 Consistent truncations in 2.01 dimensions

We are interested in deformations that can be turned on in $d = 2 + \varepsilon$ without inducing all of the other $\mathcal{O}_n$ vertices at the same order. We know there should be at least one example based on the successful determination of higher-loop critical exponents in the Gross-Neveu model [177]. We will now show that all other cases of the generalized Thirring model (3.74) lead to infinitely many coupling constants that are $O(\varepsilon)$. This is different from saying that *every* coupling is present at this order. We will see that there are infinite towers of $u_n$ that may be set to zero based on the value of $n$ modulo 4.

This one-loop analysis can be done by only looking at the $L_p^{mn}(0) - R_p^{mn}(0)$ part of (3.78). For this to contribute, two necessary conditions are

$$m + n - p + 1 \in 2\mathbb{Z} \ , \ mn + m + n + \frac{m + n - p + 1}{2} \in 2\mathbb{Z} + 1 \ . \tag{3.87}$$

The first permits $L_p^{mn}(0)$ and $R_p^{mn}(0)$ to be non-vanishing on their own while the second ensures that they do not cancel. It is now a simple matter to go through the four possible cases and find

$$\begin{aligned}
n - m &\equiv 0 \pmod 4 \quad \Longrightarrow \quad p \equiv 3 \pmod 4 \\
n - m &\equiv 1 \pmod 4 \quad \Longrightarrow \quad p \equiv 2m + 2, \ 2n \pmod 4 \\
n - m &\equiv 2 \pmod 4 \quad \Longrightarrow \quad p \equiv 1 \pmod 4 \\
n - m &\equiv 3 \pmod 4 \quad \Longrightarrow \quad p \equiv 2m, \ 2n + 2 \pmod 4 \ .
\end{aligned} \tag{3.88}$$

These implications tell us when a product $u_m u_n$ can appear in the one-loop beta function $\beta_p^{(1)}$. They may be economically presented as a set of "fusion rules" for congruence classes

$$\begin{array}{lll}
[3] \times [0] = [0] & [0] \times [0] = [3] + [0] & [0] \times [1] = [2] \\
[3] \times [1] = [1] & [1] \times [1] = [3] + [1] & [1] \times [2] = [0] \\
[3] \times [2] = [2] & [2] \times [2] = [3] + [2] & [2] \times [0] = [1]
\end{array} \tag{3.89}$$

with [3] playing the role of the identity. Note that each coupling clearly generates a running of itself due to the other terms in (3.78). A consequence is that (3.80) can indeed be made to vanish without turning on every four-fermi scalar. It is enough to take the identity [3] and optionally one other class [0], [1] or [2]. There may be further truncations that allow [3] to be

left out at one loop as in the case of Gross-Neveu. This is possible because $L_p^{mn}(0) - R_p^{mn}(0)$ takes the form

$$\pm \frac{1}{p!}\partial_1^m \partial_2 \partial_3^n \left[(1 - x_1x_2 - x_1x_3 - x_2x_3)^{2-p}(x_1 + x_2 + x_3 - x_1x_2x_3)^p\right]\Big|_{x=0}, \tag{3.90}$$

which vanishes for sufficiently large $p$. Said another way, all rows in

$$L_p^{mm}(0) - R_p^{mm}(0) = \left[\begin{array}{ccc|ccccccc} 0 & 0 & 0 & 0 & \dots & & & & & \\ 0 & 0 & 0 & * & 0 & \dots & & & & \\ 0 & 0 & 0 & * & 0 & \dots & & & & \\ \hline 0 & 0 & 0 & * & 0 & 0 & 0 & * & 0 & \dots \\ 0 & 0 & 0 & * & 0 & 0 & 0 & * & 0 & \dots \\ \vdots & \vdots & \vdots & \vdots & \vdots & \vdots & \vdots & \vdots & \vdots & \ddots \end{array}\right] \tag{3.91}$$

must be zero after a certain point. The schematic expression (3.91) indicates that once $\mathcal{O}_3$ is present, we need to deal with the full tower $\mathcal{O}_7, \mathcal{O}_{11}, \dots$ and so on. We can avoid this runaway generation of vertices by looking at the one row of (3.91) that vanishes identically. This is precisely the theory closest to the $u_0$ axis in the approach that was advocated in [176].

It is worth pointing out that higher-loop calculations retain the property that only finitely many verties are generated by a given diagram. In view of this fact, solving an infinite system of fixed-point equations will never be necessary to find the Gross-Neveu CFT. Consider an order $L$ diagram built from the couplings $u_{(1)}, \dots u_{(L)}$. If this generates a new vertex, its coupling will be $O\left(\varepsilon^{-1}\prod_i u_{(i)}\right)$. For an infinite cascade to start, this vertex must help us generate others whose powers of $\varepsilon$ do not exceed those that have already been encountered.

$$\begin{aligned} (\varepsilon^{a_1}, \dots, \varepsilon^{a_L}) &\mapsto \varepsilon^{\sum a - 1} \\ (\varepsilon^{\sum a - 1}, \varepsilon^{b_1}, \dots, \varepsilon^{b_M}) &\mapsto \varepsilon^{\sum a + \sum b - 2} \end{aligned} \tag{3.92}$$

For the order not to grow, we need $M = 1$ and $b_1 = 1$. But the only $O(\varepsilon)$ coupling in the Gross-Neveu model is the original $u_0$ itself and we have already seen that the set

$$(u_{4k-1}, u_{4k}, u_{4k+1}, u_{4k+2}) \tag{3.93}$$

closes among itself when considered in one-loop diagrams alongside $u_0$.

We have shown that, although Gross-Neveu is not the only example of a generalized Thirring model, it is the only one whose $d = 2 + \varepsilon$ fixed-point can be systematically analyzed by the methods of finite-dimensional algebraic geometry. Next, we will show that this is a special case of a more general theorem.

### 3.3.4 Smaller symmetry groups

Interesting things happen when we consider interactions that break $U(N)$ to a proper subgroup. Such theories

$$S = \int \bar{\psi}\partial\!\!\!/\psi + \sum_{m=0}^{\infty} T(m)^{ik}{}_{jl} \left(\bar{\psi}_i \Gamma_A^{(m)} \psi^j\right) \left(\bar{\psi}_k \Gamma^A_{(m)} \psi^l\right) \mathrm{d}^2x \tag{3.94}$$

involve a sequence of rank-4 tensors which do not need to be $g_m \delta^i_j \delta^k_l$. We should look for fixed-points that are well controlled in the same sense as Gross-Neveu. As shown above, only a one-loop check is needed to see if finitely many couplings will turn on at each loop order. The one-loop diagrams, which were all proportional to $\delta^i_j \delta^k_l$ in (3.76), now need to have their tensor structures written out explicitly. For reference, we collect the four expressions in Table 3.7. As in [182, 183], an important role is played by the number of quartic invariants

| Spinor index structure | Global index structure |
|---|---|
| $\Gamma_A^{(m)} \otimes \Gamma_B^{(n)} \mathrm{Tr}\left(\gamma^\mu \Gamma_A^{(m)} \gamma_\mu \Gamma_B^{(n)}\right)$ | $T(m)^{ia}{}_{jb} T(n)^{bk}{}_{al}$ |
| $\left(\Gamma_A^{(m)} \gamma^\mu \Gamma_B^{(n)} \gamma_\mu \Gamma_A^{(m)}\right) \otimes \Gamma_B^{(n)}$ | $T(m)^{ia}{}_{bj} T(n)^{bk}{}_{al} + T(m)^{ka}{}_{bl} T(n)^{bi}{}_{aj}$ |
| $\left(\Gamma_A^{(m)} \gamma^\mu \Gamma_B^{(n)}\right) \otimes \left(\Gamma_A^{(m)} \gamma_\mu \Gamma_B^{(n)}\right)$ | $T(m)^{ik}{}_{ab} T(n)^{ab}{}_{jl}$ |
| $\left(\Gamma_A^{(m)} \gamma^\mu \Gamma_B^{(n)}\right) \otimes \left(\Gamma_B^{(n)} \gamma_\mu \Gamma_A^{(m)}\right)$ | $T(m)^{ib}{}_{al} T(n)^{ak}{}_{jb}$ |

Table 3.7: The gamma matrix combinations that arise from the one-loop diagrams in Figure 3.9 along with their corresponding contractions of $T(m)^{ik}{}_{jl}$ and $T(n)^{ik}{}_{jl}$. What was previously written with a factor of 2 becomes a sum of two contractions in the general case.

for the symmetry group under consideration. The form of (3.94) allows us to take

$$T(m)^{ik}{}_{jl} = T(m)^{ki}{}_{lj} \tag{3.95}$$

but other permutations of indices should be considered distinct.

We previously showed that with the quartic invariant $\delta^i_j \delta^k_l$, gamma forms with at least one index lead to a runaway evanescent tower. It turns out that when $T(m)^{ik}_{jl} = g_m T^{ik}_{jl}$, the maximal rank $M$ of a gamma form can at most increase by one. The point is that the third and fourth diagrams in Figure 3.9 produce $\Gamma_C^{(p)} \otimes \Gamma_C^{(p)}$ structures beyond $p = M$ when $g_M$ is inserted twice.

Looking at the sums $\sum_{p=0}^{2M+1} L_p^{M,M} \Gamma_C^{(p)} \otimes \Gamma_C^{(p)}$ and $\sum_{p=0}^{2M+1} R_p^{M,M} \Gamma_C^{(p)} \otimes \Gamma_C^{(p)}$, the coefficient of $\Gamma_C^{(2M+1)} \otimes \Gamma_C^{(2M+1)}$ is

$$g_M^2 R^{M,M}_{2M+1} \left[T^{ib}{}_{al} T^{ak}{}_{jb} - (-1)^{M^2} T^{ik}{}_{ab} T^{ab}{}_{jl}\right] , \tag{3.96}$$

where we have used Table 3.7 and the basic relation in (3.77). There is always another potential vertex that can be built in a unique way. If $g_{M-1} = 0$, it is $\Gamma_C^{(2M-1)} \otimes \Gamma_C^{(2M-1)}$, otherwise it is $\Gamma_C^{(2M)} \otimes \Gamma_C^{(2M)}$. The coefficients of these are

$$\begin{aligned} g_M^2 R_{2M-1}^{M,M} \left[ T^{ib}{}_{al} T^{ak}{}_{jb} + (-1)^{M^2} T^{ik}{}_{ab} T^{ab}{}_{jl} \right] , \\ g_M g_{M-1} R_{2M}^{M,M-1} \left[ T^{ib}{}_{al} T^{ak}{}_{jb} - (-1)^{M^2+M-1} T^{ik}{}_{ab} T^{ab}{}_{jl} \right] . \end{aligned} \tag{3.97}$$

If $M \geq 2$, (3.96) and (3.97) must vanish. For even $M$, this requires $T^{ib}{}_{al} T^{ak}{}_{jb} = T^{ik}{}_{ab} T^{ab}{}_{jl} = 0$. For odd $M$, there appears to be a way out until we realize that $\Gamma_C^{(2M-2)} \otimes \Gamma_C^{(2M-2)}$ must now vanish as well. Looking at its three contributions, the $O(g_M g_{M-3})$ and $O(g_{M-1} g_{M-2})$ coefficients are already being set to zero as they are proportional to (3.96) when $M$ is odd. The only remaining piece is

$$g_M g_{M-1} R_{2M-2}^{M,M-1} \left[ T^{ib}{}_{al} T^{ak}{}_{jb} - (-1)^{M^2+M} T^{ik}{}_{ab} T^{ab}{}_{jl} \right] \tag{3.98}$$

which has the precise form needed to ensure that $T^{ik}{}_{jl}$ is nilpotent. The non-existence of such a fixed-point follows from the fact that $T^{ik}{}_{jl} = 0$ is the only solution to the system

$$\begin{cases} T^{ib}{}_{al} T^{ak}{}_{jb} = T^{ik}{}_{ab} T^{ab}{}_{jl} = 0 \\ T^{ik}{}_{jl} = c_1 T^{ia}{}_{jb} T^{bk}{}_{al} + c_2 \left( T^{ia}{}_{bj} T^{bk}{}_{al} + T^{ai}{}_{bj} T^{kb}{}_{al} \right) \end{cases} \tag{3.99}$$

of coupled quadratic equations. It would be interesting to generalize this theorem to fixed-points with multiple quartic invariants. Some steps toward this are taken in Appendix D.

Without a theorem in hand for the more general case, we have nevertheless searched for fixed-points with a separation of powers and found some examples. A family that can be summarized nicely has $SO(2)^M \times U(N) \subset U(2^M N)$ symmetry. For an action consistent at one loop, we may write

$$\begin{aligned} S_{M,N} = \int \bar{\psi} \partial\!\!\!/ \psi - \frac{1}{2} g \; \bar{\psi}_{I,i_1,\ldots i_M} \delta^I_J (\sigma_2)^{i_1}{}_{j_1} \ldots (\sigma_2)^{i_M}{}_{j_M} \psi^{J,j_1,\ldots,j_M} \\ \bar{\psi}_{K,k_1,\ldots k_M} \delta^K_L (\sigma_2)^{k_1}{}_{l_1} \ldots (\sigma_2)^{k_M}{}_{l_M} \psi^{L,l_1,\ldots,l_M} \; \mathrm{d}^2 x \; , \end{aligned} \tag{3.100}$$

where uppercase indices transform in the fundamental of $U(N)$ and $\sigma_2$ is the generator of $SO(2)$. It is illuminating to look at the simplest member of this family (other than $S_{0,N}$ which is Gross-Neveu):

$$S_{1,1} = \int \bar{\psi} \partial\!\!\!/ \psi - \frac{1}{2} g \left[ (\bar{\psi}_i \psi^j)(\bar{\psi}_j \psi^i) - (\bar{\psi}_i \psi^j)(\bar{\psi}_i \psi^j) \right] \mathrm{d}^2 x \; . \tag{3.101}$$

We emphasize that the interaction preserving $U(2)$ in (3.101) cannot be constructed from just $\mathcal{O}_0$, $\mathcal{O}_1$ and $\mathcal{O}_2$. We have had to use $\mathcal{O}'_0$ as well, defining $\mathcal{O}'_n$ as in (3.69) except with global indices and spinor indices contracted in opposite ways. In two dimensions, where it is redundant to include both sets of operators, one may equivalently use the action

$$\begin{aligned} S'_{1,1} = \int \bar{\psi}\partial\!\!\!/\psi \quad &- \quad \frac{1}{2}g\left[\frac{1}{2}(\bar{\psi}_i\psi^i)(\bar{\psi}_j\psi^j) + \frac{1}{2}(\bar{\psi}_i\gamma^\mu\psi^i)(\bar{\psi}_j\gamma_\mu\psi^j) - \frac{1}{4}(\bar{\psi}_i\gamma^{\mu\nu}\psi^i)(\bar{\psi}_j\gamma_{\mu\nu}\psi^j)\right] \\ &+ \quad \frac{1}{2}g(\bar{\psi}_i\psi^j)(\bar{\psi}_i\psi^j)\mathrm{d}^2x \end{aligned} \tag{3.102}$$

but this is no longer true for $d = 2 + \varepsilon$. The point is that (3.71) is really a truncation of the full Fierz identity which contains infinitely many $O(1)$ coefficients. When the higher $\Gamma$ structures are non-vanishing, the full $\{\mathcal{O}_n\}_{n=1}^{\infty}$ basis is needed to remove the dependence on $\mathcal{O}'_0$. Hence, for the purposes of analytic continuation, (3.101) and (3.102) should be regarded as different theories.

# Chapter 4

# The long-range Ising model

The 2D Ising model, solved exactly in [184], was the first theory observed to saturate numerical bootstrap bounds. It was later seen that this also applies to the 3D Ising model and subsequent work led to the most precise determination of its critical exponents [78, 95, 129, 185]. On the other hand, long-range Ising (LRI) models, defined by relaxing the requirement for spins to interact with nearest neighbours, have not been solved in any dimension, despite exhibiting critical behaviour in all $1 \leq d < 4$ [186]. The models we consider will have ferromagnetic ($J > 0$) interactions that fall off as a power-law:

$$H_{\text{LRI}} = -J \sum_{i,j} \frac{\sigma_i \sigma_j}{|i-j|^{d+s}} \,. \tag{4.1}$$

On the fixed line parameterized by $s$, two regimes are well understood. If $s$ exceeds a certain crossover value, which we call $s_*$, the critical exponents become those of the (short-range) Ising model. For the critical exponents to become those of mean-field theory instead, we must have $s < \frac{d}{2}$. The most interesting range is therefore $\frac{d}{2} < s < s_*$. Choosing several such values of $s$ and $d = 3$, it would be interesting to do, for (4.1), what [95, 185] did for its short-range counterpart. We will now explain why long-range Ising models are indeed prime candidates for a non-perturbative bootstrap study.

## 4.1 Conformality

Due to the work of [158], there is strong evidence that the second-order phase transition of the LRI is described by a CFT. Perhaps unsurprisingly, this CFT is nonlocal and in particular lacks a stress-energy tensor. This does not conflict with the Ward identity argument for conformal invariance as the presence of a traceless stress-energy tensor is only a *sufficient*

condition for having a CFT.[1] On the other hand, nonlocality can certainly make conformal invariance more difficult to check. Let us review the continuum description of the LRI which, among other things, will give us a clearer indication that the bootstrap approach should work.

The nonlocal action

$$S = \int -\frac{1}{2}\phi\partial^s\phi + \frac{\lambda}{4!}\phi^4 \mathrm{d}x \tag{4.2}$$

was first introduced by [188] to study the LRI with the renormalization group.[2] The kinetic term, with momentum space propagator $|k|^{-s}$, is exactly the action for a generalized free scalar of dimension $\frac{d-s}{2}$. The $\phi^4$ perturbation drives the system to the LRI fixed point in the spirit of Wilson-Fisher. When $s > \frac{d}{2}$, this interaction is relevant which makes the fixed point non-trivial. It is therefore natural to compute observables as an expansion in $\varepsilon \equiv 2s - d$. In terms of this parameter, the beta function is

$$\beta(\lambda) = -\varepsilon\lambda + \frac{3\lambda^2}{\Gamma\left(\frac{d}{2}\right)(4\pi)^{\frac{d}{2}}} + O(\lambda^3)\,. \tag{4.3}$$

For future reference let us write down some relations between bare and renormalized quantities in $\overline{\text{MS}}$.[3]

$$\begin{aligned} \lambda_0 &= \left(\lambda + \frac{3}{\Gamma\left(\frac{d}{2}\right)(4\pi)^{\frac{d}{2}}}\frac{\lambda^2}{\varepsilon} + O(\lambda^3)\right)\mu^\varepsilon \\ \phi^n &= \left(1 - \frac{n(n-1)}{6}\frac{3\lambda}{\Gamma\left(\frac{d}{2}\right)(4\pi)^{\frac{d}{2}}\varepsilon} + O(\lambda^2)\right)[\phi^n] \end{aligned} \tag{4.4}$$

The first line is equivalent to (4.3) while the second is a simple exercise. Renormalizability of (4.2) is on solid footing just like its local version [190].

[1] Without a stress-energy tensor, we can have a theory satisfying all of the usual conformal field theory axioms except locality. Although we will continue to call this object a CFT, it is also commonly referred to as a conformal theory or CT [5, 187].

[2] The fractional derivative is a shorthand for the nonlocal operator that acts as $\partial^s\phi(x) \equiv \int \frac{\phi(y)}{|x-y|^{d+s}}\mathrm{d}y$.

[3] Note that $\varepsilon$ is finite for us so we are not obligated to subtract $\varepsilon^{-1}$ terms. Nevertheless, it is helpful to do so as this preserves the property that $O(\varepsilon^n)$ accuracy can be achieved with an expansion up to $O(\lambda^n)$. The correlators we derive could in principle be obtained without any subtraction by resumming terms enhanced by poles in $\varepsilon$. The RG technology is nothing but a systematic way to perform such resummations [189].

### 4.1.1 Mixed two-point functions

A readily calculable quantity in the theory (4.2) is the two-point function of scalars, which scale invariance only constrains as

$$\langle \mathcal{O}_1(x_1)\mathcal{O}_2(x_2)\rangle = \frac{c_{12}}{|x_{12}|^{\Delta_1+\Delta_2}} \ . \tag{4.5}$$

By computing some $\Delta_1 \neq \Delta_2$ examples of (4.5) and seeing that they vanish, we arrive at a hint that this scale invariance is enhanced to the full conformal group under which $\mathcal{O}_1$ and $\mathcal{O}_2$ transform as primaries [158].

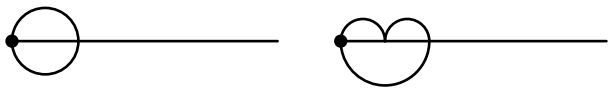

Figure 4.1: The first two diagrams that allow us to compute (4.9). The dot represents a $\phi^3$ operator with three legs.

Consider the correlator

$$F(\mu, x, \lambda) = \big\langle \phi(0)[\phi^3](x)\big\rangle = f(\mu|x|, \lambda)|x|^{-\Delta_\phi - 3\Delta_\phi} \tag{4.6}$$

where $[\phi^3] = Z_3(\lambda, \varepsilon)^{-1}\phi^3$ is a renormalized operator. The Callan-Symanzik equation

$$\left[\mu\frac{\partial}{\partial\mu} + \beta(\lambda)\frac{\partial}{\partial\lambda} + \gamma_3(\lambda)\right] F(\mu, x, \lambda) = 0 \ , \tag{4.7}$$

when converted into an equation for $f$, has a solution of

$$f(\mu|x|, \lambda) \sim C\,|\mu x|^{-\gamma_3(\lambda_*)} \tag{4.8}$$

at large distances. Matching against perturbation theory is what will determine $C = f(1, \lambda_*)$. The first step is to evaluate the bare correlator using the diagrams in Figure 4.1. We arrive at

$$\big\langle \phi(x)\phi^3(0)\big\rangle = R_1\frac{\lambda_0}{|x|^{d-2\varepsilon}} + R_2\frac{\lambda_0^2}{|x|^{d-3\varepsilon}} + O(\lambda_0^3) \ , \tag{4.9}$$

where the coefficients are

$$\begin{aligned} R_1 &= -\varepsilon \frac{\Gamma\left(-\frac{d}{4}\right)\Gamma\left(\frac{d}{2}\right)}{(4\pi)^{\frac{d}{2}}\Gamma\left(\frac{3d}{4}\right)} + O(\varepsilon^2) \\ R_2 &= 9\frac{\Gamma\left(-\frac{d}{4}\right)}{(4\pi)^d\Gamma\left(\frac{3d}{4}\right)} + O(\varepsilon) \ . \end{aligned} \tag{4.10}$$

Next, we improve the correlator by substituting (4.4).

$$\begin{aligned} F(\mu,x,g) &= \lambda R_1|\mu x|^{\varepsilon}|x|^{\varepsilon-d} + \lambda^2\left[R_1\frac{6}{\Gamma\left(\frac{d}{2}\right)(4\pi)^{\frac{d}{2}}\varepsilon}|\mu x|^{\varepsilon} + R_2|\mu x|^{2\varepsilon}\right]|x|^{\varepsilon-d} + O(\lambda^3) \\ f(1,\lambda) &= \lambda R_1 + \lambda^2\left[R_1\frac{6}{\Gamma\left(\frac{d}{2}\right)(4\pi)^{\frac{d}{2}}\varepsilon} + R_2\right] + O(\lambda^3) \\ &= -R_1\varepsilon^{-1}\beta(\lambda) \end{aligned} \tag{4.11}$$

The overall factor of the beta function tells us that $C = 0$ at the fixed-point.

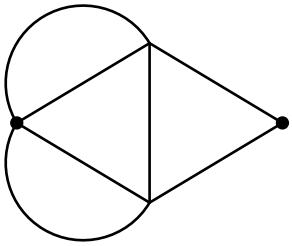

Figure 4.2: One of three two-loop diagrams that contributes to (4.12). Unlike the others, this one has only been computed recently.

As we will see shortly, (4.6) is a very special two-point function. It is beneficial to check a more complicated two-point function like

$$H(\mu,x,\lambda) = \left\langle [\phi^2](0)[\phi^4](x)\right\rangle = h(\mu|x|,\lambda)|x|^{-2\Delta_\phi-4\Delta_\phi} \ . \tag{4.12}$$

The idea here completely echoes the previous calculation so we will only discuss the method in [158] for evaluating the hardest diagram in (4.12). This is the one in Figure 4.2. The method starts by writing

$$\begin{aligned} \frac{\Upsilon}{|x|^{\frac{3d-7\varepsilon}{2}}} &= \iint \frac{\mathrm{d}y\mathrm{d}z}{|x-y|^{2\alpha}|x-z|^{2\alpha}|y-z|^{2\alpha}|y|^{2\beta}|z|^{2\beta}} \\ &= \int \frac{1}{|x-z|^{2\alpha}|z|^{2\beta}} I(x,z)\mathrm{d}z \end{aligned} \tag{4.13}$$

in position space. Here, $\beta = 2\alpha = \frac{d-\varepsilon}{2}$. A Mellin space version of the inner integral can be written if we insert a factor of $|y-w|^{-2\varepsilon}$ and take $w \to \infty$ [191, 192].

$$I(x,z) = \frac{\pi^{\frac{d}{2}}}{|x-z|^{d-2\varepsilon}} \iint \frac{\mathcal{M}(s,t)}{\Gamma(\varepsilon)\Gamma\left(\frac{d-\varepsilon}{4}\right)^2\Gamma\left(\frac{d-\varepsilon}{2}\right)} \left|\frac{x}{x-z}\right|^{2s} \left|\frac{z}{x-z}\right|^{2t} \frac{\mathrm{d}s\mathrm{d}t}{(2\pi i)^2} \tag{4.14}$$

$$\mathcal{M}(s,t) = \Gamma(-s)\Gamma(-t)\Gamma\left(\frac{3\varepsilon-d}{4}-s\right)\Gamma\left(\frac{3\varepsilon-d}{4}-t\right)\Gamma\left(s+t+\frac{d-\varepsilon}{2}\right)\Gamma\left(s+t+\frac{d-2\varepsilon}{2}\right)$$

For (4.14) to be valid, the contour must be of the form $(s,t) = (s_0+i\mathbb{R}, t_0+i\mathbb{R})$ where $(s_0,t_0)$ is chosen so that poles and shadow poles lie on opposite sides of the contour. If one of the variables (say $t$) is moved out of this region, an extra term is encountered for each pole $t_*$ that we cross.

$$\frac{\Upsilon}{|x|^{\frac{3d-7\varepsilon}{2}}} = \int \frac{1}{|x-z|^{2\alpha}|z|^{2\beta}} \left[\iint \frac{\mathrm{d}s\mathrm{d}t}{(2\pi i)^2} - \sum_{t_*}\int \frac{\mathrm{d}s}{2\pi i}\mathrm{Res}_{t=t_*}\right] \frac{\mathcal{M}(s,t)}{\Gamma(\varepsilon)\Gamma\left(\frac{d-\varepsilon}{4}\right)^2\Gamma\left(\frac{d-\varepsilon}{2}\right)} \left|\frac{x}{x-z}\right|^{2s} \left|\frac{z}{x-z}\right|^{2t} \mathrm{d}z \tag{4.15}$$

Precisely such a shift, with $t_* \in \{0, \frac{3\varepsilon-d}{4}\}$, is needed in order to make the $z$ integral commute with the others. This results in

$$\begin{aligned}
\Upsilon &= \frac{\pi^d}{\Gamma(\varepsilon)\Gamma\left(\frac{d-\varepsilon}{4}\right)^2\Gamma\left(\frac{d-\varepsilon}{2}\right)} \left[\iint \frac{\mathrm{d}s\mathrm{d}t}{(2\pi i)^2} - \int \frac{\mathrm{d}s}{2\pi i}\mathrm{Res}_{t=0} - \int \frac{\mathrm{d}s}{2\pi i}\mathrm{Res}_{t=\frac{3\varepsilon-d}{4}}\right] \tilde{\mathcal{M}}(s,t) \\
\tilde{\mathcal{M}}(s,t) &= \mathcal{M}(s,t)\frac{\Gamma\left(\frac{3d-7\varepsilon}{4}+s\right)\Gamma\left(\frac{\varepsilon}{2}+t\right)\Gamma\left(\frac{5\varepsilon-d}{4}-s-t\right)}{\Gamma\left(\frac{d-\varepsilon}{2}-t\right)\Gamma\left(\frac{3d-5\varepsilon}{4}+s+t\right)\Gamma\left(\frac{7\varepsilon-d}{4}-s\right)} .
\end{aligned} \tag{4.16}$$

Isolating the $\varepsilon^{-1}$ poles in the three integrals that cancel the overall $\Gamma(\varepsilon)^{-1}$, the leading behaviour is found to be

$$\Upsilon = 4\pi^d \frac{\Gamma\left(-\frac{d}{4}\right)}{\Gamma\left(\frac{3d}{4}\right)} + O(\varepsilon) . \tag{4.17}$$

### 4.1.2 The Caffarelli-Silvestre trick

An idea in [193], which has some parallels with the AdS / CFT literature, is to realize generalized free theory using a local theory in a higher number of dimensions. The nonlocal part of (4.2) becomes the effective action for a defect obtained by integrating out the orthogonal directions. The two-point function tells us that there should be $2-s$ such co-ordinates, a

number which is in general not an integer. Consider

$$S = \int (\partial_x \Phi)^2 + (\partial_y \Phi)^2 \mathrm{d}x\mathrm{d}y \tag{4.18}$$

which is a lift of

$$\phi(x) = \Phi(x, 0) \ . \tag{4.19}$$

A solution of the equation of motion is just a spherical harmonic times a solution of the radial equation

$$\partial_x^2 \Phi + \frac{1-s}{z} \partial_z \Phi + \partial_z^2 \Phi = 0 \ . \tag{4.20}$$

Here, we have defined $z = |y|$ and abused notation in order to work with $\Phi(x, z)$ instead of $\Phi(x, y)$. The solution of (4.20) for the boundary condition (4.19) has the short-distance expansion

$$\Phi(p, z) = \left[1 + C|pz|^s + O(z^2)\right] \phi(p) \tag{4.21}$$

where we have only Fourier transformed in $x$. We may now substitute (4.21) into (4.18) to obtain the pure boundary term

$$S \propto \int |p|^s \phi(p) \phi(-p) \mathrm{d}p \ . \tag{4.22}$$

From the above, it is clear that the LRI may be reached from an interaction confined to the defect;

$$S = \int \frac{1}{2} \partial_M \Phi \partial^M \Phi \mathrm{d}X + \frac{\lambda}{4!} \int \Phi^4 \mathrm{d}x \tag{4.23}$$

where $X = (x, y)$. This gives us the benefit of a local stress-energy tensor in the ambient space.

$$\begin{aligned} T_{MN} &= \partial_M \Phi \partial_N \Phi - \frac{1}{2}(\partial \Phi)^2 - \frac{\lambda_0}{4!} \Phi^4 \delta(y) \delta_{MN} \theta(M, N \leq d) \\ &= \partial_M \Phi \partial_N \Phi - \frac{1}{2}(\partial \Phi)^2 + \varepsilon^{-1} \mu^\varepsilon \frac{\beta(\lambda)}{4!} [\phi^4] \delta_{MN} \theta(M, N \leq d) \end{aligned} \tag{4.24}$$

Computing divergences of the dilation and special conformal currents in the usual way (retaining terms proportional to the equation of motion), we arrive at the Ward identities

$$\sum_i \left[ X_i \cdot \frac{\partial}{\partial X_i} + \Delta_\phi \right] \left\langle \prod_j \Phi(X_j) \right\rangle = \beta(\lambda) \frac{\mu^\varepsilon}{4!} \int \left\langle \prod_j \Phi(X_j) [\phi^4](x) \right\rangle \mathrm{d}x \tag{4.25}$$

$$\sum_i \left[ \left(2 X_i^M X_i^\lambda - \delta^{M\lambda} X_i^2\right) \frac{\partial}{\partial X_i^M} + 2\Delta_\phi X_i^\lambda \right] \left\langle \prod_j \Phi(X_j) \right\rangle = 2\beta(\lambda) \frac{\mu^\varepsilon}{4!} \int x^\lambda \left\langle \prod_j \Phi(X_j) [\phi^4](x) \right\rangle \mathrm{d}x \ .$$

These may now be freely restricted to the defect. Conformal invariance, following from $\beta(\lambda_*) = 0$, is often taken for granted once a Ward identity like (4.25). The main improvement to the situation, offered in [158], is a proof that the integrals on the right-hand side do not overpower the suppression from the beta function. These are the integrals to which a pessimist would point as the source of a possible virial current due to non-perturbative effects.

The Caffarelli-Silvestre trick, rewriting (4.2) as (4.23), has been instrumental in this proof of conformal invariance to all orders in perturbation theory. However, it can (and should) be further used to argue that a convergent OPE is inherited from the ambient space. The ability to write higher-point correlators as sums of lower-point correlators is certainly important for the non-perturbative study we have in mind. And yet, the standard proof of this in CFT appeals to the notion of a Hilbert space — something that requires a local Hamiltonian. As far as we are aware, "conformal invariance without OPE" and "conformal invariance with OPE" should both be considered plausible properties for nonlocal theories *a priori*, with the latter fortunately being realized in this case.

## 4.2 A theory for the crossover

The flow we have discussed above goes back to [188], with significant improvements in [194]. This enables perturbation theory around $s = \frac{d}{2}$ but we have yet to discuss $s = s_*$. If this really caputres short-range behaviour, we should expect *e.g.* $\phi$ and $\phi^2$ to take on scaling dimensions of $\Delta_\sigma^{\text{SRI}}$ and $\Delta_\epsilon^{\text{SRI}}$ respectively for this value of $s$. An ideal scenario would explain how these exactly known dimensions are approached perturbatively. A solution to this problem, recently found in [159, 160], is what we now discuss.

Cardy and Sak [195, 196] proposed a nonlocal perturbation around the crossover given by

$$S = S_{\text{SRI}} + \int \frac{\sigma(x)\sigma(y)}{|x-y|^{d+s}} \mathrm{d}x\mathrm{d}y \ , \tag{4.26}$$

where $\sigma$ is the short-range spin operator. If $s$ is just slightly below $s_*$, Sak's perturbation is weakly relevant, and in principle it should be possible to study the flow perturbatively. However, it is unclear how to adapt the rules of conformal perturbation theory to this nonlocal case. To the best of our knowledge this has not been done.[4] This leaves us in a situation analogous to the original Wilson-Fisher flow (Figure 4.3) where an expansion is known for $d = 4 - \varepsilon$ but not $d = 2 + \delta$.

This lack of computability may be dismissed as a technical problem, but there are related conceptual puzzles. If the crossover is continuous, the spectrum of all operators should vary continuously. In particular, the number of operators should be the same on both sides of the

[4] There has recently been a growing interest in deformations with similar position dependence in boundary CFT [197].

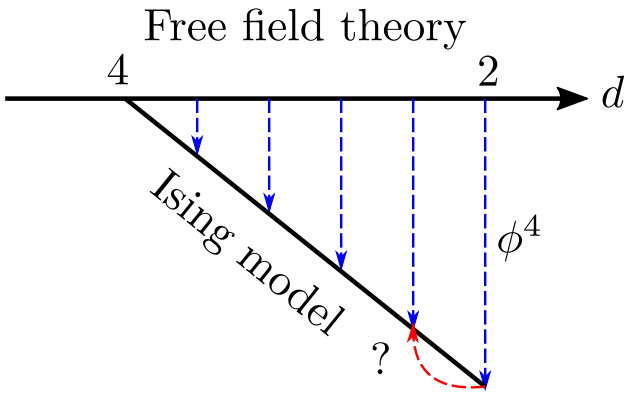


Figure 4.3: A standard RG flow diagram where long arrows are strongly coupled and short arrows are weakly coupled. In this case, we show the standard approach to the short-range Ising model where perturbation theory can only be done close to $d = 4$ despite the fact that $d = 2$ is a solved case as well. This is what the long-range RG flow diagram looked like before the work of [159, 160].

crossover. However, for some LRI operators no counterpart SRI operators appear to exist. One such operator is $\phi^3$. As (4.2) has a nonlocal equation of motion rather than a local one, $\phi^3$ is a primary in the LRI — one which we can easily show to be relevant. This is puzzling, because the SRI contains, both in $d = 2$ and $d = 3$, a *single* relevant $\mathbb{Z}_2$ odd scalar.

Another puzzle involves the stress tensor operator. The SRI has a local conserved stress tensor $T_{\mu\nu}$. Moving to the long-range regime, this operator is expected to acquire an anomalous dimension so that it is no longer conserved. The divergence $V_\nu = \partial^\mu T_{\mu\nu}$ is thus a non-trivial operator in the LRI. At the crossover point the dimension of this vector operator is exactly $d+1$. Is there such an operator in SRI? 2D Ising is a solvable minimal model and it is easy to see by inspection that there is no such operator. For $d$ close to 4 one can use the weakly coupled Wilson-Fisher description, and again there is no such operator. While in $d = 3$ its existence cannot be rigorously excluded at present, it seems very unlikely.[5]

The puzzle of the missing $V_\mu$ can be stated more formally in terms of "recombination rules" of unitary representations of the $\mathfrak{so}(d+1,1)$ conformal algebra. The standard stress tensor of the SRI is the lowest weight state (conformal primary) of the *shortened* spin-2 representation $\mathcal{C}^d_{\ell=2}$, while the non-conserved spin-2 operator of the LRI is the conformal primary of the *long* spin-two representation $\mathcal{A}^\Delta_{\ell=2}$, with $\Delta \geq d$ for unitarity. When the unitarity bound is saturated, the long spin-2 representation decomposes into the semi-direct sum $\mathcal{A}^d_{\ell=2} \simeq \mathcal{C}^d_{\ell=2} \oplus \mathcal{A}^{d+1}_{\ell=1}$. In other terms, the shortened spin-2 representation can become long only by recombining with ("eating") an additional spin-one representation, $\mathcal{A}^{d+1}_{\ell=1}$, whose conformal primary $V_\mu$ is however missing in the SRI.

[5] $\mathbb{Z}_2$-even operators of odd spin have not yet been probed by the numerical conformal bootstrap.

### 4.2.1 Review of standard flow


Figure 4.4: The first non-vanishing correction to the two-point function of $\phi$.

We will first review some key features of the standard flow (4.2) that have not been mentioned yet. The first is that the $\phi$ and $\phi^3$ operators are protected. We have already seen from (4.4) that there is no anomalous dimension $\gamma_\phi$ at one-loop. However, it may be seen more generally that $\gamma_\phi = 0$ at any number of loops. The intuitive justification for this is that a nonlocal kinetic term cannot be modified by local divergences. A useful test is evaluating the first two-loop diagram that could potentially influence $\gamma_\phi$. Using analytic regularization, the diagram in Figure 4.4 yields

$$\begin{aligned} G(k) &= \frac{\lambda^2}{6(4\pi)^d}\frac{\Gamma\left(\frac{3s}{2}-d\right)\Gamma\left(\frac{d-s}{2}\right)^3}{\Gamma\left(\frac{3d-3s}{2}\right)\Gamma\left(\frac{s}{2}\right)^3}\left|\frac{k}{\mu}\right|^{2d-3s} \\ &= \frac{\lambda^2}{6(4\pi)^d}\frac{\Gamma\left(\frac{3\varepsilon-d}{4}\right)\Gamma\left(\frac{d-\varepsilon}{4}\right)^3}{\Gamma\left(\frac{3d-3\varepsilon}{4}\right)\Gamma\left(\frac{d+\varepsilon}{4}\right)^3}\left|\frac{k}{\mu}\right|^{\frac{d-3\varepsilon}{2}} . \end{aligned} \tag{4.27}$$

This requires no minimal subtraction as the $\varepsilon \to 0$ limit is finite for all $1 \leq d < 4$. Indeed, $\Gamma\left(-\frac{d}{4}\right)$ is the only gamma function with a non-positive argument. We have already seen a preference for such gamma functions in (4.10). It is reassuring that a pole appears for $d = 4$, which is precisely the value that turns (4.2) into a local theory.[6] The upshot is that the dimension of $\phi$ has the exact expression

$$\Delta_\phi = \frac{d-s}{2} , \tag{4.28}$$

a relation which has been proven rigorously in [202].[7] By demanding that the short-range scaling dimensions are approached continuously, we can take $\Delta_\sigma^{\text{SRI}} = \frac{d-s_*}{2}$ as the definition of $s_*$. This is a correction to [188] which initially predicted $s_* = 2$. The correct behaviour at the crossover was explicitly demonstrated in [194] by taking $d \to 4$ to make the entire

[6] Because (4.27) is a two-loop contribution, we must be careful when using it to solve for $\gamma_\phi$ in the Wilson-Fisher fixed point. Setting $d = 4$ in the second line is not valid. We must instead set $(s, d) = (2, 4-\varepsilon)$ in the first line. This diagram therefore provides a counter-example to the widely discussed "effective dimension" idea [198–201], which we do not find convincing.

[7] Earlier work had rigorously proven that the anomalous dimension must be non-negative [203]. The vanishing can be established for any nonlocal theory that can be realized as a defect where the bulk is free (such as the LRI, given (4.23)). This comes from writing the bulk field in terms of the defect OPE and demanding that the Laplacian still kill the right-hand side [140].

flow perturbative. When this is done, one sees that the weakly irrelevant operator $\phi\partial^2\phi$ is responsible for the breakdown of (4.28).

The second operator with an exactly known scaling dimension is $\phi^3$. This is obvious in the Wilson-Fisher fixed point as the equation of motion $\partial^2\phi = \frac{\lambda}{3!}\phi^3$ places $\phi^3$ squarely in the $\phi$ multiplet.[8] In the LRI, this protected dimension is instead a consequence of the *nonlocal* equation of motion

$$\partial^s\phi = \frac{\lambda}{3!}\phi^3 \ , \tag{4.29}$$

with $\phi^3$ remaining an independent primary. From (4.29), we read off

$$\Delta_{\phi^3} = \frac{d+s}{2} \ . \tag{4.30}$$

These operators, satisfying $\Delta_\phi + \Delta_{\phi^3} = d$, are often said to form a *shadow pair* [158]. Although this relation will come out of many integrals that will be evaluated soon, we now give another proof which demonstrates the role of the Callan-Symanzik equation.

In perturbation theory, the nonlocal equation of motion simply means that the diagrams contributing to correlation functions of $\phi^3$ are the diagrams of $\phi$ amputated by one propagator.[9] In other words correlators of $\phi^3$ are related to those of $\phi$ by (in momentum space)

$$\begin{aligned} \frac{\lambda_0}{3!}\langle\phi^3(p)\ldots\rangle &= |p|^s\langle\phi(p)\ldots\rangle \\ \frac{\mu^\varepsilon\lambda}{3!}\langle[\phi^3](p)\ldots\rangle &= |p|^s\langle\phi(p)\ldots\rangle \ . \end{aligned} \tag{4.31}$$

Now, (4.31) implies that the correlation functions of the so defined $[\phi^3]$ are free of poles in $\varepsilon$. Since $Z_\lambda = Z_3^{-1}$, a short computation allows us to express $\gamma_{\phi^3}$ via the beta function all along the flow:

$$\gamma_{\phi^3}(\lambda) = \varepsilon + \beta(\lambda)\lambda^{-1} \ . \tag{4.32}$$

In particular in the IR we have $\gamma_{\phi^3} \to \varepsilon$, which given the dimension of $\phi$, is equivalent to the shadow relation. This argument proves the shadow relation to all orders in perturbation theory.

### 4.2.2 An infrared duality

We will now explain how the situation of Figure 4.3 is improved to that of Figure 4.5. Where this differs from standard (incorrect) lore is that the LRI does not crossover to the SRI, but

[8] The implications of this for anomalous dimensions were explored in [204].

[9] This amputation relation is true for the diagrams which connect $\phi$ to an interaction vertex. Diagrams which connect $\phi$ directly to another $\phi$ in the correlator do not have a counterpart for the correlators of $\phi^3$. The equation of motion maps such diagrams into local terms, and is thus valid modulo such local terms. These local terms are not important for the present discussion.

to a larger theory which consists of the SRI and a decoupled mean-field which we call $\chi$. Assuming this, we can construct the flow from the larger theory to the LRI by turning on the perturbation

$$S = S_{\rm SRI} + \int -\frac{1}{2}\chi\partial^{-s}\chi + g_0\sigma\chi \mathrm{d}x \tag{4.33}$$

The sign of $g_0$ is arbitrary since it can be flipped by the symmetry $\chi \to -\chi$. In fact the decoupled theory has an enlarged $\mathbb{Z}_2 \times \mathbb{Z}_2$ symmetry which is broken to the diagonal when the perturbation $\sigma\chi$ is turned on. This is as it should be, since the LRI has only a single $\mathbb{Z}_2$ symmetry $\sigma \to -\sigma$. The enlarged symmetry leads to selection rules, which will appear many times in the RG calculations below.

Connection to the standard picture is established by integrating out $\chi$, which should generate precisely Sak's non-local perturbation (4.26).[10] This fixes the dimension $\Delta_\chi = \frac{d+s}{2}$, so that the local deforming operator $\mathcal{O}$ satisfies

$$\Delta_{\mathcal{O}} = \Delta_\chi + \Delta_\sigma = d - \delta \ , \ \delta = \frac{s_* - s}{2} \ . \tag{4.34}$$

This crosses from relevant to irrelevant at the same location as before. We emphasize however that $\chi$ is not simply a theoretical construct but a physical field.

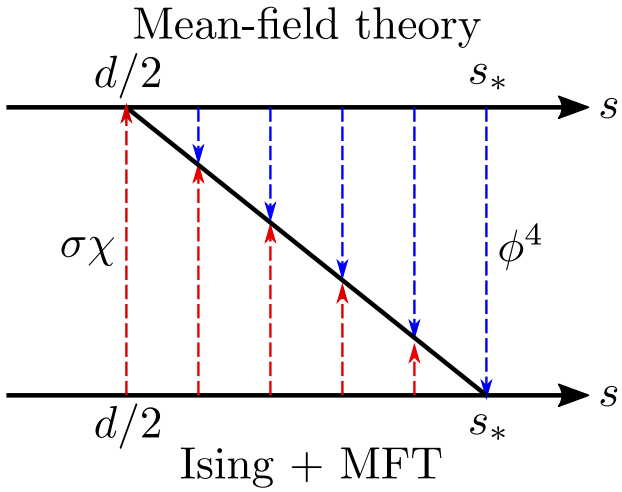


Figure 4.5: The RG flow diagram showing the two flows to the LRI where one is weakly coupled precisely when the other is strongly coupled.

The existence of $\chi$ allows us to resolve the difficulties concerning the crossover description. First of all, since $\chi$ and $\phi$ satisfy the shadow relation, $\chi$ can be identified with $\phi^3$ at the crossover point. This identification and its consequences will be discussed in detail below. We will also see that using $\chi$ one can construct a vector operator playing the role of $V_\mu$. Finally,

[10] Notice that for real $g_0$, the generated operator has ferromagnetic, negative, sign, as it should.

since $\mathcal{O}$ is a local operator, we will be able to use the well-developed framework of conformal perturbation theory to compute the long-range critical exponents near the crossover point.

We have a situation predicting that two flows (one perturbative for $\varepsilon \to 0$, the other for $\delta \to 0$) have the same IR endpoint. In quantum field theoretic parlance, this is referred to as "infrared duality". A famous example is the Seiberg duality which establishes the IR equivalence of UV-distinct $\mathcal{N} = 1$ supersymmetric gauge theories [205]. Another example is the particle / vortex duality between the $XY$ model and the $U(1)$ Abelian Higgs model in 3D, both flowing to the same $O(2)$ Wilson-Fisher critical point [206, 207]. The novelty of our example is that the IR fixed-point does not have a local stress tensor.

### 4.2.3 All-order predictions

Something to see right away is that $\gamma_\chi(g) = 0$ all along the flow. This is motivated in the same way as for $\phi$ in the $\phi^4$ flow. Namely, that poles in $\delta$ correspond to short-distances divergences of the integral for $\delta = 0$, the divergences are local, and the action of $\chi$ is non-local, so it cannot be renormalized. We then obtain that the anomalous dimension of $\chi$ at the fixed-point is identically zero.

We can argue that the IR fixed-point of the $\sigma\chi$-flow should be conformally invariant. Indeed, we can derive the broken conformal Ward identities for the $\sigma\chi$-flow by the same Caffarelli-Silvestre trick. We can then show that these Ward identities imply the conformal invariance in the IR.

We also have the nonlocal equation of motion

$$\partial^{-s}\chi = g\sigma \ , \tag{4.35}$$

and therefore all the same shadow relation consequences.

We now see that the both the $\phi^4$ and $\sigma\chi$ flows have a conformally invariant IR fixed-point. The dimensions of two operators at the fixed-point are exactly known (one by non-renormalization, another by the shadow relation):

$$\begin{aligned} \Delta_\phi &= \tfrac{d-s}{2} &&= \Delta_\sigma \\ \Delta_{\phi^3} &= \tfrac{d+s}{2} &&= \Delta_\chi \ . \end{aligned} \tag{4.36}$$

The $\phi^4$ statements have been proven to all orders while the analogous $\sigma\chi$ statements hold as well under the reasonable assumption of renormalizability.

The most natural interpretation of these results is that there is only one CFTs for each $s$, which describes the fixed points of both flows (infrared duality). The fields $\phi$ and $\phi^3$ for the first flow have to be identified in the IR with $\sigma$ and $\chi$ for the second flow (up to proportionality coefficients). As such, we will often use the two notations interchangeably. Finally, the above equations for the IR field dimensions are valid *exactly* and not just in perturbation theory. Indeed, if there were nonperturbative corrections to one set of equations, they would

presumably become largest near the short-range crossover, but this is where the other set of equations becomes accurate and shows that there are no corrections.

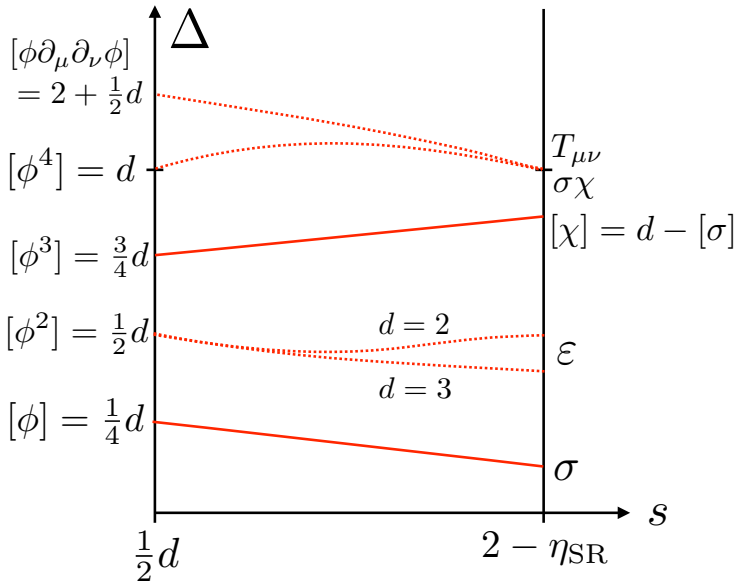


Figure 4.6: The dependence of dimensions of several important operators on $s$. The main text uses $[\mathcal{O}]$ to denote the renormalized version of $\mathcal{O}$ but here it is a shorthand for $\Delta_{\mathcal{O}}$.

Figure 4.6 predicts the dependence of the most important LRI operator dimensions on $s$ between the $s = \frac{d}{2}$ and $s = s_*$ points. The solid lines joining $\phi$ to $\sigma$ and $\chi$ to $\phi^3$ are straight lines. The other lines are known only approximately in the $\varepsilon$ and $\delta$ expansions. The shown shape of the lines is the simplest consistent with these asymptotics. The line joining $\phi^2$ to $\epsilon$ will be shown to have a vanishing first derivative at $s_*$ in $d = 2$ but not $d = 3$ momentarily.

After the section that deals with anomalous dimensions, we include a section that focuses on OPE coefficients. These allow a non-trivial check of the duality which we will now explore. First, we can scale the coupling out of the nonlocal equation of motion to write

$$\phi^3(x) = \int \frac{\phi(y)}{|x-y|^{2\Delta_{\phi^3}}} \mathrm{d}y \ . \tag{4.37}$$

Since two-point functions change with $s$, we can use this to relate the normalization of $\phi^3$ to the normalization of $\phi$. We will act twice on

$$\langle \phi(x)\phi(0)\rangle = \frac{1+\rho(\varepsilon)}{|x|^{2\Delta_\phi}} \tag{4.38}$$

where $\rho(\varepsilon) > -1$ is expected from unitarity. The result is

$$\begin{aligned} \left\langle \phi^3(x)\phi^3(0)\right\rangle &= \frac{\rho(\varepsilon) M_2}{|x|^{2\Delta_{\phi^3}}} \\ M_2 &= \pi^d \frac{\Gamma\left(\Delta_\phi - \frac{d}{2}\right)\Gamma\left(\Delta_{\phi^3} - \frac{d}{2}\right)}{\Gamma(\Delta_\phi)\Gamma(\Delta_{\phi^3})} \end{aligned} \tag{4.39}$$

after properly handling the local terms. By complete analogy, we may start with

$$\langle \chi(x)\chi(0)\rangle = \frac{1+\kappa(\delta)}{|x|^{2\Delta_\chi}} \tag{4.40}$$

and act with the dual version of (4.37). This yields

$$\begin{aligned} \langle \sigma(x)\sigma(0)\rangle &= \frac{\kappa(\varepsilon)\hat{M}_2}{|x|^{2\Delta_\sigma}} \\ \hat{M}_2 &= \pi^d \frac{\Gamma\left(\Delta_\sigma - \frac{d}{2}\right)\Gamma\left(\Delta_\chi - \frac{d}{2}\right)}{\Gamma(\Delta_\sigma)\Gamma(\Delta_\chi)} \,. \end{aligned} \tag{4.41}$$

We would now like to divide OPE coefficients and consider $\phi$, $\phi^3$, $\sigma$ and $\chi$ to be unit-normalized for the purposes of these ratios. Although we will eventually discuss more complicated ratios, there is a remarkable comment to make about

$$\begin{aligned} \frac{\lambda_{12\phi^3}}{\lambda_{12\phi}} &= M_3 \sqrt{\frac{1+\rho(\varepsilon)}{\rho(\varepsilon) M_2}} \\ \frac{\lambda_{12\sigma}}{\lambda_{12\chi}} &= \hat{M}_3 \sqrt{\frac{1+\kappa(\delta)}{\kappa(\delta)\hat{M}_2}} \end{aligned} \tag{4.42}$$

where $M_3$ and its shadow $\hat{M}_3$ are combinations of gamma functions which we will compute. This is the identity

$$M_2 = M_3 \hat{M}_3 = \hat{M}_2 \tag{4.43}$$

which guarantees that both lines of (4.42) depend on $\Delta_1$, $\Delta_2$, $\ell_1$ and $\ell_2$ in the same way. In order to make both lines equal, not just in their quantum number dependence, we need

$$\frac{\kappa(\delta)}{1+\kappa(\delta)} = \frac{1+\rho(\varepsilon)}{\rho(\varepsilon)} \tag{4.44}$$

which is a non-trivial prediction.

Since $\kappa(\delta) = O(\delta)$ for small $\delta$, we conclude that the normalization of the two-point

function of $\phi$ must vanish linearly in $s$ close to the short-range crossover:

$$1 + \rho(\varepsilon) = O(s_* - s) \ . \tag{4.45}$$

This was previously argued by a different method in [208]. Analogously, we must have

$$1 + \kappa(\delta) = O((2s - d)^2) \tag{4.46}$$

when approaching the mean-field regime. In this case the vanishing is expected to be quadratic since $\rho(\varepsilon) = O(\varepsilon^2)$.

## 4.3 Running coupling from conformal perturbation theory

According to our proposal, the LRI can be described as the IR fixed-point of (4.33) which is weakly coupled for $\delta \ll 1$, when the $\sigma\chi$ perturbation is weakly relevant. This allows to us compute the LRI critical exponents in terms of the SRI conformal data, known exactly in $d = 2$ [12], and with an impressive precision in $d = 3$ thanks to the recent progress in the numerical conformal bootstrap.

The standard framework to describe CFTs with weakly relevant local perturbations turned on is conformal perturbation theory (see *e.g.* [209, 210] for $d = 2$ and [196, 211] for general $d$). As usual in quantum field theory, we consider the perturbative expansion of observables in the bare coupling constant in a regulated theory, and then add counterterms to cancel the dependence on the short-distance regulator. The order $n$ perturbative correction to an observable $\Xi$ is given by

$$\frac{g_0^n}{n!} \int \langle \mathcal{O}(x_1) \dots \mathcal{O}(x_n)\, \Xi \rangle \, \mathrm{d}x_1 \dots \mathrm{d}x_n \ . \tag{4.47}$$

In general, this integral is divergent when points $x_i$ collide. A convenient way to regulate is by point splitting, restricting integration to the region where all $|x_i - x_j| > a$ (short-distance cutoff). If $\Xi$ is a local operator, there will also be divergences where $x_i$ approach $\Xi$, but those are associated not with the running of the coupling but with the renormalization of $\Xi$. They will be discussed and interpreted separately below.

The first quantity we need is the beta function. Let $g = a^\delta g_0$ be the dimensionless coupling at the cutoff scale. The beta function has the form

$$\beta(g) \equiv \frac{\mathrm{d}g}{\mathrm{d}\log(1/a)} = -\delta\, g + \dots \ , \tag{4.48}$$

where $-\delta\, g$ is the classical term and $\dots$ are the quantum corrections.

The order $g^2$ correction to the beta function is proportional to the three-point function coefficient $\lambda_{\mathcal{OOO}}$. This is well known and sufficient for most applications [196, 209, 210]. However, in our case $\lambda_{\mathcal{OOO}}$ vanishes, because $\mathcal{O}$ is odd under the symmetry $\chi \to -\chi$. Analogously all even-order contributions to $\beta(g)$ will vanish as well.

The lowest nonvanishing contribution will appear at order $g^3$, and that is the only one we will need. So we have:

$$\beta(g) = -\delta g + \beta_3 g^3 \,, \tag{4.49}$$

neglecting the higher order terms. We will now review how one computes the coefficient $\beta_3$. We aim to discuss the fixed-point properties at the leading non-trivial order in $\delta$. For this we may neglect the dependence of $\beta_3$ on $\delta$, so we will compute it in the limit $\delta = 0$.[11] We will also specialize to the case $\lambda_{\mathcal{OOO}} = 0$ of interest to us, as this simplifies some details. See [212, 213] for prior work involving third-order corrections. Our discussion owes a lot to [99], which covers also the general case $\lambda_{\mathcal{OOO}} \neq 0$.

For $\delta = 0$ the coupling $g$ is marginal and its running is related to the logarithmic short-distance divergence of (4.47). At order $g^3$, we are interested in the divergence where three points come close together. In this region we can use the so called "triple OPE" which is easily seen to be nothing but the four-point function.[12]

$$\begin{aligned} \mathcal{O}(0)\mathcal{O}(x_2)\mathcal{O}(x_3) &\sim f(x_2,x_3)\mathcal{O}(0) \\ &= \langle \mathcal{O}(0)\mathcal{O}(x_2)\mathcal{O}(x_3)\mathcal{O}(\infty)\rangle\, \mathcal{O}(0) \end{aligned} \tag{4.50}$$

This is similar to the well-known relation between the usual OPE of two operators and the three-point function.

Using (4.50), we see that the divergence of the integral with three $\mathcal{O}$ insertions is equal to the integral with one $\mathcal{O}$ insertion times a divergent coefficient, computed by integrating the four-point function:

$$\int_V \langle \mathcal{O}(x_1)\mathcal{O}(x_2)\mathcal{O}(x_3)\mathcal{O}(\infty)\rangle \mathrm{d}x_1 \mathrm{d}x_2 \mathrm{d}x_3 = AV \log(1/a) + \dots \tag{4.51}$$

Integration is over the region $|x_i - x_j| > a$ with all three points belonging to a finite region of volume $V$, which serves as an IR cutoff. The IR cutoff is needed since we are interested only in the short-distance part of the divergence.

The divergence at $O(g^3)$ can thus be cancelled, and the cutoff dependence removed, by a variation of the $O(g)$ term, adjusting the bare coupling by $-A\log(1/a)\frac{g^3}{3!}$. Therefore, the beta function can be specified to this order by $\beta_3 = -\frac{A}{3!}$. To isolate the coefficient $A$, we use translational invariance to fix one of the points, say $x_3$, to 0. The volume factor $V$ cancels,

[11] To compute higher order corrections, we would have to keep $\delta$ nonzero and set up a minimal subtraction scheme. This will not be carried out here.

[12] As usual $\mathcal{O}(\infty) = \lim_{x\to\infty} |x|^{2\Delta_\mathcal{O}} \mathcal{O}(x)$.

and we are left with an integral of the function $f(x_1, x_2)$. We then separate the integration over the overall "size" of the pair of points $(x_1, x_2)$ and over their relative position. Rescaling the pair by, *e.g.* $|x_1|$, and using the fact that $f$ has dimension $2d$, we have

$$\int f(x_1,x_2)\mathrm{d}x_1\mathrm{d}x_2 = \int \frac{1}{|x_1|^{2d}} f\left(\frac{x_1}{|x_1|}, \frac{x_2}{|x_1|}\right)\mathrm{d}x_1\mathrm{d}x_2 = \mathrm{S}_d \int \frac{1}{|x_1|}\int f(\hat{e},y)\mathrm{d}y\mathrm{d}|x_1| \quad (4.52)$$

where $\hat{e}$ is an arbitrary unit length vector and $\mathrm{S}_d = 2\pi^{d/2}/\Gamma(d/2)$. The log divergence $\sim \log(L/a)$ now arises from integrating over $a < |x_1| < L$, which is basically the pair size. So we conclude

$$A = \mathrm{S}_d \int [f(\hat{e},y) - \dots]\,\mathrm{d}y \quad (4.53)$$

where the implicit terms cancel whatever power-law divergences may have been present in (4.51) without changing the log. These power divergences have nothing to do with the running of $g$. Instead, they renormalize coefficient of the relevant operators appearing in the OPE $\mathcal{O}\times\mathcal{O}$. In our case there are two such operators, the unit operator and the SRI energy density operator $\epsilon$.[13] The unit operator coefficient is unimportant, while that of $\epsilon$ has to be anyway tuned to zero to reach the fixed point, as this corresponds to tuning the temperature to the critical temperature. The bottom line is that the power divergences need to be subtracted away.

There are two methods to do this, which give equivalent, although not manifestly identical, final results. Method 1 subtracts the divergent terms, given by the relevant operators, from the integrand $f$. Method 2 computes the integral (4.53) with a cutoff and drop the terms that diverge when the cutoff is sent to zero. In both case we are just dropping power divergences of the integral (4.52) and we are not changing the coefficient of the logarithm divergence. Once one of these methods has been employed, the integral is convergent.

*Method 1.* We subtract from the integrand $f$ in (4.52) the singularities associated with the two relevant operators in the limits $x_1 \to 0$, $x_2 \to 0$, $x_1 \to x_2$. The subtraction terms have to be chosen so that they fully subtract the power divergence but do not modify the logarithmic divergence. The following simple choice satisfies these constraints:

$$\begin{aligned} f \to \tilde{f} &= f - r_1 - r_\epsilon \\ r_1 &= \frac{1}{|x_1|^{2d}} + \frac{1}{|x_2|^{2d}} + \frac{1}{|x_1-x_2|^{2d}} \\ r_\epsilon &= \lambda^2_{\sigma\sigma\epsilon}\left(\frac{1}{|x_1|^{2d-\Delta_\epsilon}|x_2|^{\Delta_\epsilon}} + \frac{1}{|x_2|^{2d-\Delta_\epsilon}|x_1|^{\Delta_\epsilon}} + \frac{1}{|x_1-x_2|^{\Delta_\epsilon}|x_1|^{2d-\Delta_\epsilon}}\right). \end{aligned} \quad (4.54)$$

Here $\lambda_{\sigma\sigma\epsilon}$ is the SRFP OPE coefficient: $\sigma\times\sigma = I + \lambda_{\sigma\sigma\epsilon}\epsilon + \dots$. The crucial point is that these subtraction terms themselves only have power divergences. This is obvious for $r_1$. For

[13] Another low-dimension scalar operator in the $\mathcal{O}\times\mathcal{O}$ OPE is $\chi^2$, but this one is irrelevant since $s > 0$.

$r_\epsilon$, notice that the $x_1$ and $x_2$ integrals of each term factorize into a product of two integrals each of which has only power divergences. So the logarithmic divergence is not modified by the subtraction procedure.

The regulated expression for $A$ is the obtained by changing $f(\hat{e}, y) - \cdots \to \tilde{f}(\hat{e}, y)$ in (4.53). This integral is now convergent, although not absolutely convergent. The lack of absolute convergence is due to the presence of relevant or marginal operators with nonzero spin in the $\mathcal{O} \times \mathcal{O}$ OPE. These are $\partial_\mu \epsilon$ and the stress tensor $T_{\mu\nu}$. Since these operators have nonzero spin, their contributions vanish when integrated over the angular directions. So the integral has to be understood in the sense of principal value, introducing and then removing spherical cutoffs around 0, $\hat{e}$ and $\infty$. These cutoffs are remnants of the original cutoffs on $|x_2|$ and $|x_1 - x_2|$, since $y$ is the rescaled $x_2$.

*Method 2.* In this method we start by spliting the integration region of (4.51) into three parts. We consider one region in which $x_{12}$ is the shortest distance:

$$\mathcal{R}_{12} = \{x_1, x_2, x_3 : |x_{12}| < |x_{13}|, |x_{12}| < |x_{23}|\} \ , \tag{4.55}$$

and the two other regions $\mathcal{R}_{23}$ and $\mathcal{R}_{13}$, given by permutations of the three points. It is clear that these three regions contribute equally to the integral (4.51), so we can focus on $\mathcal{R}_{12}$. As before, we set one of the points to zero and we rescale $x_1$ and $x_2$ by $|x_1|$. The logarithmic divergence arises when integrating over $|x_1|$. We obtain

$$A = 3\mathrm{S}_d \int_{\mathcal{R}} \langle \mathcal{O}(0)\mathcal{O}(y)\mathcal{O}(\hat{e})\mathcal{O}(\infty)\rangle \, \mathrm{d}y \tag{4.56}$$

where

$$\mathcal{R} = \{y : |y| < 1, |y| < |y - \hat{e}|\} \tag{4.57}$$

which is a rescaled $\mathcal{R}_{12}$. Such an integral is not yet convergent when integrating $y$ around 0 due to the presence of relevant operators being exchanged. These divergences may be subtracted again by introducing a UV cutoff but now they have the advantage of only appearing in one place.

Although these methods are not manifestly identical, the logic of their derivation shows that they should give identical answers (and they do, in all cases we checked). In practical computations, both ways of proceeding have advantages and disadvantages. Method 2 fully takes advantage of the symmetry among $0, 1, \infty$, while the integrands in Method 1 do not respect this symmetry (it is broken by the subtraction terms). Still, if one were to aim for analytic expressions, Method 1 seems preferable. The shape of the integration region in Method 2 makes it hard to compute the integral analytically. However, Method 2 will prove useful and yield more precise results when the integral needs to be evaluated numerically. Besides, in $d = 3$, where the correlation function is not known exactly but will be constructed approximately from the bootstrap data, Method 2 allows to consider the conformal block expansion in the s-channel only, without any need to deal with the other decompositions.

We adopted Method 2 as the principal method for the beta function computation both in $d = 2$ and $d = 3$, since as we will see the integrals have to be computed numerically. While Method 1 is less precise for the numerical evaluation, we still checked that it gives the same results within its reduced precision.

### 4.3.1 2D beta function

The 2D SRI is the minimal model CFT $\mathcal{M}(3,4)$ and everything about it is known exactly [12]. In particular, we have $\Delta_\sigma = \frac{1}{8}$, $\Delta_\epsilon = 1$ and $\lambda_{\sigma\sigma\epsilon} = \frac{1}{2}$. The four-point function of $\sigma$ is given by

$$\langle \sigma(0)\sigma(1)\sigma(z)\sigma(\infty)\rangle = \frac{|1+\sqrt{1-z}|+|1-\sqrt{1-z}|}{2|z|^{1/4}|1-z|^{1/4}}\,. \tag{4.58}$$

Comparing the notation to our previous expression, we have fixed $\hat{e}$ at 1 on the real axis, while $y = z$ runs over the full complex plane. In spite of the appearance the four-point function is smooth across $z \in (1,\infty)$.

The four-point function of $\chi$ is Gaussian, given by the sum of three Wick contractions. In the same kinematics,

$$\langle \chi(0)\chi(1)\chi(z)\chi(\infty)\rangle = 1 + \frac{1}{|z|^{2\Delta_\chi}} + \frac{1}{|1-z|^{2\Delta_\chi}}\,, \quad \Delta_\chi = 2 - \Delta_\sigma = \frac{15}{8}\,. \tag{4.59}$$

The four-point function of $\mathcal{O}$ is given by the product of (4.58) and (4.59):

$$F(z,\bar{z}) = \left[1 + \frac{1}{|z|^{\frac{15}{4}}} + \frac{1}{|z-1|^{\frac{15}{4}}}\right] \frac{|1+\sqrt{1-z}|+|1-\sqrt{1-z}|}{2|z|^{\frac{1}{4}}|z-1|^{\frac{1}{4}}}\,. \tag{4.60}$$

We were not able to evaluate the integral of $F(z)$ analytically, so we will report the results of the numerical evaluation. We employ Method 2, so that we have to integrate over the region $\mathcal{R}$.

As discussed after (4.53), the integral is not convergent around 0. If we expand $F(z,\bar{z})$ around $z = 0$, we encounter several terms responsible for the non-convergence. The terms $|z|^{-4}$ and $|z|^{-2}$ correspond to contributions of the identity operator and energy density $\epsilon$ respectively. Other terms, such as $z/|z|^3$ and $z^2/|z|^4$ (along with their conjugates), are the contributions of $\partial_\mu\epsilon$ and $T_{\mu\nu}$ in the $\mathcal{O}\times\mathcal{O}$ OPE — these vanish upon angular integration.

To deal with the divergences, we remove from the region $\mathcal{R}$ a small disk $|z| < a$ around the origin, and divide the rest into two regions: the annulus $\mathcal{A}(a < |z| < r_0)$ centered around zero and its complement $\bar{\mathcal{A}}$, see Fig. 4.7. Here $r_0$ is arbitrary subject to $a < r_0 < 1/2$. In $\mathcal{A}$ we expand $F(z)$ functions as a series in $z$ and $\bar{z}$ up to some high order. We can then drop the terms that vanish upon angular integration, and we integrate exactly the remaining terms. The power-law divergent, as $a \to 0$, part of the answer is dropped. In the complement of

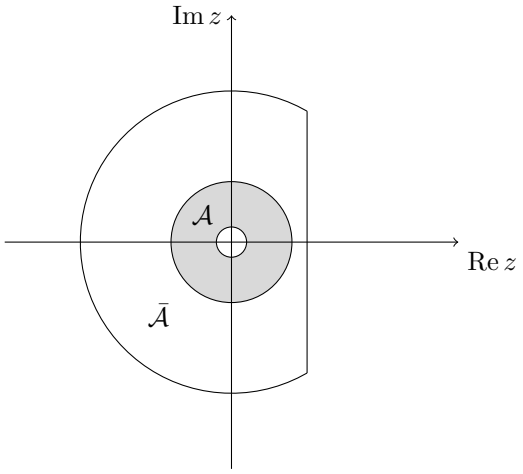


Figure 4.7: The integration region $\mathcal{R}$.

the annulus we integrate $F(z)$ numerically. The so regulated integral over $\mathcal{R}$ is then:

$$I_{d=2} = \int_{\mathcal{R}} d^2z\, F(z,\bar{z}) = -0.403746\ldots \tag{4.61}$$

All the shown digits are exact, and we checked that the result is stable against changes of $r_0$. This implies

$$\beta_3 = -3(2\pi) I_{d=2} \frac{1}{3!} = 1.268404 \quad (d=2). \tag{4.62}$$

### 4.3.2 3D beta function

The 3D SRI is not yet exactly solved but high precision results are available thanks to the progress of the numerical conformal bootstrap [77, 94, 95, 129, 185]. Recently, the approximate critical 3D Ising four-point function extracted from the bootstrap data was used in [99] to study the random-bond Ising critical point. It was also used in [100] to qualify the non-Gaussianity of the 3D Ising model.

Here we proceed analogously and will use the OPE coefficients $\lambda_{\sigma\sigma\mathcal{O}}$ and dimensions $\Delta_{\mathcal{O}}$ of the lowest lying operators (such that $\Delta_{\mathcal{O}}$ is smaller than some cutoff in the spectrum $\Delta_*$) to construct an approximate four-point function for the $\sigma$ field:

$$\langle \sigma(0)\sigma(\hat{e})\sigma(y)\sigma(\infty)\rangle \simeq \frac{1}{|x|^{2\Delta_\sigma}} \sum_{\mathcal{O}:\Delta_{\mathcal{O}}<\Delta_*} \lambda^2_{\sigma\sigma\mathcal{O}}\, g_{\Delta_{\mathcal{O}},\ell_{\mathcal{O}}}(z,\bar{z})\,, \tag{4.63}$$

where $g_{\Delta,\ell}$ are the conformal blocks. Let us fix $\hat{e} = (1,0,\ldots,0)$. Then $z$ is the complex

coordinate related to $y$ by

$$z = y_1 + i|y_\perp|, \quad y_\perp = (y_2, \ldots, y_d)\,. \tag{4.64}$$

The four-point function only depends on $|y_\perp|$ because of rotation invariance around the $x_1$ axis. The usual conformal cross ratios $u$, $v$ are $u = |z|^2$, $v = |1-z|^2$. Instead of $z$, it will be convenient to work with the radial coordinate of [84].

$$\rho(z) = \frac{z}{\left(1+\sqrt{1-z}\right)^2} \tag{4.65}$$

In three dimensions, the conformal blocks are not known exactly. However, they can be computed efficiently as a series in $r$ and $\eta = \cos\theta$, where $\rho = re^{i\theta}$, using a recursion relation [24, 214]. The conformal block expansion converges for $r < 1$ [40], while in the integration region $\mathcal{R}$ the maximum value of $r$ is $2-\sqrt{3} \simeq 0.27 < 1$, so our series expansion will converge exponentially fast.

When approximating the four-point function, we have to take into account three different sources of error:

1. We do not know the OPE coefficients and the operator dimensions exactly, as they are obtained through the numerical conformal bootstrap. The uncertainty due to this will turn out to be subleading;

2. We compute the conformal blocks as a series expansion in $r$. Here we did it up to order $O(r^{12})$, which provided sufficient accuracy, but it would be straightforward to compute them to a higher order;

3. We know the dimensions and the OPE coefficients of primary operators only up to a dimension $\Delta_*$. The error introduced is of order $r^{\Delta_*}$ [40]. We use data from the numerical conformal bootstrap on operators up to dimension $\Delta_* = 8$.

We will focus on the last source of error, since it will be the dominant one. The error one introduces when truncating the conformal block expansions of a four-point function of identical scalars $\sigma$ to some dimension $\Delta_*$ was estimated in [40, 41] to be

$$\left|\sum_{\mathcal{O}:\Delta_\mathcal{O}\geq\Delta_*} \lambda^2_{\sigma\sigma\mathcal{O}}\, g_{\Delta_\mathcal{O},\ell_\mathcal{O}}(z,\bar{z})\right| \lesssim \frac{2^{4\Delta_\sigma}}{\Gamma(4\Delta_\sigma+1)}\Delta_*^{4\Delta_\sigma}|\rho(z)|^{\Delta_*}\,. \tag{4.66}$$

This error estimate is essentially optimal for real $0 < z < 1$, when the four-point function is in a reflection positive configuration, and all conformal blocks are positive. This corresponds to the configuration with $\eta = 1$ in the $\rho$ plane. For configurations with $\eta < 1$, conformal blocks decrease in absolute value by unitarity, and hence the same estimate (4.66) applies, although it is no longer optimal. When we integrate the 4pt function over the $\eta$ coordinate, we will

not be in a reflection positive configuration, but we will nonetheless bound the truncated operators contribution by its largest possible value, obtained for $\eta = 1$. Clearly, the obtained error estimate will be overly conservative, since it does not take into account cancelations due to the varying sign of contributions of operators with spin.

Once we have constructed the approximated four-point function, we integrate it in the region $\mathcal{R}$.[14] We follow the procedure outlined in Appendix C of [99]: this consists in expanding the four-point function as a power series in $r$ and $\eta$, then integrating over $r$ and dropping the diverging contributions of the identity and the energy operator. Finally we series-expand again with respect to $\eta$ and we integrate the result exactly.

The data concerning the operator dimensions up to $\Delta_* = 8$ and their OPE coefficients can be found in Table 2 of [94] (our $\lambda_{\sigma\sigma\mathcal{O}}$ is $f_{\sigma\sigma\mathcal{O}}$ given in that table). The OPE coefficients given there are in the normalization for which the small $r$ limit of the conformal block is $g_{\Delta,\ell} \simeq \frac{\ell!}{(\nu)_\ell}(-1)^\ell C_\ell^\nu(\eta)(4r)^\Delta + \ldots$, where $C_\ell^\nu$ is a Gegenbauer polynomial, $\nu = \frac{d-2}{2}$ and $(\nu)_\ell$ is the Pochhammer symbol. Using these values, we obtain $I_{d=3} = -1.950 \pm 0.005$. The error is dominated by the truncation error, which we estimate by integrating (4.66).[15] The $g^3$ term of the beta function is then

$$\beta_3 = 12.26 \pm 0.03 \quad (d = 3). \tag{4.67}$$

### 4.3.3 Fixed-point existence

The last two calculations have shown us that for $d = 2$ and $d = 3$, we get a $\delta \ll 1$ fixed point at

$$g^2 = g_*^2 = \delta/\beta_3 \tag{4.68}$$

for a real value of the coupling. The sign of $\beta_3$ was not manifest in the above calculations, since the regulated integrals are not sign-definite.[16] Still, we have seen that $\beta_3$ is positive in both 2D and 3D. This provides a non-trivial check on our picture and allows us to proceed to the calculation of anomalous dimensions.

## 4.4 Anomalous dimensions

When deforming a CFT with a local perturbation, operators renormalize and acquire anomalous dimensions. Let us recall how these are computed in conformal perturbation theory. As usual, we require observables to be cutoff independent. To find the anomalous dimension of

[14] In $r$ and $\eta$ coordinates, the region $\mathcal{R}$ is given by $0 < r < r_*(|\eta|)$ and $-1 < \eta < 1$, with $r_*(\eta) = 2 + \eta - \sqrt{\eta^2 + 4\eta + 3}$.

[15] For comparison, if we only use operators up to $\Delta_* = 6$, we obtain the same central value but with a much larger error estimate: $I_{d=3} = -1.95 \pm 0.08$. This confirms that the error estimate is overly conservative.

[16] As a curiosity we notice that if it were not for the subtraction terms which had to be introduced in the process of disentangling short-distance divergences, then $A$ would be positive, and $\beta_3$ negative.

a local operator $\Phi(x)$, assumed unit-normalized, we look at an observable with one insertion of $\Phi$, $\langle\Phi(0)\Xi\rangle$. Perturbative corrections will be given by

$$\frac{g^n}{n!}\int\langle\Phi(0)\mathcal{O}(x_1)\dots\mathcal{O}(x_n)\Xi\rangle\,\mathrm{d}x_1\dots\mathrm{d}x_n. \tag{4.69}$$

We regulate the integral by point splitting, with a short distance cutoff $a$, like in the previous section. There we dealt with the divergences and cutoff dependence which appear when operators $\mathcal{O}$ approach each other. Those were taken care of by renormalization of the coupling, leading to the nontrivial beta function. We are interested in the additional divergences, in particular the logarithmic ones, which appear when the positions of $\mathcal{O}$ collide with those of $\Phi$.

We define a renormalized operator $[\Phi]$, whose correlation functions remain finite in the $a\to 0$ limit. This is related to the bare operator by

$$\Phi = Z_\Phi(g,a)[\Phi]\,. \tag{4.70}$$

The anomalous dimension of $\Phi$ will then be given by

$$\gamma_\Phi = -\frac{1}{Z_\Phi}\frac{\partial Z_\Phi}{\partial\log(1/a)}\,. \tag{4.71}$$

The above discussion was general, but now let us specialize to the flow which interests us, namely (4.33). We are ultimately interested in $\delta>0$ small, but at the leading order we can compute the anomalous dimension for $\delta=0$, when it is related to the log divergence as above. Moreover, order $g$ corrections will vanish thanks to the $\mathbb{Z}_2$ symmetry of the unperturbed theory, since $\Phi\mathcal{O}\Phi$ will be odd under flipping $\chi$ regardless of whether $\Phi$ is even or odd. We will therefore be interested in the anomalous dimension to order $g^2$. The computation of this anomalous dimension parallels the beta function computation. To extract the short-distance divergence giving rise to the cutoff dependence of $\Phi$, we consider the "triple OPE"

$$\begin{aligned}\Phi(0)\mathcal{O}(x_1)\mathcal{O}(x_2) &\sim h(x_1,x_2)\Phi(0)\\ &= \langle\Phi(0)\mathcal{O}(x_1)\mathcal{O}(x_2)\Phi(\infty)\rangle\,\Phi(0)\,.\end{aligned} \tag{4.72}$$

If the short-distance logarithmic divergence is

$$\int_V\langle\Phi(0)\mathcal{O}(x_1)\mathcal{O}(x_2)\Phi(\infty)\rangle\mathrm{d}x_1\mathrm{d}x_2 = B\log\frac{1}{a}+\dots \tag{4.73}$$

the renormalized operator will be made cutoff-independent by the choice

$$Z_\Phi = 1+\frac{g^2}{2}B\log\frac{1}{a}+O(g^3)\,. \tag{4.74}$$

It follows that at the fixed point, where $g = g_*$, the operator $\Phi$ will acquire an anomalous dimension of

$$\gamma_\Phi = -\frac{g_*^2}{2} B + O(g_*^3)\,. \tag{4.75}$$

As before, we rescale the two integration points $x_1$ and $x_2$ by $|x_1|$. The logarithmic divergence of the integral (4.73) is then

$$B = \mathrm{S}_d \int [h(\hat{e}, y) - \dots] \mathrm{d}y \tag{4.76}$$

where we have again prepared for necessary subtractions. Excluding the case $\Phi = \mathcal{O}$, the OPE $\Phi \times \mathcal{O}$ does not contain the unit operator or the stress tensor. Nor does it contain $\Phi$ since $\lambda_{\Phi\Phi\mathcal{O}} = 0$. Assuming all other operators in the OPE have dimension larger than that of $\Phi$, the above integral is convergent near 0 and $\infty$. Let us proceed under the above assumptions, otherwise minor obvious modifications will be required.

The integral presents power-law divergences for $y$ close to $\hat{e}$. These divergences are due to the unit operator and $\epsilon$ in the $\mathcal{O} \times \mathcal{O}$ OPE. As already mentioned in the beta function discussion, they do not have anything to do with the critical point physics. We have to drop these divergences, but in a way which does not modify the log divergence influencing the anomalous dimension of the operator $\Phi$. We have again two different ways to proceed, with minor modifications compared to the beta function computation.

*Method 1.* We subtract the contributions of the relevant operators at the level of (4.73), so that the logarithmic divergences are unchanged. Since all divergences come from $x_1 \to x_2$, we may write

$$\begin{aligned} h \to \tilde{h} &= h - s_1 - s_\epsilon \\ s_1 &= \frac{1}{|x_1 - x_2|^{2d}} \\ s_\epsilon &= \lambda_{\Phi\Phi\epsilon}\lambda_{\mathcal{O}\mathcal{O}\epsilon} \frac{1}{|x_1 - x_2|^{2d-\Delta_\epsilon}|x_1|^{\Delta_\epsilon}} \end{aligned} \tag{4.77}$$

knowing the relevant operators. It is then a matter of taking $h(\hat{e}, y) - \dots \to \tilde{h}(\hat{e}, y)$ to compute the value of $B$.

*Method 2.* We split again the integration region of (4.73) into three smaller subregion. This will make the numerical evaluation of the integral simpler. Clearly, the contribution of the integration region with $x_1$ close to zero, $|x_1| < |x_2|$ and $|x_1| < |x_1 - x_2|$, is the same as that of the region with $x_2$ close to zero. However, the contribution of the region where $x_1$ and $x_2$ are close together will be different. By the same logic as before, we obtain a regulated

expression for (4.76):

$$B = \mathrm{S}_d \int_{\mathcal{R}} 2\langle \Phi(0)\mathcal{O}(y)\mathcal{O}(\hat{e})\Phi(\infty)\rangle + \langle \mathcal{O}(0)\mathcal{O}(y)\Phi(\hat{e})\Phi(\infty)\rangle \mathrm{d}y\,. \tag{4.78}$$

The integration region $\mathcal{R}$ is the same as in the previous section. The first term is finite since $y$ is separated from $\hat{e}$. The second term has a power-law divergences, but no log divergences for small $y$ — we make it finite by dropping the divergent terms.

### 4.4.1 Protected operator dimensions

Let us keep $d$ general and consider the field $\chi$. This is described by a nonlocal action in the UV. As a consequence, we expect that $\chi$ does not get an anomalous dimension to all orders in $\delta$. This is similar to what happens for the $\phi$ field in the 4.2. Here we will check this expectation at leading non-trivial order. Observe that the integral (4.73), with $\Phi = \chi$ and $\mathcal{O} = \sigma\chi$, only has power-law divergences, and no logarithmic divergences. Indeed its integrand is

$$\frac{1}{|x_1 - x_2|^{2\Delta_\sigma}} \left( \frac{1}{|x_1|^{2\Delta_\chi}} + \frac{1}{|x_1|^{2\Delta_\chi}} + \frac{1}{|x_1 - x_2|^{2\Delta_\chi}} \right) . \tag{4.79}$$

The integral only has power divergences by the same argument as that given for the beta function subtraction terms (4.54). If we were to apply Method 1 to this integral, we would end up with an identically vanishing integrand. Notice that in this case the OPE $\Phi \times \mathcal{O}$ contains an operator $\sigma$ with dimension $\Delta_\sigma < \Delta_\Phi$, So more subtraction terms are needed than the ones given before. After these subtractions, the integrand is identically zero.

Next we consider the field $\sigma$. It is also special, because it acts as a source for $\chi$, and so the classical equation of motion sets a linear nonlocal relation between the two. As we have mentioned, non-renormalization of the type (4.30) is a direct consequence. To check this at leading order, the anomalous dimension of $\sigma$ can be reduced by a trick to the $g^3$ term of the beta function, which we already computed. Let us consider the original integral (4.73) for $\Phi = \sigma$. It is easy to see that this integral (multiplied by the overall volume) is exactly one third of the integral (4.51) in the beta function calculation. Indeed, the integrand in both cases involves the four-point function of $\sigma$ multiplied by a correlation function of $\chi$, which has one term in the first case and three terms in the second one. These three terms all contribute equally, and so we obtain $B = A/3$. This fact is not manifest in the expressions provided by Methods 1 and 2, but we checked it numerically. The anomalous dimension of $\sigma$ is now found to be:

$$\gamma_\sigma = \delta + O(\delta^2)\,. \tag{4.80}$$

Note that the classic RG result that reads $\gamma_{\mathcal{O}}(g) = \beta'(g)$, for the deforming operator itself, follows here from the fact that $B = A$ for the renormalization of $\mathcal{O}$.

### 4.4.2 Unprotected operator dimensions

Let us now compute the anomalous dimension of $\epsilon$ in two and three dimensions. For $d = 2$, we should use the result from the Ising minimal model [215]

$$\langle \epsilon(0)\sigma(z)\sigma(1)\epsilon(\infty)\rangle = \frac{|1+z|^2}{4|z||1-z|^{1/4}}\,. \tag{4.81}$$

To obtain the correlation function $\langle \epsilon\mathcal{O}\mathcal{O}\epsilon\rangle$ we multiply (4.81) by $\langle\chi(z)\chi(1)\rangle$. This time we will use Method 1, and we will be able to carry out the integration analytically. We need to subtract the divergent terms due to the relevant operators, as shown in (4.77). The $\epsilon$ subtraction term is absent since $\lambda_{\epsilon\epsilon\epsilon} = 0$, which is part of Kramers-Wannier duality in two dimensions. We obtain the integral

$$\int_{\mathbb{C}} f(z,\bar{z})\mathrm{d}z \equiv \int_{\mathbb{C}} \frac{1}{|1-z|^4}\left(\frac{|1+z|^2}{4|z|}-1\right)\mathrm{d}z = 0 \tag{4.82}$$

as a principal value with circular cutoffs around 0, 1 and $\infty$. The fact that this integral vanishes was noticed numerically in [99]. We have obtained the following proof which still makes it seem like an accident.

We divide the complex plane into the three regions in Figure 4.8.

$$R_1 = \{z : a < |z| < 1-b\}\,, \tag{4.83}$$
$$A = \{z : 1-b < |z| < 1+b, |z-1| > a\}\,, \tag{4.84}$$
$$R_2 = \left\{z : 1+b < |z| < a^{-1}\right\}\,. \tag{4.85}$$

We need to compute the integral for small but finite values of $a$ and then take $a \to 0$ limit.

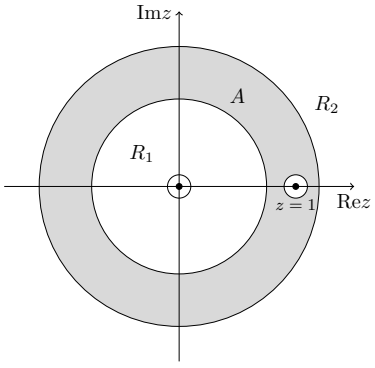


Figure 4.8: The three integration regions (4.85).

The quantity $b$ is introduced for convenience since all three integrals simplify for $b \ll 1$. We take the $b \to 0$ after $a \to 0$. It will turn out that the contribution of the region $A$ approaches

a nonzero constant. It is easy to forget about this contribution and get a wrong answer. The

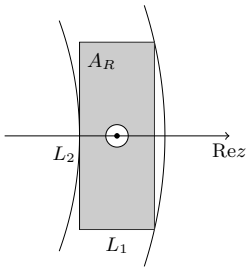


Figure 4.9: Deformation of the region $A$, which yields the same result in the $\delta \to 0$ limit.

integrals over $R_1$ and $R_2$ can be computed via

$$\int f(re^{i\theta}, re^{i\theta}) r \mathrm{d}r \mathrm{d}\theta = \int \oint f(r\rho, r/\rho) \frac{\mathrm{d}\rho}{i\rho} r \mathrm{d}r \tag{4.86}$$

and doing the $\rho$ integrals by residues. This way one obtains

$$\lim_{a\to 0} \int_{R_1} f(z,\bar{z}) \mathrm{d}z = \frac{\pi}{8} + O(b)\,, \tag{4.87}$$

$$\lim_{a\to 0} \int_{R_2} f(z,\bar{z}) \mathrm{d}z = \frac{\pi}{8} + O(b)\,. \tag{4.88}$$

We are left with computing the integral over the region $A$. When $b \to 0$ is taken, and the annulus shrinks, the integral gives a nonzero contribution because of the singularity at $z = 1$. We can restrict the integration region $A$ to a rectangle around $z = 1$, as the regions where the integrand is regular yield a zero contribution in this limit. We consider therefore the region in Figure 4.9. Let us perform a $z \mapsto z + 1$ shift and call this region $A_R = \left\{ z : -\frac{L_1}{2} < \mathrm{Re}\, z < \frac{L_1}{2}, -\frac{L_2}{2} < \mathrm{Im}\, z < \frac{L_2}{2}, |z| > a \right\}$. We expand the integrand around $z = 0$, keeping only divergent terms, to find

$$\begin{aligned} \lim_{b\to 0}\lim_{a\to 0} \int_A f(z,\bar{z}) \mathrm{d}z &= \lim_{b\to 0}\lim_{a\to 0} \int_{A_R} \left( \frac{1}{8z^2} + \frac{1}{8\bar{z}^2} \right) \mathrm{d}z \\ &= \lim_{b\to 0} \frac{1}{4} \left[ \pi - 4 \arctan\left( \frac{L_2}{L_1} \right) \right] . \end{aligned} \tag{4.89}$$

By inspection, $L_1 \sim \delta$ while $L_2 \sim \sqrt{\delta}$, telling us that the arctangent approaches $\frac{\pi}{2}$. This gives us a $-\frac{\pi}{4}$ value for (4.89) exactly cancelling (4.88).

Going back to (4.82), the anomalous dimension of $\epsilon$ in $d = 2$ vanishes at order $g_*^2$, while order $g_*^3$ will be zero by the $\mathbb{Z}_2$ selection rules. Therefore

$$\gamma_\epsilon = O(g_*^4) = O(\delta^2) \qquad (d = 2)\,. \tag{4.90}$$

Moving onto $d = 3$, we set up a numerical computation for this anomalous dimension using the CFT data from the numerical conformal bootstrap. In order to compute the four-point function $\langle \epsilon\sigma\sigma\epsilon\rangle$, we will need the operator dimensions and the OPE coefficients of the operators appearing in the $\sigma \times \sigma$, $\sigma \times \epsilon$ and $\epsilon \times \epsilon$ OPEs. For operators up to $\Delta_* = 8$, these can be found in [94], with a clear preference for Method 2. We construct the four-point function in the region where one $\epsilon$ is close to one $\mathcal{O}$ and the region where the two copies of $\mathcal{O}$ are close together:

$$\begin{aligned}\langle \epsilon(0)\sigma(z)\sigma(1)\epsilon(\infty)\rangle &= \frac{1}{|z|^{\Delta_\sigma+\Delta_\epsilon}} \sum_{\mathcal{O}:\Delta_\mathcal{O}<\Delta_*} \lambda^2_{\sigma\epsilon\mathcal{O}} g^{\Delta_{\epsilon\sigma},\Delta_{\sigma\epsilon}}_{\Delta_\mathcal{O},l_\mathcal{O}}(z,\bar{z})\,,\\ \langle \sigma(0)\sigma(z)\epsilon(1)\epsilon(\infty)\rangle &= \frac{1}{|z|^{2\Delta_\sigma}} \sum_{\mathcal{O}:\Delta_\mathcal{O}<\Delta_*} \lambda_{\sigma\sigma\mathcal{O}}\lambda_{\epsilon\epsilon\mathcal{O}} g^{0,0}_{\Delta_\mathcal{O},l_\mathcal{O}}(z,\bar{z})\,.\end{aligned} \tag{4.91}$$

Here $g_{\Delta_\mathcal{O},l_\mathcal{O}}$ with upper indices are the conformal blocks for the external scalars with unequal dimensions, which we compute via recursion relations from [78]. The operators entering the sum in the first (second) equation are $\mathbb{Z}_2$ odd (even). In both cases, we will be integrating over the now familiar region $\mathcal{R}$.

Once again, the largest error contribution when approximating the four-point function will come from the truncation of the spectrum at dimension $\Delta_*$. The same line of reasoning used to obtain the truncation error for four identical scalar in [40] will go through in the first line of (4.91). Analyzing the proof in [40], it is possible to see that the truncation error will be given by (4.66) with the change $\Delta_\sigma \to (\Delta_\sigma + \Delta_\epsilon)/2$ in all occurrences in the right-hand side.

For the second line, on the other hand, we cannot map the four-point function onto a reflection positive configuration, and therefore we cannot find a bound on the contribution of the truncated operators in the same way. We need to first use Cauchy's inequality so that the tail of $\langle\sigma\sigma\epsilon\epsilon\rangle$ can be bounded by the tails of $\langle\sigma\sigma\sigma\sigma\rangle$ and $\langle\epsilon\epsilon\epsilon\epsilon\rangle$. At this point we can use again the result of [40], and we obtain

$$\left|\sum_{\mathcal{O}:\Delta_\mathcal{O}>\Delta_*} \lambda_{\sigma\sigma\mathcal{O}}\lambda_{\epsilon\epsilon\mathcal{O}} g^{0,0}_{\Delta_\mathcal{O},l_\mathcal{O}}(z,\bar{z})\right| \lesssim \frac{2^{2\Delta_\sigma+2\Delta_\epsilon}}{\sqrt{\Gamma(4\Delta_\sigma+1)\Gamma(4\Delta_\epsilon+1)}} \Delta_*^{2\Delta_\sigma+2\Delta_\epsilon} |\rho(z)|^{\Delta_*}\,. \tag{4.92}$$

Truncating the CFT data up to $\Delta_* = 8$ and carrying out the integration in the region $\mathcal{R}$, we obtain a nonzero value, unlike in $d = 2$. The order $g_*^2$ anomalous dimension is

$$\gamma_\epsilon \approx 3.3 g_*^2 + O(g_*^4) \approx 0.27\,\delta + O(\delta^2) \quad (d = 3), \tag{4.93}$$

where in the second equality we plugged in the fixed-point. The total truncation error on the coefficient 3.3, estimated as above, is $\pm 0.5$. So we are confident that $\epsilon$ gets a nonzero anomalous dimension in $d = 3$ already at the lowest order allowed by the $\mathbb{Z}_2$ selection rules.

### 4.4.3 Broken currents

We now come to a discussion of the stress tensor operator, the source of a long-standing paradox. The UV theory contains an Ising subsector and a $\chi$ subsector, where only the first contains a $T_{\mu\nu}$. When we perturb the UV theory with the operator $\sigma\chi$, the two sectors are no longer decoupled and locality is lost. This implies that, at the IR fixed-point, the operator $T_{\mu\nu}$ will acquire an anomalous dimension. We will still call it $T_{\mu\nu}$ and will sometimes refer to it as the "stress tensor", but it has to be kept in mind that this operator is non-conserved. We will first compute $\gamma_T$ directly in the 2D case. We will then exhibit an alternative method, involving multiplet recombination, which clarifies our understanding of the crossover and makes the 3D answer apparent as well.

For the direct computation, it is sufficient to consider only one tensor component, say $T \equiv T_{zz}$, as all the components will acquire the same anomalous dimension. The stress tensor in the UV is conventionally normalized as

$$\langle T(z,\bar{z})T(0)\rangle = \frac{c}{2}\frac{1}{z^4}\,. \tag{4.94}$$

In the case of the two dimensional Ising model, the central charge is $c = \frac{1}{2}$. The 4pt function $\langle T(0)\sigma(z)\sigma(1)T(\infty)\rangle$ is then recovered in the standard way using the Ward identity twice on the two-point function of $\sigma$. For the four-point function involving two $\mathcal{O}$ insertions we obtain:

$$\langle T(0)\sigma\chi(z)\sigma\chi(1)T(\infty)\rangle = \frac{1}{|1-z|^4}\left(\frac{1}{4} + \frac{(1-z)^2(z^2+30z+1)}{256z^2}\right)\,. \tag{4.95}$$

Although the stress tensor is not a scalar operator, our discussion pertaining to anomalous dimensions still applies. We aim for an analytic result and use Method 1. Since $\lambda_{TT\varepsilon} = 0$ in $d = 2$, we only need to subtract the contribution of the identity. Note that, since the stress tensor is not unit-normalized, subtracting the contribution of the identity means subtracting $(4|z-1|^4)^{-1}$. The resulting integral can be evaluated exactly:

$$\int_{\mathbb{C}} \frac{1}{(1-\bar{z})^2}\frac{(z^2+30z+1)}{256z^2}\mathrm{d}z = -\frac{15}{128}\pi \tag{4.96}$$

where we have again accounted for the finite contribution of a vanishingly small annulus that contains $z = 1$. To apply (4.75), we recall that it is valid for the unit-normalized operators. To make up for the fact that $T$ is not, we need to multiply by an extra factor of $\frac{2}{c}$.

$$\gamma_T = \frac{15}{32}\pi^2 g_*^2 + O(g_*^4) \approx 3.65\,\delta + O(\delta^2) \quad (d=2)\,. \tag{4.97}$$

We will now recompute the same anomalous dimension using the recombination of mul-

tiplets.[17] As we will see, this method requires only the integration of a three-point function fixed by a Ward identity, and gives $\gamma_T$ as a function of $\Delta_\sigma$ and of the central charge $c$ for arbitrary $d$.

The stress tensor in the UV satisfies the conservation equation $\partial^\mu T_{\mu\nu} = 0$, meaning that some of its descendants are zero. As we say, it belongs to a short multiplet. The same operator taken to the nonlocal IR fixed-point, is not expected to be conserved: $\partial^\mu T_{\mu\nu} \propto V_\nu \neq 0$. In other words, the stress tensor multiplet becomes long by eating the $V_\nu$ multiplet. The vector $V_\nu$ must exist in the UV theory as well; this was puzzling in the standard picture. The puzzle is neatly resolved in our picture, since this multiplet can be easily constructed with the help of the $\chi$ field. Namely, we have:

$$V_\nu = \sigma(\partial_\nu \chi) - \frac{\Delta_\chi}{\Delta_\sigma}(\partial_\nu \sigma)\chi\,. \tag{4.98}$$

This is clearly a vector field and of dimension $d+1$ at the crossover point. The relative coefficient between the two terms is fixed by requiring that $V_\nu$ be a (non-unit normalized) vector primary at the crossover. For this it is sufficient to check that the two-point function of $V_\nu$ and of the descendant $\partial_\nu(\sigma\chi)$ vanishes.

Since $V_\mu$ given above is the only candidate to be eaten, at the IR fixed-point we expect

$$\partial^\mu T_{\mu\nu} = b(g) V_\nu\,, \tag{4.99}$$

where $b(g) \to 0$ as $g \to 0$. We will be interested in the first nontrivial order: $b(g) = b_1 g + O(g^2)$. The value of $b_1$ can be determined by studying the two-point function of $V_\mu$ with $T_{\mu\nu}$, computed at first-order in perturbation theory. It will be more convenient to utilise the descendant $\partial^\mu T_{\mu\nu}$, as this will allow us to use the Ward identity. On the one hand from multiplet recombination (4.99) we expect at the lowest order in $g_*$:

$$\langle \partial^\mu T_{\mu\nu}(x) V_\rho(y)\rangle_g \approx b_1 g_* \langle V_\nu(x) V_\rho(y)\rangle_0\,. \tag{4.100}$$

Here and below we mark with subscript $g$ the IR fixed-point correlators, while the subscript 0 corresponds to the UV theory. The two-point function of $V_\mu$ entering this equation can be computed explicitly given its definition:

$$\langle V_\mu(x) V_\nu(0)\rangle_0 = 2d\frac{\Delta_\chi}{\Delta_\sigma}\frac{I_{\mu\nu}(x)}{|x|^{2d+2}}, \quad I_{\mu\nu}(x) = \delta_{\mu\nu} - 2\frac{x_\mu x_\nu}{x^2}\,. \tag{4.101}$$

Notice that this functional form is consistent with the conformal primary nature of $V_\mu$.

On the other hand perturbation theory predicts for the correlator in the left-hand side

[17] For recent discussions of multiplet recombination in various CFT contexts see *e.g.* [204, 216–218].

of (4.100)

$$\langle \partial^\mu T_{\mu\nu}(x) V_\rho(y)\rangle_g = g_* \int \langle \partial^\mu T_{\mu\nu}(x) V_\rho(y)\mathcal{O}(z)\rangle_0 \mathrm{d}z\,. \tag{4.102}$$

The three-point function that we need to integrate is the sum of two factorized terms:

$$\begin{aligned}\langle \partial^\mu T_{\mu\nu}(x) V_\rho(y)\mathcal{O}(z)\rangle_0 &= \langle \partial^\mu T_{\mu\nu}(x)\sigma(y)\sigma(z)\rangle\langle \partial_\rho\chi(y)\chi(z)\rangle_0 \\ &- \frac{\Delta_\chi}{\Delta_\sigma}\langle \partial^\mu T_{\mu\nu}(x)\partial_\rho\sigma(y)\sigma(z)\rangle\langle \chi(y)\chi(z)\rangle_0\,.\end{aligned} \tag{4.103}$$

When the three-point functions in the right-hand side are expressed using the Ward identity of the unperturbed theory, we get terms proportional to $\delta(x-y)$ and to $\delta(x-z)$.[18] We assume that $x\neq y$, so only $\propto \delta(x-z)$ terms are important. They yield a nonzero contribution when we integrate over $z$. We obtain

$$\int \langle \partial^\mu T_{\mu\nu}(x) V_\rho(0)\mathcal{O}(z)\rangle_0 \mathrm{d}z \tag{4.104}$$

$$= -\langle\sigma(x)\partial_\nu\sigma(0)\rangle\langle\partial_\rho\chi(x)\chi(0)\rangle + \frac{\Delta_\chi}{\Delta_\sigma}\langle\partial_\nu\sigma(x)\partial_\rho\sigma(0)\rangle\langle\chi(x)\chi(0)\rangle = 2\Delta_\chi \frac{I_{\nu\rho}(x)}{|x|^{2d+2}} \tag{4.105}$$

Using (4.100), (4.101), (4.102), we fix the value $b_1 = \frac{\Delta_\sigma}{d}$.

Now let us compute the anomalous dimension of $T_{\mu\nu}$. The two-point function normalization customary for $d$-dimensional CFT is [20, 219]:

$$\langle T_{\mu\nu}(x) T_{\rho\sigma}(0)\rangle = \frac{c_T}{2\mathrm{S}_d^2}\frac{1}{|x|^{2\Delta_T}}\left[I_{\mu\rho}(x)I_{\nu\sigma}(x) + (\mu\leftrightarrow\nu) - \frac{2}{d}\delta_{\mu\nu}\delta_{\lambda\sigma}\right]\,. \tag{4.106}$$

In this normalization, and assuming the Ward identities are normalized as in note 18, the free massless scalar has $c_T = \frac{d}{d-1}$.

To specify (4.106), we used only conformal invariance and the fact that $T_{\mu\nu}$ transforms as a rank 2 symmetric traceless primary. It is therefore valid both at the UV and IR.[19] In the UV we have $c_T = c_T^{\mathrm{SRI}}$ and $\Delta_T = d$, corresponding to the conserved local stress tensor. In the IR both $c_T$ and $\Delta_T$ receive $O(g_*^2)$ corrections.

The quantity of interest is the two-point function of the divergence of $T_{\mu\nu}$ at the fixed-point which can be found by an explicit differentiation of (4.106). This vanishes for $\gamma_T = 0$,

[18] In this general $d$ argument we normalize the stress tensor so that the Ward identity takes the form $\langle \partial^\mu T_{\mu\nu}(x)\mathcal{O}_1(x_1)\dots\mathcal{O}_n(x_n)\rangle = -\sum_i \delta(x-x_i)\,\partial_\nu^{x_i}\langle\mathcal{O}_1(x_1)\dots\mathcal{O}_n(x_n)\rangle$. Notice that it is not the same as the normalization usually used in 2D.

[19] It is also possible to see without invoking conformal invariance that the tensor structure of the 2pt function is preserved along the RG flow. This follows from the fact that the rescaling needed to make the operator finite depends only on the indices of the operator and not on any other insertions in the correlation function. It is part of the same argument which shows that all tensor components get the same anomalous dimension.

consistent with the fact that $T_{\mu\nu}$ is conserved in the UV. For nonzero $\gamma_T$, it is given by:

$$\langle \partial^\mu T_{\mu\nu}(x) \partial^\rho T_{\rho\sigma}(0) \rangle_g \approx \frac{c_T}{\mathrm{S}_d^2} \gamma_T \left( d + 1 - \frac{2}{d} \right) \frac{I_{\nu\sigma}}{|x|^{2d+2}} \,, \tag{4.107}$$

In (4.107) we dropped terms higher order in $g_*^2$. One such higher order term is the correction to $c_T$ which will not play any role, so in all subsequent equations $c_T = c_T^{\mathrm{SRI}}$.

At the same order, using the recombination of multiplets equation (4.99), we have:

$$\langle \partial^\mu T_{\mu\nu}(x) \partial^\rho T_{\rho\sigma}(0) \rangle_g \approx b_1^2 g_*^2 \langle V_\nu(x) V_\sigma(0) \rangle_0 \,. \tag{4.108}$$

From the last two equations, the two-point function of $V_\mu$ and the value of $b_1$, we find the lowest-order anomalous dimension of the stress tensor:

$$\gamma_T = \frac{2\mathrm{S}_d^2}{c_T} \frac{\Delta_\sigma (d - \Delta_\sigma)}{d^2 + d - 2} g_*^2 + O(g_*^4) \,. \tag{4.109}$$

In $d = 2$, this agrees with (4.97). In $d = 3$, it gives

$$\gamma_T = 28.60555(6) g_*^2 + O(g_*^4) \approx 2.33\, \delta + O(\delta^2) \quad (d = 3) \tag{4.110}$$

where we have used $\Delta_\sigma = 0.5181489(10)$ from [129] and $c_T / c_T^{\mathrm{free}} = 0.946539(1)$ from [99].

### 4.4.4 Standard flow

These results for unprotected operators in the $\sigma\chi$ flow should be compared to corresponding calculations in the $\phi^4$ flow. The partner of $\Delta_\epsilon$ has been computed, with [188] finding

$$\Delta_{\phi^2} = \frac{d - \varepsilon}{2} + \frac{\varepsilon}{3} + \left[ \psi(1) - 2\psi\left(\frac{d}{4}\right) + \psi\left(\frac{d}{2}\right) \right] \left(\frac{\varepsilon}{3}\right)^2 + O(\varepsilon^3) \,, \tag{4.111}$$

but the partner for $\Delta_T$ has not. We would therefore like to compute the dimension of the leading spin-2 double-twist operator in $\phi \times \phi$, also called $T_{\mu\nu}$. We can use $\Delta_T$ to distinguish between different long-range Ising models since it gives a rough measure of how nonlocal a theory is. This makes it important for the bootstrap which is agnostic to microscopic parameters like $s$. Constructing the operator

$$T_{\mu\nu} = \left( \phi \partial_\mu \partial_\nu \phi - \frac{1}{d} \delta_{\mu\nu} \phi \partial^2 \phi \right) + y \left( \partial_\mu \phi \partial_\nu \phi - \frac{1}{d} \delta_{\mu\nu} (\partial \phi)^2 \right) \,, \tag{4.112}$$

we choose $y = -\frac{\Delta_\phi+1}{\Delta_\phi}$ in order to make it a conformal primary.[20] The one-loop diagram that one might expect to give anomalous scaling to $\langle\phi(-k_1-k_2)\phi(k_1)T_{\mu\nu}(k_2)\rangle$ is shown in Figure 4.10.

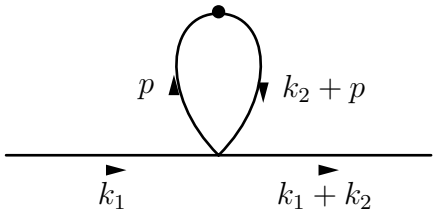


Figure 4.10: The $T_{\mu\nu}$ operator, represented by a dot at the top with momentum flowing in, has its legs saturated by $\phi$.

After Feynman parameters are first invoked, the integral takes the form

$$\begin{aligned} G(k_1,k_2) &= \lambda\mu^\varepsilon \frac{\Gamma(s)}{\Gamma\left(\frac{s}{2}\right)^2}\int_0^1\int_{\mathbb{R}^d}\frac{x^{\frac{s}{2}-1}(1-x)^{\frac{s}{2}-1}}{[(k_2+p)^2x+p^2(1-x)]^s} \\ &\quad [(k_2+p)_\nu((k_2+p)_\mu - yp_\mu) + p_\nu(p_\mu - y(k_2+p)_\mu) - \text{trace}]\,\frac{\mathrm{d}p}{(2\pi)^d}\mathrm{d}x\ . \end{aligned} \tag{4.113}$$

After making the denominator spherically symmetric in $p$, the piece in brackets becomes $(p+(1-x)k_2)_\nu[(p+(1-x)k_2)-y(p-xk_2)_\mu]+(p-xk_2)_\nu[(p-xk_2)_\mu - y(p+(1-x)k_2)_\mu]$ with the trace subtracted. Expanding this, all parts that are odd in a given component of $p_\mu$ must vanish. This reveals an overall factor of $k_{2\mu}k_{2\nu} - \frac{1}{d}\delta_{\mu\nu}k_2^2$ which we omit in what follows. The other parts of (4.113) become

$$\begin{aligned} G(k_1,k_2) &\propto \frac{\lambda}{(4\pi)^{\frac{d}{2}}}\frac{\Gamma\left(s-\frac{d}{2}\right)}{\Gamma\left(\frac{s}{2}\right)^2}\left[\frac{\Gamma\left(\frac{d-s}{2}\right)^2}{\Gamma(d-s)} - 2(1-y)\frac{\Gamma\left(\frac{d-s}{2}+1\right)^2}{\Gamma(d-s+2)}\right]\left|\frac{k_2}{\mu}\right|^{-\varepsilon} \\ &= \frac{1}{\varepsilon}\frac{\lambda}{(4\pi)^{\frac{d}{2}}\Gamma\left(\frac{d}{2}\right)}\left[2-(1-y)\frac{d}{d+2}\right]\left|\frac{k_2}{\mu}\right|^{-\varepsilon} + O(1)\ . \end{aligned} \tag{4.114}$$

After inserting the leading order value of $y$, it becomes clear that (4.114) is completely regular. This vanishing one-loop anomalous dimension, which had to be the case in $d=4$, is actually true for all other values of $d$ as well.[21] A two-loop diagram is therefore necessary to see perturbative corrections in $\Delta_T$.

[20] It is easy to check that for $(\Delta_\phi, d) = (1,4)$, (4.112) is the improved stress-energy tensor of a free scalar up to a constant factor.

[21] This is in fact reassuring given that $k_{1\mu}k_{1\nu} + (k_1+k_2)_\mu(k_1+k_2)_\nu - yk_{1\mu}(k_1+k_2)_\nu - yk_{1\nu}(k_1+k_2)_\mu$ is the tree level contribution to $\langle\phi(-k_1-k_2)\phi(k_1)T_{\mu\nu}(k_2)\rangle$. This cannot be produced by Figure 4.10 whose tensor structure only involves $k_2$.

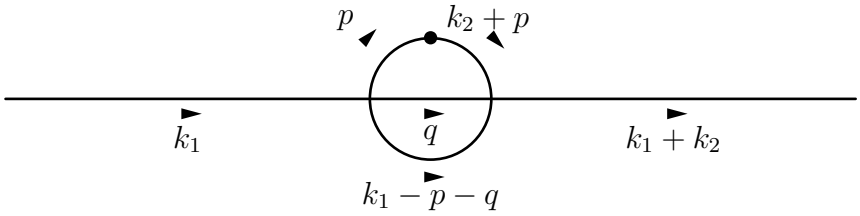


Figure 4.11: The most interesting two-loop contribution to $\langle\phi\phi T\rangle$.

The two-loop $\gamma_T$ comes from the diagram in Figure 4.11. All other candidates either involve a scaleless loop or have Figure 4.10 as a subdiagram. While standard methods are not enough to evaluate this integral in general, it is sufficient to set $k_2 = 0$ if we are only interested in the pole term. Starting with the $q$ integral already evaluated,

$$\begin{aligned} G(k_1,0) &= \frac{\lambda^2\mu^{2\varepsilon}}{(4\pi)^{\frac{d}{2}}}\frac{\Gamma\left(s-\frac{d}{2}\right)\Gamma\left(\frac{s-\varepsilon}{2}\right)^2}{\Gamma(s-\varepsilon)\Gamma\left(\frac{s}{2}\right)^2}\int_{\mathbb{R}^d}\frac{1}{|p|^{2s}|p-k_1|^{\varepsilon}} \\ &\quad [2(1-y)p_\mu p_\nu - \text{trace}]\,\frac{\mathrm{d}p}{(2\pi)^d} \\ &\propto \frac{\lambda^2\mu^{2\varepsilon}}{(4\pi)^{\frac{d}{2}}}\frac{\Gamma\left(s-\frac{d}{2}\right)\Gamma\left(\frac{s-\varepsilon}{2}\right)^2\Gamma\left(s+\frac{\varepsilon}{2}\right)}{\Gamma(s-\varepsilon)\Gamma\left(\frac{s}{2}\right)^2\Gamma(s)\Gamma\left(\frac{\varepsilon}{2}\right)} \\ &\quad \int_0^1\int_{\mathbb{R}^d}\frac{x^{\frac{\varepsilon}{2}-1}(1-x)^{s-1}}{[p^2+x(1-x)k_1^2]^{s+\frac{\varepsilon}{2}}}[x^2]\frac{\mathrm{d}p}{(2\pi)^d}\mathrm{d}x\,. \end{aligned} \tag{4.115}$$

Once there is only a Feynman paremeter left to deal with, its integral can be expanded as a series in $\varepsilon$. The first term vanishes, as it must by consistency, but the second term does not. This gives the correlator an overall $\frac{1}{\varepsilon}$ dependence.[22]

$$\begin{aligned} G(k_1,0) &\propto \frac{\lambda^2}{(4\pi)^d}\frac{\Gamma\left(s-\frac{d}{2}\right)\Gamma\left(\frac{s-\varepsilon}{2}\right)^2\Gamma\left(s+\frac{\varepsilon-d}{2}\right)}{\Gamma(s-\varepsilon)\Gamma\left(\frac{s}{2}\right)^2\Gamma(s)\Gamma\left(\frac{\varepsilon}{2}\right)}\left|\frac{k_1}{\mu}\right|^{-2\varepsilon} \\ &\quad \int_0^1 x^{\frac{\varepsilon}{2}+1}(1-x)^{s-1}\mathrm{d}x \\ &= \frac{1}{\varepsilon}\frac{\lambda^2}{(4\pi)^d\Gamma\left(\frac{d}{2}\right)^2}\frac{4}{d(d+2)}\left|\frac{k_1}{\mu}\right|^{-2\varepsilon}+O(1)\,. \end{aligned} \tag{4.116}$$

[22] At $d=4$, it is actually $\gamma_T+2\gamma_\phi$ that appears in the Callan-Symanzik equation, explaining why (4.116) still has a pole in this limit.

From this expression, $\gamma_T$ can easily be read off. Substituting the fixed point, we have

$$\Delta_T = \frac{d+4-\varepsilon}{2} - \frac{8}{d(d+2)}\left(\frac{\varepsilon}{3}\right)^2 + O(\varepsilon^3)\ . \tag{4.117}$$

Our choice to set $k_2 = 0$, imparting zero change in momentum to the composite operator, was very convenient. It allowed derivatives on the left leg to produce the same effect as derivatives on the right leg, thereby yielding an answer proportional to the tree-level contribution of $2(1-y)$. Had we set $k_1 = 0$ instead, as in [220], the integral would still be tractable, but only after accounting for the precise value of $y$. Encouraged by this simplification, we will calculate the same anomalous dimension for the general leading double-twist operator $[\phi\phi]_{0,\ell}$. Expressing this operator as

$$\begin{aligned}
[\phi_1\phi_2]_{n,\ell} &= \sum_{\substack{u_1+u_2+m=n\\ k_1+k_2=\ell}} a(k_1,k_2,u_1,u_2,m)T(k_1,k_2,u_1,u_2,m)\\
T(k,\ell-k,u_1,u_2,n-u_1-u_2)_{\alpha_1\ldots\alpha_\ell} &\equiv P_{\alpha_1}\ldots P_{\alpha_k}P_{\mu_1}\ldots P_{\mu_{n-u_1-u_2}}P^{2u_1}\phi_1\\
&\quad P_{\alpha_{k+1}}\ldots P_{\alpha_\ell}P_{\mu_1}\ldots P_{\mu_{n-u_1-u_2}}P^{2u_2}\phi_2\ ,
\end{aligned} \tag{4.118}$$

a recursion algorithm for computing the coefficients may be found in [221]. In fact in our case,

$$\begin{aligned}
&a(k,\ell-k,u_1,u_2,n-u_1-u_2) = s_{n,\ell}(k)b(u_1,u_2)\\
&s_{0,\ell}(k) = \frac{(-1)^k}{k!(\ell-k)!}\frac{1}{\Gamma(\Delta_\phi+k)\Gamma(\Delta_\phi+\ell+k)}\ ,\ b(0,0)=1
\end{aligned} \tag{4.119}$$

but we will not need this expression directly.[23] All that matters is that the extra momenta with indices bring in extra factors of the Feynman parameter, leading to

$$\Delta_{[\phi\phi]_{0,\ell}} = \frac{d+2\ell-\varepsilon}{2} - \frac{2\Gamma(\ell)}{\Gamma\left(\frac{d}{2}\right)\Gamma\left(\frac{d}{2}+\ell\right)}\left(\frac{\varepsilon}{3}\right)^2 + O(\varepsilon^3)\ . \tag{4.120}$$

The singularity at $\ell = 0$ is sensible because this results in an integral with a $\frac{1}{\varepsilon^2}$ term which has to be handled differently. Proceeding to the subleading double-twist operators $[\phi\phi]_{n,\ell}$ using this approach would be quite cumbersome. However, we can make a useful statement about them in $d = 2$ from the inversion formula (3.25).

To see how this gains us an order of perturbation theory, consider the conformal block expansion of the reduced correlator $G(z,\bar{z}) = |z|^{2\Delta_\phi}\langle\phi(0)\phi(z,\bar{z})\phi(1)\phi(\infty)\rangle$ with corrections

[23] In our previous notation, $2y = \frac{s_{0,2}(1)}{s_{0,2}(0)}$. The factor of 2 comes from the fact that (4.118) allows the two free fields to be different.

to $\Delta_{n,\ell} \equiv \Delta_{[\phi\phi]_{n,\ell}}$ and $a_{n,\ell} \equiv \lambda^2_{\phi\phi[\phi\phi]_{n,\ell}}$ plugged in.

$$\begin{aligned} G(z,\bar{z}) &= 1 + \sum_{n,\ell} \left( a^{(0)}_{n,\ell} + a^{(1)}_{n,\ell} + \dots \right) g_{\Delta_{n,\ell}+\gamma^{(1)}_{n,\ell}+\dots,\ell}(z,\bar{z}) \\ &= 1 + \sum_{n,\ell} a^{(0)}_{n,\ell} g_{\Delta_{n,\ell},\ell}(z,\bar{z}) + \sum_{n,\ell} a^{(1)}_{n,\ell} g_{\Delta_{n,\ell},\ell}(z,\bar{z}) + \gamma^{(1)}_{n,\ell} a^{(0)}_{n,\ell} g'_{\Delta_{n,\ell},\ell}(z,\bar{z}) \\ &+ \sum_{n,\ell} \Big[ a^{(2)}_{n,\ell} g_{\Delta_{n,\ell},\ell}(z,\bar{z}) + 2\gamma^{(1)}_{n,\ell} a^{(1)}_{n,\ell} g'_{\Delta_{n,\ell},\ell}(z,\bar{z}) \\ &\quad + \gamma^{(2)}_{n,\ell} a^{(0)}_{n,\ell} g'_{\Delta_{n,\ell},\ell}(z,\bar{z}) + \frac{1}{2}\left(\gamma^{(1)}_{n,\ell}\right)^2 a^{(0)}_{n,\ell} g''_{\Delta_{n,\ell},\ell}(z,\bar{z}) \Big] + \dots \end{aligned} \tag{4.121}$$

As conformal blocks have $|z|^{\Delta_{n,\ell}}$ asymptotics close to the origin, they produce one logarithm for each differentiation. Hence, there is precisely one double-log in (4.121), found by taking $g''_{\Delta_{n,\ell},\ell}(z,\bar{z}) \mapsto g_{\Delta_{n,\ell},\ell}(z,\bar{z}) \log^2|z|$ in the last term. Furthermore, we may identify the terms that lead to a $\log^2|1-z|$, which must be present by crossing symmetry [222]. Each conformal block that contributes must be differentiated at least once but all sums involving $\gamma^{(1)}_{n,\ell}$ are sums with a single term. This leaves us with

$$\sum_{n,\ell} a^{(0)}_{n,\ell} \gamma^{(2)}_{n,\ell} g'_{\Delta_{n,\ell},\ell}(z,\bar{z})\Big|_{\log^2|1-z|} = \left|\frac{z}{1-z}\right|^{\frac{d}{2}} \frac{\varepsilon^2}{9} g_{\frac{d}{2},0}(1-z,1-\bar{z}) \tag{4.122}$$

as the only possibility. The remarkable fact, which allows us to extract the spectral density $c(\Delta,\ell)$, is that the left-hand side of (4.122) is $\frac{1}{2\pi^2}$ times the double-discontinuity! Just as the coefficients of conformal blocks are residues for the simple poles of $c(\Delta,\ell)$, the coefficients of conformal block derivatives are residues associated with double poles. The inversion integral

$$\begin{aligned} c(\Delta,\ell) &= \frac{\varepsilon^2}{9} \frac{\Gamma\left(\frac{\Delta+\ell}{2}\right)^4}{\Gamma(\Delta+\ell-1)\Gamma(\Delta+\ell)} \int_0^1 z^{\frac{\Delta+\ell+1}{2}} {}_2F_1\left(\begin{matrix}\frac{\Delta+\ell}{2},\frac{\Delta+\ell}{2}\\ \Delta+\ell\end{matrix};z\right) {}_2F_1\left(\begin{matrix}\frac{1}{2},\frac{1}{2}\\ 1\end{matrix};1-z\right)\frac{\mathrm{d}z}{z^2} \\ &\int_0^1 \bar{z}^{\frac{\ell-\Delta+3}{2}} {}_2F_1\left(\begin{matrix}\frac{\ell-\Delta+2}{2},\frac{\ell-\Delta+2}{2}\\ \ell-\Delta+2\end{matrix};\bar{z}\right) {}_2F_1\left(\begin{matrix}\frac{1}{2},\frac{1}{2}\\ 1\end{matrix};1-\bar{z}\right)\frac{\mathrm{d}\bar{z}}{\bar{z}^2} \end{aligned} \tag{4.123}$$

may be evaluated after noticing that the crossed channel block (with the kinematic prefactors) is special enough to be a Casimir eigenfunction in the direct channel.[24] In other words, hypergeometric identities ensure that

$$f(z) \equiv z^{\frac{1}{2}} {}_2F_1\left(\begin{matrix}\frac{1}{2},\frac{1}{2}\\ 1\end{matrix};1-z\right) = {}_2F_1\left(\begin{matrix}\frac{1}{2},\frac{1}{2}\\ 1\end{matrix};\frac{z-1}{z}\right), \tag{4.124}$$

[24] This observation is due to Dalimil Mazáč.

which is part of the basis found in [136] with eigenvalue $-\frac{1}{4}$. Each integral in (4.123) is now an inner product of (4.124) with some $SL(2;\mathbb{R})$ block. The weight of the latter — which is either $\frac{\Delta+\ell}{2}$ or $\frac{\ell-\Delta+2}{2}$ — will be denoted by $h$.

$$\begin{aligned}\langle f,g\rangle &= \frac{1}{h(h-1)+\frac{1}{4}}\left[\langle Df,g\rangle-\langle f,Dg\rangle\right]\\ &= \frac{1}{h(h-1)+\frac{1}{4}}\left[(1-z)\left(\bar{f}'g-\bar{f}g'\right)\right]\Big|_0^1\\ &= \frac{h}{2h(h-1)+\frac{1}{2}}\frac{\Gamma(2h+1)}{\Gamma(h+1)^2}\end{aligned} \tag{4.125}$$

With this trick in mind, we arrive at the spectral density which reveals a nice surprise.

$$c(\Delta,\ell)=\frac{\varepsilon^2}{9}\frac{(\Delta+\ell)^2(\ell-\Delta+2)^2}{(\Delta-\ell-1)^2(\Delta+\ell-1)^2}\frac{\Gamma\left(\frac{\Delta+\ell}{2}\right)^4\Gamma(\ell-\Delta+2)}{\Gamma(\Delta+\ell-1)\Gamma\left(\frac{\Delta+\ell}{2}+1\right)^2\Gamma\left(\frac{\ell-\Delta+2}{2}+1\right)^2} \tag{4.126}$$

Evidently, there is only a single second-order pole for each spin, namely $\Delta=\Delta_{0,\ell}=\ell+1$. Subleading double-twist operators fail to renormalize in $d=2$ even at two-loops. This is the second mysterious zero for an anomalous dimension we have seen after (4.90).

## 4.5 Exploiting the shadow relation

A fundamental result which makes the LRI bootstrap worthwhile is the nonlocal equation of motion. The most general analytic constraint that has been extracted from it so far is a quadratic OPE coefficient relation with four traceless symmetric primaries $\mathcal{O}_i$. It takes the form

$$\frac{\lambda^{(m)}_{12\chi}\lambda^{(n)}_{34\sigma}}{\lambda^{(m)}_{12\sigma}\lambda^{(n)}_{34\chi}}=\frac{R^{(m)}_{12}}{R^{(n)}_{34}}\,. \tag{4.127}$$

We will derive this and then use it to understand the correlator $\langle\sigma\sigma\chi\chi\rangle$. Rich constraints on it will come from setting $\mathcal{O}_1=\sigma$, $\mathcal{O}_2=\mathcal{O}$, $\mathcal{O}_3=\chi$ and $\mathcal{O}_4=\mathcal{O}$ (which together imply $m=n=0$).

### 4.5.1 Exact OPE coefficient ratios

In addition to the non-renormalization theorems we have discussed, the nonlocal equation of motion can be used to derive an infinite family of ratios between OPE coefficients. Equations like (4.29) are statements about fields in a Lagrangian rather than unit-normalized operators in a CFT. We will therefore equip them with $s$-dependent prefactors which we call $n_\sigma$ and

$n_\chi$. Writing the integral expression for (4.29) yields

$$n_\chi(s)\chi(x) = \int \frac{n_\sigma(s)\sigma(y)}{|x-y|^{d+s}}\mathrm{d}y \ , \tag{4.128}$$

which is recognizable as the shadow transform. The idea is to use (4.128) in three-point functions containing $\sigma$ and $\chi$ in order to find

$$\frac{\lambda_{12\chi}}{\lambda_{12\sigma}} = \frac{n_\sigma(s)}{n_\chi(s)} R_{12} \ , \tag{4.129}$$

where $R_{12}$ is a known function of the quantum numbers. If we repeat this for a second pair of operators, we can arrange to have the normalizations cancel out, leaving us with

$$\frac{\lambda_{12\chi}\lambda_{34\sigma}}{\lambda_{12\sigma}\lambda_{34\chi}} = \frac{R_{12}}{R_{34}} \ . \tag{4.130}$$

The explicit $R_{ij}$ was computed for scalars in [158]. In Appendix F, we use it to test the IR duality between the flows that generate the $\varepsilon$-expansion and the $\delta$-expansion. In what follows, we aim to generalize this result to the case of spinning operators.

A natural language for this is the embedding formalism [223] which associates to each $x^\mu \in \mathbb{R}^d$ a null ray $X^M \sim \lambda X^M \in \mathbb{R}^{d+1,1}$. If one chooses representatives such that $X^+ = 1$ (the Poincaré section of the null cone), a Lorentz transformation on $X^M = (1, x^2, x^\mu)$ precisely implements a conformal transformation on $x^\mu$. Conformally invariant quantities can therefore be built out of the Lorentz scalars

$$X_{ij} \equiv -2X_i \cdot X_j = x_{ij}^2 \ . \tag{4.131}$$

An especially useful incarnation of the embedding space was developed in [224, 225] which used polarization vectors to make the formalism index-free. One such vector $Z$, in addition to being null, must satisfy a transversaity condition with $X$:

$$X_{ii} = 0 \ , \ X_i \cdot Z_i = 0 \ , \ Z_{ii} = 0 \ . \tag{4.132}$$

This is because tracelessness in $\mathbb{R}^{d+1,1}$ is stronger than tracelessness in $\mathbb{R}^d$. An important result is that correlation functions may only depend on polarization vectors through the combinations

$$\begin{aligned} H_{ij} &\equiv -2[(Z_i \cdot Z_j)(X_i \cdot X_j) - (X_1 \cdot Z_2)(X_2 \cdot Z_1)] \\ V_{i,jk} &\equiv \frac{(Z_i \cdot X_j)X_{ik} - (Z_i \cdot X_k)X_{ij}}{X_{jk}} \ . \end{aligned} \tag{4.133}$$

We will begin with the three-point function $\langle \phi_1(x_1)\mathcal{O}_2^{\mu_1,\ldots,\mu_\ell}(x_2)\sigma(x_3)\rangle$, which has a single

tensor structure. The most straightforward extension of it to the projective null cone is

$$\langle \Phi_1(X_1)\mathcal{O}_2(X_2,Z_2)\sigma(X_3)\rangle = \frac{\lambda_{12\sigma}V_{2,13}^{\ell}}{X_{13}^{\frac{\Delta_\sigma+\Delta_{12}-\ell}{2}}X_{23}^{\frac{\Delta_\sigma-\Delta_{12}+\ell}{2}}X_{12}^{\frac{\Delta_1+\Delta_2-\Delta_\sigma+\ell}{2}}} \,. \tag{4.134}$$

As a check, this is a degree-$\ell$ polynomial in $Z_2$ which is invariant under $Z_2 \mapsto Z_2 + X_2$. It also transforms with the correct weights when $X_1$, $X_2$ and $X_3$ are scaled individually. Lifting the equation of motion to the embedding space as well,

$$\langle \Phi_1(X_1)\mathcal{O}_2(X_2,Z_2)\chi(X_3)\rangle = \frac{n_\sigma(s)}{n_\chi(s)}\frac{\lambda_{12\sigma}}{X_{12}^{\frac{\Delta_1+\Delta_2-\Delta_\sigma+\ell}{2}}}\int \frac{V_{2,10}^{\ell}DX_0}{X_{01}^{\frac{\Delta_\sigma+\Delta_{12}-\ell}{2}}X_{02}^{\frac{\Delta_\sigma-\Delta_{12}+\ell}{2}}X_{03}^{d-\Delta_\sigma}} \,. \tag{4.135}$$

This type of object, which has exponents adding up to $d$, is called a conformal integral. Suitable technology for treating conformal integrals in the embedding space, including the formula

$$\int \frac{X^{A_1}\dots X^{A_n}}{(-2X\cdot Y)^{d+n}}DX = \frac{\pi^{\frac{d}{2}}\Gamma\left(\frac{d}{2}+n\right)}{\Gamma(d+n)}\frac{Y^{A_1}\dots Y^{A_n}}{(-Y^2)^{\frac{d}{2}+n}} - \text{traces} \,, \tag{4.136}$$

was developed in [226]. For similar integrals with a slight excess in the exponents, see [227]. Before returning to (4.135), it is worth expanding the tensor structure as

$$V_{2,10}^{\ell} = X_{01}^{-\ell}\sum_{n=0}^{\infty}\binom{\ell}{n}(Z_2\cdot X_1)^n(Z_2\cdot X_0)^{\ell-n}X_{02}^n X_{12}^{\ell-n} \,. \tag{4.137}$$

The result of (4.135) will contain $V_{2,13}^{\ell}$ and in particular $(Z_2\cdot X_3)^\ell$, which can only come from the first term of (4.137). It is therefore enough to focus on the $n=0$ term and infer the others from conformal invariance. Introducing Schwinger parameters and using (4.136), we have

$$\begin{aligned}\langle \Phi_1(X_1)\mathcal{O}_2(X_2,Z_2)\chi(X_3)\rangle = \frac{n_\sigma(s)}{n_\chi(s)}\frac{\lambda_{12\sigma}Z_2^{A_1}\dots Z_2^{A_\ell}}{X_{12}^{\frac{\Delta_1+\Delta_2-\Delta_\sigma-\ell}{2}}}\frac{\pi^{\frac{d}{2}}\Gamma\left(\frac{d}{2}+\ell\right)}{\Gamma(d-\Delta_\sigma)\Gamma\left(\frac{\Delta_\sigma+\Delta_{12}+\ell}{2}\right)\Gamma\left(\frac{\Delta_\sigma-\Delta_{12}+\ell}{2}\right)} \\ \int_0^\infty\int_0^\infty \frac{(X_3+\alpha X_1+\beta X_2)^{A_1}\dots(X_3+\alpha X_1+\beta X_2)^{A_\ell}}{\alpha^{-\frac{\Delta_\sigma+\Delta_{12}+\ell}{2}}\beta^{-\frac{\Delta_\sigma-\Delta_{12}+\ell}{2}}[\alpha X_{13}+\beta X_{23}+\alpha\beta X_{12}]^{\frac{d}{2}+\ell}}\frac{\mathrm{d}\alpha}{\alpha}\frac{\mathrm{d}\beta}{\beta} \\ + O(Z_2\cdot X_1) \,.\end{aligned} \tag{4.138}$$

If we again discard $Z_2\cdot X_1$ terms, we can evaluate the integral to arrive at

$$R_{12} = \pi^{\frac{d}{2}}\frac{\Gamma\left(\Delta_\sigma-\frac{d}{2}\right)\Gamma\left(\frac{d-\Delta_\sigma+\Delta_{12}+\ell}{2}\right)\Gamma\left(\frac{d-\Delta_\sigma-\Delta_{12}+\ell}{2}\right)}{\Gamma(d-\Delta_\sigma)\Gamma\left(\frac{\Delta_\sigma+\Delta_{12}+\ell}{2}\right)\Gamma\left(\frac{\Delta_\sigma-\Delta_{12}+\ell}{2}\right)} \,. \tag{4.139}$$

This logic can be repeated for correlators that have arbitrary spin in both positions. The difference here is that there is no longer a unique tensor structure:

$$\langle \mathcal{O}_1(X_1,Z_1)\mathcal{O}_2(X_2,Z_2)\sigma(X_3)\rangle = \sum_{m=0}^{\min(\ell_1,\ell_2)} \lambda^{(m)}_{12\sigma} \frac{V_{1,23}^{\ell_1-m} V_{2,13}^{\ell_2-m} H_{12}^m}{X_{13}^{\frac{\Delta_\sigma+\tau_{12}}{2}} X_{23}^{\frac{\Delta_\sigma-\tau_{12}}{2}} X_{12}^{\frac{\tau_1+\tau_2-\Delta_\sigma}{2}}} \,. \tag{4.140}$$

However, the factor of $H_{12}^m$ is untouched by the integration. This means that $\lambda^{(m)}_{12\chi}$ is proportional to $\lambda^{(m)}_{12\sigma}$ and $R_{ij}$ acquires one extra index instead of two. Carrying out the computation, we find

$$R_{12}^{(m)} = \pi^{\frac{d}{2}} \frac{\Gamma\left(\Delta_\sigma - \frac{d}{2}\right)\Gamma\left(\frac{d-\Delta_\sigma+\Delta_{12}+\ell_1+\ell_2-2m}{2}\right)\Gamma\left(\frac{d-\Delta_\sigma-\Delta_{12}+\ell_1+\ell_2-2m}{2}\right)}{\Gamma(d-\Delta_\sigma)\Gamma\left(\frac{\Delta_\sigma+\Delta_{12}+\ell_1+\ell_2-2m}{2}\right)\Gamma\left(\frac{\Delta_\sigma-\Delta_{12}+\ell_1+\ell_2-2m}{2}\right)} \,. \tag{4.141}$$

As a further generalization, one could consider mixed-symmetry tensors using the formalism of [228]. Note that (4.43) is clearly true from the way $\Delta_\sigma$ and $\Delta_\chi$ appear in (4.141). This can be seen as a manifestation of the fact that fractional derivatives still satisfy $\partial^{-s}A = B \Leftrightarrow A = \partial^s B$.

### 4.5.2 A tower of protected operators

We now specialize to an important four-point function of relevant operators. Let us choose three-point functions that involve the two shadow operators and a traceless symmetric primary $\mathcal{O}$. The quadratic equality

$$\lambda^2_{\sigma\chi\mathcal{O}} = \frac{R_{\sigma\mathcal{O}}}{R_{\chi\mathcal{O}}}\lambda_{\sigma\sigma\mathcal{O}}\lambda_{\chi\chi\mathcal{O}} \tag{4.142}$$

immediately follows. Two results related to (4.142) are worth fleshing out in detail as both of them provide useful input to the numerical bootstrap.

We will first consider a primary $\mathcal{O}$ whose spin is odd. In this case, the OPE coefficients on the right-hand side of (4.142) vanish by Bose symmetry. For the left-hand side to be nonzero, the dimension of $\mathcal{O}$ must be a pole of the following expression.

$$\frac{R_{\sigma\mathcal{O}}}{R_{\chi\mathcal{O}}} = \frac{\Gamma\left(\frac{d-\Delta+\ell}{2}\right)^2\Gamma\left(\frac{d-2\Delta_\sigma+\Delta+\ell}{2}\right)\Gamma\left(\frac{2\Delta_\sigma-d+\Delta+\ell}{2}\right)}{\Gamma\left(\frac{\Delta+\ell}{2}\right)^2\Gamma\left(\frac{2\Delta_\sigma-\Delta+\ell}{2}\right)\Gamma\left(\frac{2d-2\Delta_\sigma-\Delta+\ell}{2}\right)} \tag{4.143}$$

The poles above the unitarity bound, which come entirely from the squared gamma function in the numerator, are

$$\Delta = d+\ell+2n = \Delta_\sigma+\Delta_\chi+\ell+2n \,. \tag{4.144}$$

These are nothing but the dimensions of the double-twist operators $[\sigma\chi]_{n,\ell} \sim \chi\partial_{\mu_1}\ldots\partial_{\mu_\ell}\partial^{2n}\sigma$

at $s = s_*$. The first element of this list, $[\sigma\chi]_{0,1}$, is known to renormalize upon lowering the value of $s$. As its dimension leaves the pole (4.144), the left-hand side of (4.142) is able to remain nonzero. This is because $[\sigma\chi]_{0,1}$ recombines with the stress-energy tensor and Bose symmetric OPEs are allowed to contain odd-spin descendants. All of the other double-twist operators stay primary (at least in three dimensions) and thus face a radically different situation. Bose symmetry continues to enforce $\lambda_{\sigma\sigma\mathcal{O}} = \lambda_{\chi\chi\mathcal{O}} = 0$ which means that $\Delta$ can only change continuously if $\lambda^2_{\sigma\chi\mathcal{O}}$ jumps to zero discontinuously. We therefore arrive at the following proposal.

*In the long-range Ising model given by a generic $\frac{d}{2} < s < s_*$, all odd-spin primaries in $\sigma \times \chi$ (the double-twist operators other than the first one) have a scaling dimension that is independent of $s$.*

This result, which should strictly be called a conjecture, would represent the most natural scenario even if we did not have continuity in $s$. It also follows from the earlier form of the OPE ratio (4.129) after a simple check that the normalizations $n_\sigma(s)$ and $n_\chi(s)$ are nonzero. One possibility that we cannot rule out is that these odd-spin primaries are only protected within a finite interval starting at $s = s_*$. This is because we used the fact that $\lambda^2_{\sigma\chi\mathcal{O}}$ was strictly positive. If this coefficient were to smoothly approach zero at some value of $s$, we would have to worry about the behaviour in Figure 4.12.

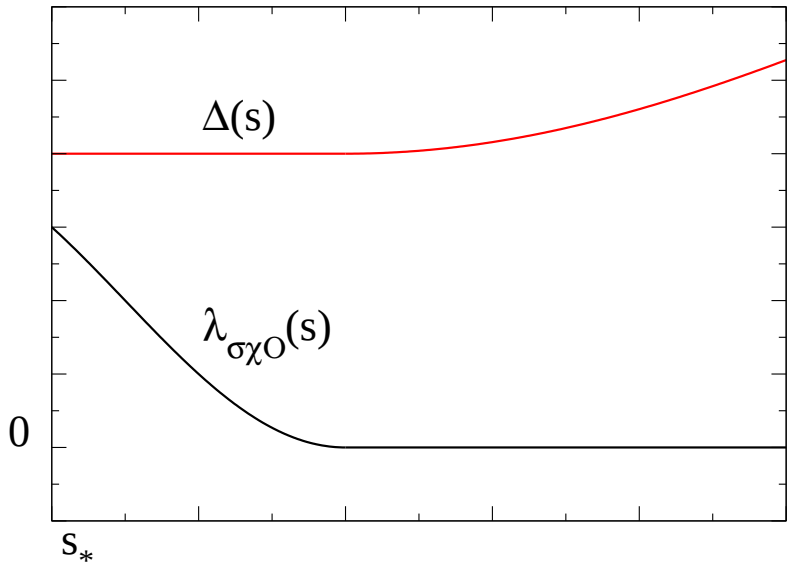


Figure 4.12: A possible way out of our non-renormalization theorem for odd-spin primary operators in $\sigma \times \chi$. The strongest statement we can make is that their dimensions are protected in an open neighbourhood of any point where $\lambda^2_{\sigma\chi\mathcal{O}} > 0$. It could be the case that at least one renormalizes after decoupling at an intermediate value of $s$.

Running this argument around the other side of the duality is more subtle since $\phi$ and $\phi^3$

cannot be treated as independent fields. At small values of the spin, however, it is clear how the protected operators in $\phi \times \phi^3$ match up with those in $\sigma \times \chi$. Taking $n = 0$ for example,

$$\begin{aligned} T_{\mu\nu} \ni \chi\partial_\mu\sigma \quad & \quad \phi^3\partial_\mu\phi \in \phi^4 \\ \chi\partial_\mu\partial_\nu\partial_\rho\sigma \quad & \leftrightarrow \quad \phi^3\partial_\mu\partial_\nu\partial_\rho\phi \\ \chi\partial_\mu\partial_\nu\partial_\rho\partial_\sigma\partial_\tau\sigma \quad & \leftrightarrow \quad \phi^3\partial_\mu\partial_\nu\partial_\rho\partial_\sigma\partial_\tau\phi \\ & \quad \dots \end{aligned} \tag{4.145}$$

Starting at $\ell = 7$, the conformal primary where four copies of $\phi$ are saturated by derivatives is not unique. A generating function counting the number of such primaries for all $\ell$ can be found in [218]. Looking at one example, the primary subspace for operators of the form

$$\begin{aligned} \mathcal{O}_7 \quad = \quad & c_0\phi^3\partial^7\phi + c_1\phi^2\partial\phi\partial^6\phi + c_2\phi^2\partial^2\phi\partial^5\phi + c_3\phi\partial\phi\partial\phi\partial^5\phi \\ & + c_4\phi^2\partial^3\phi\partial^4\phi + c_5\phi\partial\phi\partial^2\phi\partial^4\phi + c_6\partial\phi\partial\phi\partial\phi\partial^4\phi + c_7\phi\partial\phi\partial^3\phi\partial^3\phi \\ & + c_8\phi\partial^2\phi\partial^2\phi\partial^3\phi + c_9\partial\phi\partial\phi\partial^2\phi\partial^3\phi + c_{10}\partial\phi\partial^2\phi\partial^2\phi\partial^2\phi \end{aligned} \tag{4.146}$$

is two-dimensional. We should therefore only expect one linear combination to be protected. Given a basis consisting of $\left\{\mathcal{O}_7^{(1)}, \mathcal{O}_7^{(2)}\right\}$, we may choose $t$ such that $t\mathcal{O}_7^{(1)} + \mathcal{O}_7^{(2)}$ decouples from $\phi \times \phi^3$. This gives an operator that is free to renormalize since it has vanishing OPE coefficients on either side of (4.142). It is only the orthogonal operator that maintains its exact double-twist dimension. More generally, when the subspace is $N$-dimensional, the solutions to

$$t_1 \left\langle \phi(x_1)\phi^3(x_2)\mathcal{O}_\ell^{(1)} \right\rangle + \dots + t_{N-1} \left\langle \phi(x_1)\phi^3(x_2)\mathcal{O}_\ell^{(N-1)} \right\rangle + \left\langle \phi(x_1)\phi^3(x_2)\mathcal{O}_\ell^{(N)} \right\rangle = 0 \tag{4.147}$$

are $(N-1)$-dimensional, pointing us to a unique protected operator once again. It is not surprising that $\phi \times \phi^3$ contains only one leading-twist operator of each spin in a suitable basis. Indeed if the degeneracy could not be removed, one would be able to repeat our non-renormalization argument based on the nonlocal equation of motion $\partial^s\phi \propto \phi^3$ in the local fixed point governed by $\partial^2\phi \propto \phi^3$. It is clear that the Wilson-Fisher fixed point does not have an odd-spin protected tower. Instead, the odd-spin operators which have the dimensions (4.144) in $d = 4$ are able to avoid the Bose symmetry constraints for primaries by recombining with higher spin currents. It would be interesting to see how this structure is reproduced in perturbation theory.

The 2D case would also be very interesting to study further. This describes a fixed line obtained by deforming a Virasoro symmetric theory. As a result, the definition of $[\sigma\chi]_{n,\ell}$ is ambiguous just like the double-twist operator $[\phi\phi^3]_{n,\ell}$. This time, rotating the bases to remove the maximal number of operators from $\sigma \times \chi$ is probably not the right solution to

the mixing problem. Consider the operators with $(h,\bar{h}) = (4,1)$ where

$$\begin{aligned}\mathcal{O}_3^{(1)} &= \sigma L_{-1}^3\chi - 93 L_{-1}\sigma L_{-1}^2\chi + \frac{713}{3}L_{-1}^2\sigma L_{-1}\chi - \frac{3565}{51}L_{-1}^3\sigma\chi \\ \mathcal{O}_3^{(2)} &= L_{-3}\sigma\chi - \frac{128}{153}L_{-1}^3\sigma\chi \end{aligned} \tag{4.148}$$

is a valid basis.[25] The previous logic would suggest splitting these into one combination with $\lambda_{\sigma\chi\mathcal{O}} = 0$ and another combination with $\lambda_{\sigma\chi\mathcal{O}} \neq 0$. This presents a problem as both operators in such a splitting would have nonzero overlap with

$$\Lambda = \left(L_{-4} - \frac{5}{3}L_{-2}^2\right) I \ . \tag{4.149}$$

There is only room for a higher spin current to recombine with one multiplet so we must demand that the protected spin-3 operator is the one that fails to give an anomalous dimension to (4.149). To solve for this operator, we have evaluated the three-point functions

$$\begin{aligned}\left\langle \Lambda(z_1,\bar{z}_1)\mathcal{O}_3^{(1)}(z_2,\bar{z}_2)\sigma\chi(z_3,\bar{z}_3)\right\rangle &= \frac{124775/544}{z_{12}^7 z_{13}z_{23}\bar{z}_{23}^2} \\ \left\langle \Lambda(z_1,\bar{z}_1)\mathcal{O}_3^{(2)}(z_2,\bar{z}_2)\sigma\chi(z_3,\bar{z}_3)\right\rangle &= \frac{1225/3264}{z_{12}^7 z_{13}z_{23}\bar{z}_{23}^2} \end{aligned} \tag{4.150}$$

using the Virasoro Ward identity.[26] This allows us to repeat the calculation that [159] did for the stress-energy tensor and say that

$$\begin{aligned}&\int \left\langle \bar{\partial}_1\Lambda(z_1,\bar{z}_1)\left[\frac{544}{124775}\mathcal{O}_3^{(1)} - \frac{3264}{1225}\mathcal{O}_3^{(2)}\right](z_2,\bar{z}_2)\sigma\chi(z_3,\bar{z}_3)\right\rangle \mathrm{d}z_3\mathrm{d}\bar{z}_3 = 0 \\ &\int \left\langle \bar{\partial}_1\Lambda(z_1,\bar{z}_1)\left[\frac{713}{1513}\mathcal{O}_3^{(1)} + \frac{3422400}{10591}\mathcal{O}_3^{(2)}\right](z_2,\bar{z}_2)\sigma\chi(z_3,\bar{z}_3)\right\rangle \mathrm{d}z_3\mathrm{d}\bar{z}_3 \propto \gamma_\Lambda \end{aligned} \tag{4.151}$$

Based on this, one might hope that all $\sigma\times\chi$ operators in the 2D theory are either protected or eaten. The first counter-example to this appears at the next level which has three $\ell = 5$ operators built from $\sigma$ and $\chi$ but only one $\ell = 6$ current that needs to be broken.

[25] We have implicitly used the null state condition to write $L_{-2}\sigma$ as a multiple of $L_{-1}^2\sigma$. Similarly, we do not have any higher Virasoro generators acting on $\chi$ since the theory it comes from is already nonlocal at $s = s_*$.

[26] The form $\langle L_{-m}I(z_1)L_{-n}\sigma(z_2)\sigma(z_3)\rangle = \oint_{z_1}\oint_{z_2}(y_1-z_1)^{1-m}(y_2-z_2)^{1-n}\langle T(y_1)T(y_2)\sigma(z_2)\sigma(z_3)\rangle \frac{\mathrm{d}y_2}{2\pi i}\frac{\mathrm{d}y_1}{2\pi i}$ is the one most useful for our purposes.

### 4.5.3 Consequences for crossing

We will now discuss the treatment of $[\sigma\chi]_{n,\ell}$ operators with even spin. Looking at (4.142) for $s = s_*$, we again have a removable singularity since $\mathcal{O}$ has a dimension given by (4.144) while decoupling from the $\sigma \times \sigma$ and $\chi \times \chi$ OPEs. The difference is that the coefficients $\lambda_{\sigma\sigma\mathcal{O}}$ and $\lambda_{\chi\chi\mathcal{O}}$ turn on for $s < s_*$ as they are not constrained by any kinematic principle. This allows the right-hand side of (4.142) to become a ratio of finite numbers. The shadow relation then becomes a statement about operators of an unknown dimension still having constrained OPE coefficients.

This situation is ubiquitous in the superconformal bootstrap. It allows four-point functions to be decomposed into blocks that include the contributions of many conformal primaries. These superconformal blocks have been computed in [229] and many subsequent works. In the long-range Ising model which is non-supersymmetric, it is the nonlocal operator in (4.29) rather than a supercharge, which allows certain conformal blocks to be combined.

To make this precise, consider the general form of the four-point function for scalar primaries

$$\langle\phi_i(x_1)\phi_j(x_2)\phi_k(x_3)\phi_l(x_4)\rangle = \left(\frac{|x_{24}|}{|x_{14}|}\right)^{\Delta_{ij}}\left(\frac{|x_{14}|}{|x_{13}|}\right)^{\Delta_{kl}}\frac{G^{ijkl}(u,v)}{|x_{12}|^{\Delta_i+\Delta_j}|x_{34}|^{\Delta_k+\Delta_l}}\,. \tag{4.152}$$

The unknown function, depending on the cross-ratios $u = \frac{x_{12}^2x_{34}^2}{x_{13}^2x_{24}^2}$ and $v = \frac{x_{14}^2x_{23}^2}{x_{13}^2x_{24}^2}$, has the conformal block expansion

$$G^{ijkl}(u,v) = \sum_{\mathcal{O}}\lambda_{ij\mathcal{O}}\lambda_{kl\mathcal{O}}g_{\mathcal{O}}^{\Delta_{ij},\Delta_{kl}}(u,v)\,. \tag{4.153}$$

By demanding crossing symmetry for the $\langle\sigma\sigma\chi\chi\rangle$ correlator, we derive the crossing equations

$$\begin{aligned}
&\sum_{\mathcal{O}^+_{2|\ell}}\lambda_{\sigma\sigma\mathcal{O}}\lambda_{\chi\chi\mathcal{O}}F^{\sigma\sigma;\chi\chi}_{-,\Delta,\ell}(u,v) + \sum_{\mathcal{O}^+_{2|\ell}}\lambda^2_{\sigma\chi\mathcal{O}}F^{\chi\sigma;\sigma\chi}_{-,\Delta,\ell}(u,v) - \sum_{\mathcal{O}^+_{2\nmid\ell}}\lambda^2_{\sigma\chi\mathcal{O}}F^{\chi\sigma;\sigma\chi}_{-,\Delta,\ell}(u,v) = 0\\
&\sum_{\mathcal{O}^+_{2|\ell}}\lambda_{\sigma\sigma\mathcal{O}}\lambda_{\chi\chi\mathcal{O}}F^{\sigma\sigma;\chi\chi}_{+,\Delta,\ell}(u,v) - \sum_{\mathcal{O}^+_{2|\ell}}\lambda^2_{\sigma\chi\mathcal{O}}F^{\chi\sigma;\sigma\chi}_{+,\Delta,\ell}(u,v) + \sum_{\mathcal{O}^+_{2\nmid\ell}}\lambda^2_{\sigma\chi\mathcal{O}}F^{\chi\sigma;\sigma\chi}_{+,\Delta,\ell}(u,v) = 0\,,
\end{aligned} \tag{4.154}$$

where we have used the (2.66) shorthand

$$F^{ij;kl}_{\pm,\Delta,\ell}(u,v) = v^{\frac{\Delta_j+\Delta_k}{2}}g^{\Delta_{ij},\Delta_{kl}}_{\Delta,\ell}(u,v) \pm u^{\frac{\Delta_j+\Delta_k}{2}}g^{\Delta_{ij},\Delta_{kl}}_{\Delta,\ell}(v,u)\,. \tag{4.155}$$

We can modify (4.154) to account for the protected operators

$$\sum_{\mathcal{O}^+_{2|\ell}} \lambda_{\sigma\sigma\mathcal{O}}\lambda_{\chi\chi\mathcal{O}} F^{\sigma\sigma;\chi\chi}_{-,\Delta,\ell}(u,v) + \sum_{\mathcal{O}^+_{2|\ell}} \lambda^2_{\sigma\chi\mathcal{O}} F^{\chi\sigma;\sigma\chi}_{-,\Delta,\ell}(u,v) - \sum_{\ell=1,3,\ldots}\sum_{n=0}^{\infty} \lambda^2_{\sigma\chi\mathcal{O}} F^{\chi\sigma;\sigma\chi}_{-,d+\ell+2n,\ell}(u,v) = 0$$
$$\sum_{\mathcal{O}^+_{2|\ell}} \lambda_{\sigma\sigma\mathcal{O}}\lambda_{\chi\chi\mathcal{O}} F^{\sigma\sigma;\chi\chi}_{+,\Delta,\ell}(u,v) - \sum_{\mathcal{O}^+_{2|\ell}} \lambda^2_{\sigma\chi\mathcal{O}} F^{\chi\sigma;\sigma\chi}_{+,\Delta,\ell}(u,v) + \sum_{\ell=1,3,\ldots}\sum_{n=0}^{\infty} \lambda^2_{\sigma\chi\mathcal{O}} F^{\chi\sigma;\sigma\chi}_{+,d+\ell+2n,\ell}(u,v) = 0\ , \tag{4.156}$$

but this only imposes the odd-spin case of the shadow relation. Imposing the even-spin case as well leads to

$$\sum_{\mathcal{O}^+_{2|\ell}} \lambda_{\sigma\sigma\mathcal{O}}\lambda_{\chi\chi\mathcal{O}} \mathcal{F}_{-,\Delta,\ell}(u,v) - \sum_{\ell=1,3,\ldots}\sum_{n=0}^{\infty} \lambda^2_{\sigma\chi\mathcal{O}} F^{\chi\sigma;\sigma\chi}_{-,d+\ell+2n,\ell}(u,v) = 0$$
$$\sum_{\mathcal{O}^+_{2|\ell}} \lambda_{\sigma\sigma\mathcal{O}}\lambda_{\chi\chi\mathcal{O}} \mathcal{F}_{+,\Delta,\ell}(u,v) + \sum_{\ell=1,3,\ldots}\sum_{n=0}^{\infty} \lambda^2_{\sigma\chi\mathcal{O}} F^{\chi\sigma;\sigma\chi}_{+,d+\ell+2n,\ell}(u,v) = 0\ , \tag{4.157}$$

where we have defined the convolved superblocks

$$\mathcal{F}_{\pm,\mathcal{O}}(u,v) = F^{\sigma\sigma;\chi\chi}_{\pm,\Delta,\ell}(u,v) \mp \frac{R_{\sigma\mathcal{O}}}{R_{\chi\mathcal{O}}} F^{\chi\sigma;\sigma\chi}_{\pm,\Delta,\ell}(u,v)\ . \tag{4.158}$$

It is easy to read off what the non-convolved superblocks are.

In contrast to other known superblocks, *e.g.* the 4D $\mathcal{N}=1$ classification in [230], the relative coefficient in (4.158) is not a rational function of $\Delta$. Indeed (4.143) has infinitely many poles. It may therefore be of interest to compute rational approximations for the coefficient, similar to what is already standard practice for the conformal blocks themselves. We discuss this problem in Appendix E.

## 4.6 Numerical results

We are now ready to combine our exact results with the numerical bootstrap in three dimensions. For perspective, it is interesting that the 3D LRI is still considered prohibitive for a Monte Carlo simulation. Even the 2D LRI has only been simulated relatively recently [200, 201, 231–233]. By contrast, $d$ is a parameter in the conformal bootstrap that can be varied without changing the difficulty of the problem. Let us look at the crossing equations that come into play.

We have already written two of the crossing equations which take the form (4.154),

(4.156) or (4.157) depending on how much non-perturbative information is imposed. These are part of a larger system, given in Appendix E, which has the schematic form

$$\sum_{\mathcal{O}^+_{2|\ell}} (\lambda_{\sigma\sigma\mathcal{O}}\ \lambda_{\epsilon\epsilon\mathcal{O}}\ \lambda_{\chi\chi\mathcal{O}})\, V^{(0)}_{\Delta,\ell} \begin{pmatrix} \lambda_{\sigma\sigma\mathcal{O}} \\ \lambda_{\epsilon\epsilon\mathcal{O}} \\ \lambda_{\chi\chi\mathcal{O}} \end{pmatrix} + \sum_{\mathcal{O}^-} \lambda^2_{\sigma\epsilon\mathcal{O}} V^{(1)}_{\Delta,\ell} + \lambda^2_{\epsilon\chi\mathcal{O}} V^{(3)}_{\Delta,\ell} + \sum_{\mathcal{O}^+} \lambda^2_{\sigma\chi\mathcal{O}} V^{(2)}_{\Delta,\ell} = 0\ . \quad (4.159)$$

The components of $V^{(1)}$, $V^{(2)}$ and $V^{(3)}$ live in $\mathbb{R}$, while the components of $V^{(0)}$ live in $\mathbb{R}^{3\times 3}$. To rule out potential solutions, the numerical bootstrap searches for a functional that gives a positive-definite matrix when acting on $V^{(0)}$ and a positive number when acting on the other vectors. Finding such a functional becomes easier when we only demand positivity on specific linear combinations of the vectors above. To this end, we have three options for how to proceed.

1. If we do not impose (4.142) at all, we use (4.159) where the dimensions exchanged by $\sigma \times \chi$ run over all values consistent with unitarity and the presence of three relevant scalar primaries.

2. If we demand the existence of the protected tower discussed in the last section, the last sum in (4.159) for odd spin is modified so that it only contains the dimensions of (4.156).

3. If we use superblocks, we only demand positivity on the linear combinations (4.158) instead of their individual components. This means that the last sum in (4.159) for even spin is removed altogether and replaced by additional terms in the upper-right and lower-left corners of the matrices in $V^{(0)}$.

In all cases, we impose the basic relations

$$\begin{aligned} \Delta_\sigma + \Delta_\chi &= d \\ \lambda^2_{\sigma\chi\epsilon} &= \frac{R_{\sigma\epsilon}}{R_{\chi\epsilon}} \lambda_{\sigma\sigma\epsilon}\lambda_{\chi\chi\epsilon} \end{aligned} \quad (4.160)$$

which means that the isolated operator $\epsilon$ appears in a superblock. When combined with permutation symmetry, this allows $\sigma$, $\epsilon$ and $\chi$ to be accounted for with a single entry to the first sum of (4.159). Denoting the $m, n$ component of a matrix by $[M]_{mn}$, this entry is

$$\begin{pmatrix} \left[V^{(0)}_\epsilon\right]_{11} + V^{(1)}_\sigma & \left[V^{(0)}_\epsilon\right]_{12} & \left[V^{(0)}_\epsilon\right]_{13} + \frac{1}{2}\frac{R_{\sigma\epsilon}}{R_{\chi\epsilon}}\left(V^{(1)}_\chi + V^{(2)}_\epsilon + V^{(3)}_\sigma\right) \\ \left[V^{(0)}_\epsilon\right]_{21} & \left[V^{(0)}_\epsilon\right]_{22} & \left[V^{(0)}_\epsilon\right]_{23} \\ \left[V^{(0)}_\epsilon\right]_{31} + \frac{1}{2}\frac{R_{\sigma\epsilon}}{R_{\chi\epsilon}}\left(V^{(1)}_\chi + V^{(2)}_\epsilon + V^{(3)}_\sigma\right) & \left[V^{(0)}_\epsilon\right]_{32} & \left[V^{(0)}_\epsilon\right]_{33} + V^{(3)}_\chi \end{pmatrix}. \quad (4.161)$$

The upper-right and lower-left corners account for (4.160), while the upper-left and lower-right corners guarantee $\lambda_{\sigma\sigma\epsilon} = \lambda_{\sigma\epsilon\sigma}$ and $\lambda_{\chi\chi\epsilon} = \lambda_{\epsilon\chi\chi}$ respectively. Treating $\epsilon$ this way leads to interesting bounds on LRIs but it requires all three relevant deformations to be external operators. As we will see shortly, the standard system for the 3D Ising bootstrap — $\langle\sigma\sigma\sigma\sigma\rangle$, $\langle\sigma\sigma\epsilon\epsilon\rangle$ and $\langle\epsilon\epsilon\epsilon\epsilon\rangle$ — is not enough.

Scanning over the dimensions of the lightest scalars, our results rely on the *unreasonable effectiveness* of the bootstrap — the assumption that an interesting theory will lie on the boundary of an excluded region. To carry out the computations, we approximate conformal blocks $G_{\Delta,\ell}^{\Delta_{ij},\Delta_{kl}}(u,v)$ using the methods of [24, 84, 89]. While the full details were given in chapter 2, it is useful to repeat that these special functions are written as a certain double power series in two variables near the crossing symmetric point $u = v = \frac{1}{4}$. Truncating this expansion requires two cutoffs $(m_{\max}, n_{\max})$. The values chosen in this work are $(3,5)$, $(5,7)$ and $(7,9)$ which correspond to 54, 104 and 170 components respectively. Other choices made here are $k_{\max} = 40$ and $\ell_{\max} = 20$.

Since their initial exploration in [78], matrix crossing equations like (4.159) have played an increasingly central role in the numerical bootstrap [77, 79, 80, 129, 234–238]. They appear whenever there are operators of differing dimension in the four-point functions being analyzed. They have also appeared in the single correlator problem of [239] which had enough global symmetry for the same representation to be exchanged multiple times.[27] We believe that this is the first time a six-correlator system has been bootstrapped.

### 4.6.1 One correlator

It is easiest to start with the results that can be obtained from the $\langle\sigma\sigma\sigma\sigma\rangle$ correlator alone. In this case, there is no compelling reason to restrict our analysis to three dimensions. Our bound on the spin-2 gap $\Delta_T$, which we plot for 2D and 3D, has been known since the early work in [185].

From Figure 4.13, it appears that the $\Delta_T$ bound is saturated by generalized free field theory. This gives us an idea of how the allowed region in $(\Delta_\sigma, \Delta_\epsilon)$ space must behave. Not only must it become more restrictive as $\Delta_T$ is increased — its boundary must move from left to right at a known rate.

It is straightforward to derive an upper bound of this type. In Figure 4.14, we have done this for six different values of the spin-2 gap. In 2D, the minimum $\Delta_T$ values we sample are $\{2, 2.2, 2.4, 2.6, 2.8, 3\}$, while in 3D they are $\{3, 3.1, 3.2, 3.3, 3.4, 3.5\}$. If the previously observed saturation is correct, the edges of these plots must continue moving left as our computational power is incresaed. For instance, we expect a 5% change for the 2D red region and a 3% change for the 3D red region.

[27] Another interesting situation is the long multiplet bootstrap [157]. In this case, a mixed system of conformal primaries looks like a single correlator when all parts are combined into superfields. The recent progress [240, 241] for the superconformal bootstrap in three dimensions appears to be a partial implementation of this idea.

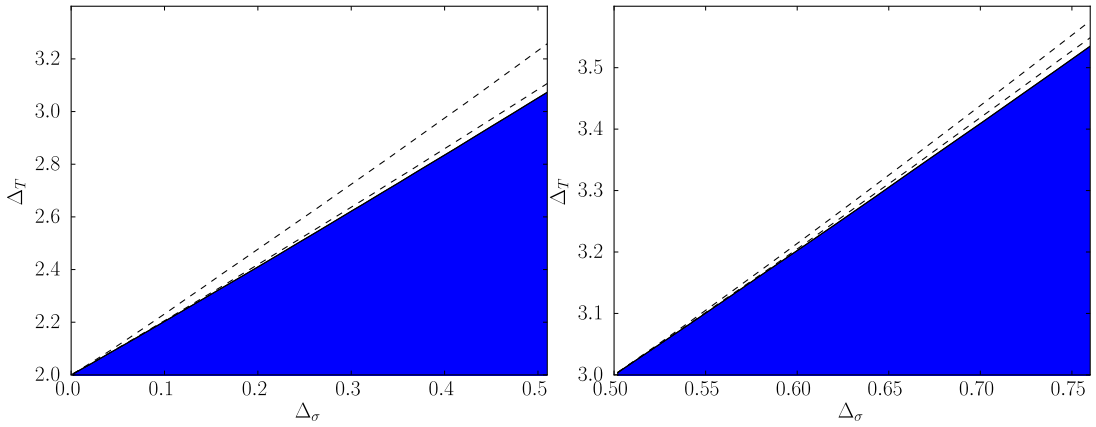


(a) 2D (b) 3D

Figure 4.13: The allowed region for the first spin-2 operator dimension $\Delta_T$ as a function of $\Delta_\sigma$. In both 2D and 3D, the bound appears to be converging to $\Delta_T = 2\Delta_\sigma + 2$. The blue region was obtained with $(m_{\max}, n_{\max}) = (7, 9)$ while $(5, 7)$ and $(3, 5)$ are shown for comparison.

Once we disallow $\Delta_T$ at the unitarity boumd, the kink corresponding to the SRI quickly disappears. The point $(\Delta_\sigma, \Delta_\epsilon) = \left(\frac{d}{4}, \frac{d}{2}\right)$, marking the first LRI to be described by mean-field theory, does not display any feature. We may therefore conclude that a single correlator gives very little information about the spectrum of non-trivial long-range Ising models.

Before proceeding to our multi-correlator results in three dimensions, we should comment on the fact that some theories can saturate numerical bootstrap bounds even when there is no kink. For a judiciously chosen quantity, there is some evidence that this is the case for the LRI in two dimensions.[28] Instead of bounding a gap, one can maximize the OPE coefficient of an operator in the spectrum. From Monte Carlo data [201], it is clear that in every 2D long-range Ising model, one such operator has a dimension close to 1. In some sense, this is explained by the perturbative calculation (4.97) around $s = s_*$, since the leading order anomalous dimension of $\epsilon$ happens to vanish. By setting $\Delta_\epsilon = 1$ and maximizing $\lambda^2_{\sigma\sigma\epsilon}$, we have extracted the low-lying spectrum using the extremal functional method of [90, 150, 242]. At $\Delta_\sigma = \frac{1}{8}$, this is guaranteed to agree with the spectrum of the SRI. However, Figure 4.15 also shows very interesting behaviour at $\Delta_\sigma = \frac{1}{2}$ as we now explain.[29]

Here, the leading spin-0 and spin-2 dimensions are both close to 3. We can see that this is exactly what happens in a generalized free field theory if we write the operators as

[28] This idea is due to Sheer El-Showk.

[29] For this step, we have used the `spectrum.py` script of [94] with parameters $(m_{\max}, n_{\max}) = (5, 7)$. The original version of [220] contained a footnote which said that values smaller than $(m_{\max}, n_{\max}) = (5, 7)$ produce solutions where the OPE coefficients are nowhere near converged. We expect this to no longer be the case after an `SDPB` bug fix by Walter Landry and Ning Su.

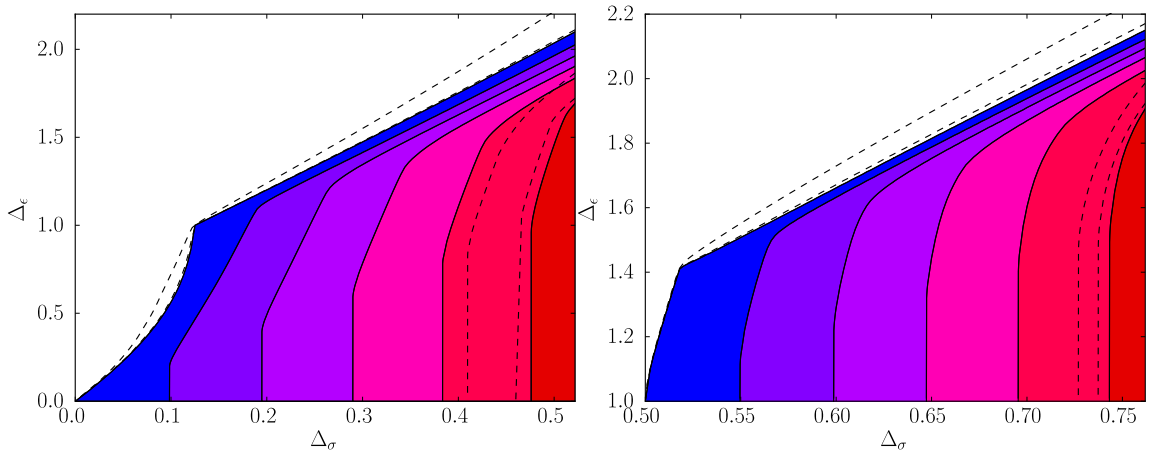


(a) 2D (b) 3D

Figure 4.14: The upper bound on $\Delta_\epsilon$ as a function of $\Delta_\sigma$. Our spin-2 constraint goes from $\Delta_T \geq d$ (blue) to $\Delta_T \geq \frac{d}{2}+2$ (red) in evenly spaced steps. Again, our main plots have $(m_{\max}, n_{\max}) = (7, 9)$ with dotted lines for $(5, 7)$ and $(3, 5)$. As expected, the convergence of the red region is slower than that of the blue region.

$\sigma\partial^2\sigma$ and $\sigma\partial_\mu\partial_\nu\sigma$ respectively. The dimensions of the next double-twist operators, found by inserting extra powers of $\partial^2$, appear somewhat too high but this could easily be an effect of the numerics. This makes it tempting to conjecture that given a long-range Ising model with dimensions $(\Delta_\sigma, \Delta_\epsilon)$, all other crossing symmetric four-point functions $\langle\sigma\sigma\sigma\sigma\rangle$ have a smaller value of $\lambda^2_{\sigma\sigma\epsilon}$. This approach to studying the LRI is ultimately perturbative since it requires the dimension of $\epsilon$ as input. Nevertheless, it could be useful for reducing the number of Feynman diagrams one encounters. Instead of computing separate diagrams for each anomalous dimension, the conjecture would enable us to compute only diagrams for $\gamma_\epsilon$ and then feed these into the bootstrap machinery to learn about other observables.

The sparseness of the spectrum in Figure 4.15 hints at another significant limitation. By perturbing around $s = s_*$ or $s = \frac{d}{2}$, it becomes clear that several additional families of operators enter the $\sigma \times \sigma$ OPE in a generic LRI. In particular, the number of scalars having $\Delta < 9$ should be much more than 4. Table 4.1 shows 16 such operators that can be constructed with the deformation of [159, 160].

The tendency for the extremal functional method to miss several operators was discussed in [94], which noticed that the numerical spectrum is dominated by double-twist families. These happen to be the families required to match the crossed channel singularity produced by a unique minimal-twist operator in the analytic bootstrap of [36, 37]. A loose conjecture arising from this is that in any crossing equation with a twist gap, several multi-twist operators with significant OPE coefficients will nevertheless provide a negligible contribution in the numerical boostrap. This is supported, for instance, by the test of the extremal func-

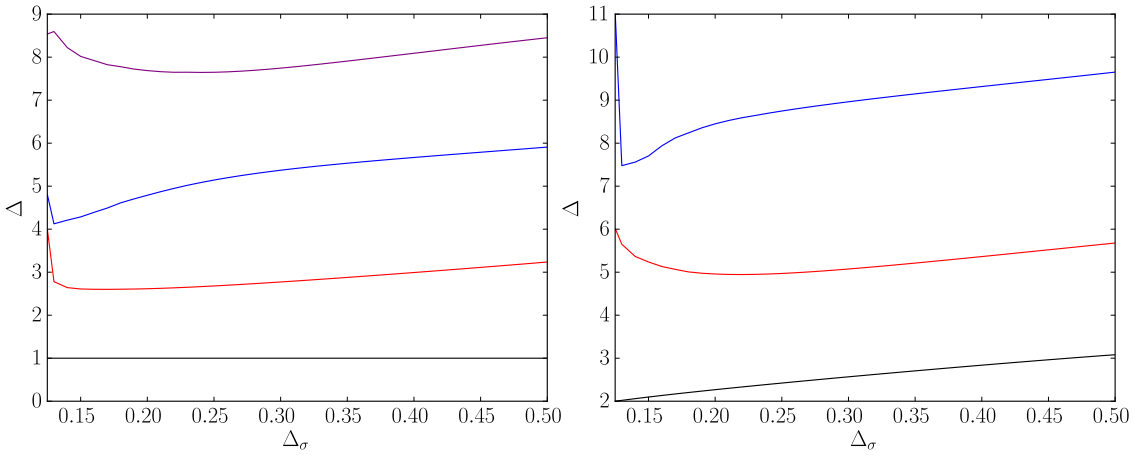


(a) Spin-0 (b) Spin-2

Figure 4.15: A few scaling dimensions in the extremal spectrum having maximal $\lambda^2_{\sigma\sigma\epsilon}$ with $\Delta_\epsilon = 1$. These are zeros of the functional that is found during the maximization procedure. For all of the spins that we have tested, it is plausible that these could approximate primary operators in the LRI.

tional method in [98], showing essential differences between the 2D and 3D Ising models. So far, the most reliable numerical bootstrap spectra all come from special cases involving a higher spin symmetry. It is worth mentioning that the analytic bootstrap has recently been extended to handle these cases as well in [38, 39]. What this means for the present case is that we only get a clear picture of the low-lying operators at $\Delta_\sigma = \frac{1}{8}$ *i.e.* the 2D Ising spectrum. As soon as we raise $\Delta_\sigma$, the theory maximizing $\lambda^2_{\sigma\sigma\epsilon}$ becomes nonlocal. Even though the nonlocality is small, we never see operators involving $\chi$ because their contributions in the $\sigma \times \sigma$ OPE are small as well.

### 4.6.2 Three correlators

In order to improve upon our single correlator results, the next logical step is to bootstrap the correlators $\langle\sigma\sigma\sigma\sigma\rangle$, $\langle\sigma\sigma\epsilon\epsilon\rangle$ and $\langle\epsilon\epsilon\epsilon\epsilon\rangle$. For this system, it makes a difference whether there are two relevant primary operators or three. Even if we did not know about the shadow relation (4.30), we would be able to infer the existence of a third relevant primary from the well known island of [78]. The assumptions that lead to an island are incompatible with the LRI because there must be a continuous line of fixed points that lead away from the SRI.

Imposing the existence of three relevant primaries, as we should, we find a reassuring exclusion plot in which all regions are connected. Figure 4.17 shows how they change as a function of $\Delta_T \in \{3, 3.1, 3.2, 3.3, 3.4, 3.5\}$. Because $3 - \Delta_\sigma$ is different from $3\Delta_\sigma$, many of the generalized free theory solutions from Figure 4.14 are excluded this time.

| Operator | Dimension | Operator | Dimension |
|---|---|---|---|
| $\epsilon$ | 1 | $\epsilon\chi\partial^2\chi$ | $\frac{27}{4}$ |
| $\sigma\chi$ | 2 | $\chi^4$ | $\frac{15}{2}$ |
| $\chi^2$ | $\frac{15}{4}$ | $\epsilon'\chi^2$ | $\frac{31}{4}$ |
| $\epsilon'$ | 4 | $\sigma\chi^2\partial^2\chi$ | $\frac{31}{4}$ |
| $\epsilon\chi^2$ | $\frac{19}{4}$ | $\chi\partial^4\chi$ | $\frac{31}{4}$ |
| $\sigma\chi^3$ | $\frac{23}{4}$ | $\epsilon''$ | 8 |
| $\chi\partial^2\chi$ | $\frac{23}{4}$ | $\epsilon\chi^4$ | $\frac{17}{2}$ |
| $\sigma'\chi$ | 6 | $\epsilon\chi\partial^4\chi$ | $\frac{35}{4}$ |

Table 4.1: Some operators having $\Delta < 9$ in the CFT obtained by coupling the 2D SRI to a generalized free field of dimension $\frac{15}{8}$. We only show the ones where both parts are scalars. Anything involving $\chi$ decouples from $\sigma \times \sigma$ at $s = s_*$ where the quoted dimensions hold exactly. At slightly smaller values of $s$ however, these operators acquire a nonzero OPE coefficient as long as they are even with respect to the diagonal $\mathbb{Z}_2$ from the two theories.

The boundary of each region has an upper branch and a lower branch. For the intermediate values $\Delta_T \in \{3.1, 3.2, 3.3, 3.4\}$, we do not observe any evidence that either branch contains a point corresponding to an LRI. If intermediate LRI models do saturate one of the branches, existing estimates for the critical exponents suggest that this should be the upper one. Lower branches for these values of $\Delta_T$ all have $\Delta_\epsilon < 1.4$. While there is no candidate LRI kink in Figure 4.17, there is a "concave kink" for some of the lower branches at $\Delta_\sigma \approx 0.58$. It appears to be a coincidence that the leftmost edge of the $\Delta_T \geq 3.1$ region of Figure 4.16 is also near this value of $\Delta_\sigma$. If any bound in Figure 4.17 were to intersect the region where CFTs can exist without $\chi$, a vanishing $\lambda^2_{\sigma\epsilon\chi}$ would signal the presence of a kink. Instead, we have found that this OPE coefficient decreases slightly at the special point without going to zero. In Figure 4.18, we maximize $\lambda^2_{\sigma\epsilon\chi}$ for $\Delta_T \in \{3, 3.05, 3.1, 3.15\}$.[30] The fact that $\chi$ decouples at a single point in the local case supports the proposal in [159]. It also agrees with the expectation that there is only one irreducible CFT with the same critical exponents as the Ising model.

### 4.6.3 Six correlators

In order to gain non-perturbative information about the LRI critical exponents, we will need to examine the minimal system of four-point functions that allows access to (4.160). This consists of $\langle\sigma\sigma\epsilon\epsilon\rangle$, $\langle\sigma\sigma\chi\chi\rangle$, $\langle\epsilon\epsilon\chi\chi\rangle$ and the three identical correlators. This system yields a much more restrictive region than Figure 4.17 and it will turn out to have interesting features.

[30] Maximizing an OPE coefficient helps to reduce any error that might have been introduced by our $10^{-4}$ bisection threshold. Once the boundary is found with sufficient precision, the spectrum is already uniquely fixed and extremization procedures are superfluous.

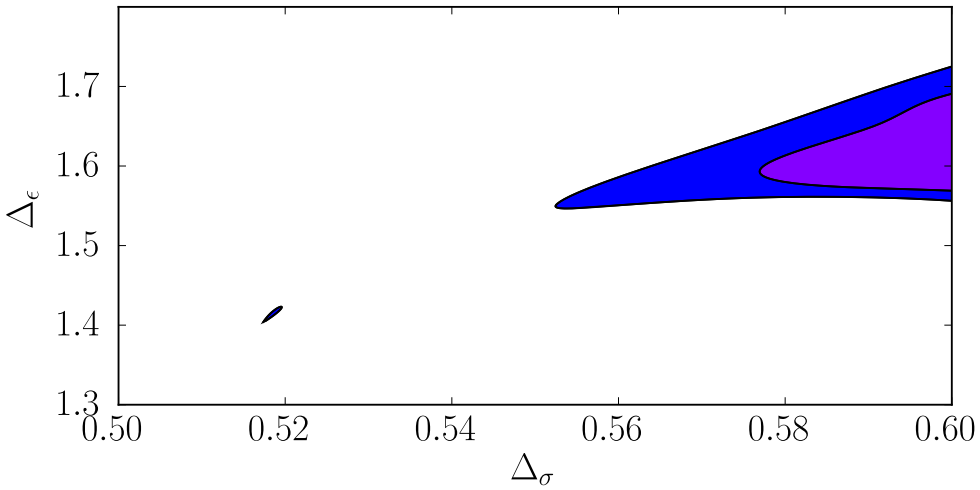


Figure 4.16: Constraints on the space of CFTs with one relevant primary operator of each parity. The allowed region for $\Delta_T \geq 3$ is blue, while the one for $\Delta_T \geq 3.1$ is purple. In the former case, an island around the 3D Ising model is separated from the rest of the region. This excludes many long-range Ising models which require $\chi$ to be present.

In order to check that they are in the right place, we have summarized our perturbative data about the LRI in Table 4.2. The last row resums the expansions around $s = \frac{d}{2}$ and $s = s_*$ using the $[3,3]$ Padé approximant. What this means is that we start with the ansatz

$$\Delta_{\mathcal{O}}(s) = \frac{a_0 + a_1 s + a_2 s^2}{1 + b_1 s + b_2 s^2} \,, \tag{4.162}$$

and fix the coefficients by demanding that (4.162) have the correct Taylor expansion around the two solvable points.

| | $\Delta_\epsilon$ | $\Delta_T$ |
|---|---|---|
| $\varepsilon$-expansion | $\frac{3}{2} - \frac{1}{6}\varepsilon + 0.18122\varepsilon^2$ | $\frac{7}{2} - \frac{1}{2}\varepsilon - 0.05926\varepsilon^2$ |
| $\delta$-expansion | $1.41263 + 0.269\delta$ | $3 + 2.333\delta$ |
| $[3,3]$-Padé | $\frac{1.3759 - 1.7116 s + 0.4013 s^2}{1 - 1.2086 s + 0.2758 s^2}$ | $\frac{4.7026 - 4.3183 s + 0.8191 s^2}{1 - 0.7812 s + 0.0850 s^2}$ |

Table 4.2: Restating our perturbative results for unprotected operators in the LRI. These expressions are specializations of (4.111) and (4.117), along with (4.93) and (4.97). To interpolate between the two expansions, we have calculated the symmetric Padé approximant.

Excluding points for $\Delta_T \in \{3, 3.1, 3.2, 3.3, 3.4, 3.5\}$ again reveals the boundaries in Figure 4.19. The lower branches are much more restrictive than those in Figure 4.17 even though we have not made use of the superblocks yet. As an example, the plot for $\Delta_T = 3$ already appears to single out the onset of mean-field theory — the blue region reaches a very narrow

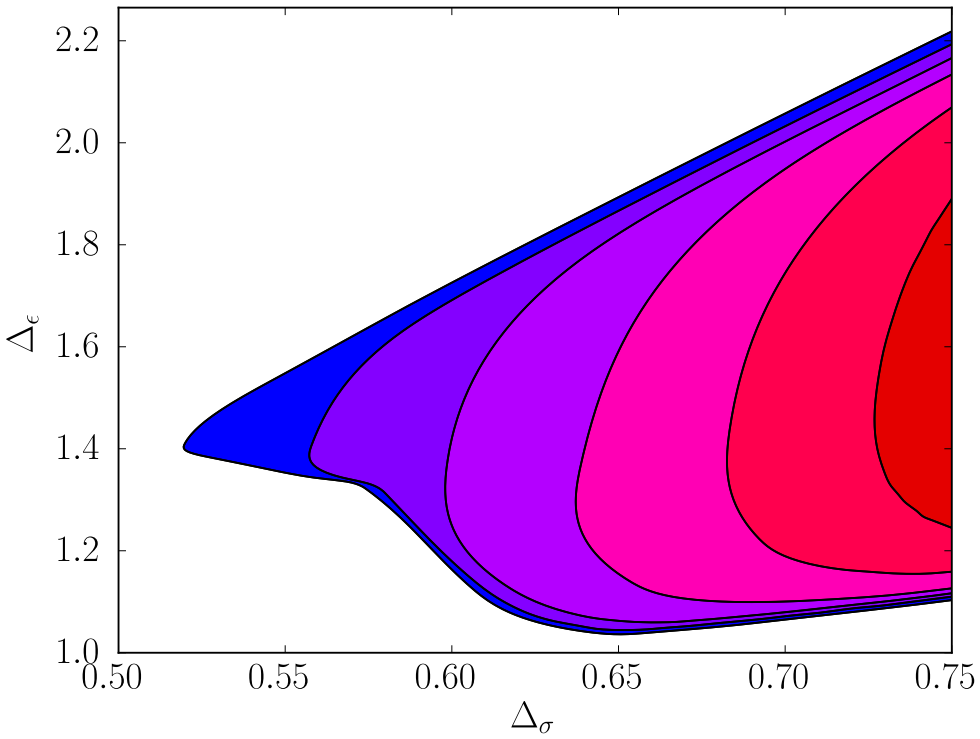


Figure 4.17: A multi-correlator version of Figure 4.14, computed with $(m_{\max}, n_{\max}) = (3, 5)$. The upper bounds are similar to the ones plotted before but the lower bounds are new. We have plotted them using a simple bisection while also testing interior points to ensure that there are no holes. Again, blue signifies $\Delta_T \geq 3$ and red signifies $\Delta_T \geq 3.5$.

throat at $(\Delta_\sigma, \Delta_\epsilon) = \left(\frac{3}{4}, \frac{3}{2}\right)$. The lower branch for this plot also experiences a jump at $\Delta_\sigma \approx 0.65$.[31] These features persist for higher values of $\Delta_T$ as well until the allowed region splits into two lobes. The bottom lobe of the $\Delta_T = 3.5$ plot stays very narrow to the left of the throat and ends at $\Delta_\sigma \approx 0.73$. This leftmost edge continues to recede as the number of derivatives is increased.

The regions shown here start to look more promising after we increase the number of derivatives. The $\Delta_T = 3.3$ region, for instance, moves to the right of the jump and develops two lobes that are connected by a narrow bridge. This makes it possible to plot a comparison between the bottom lobes and the results of Table 4.2 for $\Delta_T > 3.25$. Instead of performing this check *ceteris paribus*, we have removed the assumption that the $[\sigma\chi]_{n,\ell}$ operators are protected. The main conjecture we have made can be tested after the fact by computing an extremal spectrum at several points using the script in [94].

Allowing a continuum of odd-spin operators in the $\sigma \times \chi$ OPE we have plotted the allowed

[31] The jump here would be less pronounced if we did not assume protected operators at dimensions given by (4.144). To the left of $\Delta_\sigma \approx 0.65$, it appears to make no difference whether we impose the existence of this tower or not. We believe that most of the constraints here come from the OPE coefficient relations for

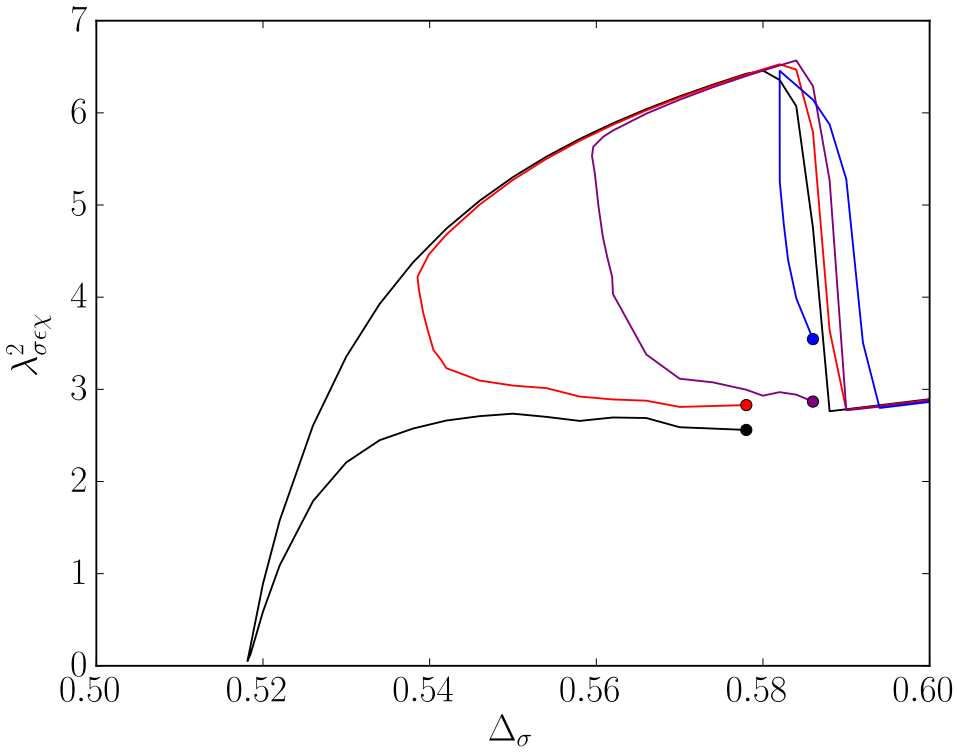


Figure 4.18: The bound on $\lambda^2_{\sigma\epsilon\chi}$ as a function of $\Delta_\sigma$ computed for $(m_{\max}, n_{\max}) = (5, 7)$. The minimum $\Delta_T$ is 3 for the black line, 3.05 for the red line, 3.1 for the purple line and 3.15 for the blue line. The OPE coefficient is maximized along the upper and lower branches of Figure 4.17. However, we have chosen not to go all the way to $\Delta_\sigma = 0.6$ along the upper branch. Doing so would yield several intersecting lines that reduce visual clarity.

regions for $\Delta_T \in \{3.25, 3.3, 3.35, 3.4, 3.45\}$ in Figure 4.20. Points on the edge, where we have extracted the spectrum, have been highlighted if they exhibit one of the following interesting properties.

1. A point is yellow if it contains a vector suitably close to $[\sigma\chi]_{1,1}$. Our threshold is that its dimension must be within 5% of 6.

2. A point is green if it additionally contains a symmetric tensor in $\sigma \times \chi$ whose dimension is within 5% of $\Delta_T$. Note that this is always true for the OPEs with Bose symmetry.

Points in the first set are likely to survive when we impose the non-renormalization of the double-twist tower. Points in the second set are likely to survive when we use superblocks or the full nine correlator system described in Appendix E.[32] Further significance to these

$\epsilon$ that are captured in (4.161).

[32]Checking what survives by producing another exclusion plot is not always instructive. In many cases, the change in a given bound is not visible to the naked eye.

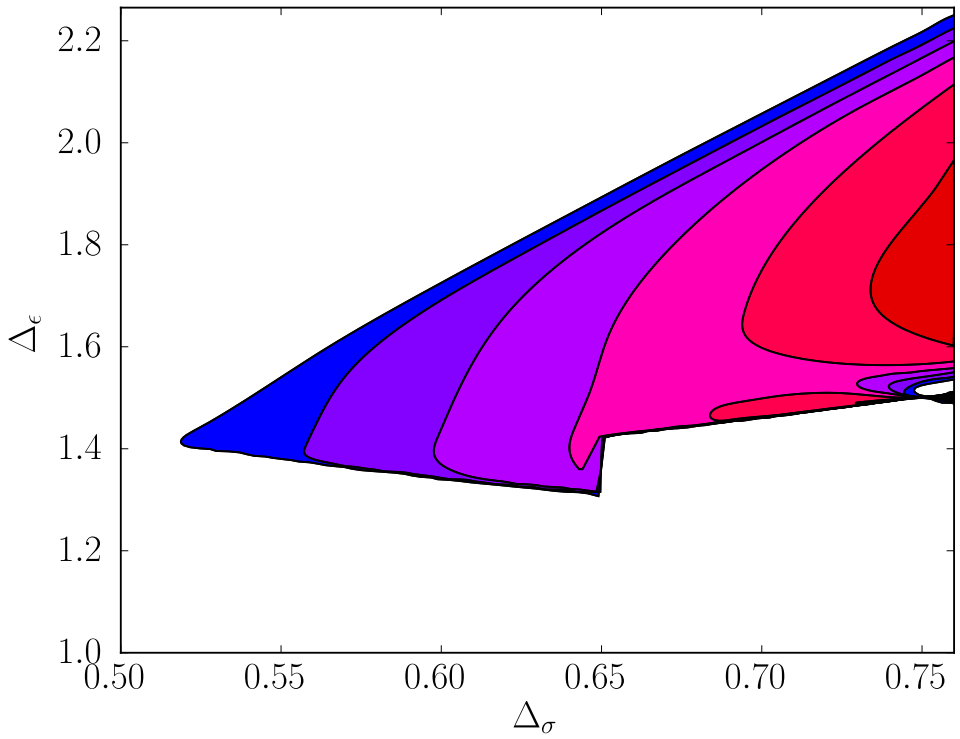


Figure 4.19: The allowed region in $(\Delta_\sigma, \Delta_\epsilon)$ space found by imposing crossing symmetry and unitarity on the six correlator system that includes $\sigma$, $\epsilon$ and $\chi$. As in Figure 4.17, the most permissive region (the blue one) allows the first $\mathbb{Z}_2$-even spin-2 operator dimension $\Delta_T$ to be as low as 3, while the most restrictive region (the red one) forces it to be at least 3.5. The other regions have $\Delta_T \in \{3.1, 3.2, 3.3, 3.4\}$. Derivative orders are $(m_{\max}, n_{\max}) = (3, 5)$. These regions account for protected double-twist operators in $\sigma \times \chi$ and use ordinary conformal blocks which means that the $\langle\sigma\sigma\chi\chi\rangle$ crossing equations are those of (4.156).

points can be seen by plotting the dimension of the first irrelevant scalar. In all long-range Ising models, we expect a value reasonably close to 3 since $\sigma\chi$ is marginally irrelevant at $s = s_*$ and $\phi^4$ is marginally irrelevant at $s = \frac{d}{2}$. Figure 4.21 shows that this is predominantly achieved at the green and yellow points which cluster around the local minimum. Several other exercises along these lines are possible, *e.g.* checking that the $\mathbb{Z}_2$-odd OPEs $\sigma \times \epsilon$ and $\epsilon \times \chi$ have low-lying operators in common as well.[33] One could also imagine a comparison involving OPE coefficients, in order to see that versions of (4.130) hold with multiple spinning operators. In practice, we have found this difficult as some of the gamma functions are highly

[33]The validity of this has nothing to do with the LRI specifically. In any bootstrap problem that includes several external scalars but not all of their mixed correlators, there are going to be OPEs that are not constrained to exchange the same operators despite being identical in terms of representation theory. In such a problem, the possibility of having two disjoint $\mathbb{Z}_2$-even OPEs, for instance, is generic but completely unphysical.

sensitive to small errors in the exchanged dimension.

Looking at the $[3,3]$ Padé approximant line in Figure 4.20, we see that it comes remarkably close to the green and yellow points. Even after a lobe becomes blunt enough that it can no longer be considered a kink, it is apparently worthwhile to locate desirable features in the extremal spectrum. This approach, advocated in [150], could perhaps reveal useful information about the smooth $\Delta_T < 3.25$ boundaries in Figure 4.19. The crosses in Figure 4.20, being offset from the green and yellow points, simply reflect the fact that convergence is noticeably slower near the $(\Delta_\sigma, \Delta_\epsilon) = \left(\frac{3}{4}, \frac{3}{2}\right)$ mean-field theory. They would appear very close to the boundaries if we continued to plot them down to $\Delta_T = 3$.

It should come as no surprise that we have not seen any islands yet. If a point satisfies crossing symmetry, unitarity and the shadow relation for some spin-2 gap $\Delta_T$, it clearly continues to satisfy these criteria when $\Delta_T$ is made less restrictive. To produce an island in this situation, one must resort to imposing whichever additional gaps appear to be most plausible [164]. It is natural to ask if an LRI island can be produced by applying this logic in the spin-2 sector — *i.e.* by setting the continuum to begin at some $\Delta_{T'} > \Delta_T$ so that the leading spin-2 operator is isolated.

It turns out that this problem demonstrates the power of the superblocks (4.158). Spectral plots analogous to Figure 4.21 tell us that the region carved out by ordinary conformal blocks is perfectly compatible with a large spin-2 gap. It is only the extra OPE relations encoded by the superblocks that ensure a more restrictive region as $\Delta_{T'}$ is increased. Figure 4.22 shows our attempt to isolate the $\Delta_T = 3.1$ LRI by imposing $\Delta_{T'} \geq 4.5$. The result is a fairly large island in which the perturbative prediction from [159] can be found near the bottom.[34] There are most likely other allowed points outside this island that we have not attempted to find. It would be interesting to check how small the spin-2 gap can be made before the two regions reunite.

## 4.7 Other issues

### 4.7.1 Off-critical behaviour

Our discussion so far has focused on the phase transition where the relevant deformation $(T - T_c)\phi^2$ has had its coefficient tuned to zero. What about correlation functions at $T \neq T_c$? More familiar statistical systems have exponentially damped two-point functions away from criticality but this is no longer true in the presence of long-range forces. Indeed, we will see that two-point functions of $\phi$ in the disordered phase (or two-point functions for the fluctuations of $\phi$ in the ordered phase) have a power-law behaviour in the IR just like they

[34] The boundary obtained by using superblocks without any $\Delta_{T'}$ gap is essentially the same as what we would get from the ordinary blocks. This is no longer true for the higher values of $\Delta_T$ that lead to lobed regions in Figure 4.19 and Figure 4.20.

do in the UV. As a result, the correlation length should be defined differently — it is a scale at which one power-law becomes more important than the other.

Consider now the two-point function of $\phi$ in position space

$$\langle \phi(x)\phi(0)\rangle = \int \frac{e^{ipx}}{|p|^s + 1} \frac{\mathrm{d}p}{(2\pi)^d} \tag{4.163}$$

where we have normalized the "mass" to 1. This can be contrasted with the two-point function of the short-range model in the disordered phase, which is obtained by setting $s = 2$. In the short-range case, the propagator is an analytic function of momenta with poles in the complex plane, leading to the exponential decay at long distances. On the other hand, non-analyticity in the long-range case leads to power-law decay.

In fact at short distances $x \ll 1$ the integral is dominated by $p \gg 1$ where we can neglect 1 in the denominator and obtain

$$\langle \phi(x)\phi(0)\rangle \sim \frac{1}{(2\pi)^d} \frac{1}{|x|^{d-s}} \qquad (x \ll 1)\ . \tag{4.164}$$

consistently with $\Delta_\phi = \frac{d-s}{2}$. On the other hand, at long distances the integral is dominated by $p \ll 1$ where we can take $\frac{1}{|p|^s+1} = 1 - |p|^s + \dots$ and find

$$\langle \phi(x)\phi(0)\rangle \sim -\frac{1}{(2\pi)^d} \frac{1}{|x|^{d+s}} \qquad (x \gg 1)\ , \tag{4.165}$$

after dropping a purely local $\delta(x)$. This gives an IR dimension of $\phi$ in the disordered phase as $\frac{d+s}{2}$. Notice that the $\phi^2$ interaction is irrelevant for this value of the $\phi$ dimension, showing the full IR stability of the disordered fixed point. Further interactions like $\phi^4$ are even more irrelevant, justifying their neglect in the above discussion. The expansions of the integrand we have used can be made rigorous with the asymptotic results of [243, 244].

### 4.7.2 Possibility of experimental observation

As the SRI is much more than a toy model, being realized in countless real-life phase transitions [245], we would be remiss not to mention the possibility of studying the LRI in the lab as well. First, it goes without saying that the validity of a $V(r) \sim \theta(r - r_0)$ potential relies on universality. Observable potentials are always more complicated than a step-function. Second, it should be just as obvious that the microscopic $V(r) \sim \frac{1}{r}$ is not the potential that matters in a physical crystal either. Many-body screening effects modify the effective potential being felt by a given atom when it is perturbed from its equilibrium position and predicting one of these from first principles is often extremely difficult. In general, the only claim we can make is that it will decay more rapidly than the Coulomb potential in a neutral material. Depending on the details of the system, this could be a potential that we have

called "short-range" — something that falls off at least as quickly as $\frac{1}{r^{d+s_*}}$. Nevertheless, it could easily be a power-law in which case the universality class should be regarded as an $s \geq s_*$ case of the LRI rather than the SRI. The difference between the two, as we have shown, is the presence of the shadow field $\chi$. Even though $\chi$ was decoupled at the crossover in all of the calculations we performed, this statement relied on the continuum limit. An experiment measuring an Ising-like phase transition that comes from a power-law potential could very well see signatures of $\chi$ as long as it has enough sensitivity to lattice operators. This would nicely complement the fact that different values of $s$ above $s_*$ can already be distinguished in materials that are taken to be continuous but finite in size [246].

A more tentative question is whether $s < s_*$ can be seen in the lab as well, signalling a breakdown of universality in the continuum limit [247]. So far there is evidence that more complicated theories (possibly outside the Ginzburg-Landau class) can be realized in this way. Examples include some high-temperature magnetic and spin-ice materials [248, 249], in which an anti-ferromagnetic short-range force is overcome by a ferromagnetic long-range force, as well as magnetic thin films where the competition is reversed [250]. Realizations of the long-range Ising model, on the other hand, currently appear to be limited to quantum simulators. See [251, 252] which achieve tunable forces using trapped ions and [253, 254] which do so using cold atoms. These experiments are useful for studying quantum phase transitions close to zero temperature but it is likely that driving the system to a thermal phase transition would introduce a radical departure from a Hamiltonian like (4.1).[35] Why have LRI physics not been seen in systems that are stable across a wide range of temperatures? Although we do not have an answer to this question, we will spend the rest of this section reviewing the force between two neutral hydrogenic atoms. This turns out to have two important components — both of them short-ranged. Such a result cannot be extrapolated to larger lattices without a severe amount of wishful thinking.

In the setup for this classic problem [259], we have protons at positions $\mathbf{r}_A$, $\mathbf{r}_B$ and electrons at positions $\mathbf{r}_1$, $\mathbf{r}_2$. The Hamiltonian $H = H_0 + H_{\text{int}}$ is given by

$$\begin{aligned} H_0 &= \frac{p_1^2}{2m} + \frac{p_2^2}{2m} - \frac{e^2}{r_{1A}} - \frac{e^2}{r_{2B}} \\ H_{\text{int}} &= e^2 \left( \frac{1}{r_{AB}} + \frac{1}{r_{12}} - \frac{1}{r_{1B}} - \frac{1}{r_{2A}} \right) . \end{aligned} \tag{4.166}$$

Corrections to the energy can be found perturbatively from the symmetric and anti-symmetric ground-states of $H_0$.

$$\psi_\pm(\mathbf{r}_1, \mathbf{r}_2) = \frac{1}{\sqrt{2 \pm 2\zeta^2}} \left[ \psi_A(\mathbf{r}_1)\psi_B(\mathbf{r}_2) \pm \psi_A(\mathbf{r}_2)\psi_B(\mathbf{r}_1) \right] \quad , \quad \psi_I(\mathbf{r}_i) \equiv \frac{1}{\sqrt{\pi a^3}} e^{-\frac{r_{iI}}{a}} \tag{4.167}$$

[35] A bootstrap approach with possible applications to this scenario was recently developed in [255–258].

Expressing the inter-atomic distance in units of the Bohr radius, one can check that

$$\zeta = e^{-\rho}\left(1+\rho+\frac{1}{3}\rho^2\right) \quad , \quad \rho \equiv \frac{r_{AB}}{a} \tag{4.168}$$

is the factor that appears in the normalization. Further integration reveals the following first-order shift.

$$\begin{aligned} E^{(1)}_{\pm} &= \langle\psi_\pm|\, H_{\rm int}\, |\psi_\pm\rangle = \frac{e^2}{r_{AB}} + \frac{e^2}{a}\frac{I_1 \pm I_2}{1\pm\zeta^2} \qquad (4.169)\\ I_1 &= -\frac{1}{\rho} + e^{-2\rho}\left(\frac{1}{\rho}+\frac{5}{8}-\frac{3}{4}\rho-\frac{1}{6}\rho^2\right)\\ I_2 &= -2\zeta e^{-\rho}(1+\rho) + e^{-2\rho}\left(\frac{5}{8}-\frac{23}{20}\rho-\frac{3}{5}\rho^2-\frac{1}{15}\rho^3\right)\\ &\quad + \frac{6}{5\rho}\left[\zeta^2(\gamma+\log\rho) - 2\left(1-\frac{1}{3}\rho^2+\frac{1}{9}\rho^4\right)\mathrm{Ei}(-2\rho) + e^{2\rho}\left(1-\rho+\frac{1}{3}\rho^2\right)^2\mathrm{Ei}(-4\rho)\right] \end{aligned}$$

The sign of $I_2$ tells us that $E^{(1)}_+ < E^{(1)}_-$. As the spatial wavefunction $\psi_+$ must be paired with an anti-symmetric spin part, this contribution to the potential is anti-ferromagnetic. Another interesting property of (4.169) is its exponential decay for large $\rho$. This result, which happens to be a 3D coincidence [260], is much stronger than what follows from dimensional analysis.

For a less symmetric state, the $\alpha^n$ term would decay as $\rho^{-3n}$ according to the multipole expansion

$$H_{\rm int} = \frac{\mathbf{r}_{1A}\cdot\mathbf{r}_{2B} - 3(\mathbf{r}_{1A}\cdot\hat{\mathbf{r}}_{AB})(\mathbf{r}_{2B}\cdot\hat{\mathbf{r}}_{AB})}{r^3_{AB}} + O\left(\frac{1}{r^4_{AB}}\right) , \tag{4.170}$$

and the first-order $E^{(1)}$ would always be dominant. The solution (4.169), on the other hand, is special because the only surviving terms are non-perturbative in $r^{-1}_{AB}$. It is therefore necessary to compute $E^{(2)}$ to find the leading contribution at large distances. This potential, called the van der Waals interaction, is proportional to $\alpha^2/r^6_{AB}$. This is reminiscent of (4.1) with $s=3$, except for the fact that we are considering a two-site lattice rather than an infinite one. We know that this is still not enough to get out of the short-range universality class since

$$s_* = d - 2\Delta^{\rm SRI}_\sigma \tag{4.171}$$

is about 1.96 in three dimensions.

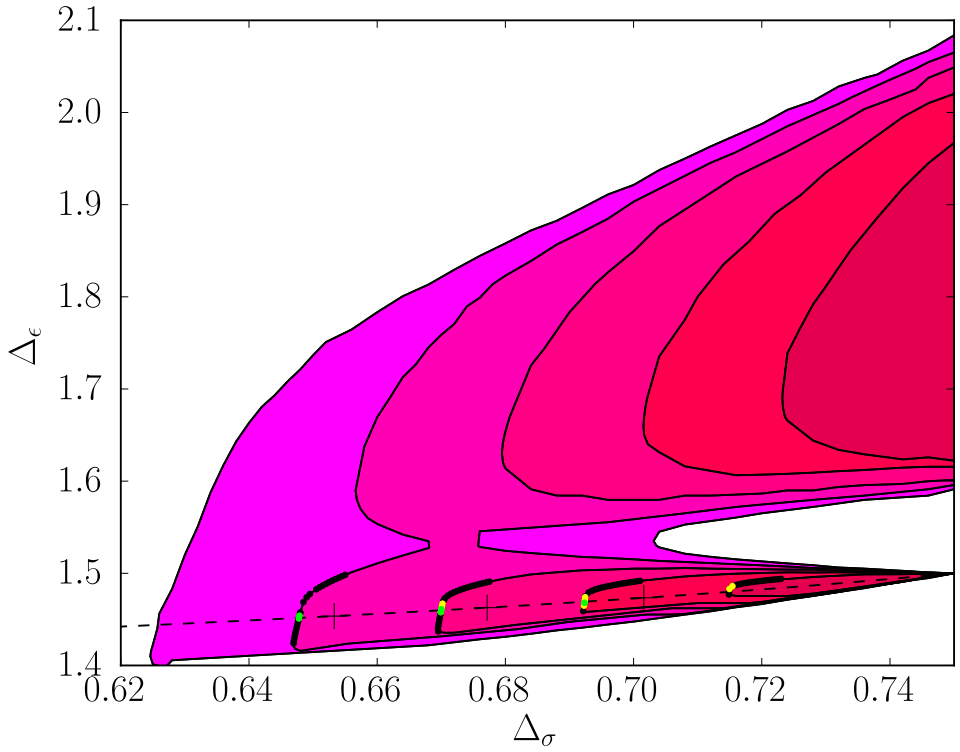


Figure 4.20: Five allowed regions whose spin-2 restrictions increment from $\Delta_T \geq 3.25$ on the left to $\Delta_T \geq 3.45$ on the right. They were found using ordinary conformal blocks with $(m_{\max}, n_{\max}) = (5, 7)$. Since no protected operators were assumed, the relevant crossing equation for $\langle\sigma\sigma\chi\chi\rangle$ is (4.154). Green points contain the operator $(\Delta, \ell) = (\Delta_T, 2)$ in all $\mathbb{Z}_2$-even OPEs instead of just one of them. Green and yellow points contain a $\mathbb{Z}_2$-even vector of dimension close to 6. All points that we have found to have neither property are marked in black. The perturbative dotted line shows $\Delta_\epsilon$ as a function of $\Delta_\sigma$ according to the Padé approximant in Table 4.2. Points on this line that are predicted to have $\Delta_T \in \{3.3, 3.35, 3.4\}$ are denoted by crosses.

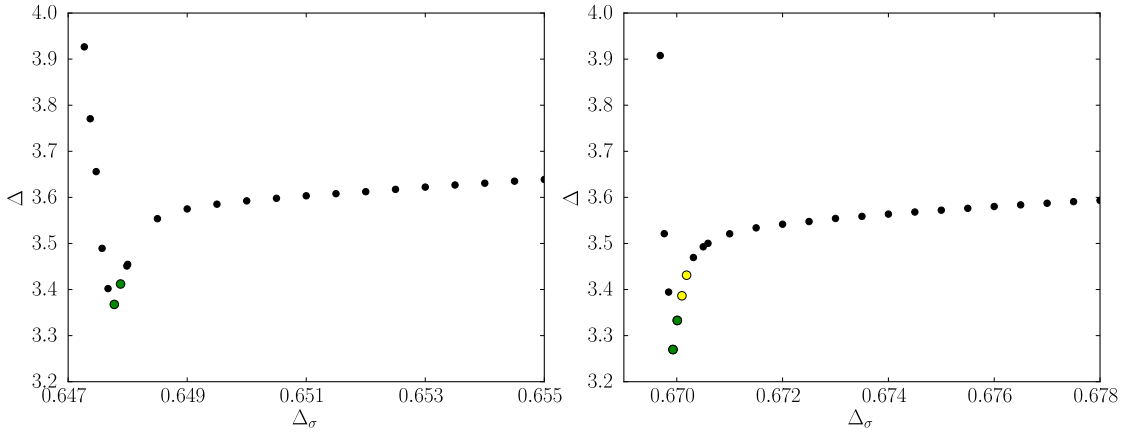


(a) $\Delta_T = 3.3$ (b) $\Delta_T = 3.35$

(c) $\Delta_T = 3.4$ (d) $\Delta_T = 3.45$

Figure 4.21: The dimension of the first irrelevant scalar in each of the four spectra extracted at the points shown in Figure 4.20. These have been taken from the $\sigma \times \sigma$, $\epsilon \times \epsilon$ and $\chi \times \chi$ OPEs as the scalars in $\sigma \times \chi$ do not show an interesting feature. Points that are yellow and green respectively satisfy property 1 and property 2 as defined in the text. These points have also been made larger.

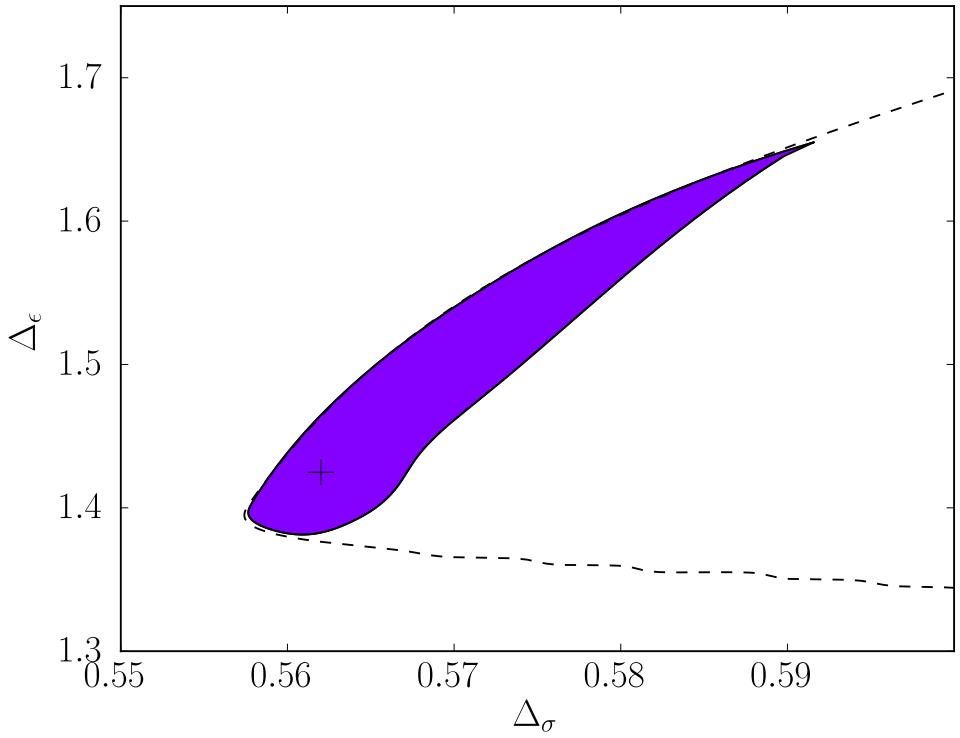


Figure 4.22: The island for the $\Delta_T = 3.1$ model computed with $(m_{\max}, n_{\max}) = (3, 5)$. Unlike Figure 4.19, which contains a much larger purple region for $\Delta_T = 3.1$, this uses the full content of the shadow relation captured in the crossing equation (4.157) — *i.e.* it was obtained by demanding crossing symmetry and unitarity for the ansatz built out of the superblocks (4.158). An island only forms because of the superblocks and the fact that we are imposing a spin-2 gap above $\Delta_T$. In this case, the gap is $\Delta_{T'} \geq 4.5$. The old $\Delta_T = 3.1$ region that would be produced from a bootstrap with ordinary conformal blocks and / or no $\Delta_{T'}$ gap is shown with a dotted line for comparison.

# Chapter 5

# Trajectories in a conformal manifold

In a $d$-dimensional conformal field theory, an exactly marginal operator is a primary scalar of dimension $d$ which does not pick up an anomalous dimension when it is added to the CFT as a deformation. The space of CFTs that can be reached in this way is referred to as a conformal manifold.[1] When the points along it describe genuinely different theories, not related by a relabelling of operators, we call a conformal manifold non-trivial. All non-trivial conformal manifolds that have been discovered so far have some enhanced symmetry beyond the conformal group $SO(d+1,1)$. In particular, all known examples in $d \geq 3$ are supersymmetric. The reason for this could simply be better analytic control which makes it easier to discover new theories, or there could be a fundamental obstruction to non-supersymmetric conformal manifolds. It is therefore worthwhile to check if there are some universal features of the operator algebra that we can associate with the presence of exactly marginal operators. Just as the modern bootstrap [16] seeks to determine whether a putative set of local operators can belong to a consistent conformal theory, there may be a test that can narrow down the space of CFTs to the space of conformal manifolds.

The original references in this subject proved non-renormalization theorems to discover conformal manifolds [261–265]. To some extent, they did so by making explicit reference to a Lagrangian. Interestingly, some of these manifolds turn out to be strongly coupled at all points. There is also a growing body of work developing the non-perturbative understanding of these theories through the superconformal algebra [266–269]. The short multiplets to which marginal operators must belong only exist in certain cases. Above 2D, these are $\mathcal{N} = 1, 2$ in 3D and $\mathcal{N} = 1, 2, 4$ in 4D [270]. In these algebras, additional requirements for finding a conformal manifold may be phrased in terms of representation theory and recombination rules. Various aspects of superconformal manifolds have been deduced from this line of reasoning including their dimensionality and the presence of complex structure.

[1] Continuous families of CFTs can arise in other ways as well. One example is the procedure in chapter 4 for constructing a line of nonlocal fixed points. Liouville theory may also be seen as a fixed line as one varies the central charge. These do not fit the definition of a conformal manifold because the lines are not traversed by deforming the CFT with a local operator.

The orthogonal approach taken here and in [271] will use conformal perturbation theory which does not rely on supersymmetry or the presence of a Lagrangian. The mnemonic

$$S \mapsto S + \int \mathrm{d}^d x g_i \hat{\mathcal{O}}^i \tag{5.1}$$

is merely an abstract statement for how we deform correlation functions. Considering a single direction on a conformal manifold that could be multi-dimensional, we will denote the associated marginal operator and its coupling by $\hat{\mathcal{O}}$ and $g$ respectively. An infinite family of constraints follows from setting $\beta(g)$, the running of the coupling, to zero. The two-loop term becomes a sum rule for even-spin CFT data analogous to the one in [16].

The local operators in a conformal manifold, even-spin or otherwise, obey many additional restrictions that require more work to state. Although there is no known way to tell if a set of scaling dimensions and OPE coefficients $\{\Delta_i, \lambda_{ijk}\}$ is part of a conformal manifold, the framework of conformal perturbation theory holds promise in telling us whether two such sets can consistently be part of the *same* conformal manifold. The key is that when there is a unique operator of each dimension, a set of differential equations exists for evolving $\{\Delta_i(g), \lambda_{ijk}(g)\}$ from one value of $g$ to another. Subtleties arise when there is degeneracy and especially when there is more than one marginal operator. In this case, there is a non-trivial Zamolodchikov metric and the curvatures built up from it become interesting observables that affect how the equations for $\frac{\mathrm{d}\Delta_i}{\mathrm{d}g}$ and $\frac{\mathrm{d}\lambda_{ijk}}{\mathrm{d}g}$ must be defined [272, 273]. Even after we limit ourselves to a single marginal operator, these equations can only be written down once the appropriate conformal block expansions are known. This yields conformal block requirements that are much steeper than those in other CFT techniques. For comparison, we note that recent studies of the analytic bootstrap use conformal blocks with small external spin that only need to be evaluated in certain limits [47, 274–276]. Bounds from spinning correlators, recently found with the numerical bootstrap, use the full expressions, but again the external spin is at most 2 [277–280]. The flow equations for conformal manifolds couple blocks of all internal and external Lorentz representations. For this reason they seem to be prohibitive in $d \geq 3$.

Nevertheless, we will see shortly that the system can in fact be analyzed sensibly in $d = 1$. The main result we have derived from this is that there is no level crossing for operators of the same symmetry. The absence of level crossing has long been predicted on general grounds but it remains a challenge to see how it is achieved. Because our argument assumes no degeneracy, we have not answered whether level crossing can occur when there is more than one marginal deformation. The program of applying our system to a known conformal manifold is similar in spirit to an algorithm that was recently developed for the numerical bootstrap. The authors of [150] saturated a dimension bound and then obtained all other solutions to crossing on the edge of that bound through a set of evolution equations. We envision an algorithm that accomplishes the same thing except in a setting where the spectra belong to the same continuous line for a physical reason.

## 5.1 Two-loop constraints

The standard framework for studying CFTs deformed by local operators is conformal perturbation theory [196, 209]. Defining $\mathcal{O}(\infty) = \lim_{x\to\infty} x^{2\Delta}\mathcal{O}(x)$, the order-$n$ correction to $\hat{\mathcal{O}}(\infty)$ is

$$\frac{g_0^n}{n!}\int \mathrm{d}^d x_1 \ldots \mathrm{d}^d x_n \left\langle \hat{\mathcal{O}}(x_1)\ldots\hat{\mathcal{O}}(x_n)\hat{\mathcal{O}}(\infty)\right\rangle \ . \tag{5.2}$$

Integrals of this form generically have logarithmic divergences which should be regulated by a UV cutoff.[2] Calling this cutoff $\Lambda$, it is enforced as a minimum distance between insertion points in the integration region: $|x_{ij}| < \Lambda^{-1}$. The divergences associated with shrinking this circle are removed from renormalized correlators by expressing them in terms of the coupling $g = \Lambda^{\hat{\Delta}-d} g_0$. The beta function is

$$\beta(g) = \frac{\mathrm{d}g}{\mathrm{d}\log\Lambda} = (\hat{\Delta}-d)g + \beta_2 g^2 + \beta_3 g^3 + \ldots \ , \tag{5.3}$$

which should vanish for marginal $\hat{\mathcal{O}}$. Putting our theory in a box of volume $V$ to handle an IR divergence, the one-loop and two-loop terms involving $\log\Lambda$ may be read off from

$$\begin{aligned}
\frac{1}{V}\int \mathrm{d}^d x_1 \mathrm{d}^d x_2 \left\langle \hat{\mathcal{O}}(x_1)\hat{\mathcal{O}}(x_2)\hat{\mathcal{O}}(\infty)\right\rangle &\sim -2\beta_2\log\Lambda \\
\frac{1}{V}\int \mathrm{d}^d x_1 \mathrm{d}^d x_2 \mathrm{d}^d x_3 \left\langle \hat{\mathcal{O}}(x_1)\hat{\mathcal{O}}(x_2)\hat{\mathcal{O}}(x_3)\hat{\mathcal{O}}(\infty)\right\rangle &\sim -6\beta_3\log\Lambda + 6\beta_2^2\log^2\Lambda \ .
\end{aligned} \tag{5.4}$$

In the first integral, the OPE with $x_2 \to x_1$ tells us that

$$\beta_2 = -\frac{S_{d-1}}{2}\lambda_{\hat{\mathcal{O}}\hat{\mathcal{O}}\hat{\mathcal{O}}} \ . \tag{5.5}$$

The second integral is more interesting as it involves a four-point function. Recently, there has been interest in approximating it using data from the numerical bootstrap [99, 159, 160]. A logarithmic divergence arises by letting $x_2$ and $x_3$ approach $x_1$ while remaining of the same order. Performing a conformal transformation, we may write $\beta_3$ as a single integral of $\left\langle \hat{\mathcal{O}}(0)\hat{\mathcal{O}}(x)\hat{\mathcal{O}}(\hat{e})\hat{\mathcal{O}}(\infty)\right\rangle$ where $\hat{e}$ is an arbitrary unit vector. For each relevant operator in the OPE $\hat{\mathcal{O}}\times\hat{\mathcal{O}}$, there is a power-law singularity. Subtracting these,

$$\beta_3 = -\frac{S_{d-1}}{6}\int \mathrm{d}^d x \left[\left\langle \hat{\mathcal{O}}(0)\hat{\mathcal{O}}(x)\hat{\mathcal{O}}(\hat{e})\hat{\mathcal{O}}(\infty)\right\rangle - \sum_{\Delta<d}\lambda^2_{\hat{\mathcal{O}}\hat{\mathcal{O}}\mathcal{O}}\left(\frac{1}{|x|^{\Delta}} + \frac{1}{|x|^{2d-\Delta}} + \frac{1}{|\hat{e}-x|^{2d-\Delta}}\right)\right] \tag{5.6}$$

[2] An approach using dimensional regularization instead was developed in [281, 282].

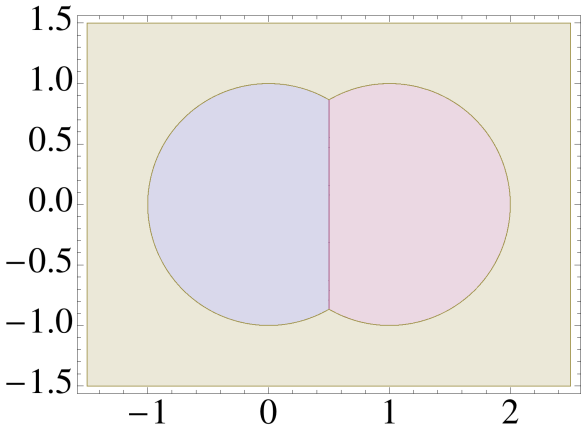


Figure 5.1: Once we send our four points to $(0, z, 1, \infty)$, $\mathcal{R}_{12}$, $\mathcal{R}_{23}$ and $\mathcal{R}_{13}$ map to the blue, red and yellow $z$-plane regions respectively. We have used a change of variables to give all integrals the blue domain, which we denote by $\mathcal{R}$.

is the net result.[3] There is a different form of (5.6) that will be more useful for our purposes [99]. It comes from writing (5.4) as an integral over $\mathcal{R}_{12} \cup \mathcal{R}_{23} \cup \mathcal{R}_{13}$ where $\mathcal{R}_{ij}$ means that $|x_{ij}|$ is smaller than the other two distances. These are precisely the regions of optimal convergence for conformal block expansions in the $s$, $t$ and $u$ channels. Figure 5.1 plots them for our desired kinematics. By covariance of the correlator, they can all be swapped for the region $\mathcal{R} \equiv \{|x| < 1, |\hat{e} - x|\}$ where the only potential singularity is at the origin. With this in mind,

$$\beta_3 = -3\frac{S_{d-1}}{6}\sum_{\mathcal{O}} \lambda^2_{\hat{\mathcal{O}}\hat{\mathcal{O}}\mathcal{O}} \int_{\mathcal{R}} \mathrm{d}^d x |x|^{-2d} g_{\mathcal{O}}(u,v)\Big|_{\text{reg}} \,. \tag{5.7}$$

The factor of 3 reflects the crossing symmetry of the four-point function. Later, when we deal with mixed correlators, we will have to treat each permutation separately. By setting the terms above to zero,

$$\boxed{\begin{aligned} &\hat{\Delta} = d \\ &\lambda_{\hat{\mathcal{O}}\hat{\mathcal{O}}\hat{\mathcal{O}}} = 0 \\ &\sum_{\mathcal{O}} \lambda^2_{\hat{\mathcal{O}}\hat{\mathcal{O}}\mathcal{O}} \int_{\mathcal{R}} \mathrm{d}^d x |x|^{-2d} g_{\mathcal{O}}(u,v)\Big|_{\text{reg}} = 0 \end{aligned}} \tag{5.8}$$

are the conditions that a conformal manifold imposes on the operator algebra. For the rest of this section, we will focus on the non-trivial line of (5.8) and refer to it as the *sum rule*. As a first step in understanding the ingredients of the sum rule, we may plot the conformal

[3] Equivalently, one could omit $\Delta = 0$ from the sum and then invoke some notation to change the four-point function to the *connected* four-point function.

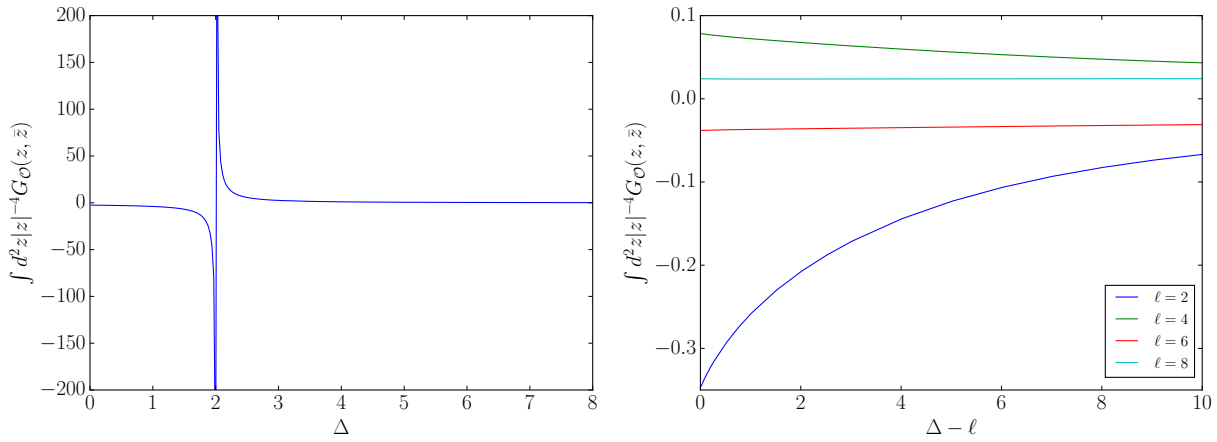


(a) Scalars, 2D

(b) Tensors, 2D

Figure 5.2: Plots showing how a primary operator in $\hat{\mathcal{O}} \times \hat{\mathcal{O}}$ contributes to the beta function. These follow from a numerical integral but they may be obtained analytically in one dimension.

block integrals as functions of the exchanged dimension $\Delta$. Figure 5.2 does this for $d = 2$ but the same basic features appear in all dimensions. Looking at the scalars, we see that relevant and irrelevant operators contribute with opposite signs. The discontinuity at $\Delta = d$ arises because the counterterm $\frac{1}{|x|^\Delta}$, introduced to cure a UV divergence, becomes IR divergent as well at marginality. Higher spin operators, which exist for $d \geq 2$, appear to have the same sign for all $\Delta$. However, they alternate with spin according to $\ell$ (mod 4). This phenomenon was noted in [283] which also included plots for $d = 4$.

### 5.1.1 Ambiguities in the sum rule

An important feature of the scalar plot in Figure 5.2 is that it does not pass through the origin. This means that in the sum rule derived from a connected four-point function in (5.6), the identity term is finite. Although this might seem strange at first sight, it is an inevitable consequence of using counterterms in bounded regions. There are different ways to do this when crossing symmetry is not manifestly satisfied, leading to a freedom in how the sum rule is presented. The point is that the minimal subtraction we have adopted for an integrated conformal block is not the same as subtracting terms of the form $\frac{1}{|x|^\Delta} + \frac{1}{|x|^{2d-\Delta}} + \frac{1}{|\hat{e}-x|^{2d-\Delta}}$ given in (5.6). If we truly wanted to do the latter, our integrals of conformal blocks would need to be regulated by subtracting finite terms as well. In this discussion, we will explore the differences between these two choices. It should also be clear that the number of choices is infinite since we are free to apply any linear combination of the two above. We should emphasize that this is not a *physical* ambiguity. Data solving one version of the sum rule will

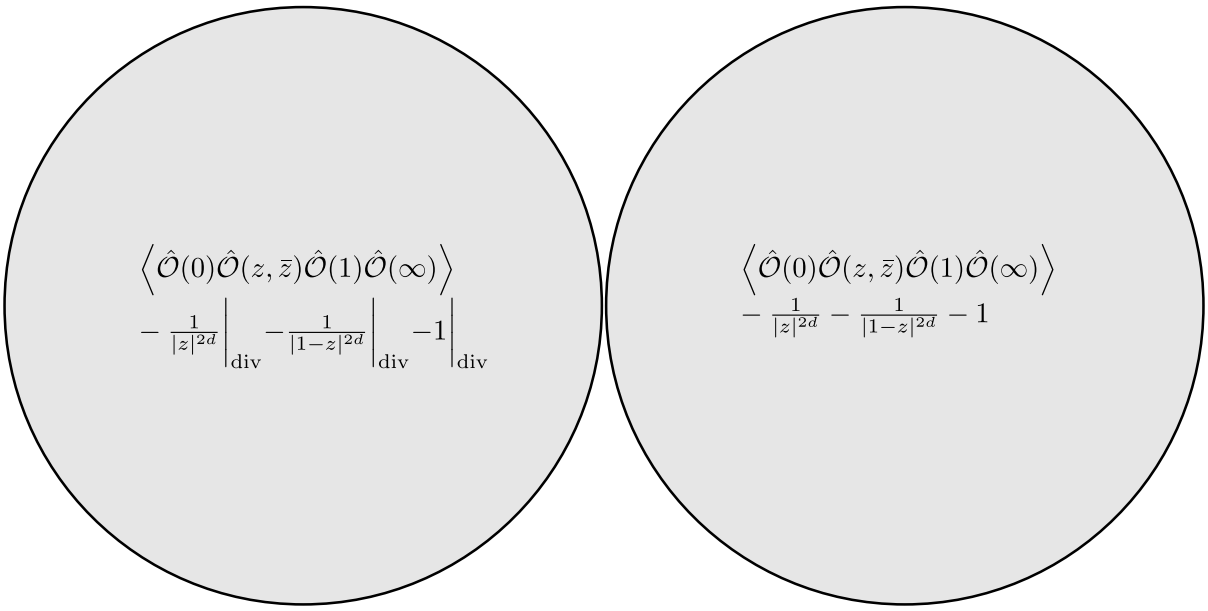


Figure 5.3: We represent $\mathbb{R}^d$ as a blob with the function to be integrated inside it. The left and right choices both compute the two-loop beta function. Because $\mathbb{R}^d$ has no boundary, the integrated power-laws being subtracted are equal to their divergent parts.

automatically solve another if it comes from a crossing symmetric theory. This reflects the fact that the beta function is well defined within our scheme. It is even scheme independent at two loops, as explained in [99]. Nevertheless, it represents an ambiguity in characterizing the beta function term of an *abstract* conformal multiplet.

For simplicity, suppose that the only relevant scalar in $\hat{\mathcal{O}}\times\hat{\mathcal{O}}$ is the identity. In this case, the right-hand side of Figure 5.3 is a cartoon that represents the integration done in (5.6). To change prescriptions, it will be helpful to distinguish between a subtracted function and its isolated divergence. We may consider a subtraction of $\frac{1}{|z|^{2d}}$ from $f(z)$, integrated over an $r$-ball for instance.

$$\begin{aligned}\int_{B(r)} \mathrm{d}^d z f(z) - \frac{1}{|z|^{2d}} &= \int_{B(r)} \mathrm{d}^d z f(z) - \frac{S_{d-1}}{d}(r^{-d} - \Lambda^d) \\ \int_{B(r)} \mathrm{d}^d z f(z) - \frac{1}{|z|^{2d}}\Big|_{\text{div}} &= \int_{B(r)} \mathrm{d}^d z f(z) + \frac{S_{d-1}}{d}\Lambda^d \end{aligned} \tag{5.9}$$

The expression that subtracts the full power-law includes an extra $\frac{S_{d-1}}{d}r^{-d}$ compared to the expression that only subtracts the divergence. Clearly, $r\to\infty$ makes these procedures equivalent, explaining why both halves of Figure 5.3 are the same.

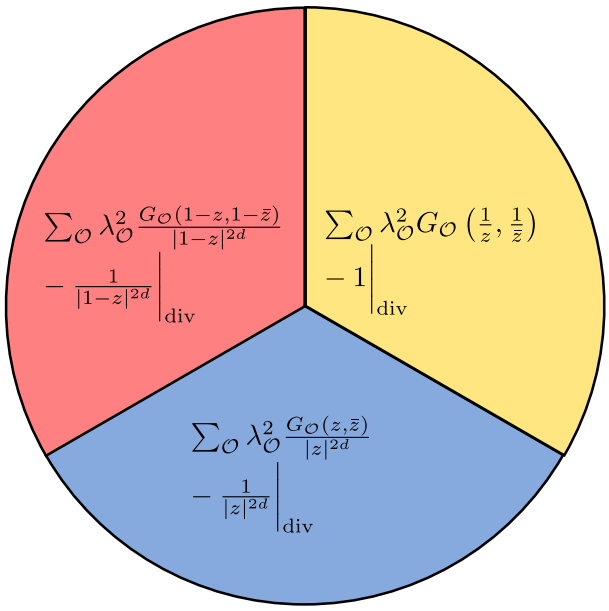


(a) Equivalent to Figure 5.3 (a)

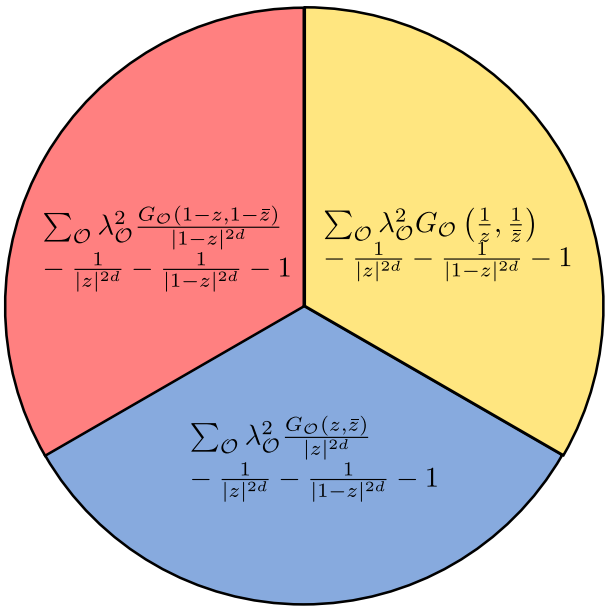


(b) Equivalent to Figure 5.3 (b)

Figure 5.4: The cartoons obtained by splitting Figure 5.3 into $s$, $t$ and $u$ channel regions. In both cases, the identity block is not annihilated. A divergence subtraction is now no longer the same as a full subtraction. In particular, removing div everywhere in the left blob would not compute a physical quantity.

As soon as we expand in conformal blocks, we must partition space into the blue, red and yellow regions from Figure 5.1. These are represented in Figure 5.4 by the same colors. The type of subtraction being performed on the left-hand side is the choice made in this chapter. It makes use of the fact that divergences are localized around special points, allowing us to keep only one in each region. It is now clear that power-laws present in the blocks for relevant scalars will not be fully removed. After divergences are subtracted, finite boundary terms will remain. Another choice that we could have made is the approach of the right-hand side — subtracting the same original counterterm in all three channels. The equivalence between the two choices relies on crossing symmetry. In this case, a power-law like $\frac{1}{|z|^{2d}}$ is fully cancelled but the additional appearances of 1 and $\frac{1}{|1-z|^{2d}}$ mean that we are subtracting too much. Finite parts will thus persist unless we find a natural way to pair these counterterms with the blocks of irrelevant operators instead. In this regard, the lightcone bootstrap has successfully matched crossed channel singularities to infinite towers of operators in the direct channel [36, 37]. However, these are the well known towers of double-twist operators which only exist asymptotically.

The observation that the two sides of Figure 5.4 are equivalent is not new. The divergence subtraction on the left-hand side was referred to as "method 2" in [159]. "Method 1" was

discussed in a context where the four-point function was known exactly, but it can also be applied in cases where we have to use the conformal block expansion. This would make it identical to the right-hand side of Figure 5.4.

### 5.1.2 The alternating sign

We now turn to the question of why the contributions plotted in Figure 5.2 have signs that alternate with spin. Although a general proof eludes us, we may show that the correct sign is predicted by the large-$\Delta$ limit. It is convenient to express everything in terms of the radial co-ordinate

$$\begin{aligned} \rho &= \frac{z}{(1+\sqrt{1-z})^2} \\ r &= |\rho| \\ \eta &= \cos \arg \rho \, . \end{aligned} \tag{5.10}$$

For the large-$\Delta$ block, we use

$$\begin{aligned} g_{\Delta,\ell}(r,\eta) &= \frac{\ell!}{(2\nu)_\ell} \frac{(4r)^\Delta C_\ell^\nu(\eta)}{(1-r^2)^\nu \sqrt{(1+r^2)^2-4r^2\eta^2}} \left(1+O\left(\frac{1}{\Delta}\right)\right) \\ \nu &= \frac{d-2}{2} \end{aligned} \tag{5.11}$$

which is the entire part from the meromorphic expansion in [24]. It is easy to check that the region $\mathbb{C} \setminus (1,\infty)$ for $z$ maps to the unit circle for $\rho$ [84]. Therefore $G_{\Delta,\ell}(r,\eta)$ vanishes for $\Delta \to \infty$ and so must an integral of it over a bounded region. Another thing to check is that $\mathcal{R}$, the region that looks like a cutoff circle, maps to $\{(r,\eta)| -1 < \eta < 1, 0 < r < r_*(|\eta|)\}$ where $r_*(|\eta|)$ is the smaller solution of $r^2 - 4r + 1 = 2r|\eta|$ [99]. With a little bit of work to find the measure, our integral is

$$I = \frac{\ell!}{(2\nu)_\ell} \int_{-1}^{1} \mathrm{d}\eta \int_0^{r_*(|\eta|)} \mathrm{d}r \sqrt{(1+r^2)^2-4r^2\eta^2} (4r)^{\Delta-d-1} (1-r^2)^\nu (1-\eta^2)^{\nu-\frac{1}{2}} C_\ell^\nu(\eta) \, . \tag{5.12}$$

Everything in the integrand except the Gegenbauer polynomial is sign-definite and peaks at $\eta = 0$. It therefore seems that the sign of $I$ should be controlled by the sign of $C_\ell^\nu(0)$. This is indeed $(-1)^{\ell/2}$ as can be seen in various ways. Perhaps most easily, we can just use the fact that each Gegenbauer is an even polynomial with $\ell$ zeros on the unit interval. The fact that $C_\ell^\nu(\pm 1) > 0$ then gives us the right sign for $C_\ell^\nu(0)$. To see why this sign persists, consider

$$\int_{-1}^{1} \mathrm{d}\eta \frac{C_\ell^\nu(\eta)}{C_\ell^\nu(0)} f(|\eta|)(1-\eta^2)^{\nu-\frac{1}{2}} \, . \tag{5.13}$$

If $f$ is identically 1, then it is a special case of a Gegenbauer polynomial and (5.13) vanishes by orthogonality. This means that the positive sign near $\eta = 0$ is exactly cancelling the negative signs that appear elsewhere. The integral should then become more positive once we change $f$ to a positive function that peaks at zero and decays in either direction. We may check that this holds for

$$f(|\eta|) = \int_0^{r_*(|\eta|)} \mathrm{d}r \sqrt{(1+r^2)^2 - 4r^2\eta^2}(4r)^{\Delta-d-1}(1-r^2)^\nu \ , \tag{5.14}$$

but this only proves our suspicion when $\ell \leq 2$. For higher spins, we will need information about $f$ beyond monotonicity. A saddle point evaluation of (5.14) leads to

$$f(|\eta|) \approx \frac{4^{\Delta-d}}{\Delta-d-1}\sqrt{1+|\eta|}(1-r_*(|\eta|)^2)^\nu r_*(|\eta|)^{\Delta-d+1} \ . \tag{5.15}$$

For sufficiently large $\Delta$, the increasing function $\sqrt{1+|\eta|}(1-r_*(|\eta|)^2)^\nu$ does not spoil the decrease of $r_*(|\eta|)^{\Delta-d+1}$. Therefore, we may consider the parts of (5.13) on either side of the first zero of $C_\ell^\nu(\eta)$. Call this point $\eta_0$. For the $\eta > \eta_0$ part of (5.13) which includes negative contributions, the crudest underestimate is

$$\begin{aligned} I_> &\geq -\frac{4^{\Delta-d}}{\Delta-d-1}K_> r_*(\eta_0)^{\Delta-d+1} \\ K_> &= |\mathrm{min} C_\ell^\nu(\eta)/C_\ell^\nu(0)|\,(1-\eta_0)\sqrt{1+\eta_0}(1-r_*(\eta_0)^2)^\nu \ . \end{aligned} \tag{5.16}$$

We may underestimate the positive contribution from $\eta \in [0,\eta_0]$ by just taking $\eta \in \left[0, \frac{\eta_0}{2}\right]$. This yields

$$\begin{aligned} I_< &\geq \frac{4^{\Delta-d}}{\Delta-d-1}K_< r_*\left(\frac{\eta_0}{2}\right)^{\Delta-d+1} \\ K_< &= \left|C_\ell^\nu\left(\frac{\eta_0}{2}\right)/C_\ell^\nu(0)\right| \frac{\eta_0}{2}\sqrt{1+\frac{\eta_0}{2}}\left(1-r_*\left(\frac{\eta_0}{2}\right)^2\right)^\nu \ . \end{aligned} \tag{5.17}$$

Since $K_>$ and $K_<$ are independent of $\Delta$, it is easy to choose $\Delta$ such that $[r_*\left(\frac{\eta_0}{2}\right)/r_*(\eta_0)]^{\Delta-d+1}$ is larger than $K_>/K_<$.

### 5.1.3 Realizations

The simplest conformal manifold is probably the compactified free boson in two dimensions.[4] While the absence of a beta function in a free theory hardly needs to be stated, it is instructive to discuss this model from symmetry considerations alone. At a generic radius, the symmetry

[4] We use the term "manifold" loosely, as the moduli space is not smooth at the self-dual radius.

is given by two copies of the affine $U(1)$ algebra. The current $J$ and its modes $a_n$ satisfy

$$\begin{aligned} J(z)J(w) &= \frac{1}{(z-w)^2} + \dots \\ [a_n, a_m] &= n\delta_{m+n,0} \, . \end{aligned} \tag{5.18}$$

The object $T =: J^2 :$, known as the Sugawara stress tensor, has all of its properties determined from (5.18). Specifically,

$$\begin{aligned} T(z)T(w) &= \frac{1}{2(z-w)^4} + \frac{2T(w)}{(z-w)^2} + \frac{\partial T(w)}{z-w} + \dots \\ L_m &= \frac{1}{2}\sum_{n\in\mathbb{Z}} : a_{m-n}a_n : \end{aligned} \tag{5.19}$$

which implies the Virasoro algebra for central charge 1. This leads to a simple relation between the charges and conformal weights of primary operators; $h = q^2$. We therefore see that $J\bar{J}$ is a marginal deformation because the two pieces have charge $\pm 1$.

Cardy found this model through a bottom-up approach while searching for a fixed line that did not require finely tuned OPE coefficients. In [284], he showed that

$$\begin{aligned} \left\langle \hat{\mathcal{O}}(0)\hat{\mathcal{O}}(z,\bar{z})\hat{\mathcal{O}}(1)\hat{\mathcal{O}}(\infty)\right\rangle &= |z|^{-4}G(z,\bar{z}) \\ &= 2\Re\left[\frac{1}{z^2} + \frac{1}{(1-z)^2} + \frac{1}{\bar{z}^2(1-z)^2}\right] + \frac{1}{|z|^4} + \frac{1}{|1-z|^4} + 1 \end{aligned} \tag{5.20}$$

is the unique crossing symmetric four-point function with a vanishing regulated integral whose singularities involve only the Virasoro identity block. We have separated the connected and disconnected pieces above. The holomorphic factorization looks like

$$\begin{aligned} G(z,\bar{z}) &= g(z)g(\bar{z}) \\ g(z) &= \left(\frac{z^2-z+1}{1-z}\right)^2 = 1 + 2z^2 + \sum_{k=2}^{\infty} k z^{k+1} \, . \end{aligned} \tag{5.21}$$

The expansion of (5.21) into $SL(2;\mathbb{R})$ blocks is

$$\begin{aligned} g(z) &= 1 + \sum_{n=1}^{\infty} c_n z^{2n} {}_2F_1(2n, 2n; 4n; z) \\ c_n &= \frac{2n-1}{4^{n-1}} \frac{(2n)!}{(4n-3)!!} \, , \end{aligned} \tag{5.22}$$

yielding explicit OPE coefficients in $\hat{\mathcal{O}} \times \hat{\mathcal{O}}$.[5] A spinning operator (labelled by non-negative integers $n, \bar{n}$) has $\lambda^2_{\hat{\mathcal{O}}\hat{\mathcal{O}}\mathcal{O}} = 2c_n c_{\bar{n}}$, while a scalar operator has $\lambda^2_{\hat{\mathcal{O}}\hat{\mathcal{O}}\mathcal{O}} = c_n^2$. Using these OPE coefficients, one can proceed to integrate the $SL(2;\mathbb{C})$ blocks in (5.20). It should be no surprise that this verifies the sum rule (5.8). The only scalar of $\Delta < 2$ in this Virasoro identity block is the quasiprimary $I$ itself. This would make it a *dead-end CFT* if we took the unusual step of regarding this subsector of the free boson as a theory in its own right. Because no relevant deformations contribute to the beta function, the model owes marginality to the appearance of both signs in Figure 5.2.

The known examples of conformal manifolds above $d = 2$ are superconformal manifolds. Let us discuss 4D theories in decreasing order of supersymmetry. The $\mathcal{N} = 4$ theories will have an exactly marginal operator whenever they have a stress-energy tensor. Both of these are in a multiplet whose primary transforms in the $\mathbf{20'}$ representation of the $SU(4)$ R-symmetry. Reassuringly, there is no way for this to recombine with another multiplet. There is a well known conjecture that all $\mathcal{N} = 4$ SCFTs fall into the Super Yang-Mills class. The situation in $\mathcal{N} = 2$ is similar with classical marginality implying exact marginality again due to recombination rules. The difference is that local $\mathcal{N} = 2$ SCFTs do not automatically require the multiplet for marginal operators to be present. Indeed, known $\mathcal{N} = 2$ SCFTs include conformal manifolds but also a large zoo of isolated fixed points [286]. Finally, classically marginal operators are ubiquitous in $\mathcal{N} = 1$ theories as descendants of scalar chiral primaries. These primaries obey $\Delta = \frac{3}{2}|r|$, where we are interested in $r$-charge 2 to get the multiplet of a superpotential. To prevent this from recombining with a conserved current multiplet, one needs extra input such as the mechanism described in [266].

Since we must have a solved theory to fully apply (5.8), we are essentially limited to examples like free $\mathcal{N} = 4$ SYM or free $\mathcal{N} = 2$ SQCD with the right matter content to make it conformal. What might be more interesting is checking the contribution of particular supermultiplets. BPS multiplets, which have fixed dimension whenever they appear, could be treated once. When an unprotected multiplet has correlators of its descendants determined by those of the primary, its contribution could be plotted as a function of $\Delta$ analogously to Figure 5.2. This is not the case for long multiplets with nilpotent superconformal invariants. In these superconformal blocks, the coefficients of bosonic blocks that appear are theory dependent [157, 230, 287]. Even before these exercises are done, it is clear that (5.8) will not allow us to see individual cancellation within a given block. As stated earlier, our current form of the sum rule is contaminated by counterterms such that even the identity — the supermultiplet with no descendants at all — contributes a finite piece. This should be addressed in any serious attempt to study the structure of the OPE applicable to the beta function.

[5] We have guessed (5.22) with the help of OEIS [285]. However, a proof should be possible with the technology of [136].

## 5.2 Evolution equations

To begin exploring the landscape of conformal manifolds, the sum rule (5.8) is the most natural starting point. We would like to emphasize, however, that CFTs with exactly marginal deformations obey a much larger set of constraints. If a continuous line of theories has a solution at one point, these constraints are in principle enough to solve for local operators in the theories at all other points. The idea is to flow along the manifold in a given direction by applying the first-order shifts

$$\begin{aligned} \delta\Delta_i &= -\delta g S_{d-1}\lambda_{ii\hat{\mathcal{O}}} \\ \delta\lambda_{ijk} &= \delta g \int_{\mathcal{R}} \mathrm{d}^d x \left\langle \mathcal{O}_i(0)\hat{\mathcal{O}}(x)\mathcal{O}_j(\hat{e})\mathcal{O}_k(\infty)\right\rangle \Big|_{\text{reg}} + \text{perms} \end{aligned} \tag{5.23}$$

repeatedly.[6] The permutations denote integrals over $\mathcal{R}$ with different $(i,j,k)$ orderings. As discussed in the last section, this is equivalent to integrating the first permutation over all of space. Because the marginal operator takes us from one CFT to another, we will always be able to use the conformal block expansion on the right-hand side of (5.23). This allows us to write the results of conformal perturbation theory in exponentiated form:

$$\begin{aligned} \frac{\mathrm{d}\Delta_i}{\mathrm{d}g} &= -S_{d-1}\lambda_{ii\hat{\mathcal{O}}} \\ \frac{\mathrm{d}\lambda_{ijk}}{\mathrm{d}g} &= \sum_{\mathcal{O}} \lambda_{i\hat{\mathcal{O}}\mathcal{O}}\lambda_{jk\mathcal{O}} \int_{\mathcal{R}} \mathrm{d}^d x \frac{g_{\mathcal{O}}(x)}{|x|^{\Delta_i+d}}\Big|_{\text{reg}} + \text{perms}\,. \end{aligned} \tag{5.24}$$

The sum rule from the last section is the special case found by taking $\mathcal{O}_i$, $\mathcal{O}_j$ and $\mathcal{O}_k$ to be $\hat{\mathcal{O}}$ itself.

Following OPE coefficients along the manifold is only meaningful if the deformation by $\hat{\mathcal{O}}$ preserves the starting normalization of all operators. In the absence of level crossing and other non-generic behaviour, it is possible to achieve this, but only in a particular scheme. This is, of course, the one we have been using which subtracts power-law divergences in the OPE. As stated in [99], other schemes — which differ by a finite part — can be recast into this language if we modify OPEs involving $\hat{\mathcal{O}}$ to include a contact term:

$$\hat{\mathcal{O}}(x)\mathcal{O}_i(0) \sim \alpha\delta(x)\mathcal{O}_i(0)\,. \tag{5.25}$$

It is clear from this that operator norms will shift by an $O(\alpha)$ amount and therefore be scheme dependent. Although we focus on non-degenerate spectra for simplicity, the situation

[6] Strictly speaking, the OPE coefficient $\lambda_{ii\hat{\mathcal{O}}}$ should be summed over all tensor structures if $\mathcal{O}_i$ is not a scalar.

becomes more interesting when we are allowed to write contact terms of the form:

$$\hat{\mathcal{O}}(x)\mathcal{O}_i(0) \sim \alpha_i^j \delta(x)\mathcal{O}_j(0) \ . \tag{5.26}$$

In this case, the field redefinitions needed to return to the initial normalization include not only rescalings but linear combinations within a degenerate subspace. While it is still possible to use a scheme that removes such mixing at a point, there is no guarantee that we may do so globally [272, 273].

Clearly, the infinite coupled system (5.24) will need to be truncated if one hopes to use it numerically. It is also unrealistic to expect a subset of the equations in (5.24) to close among themselves. In particular, this means that one will have to compute the trajectories of OPE coefficients $\lambda_{ijk}(g)$ even if she is only interested in the dimensions $\Delta_i(g)$. It also means that CFT data involving only scalars will still receive contributions from spinning conformal blocks. For this reason, (5.24) is most readily accessible in $d = 1$.

### 5.2.1 One dimension

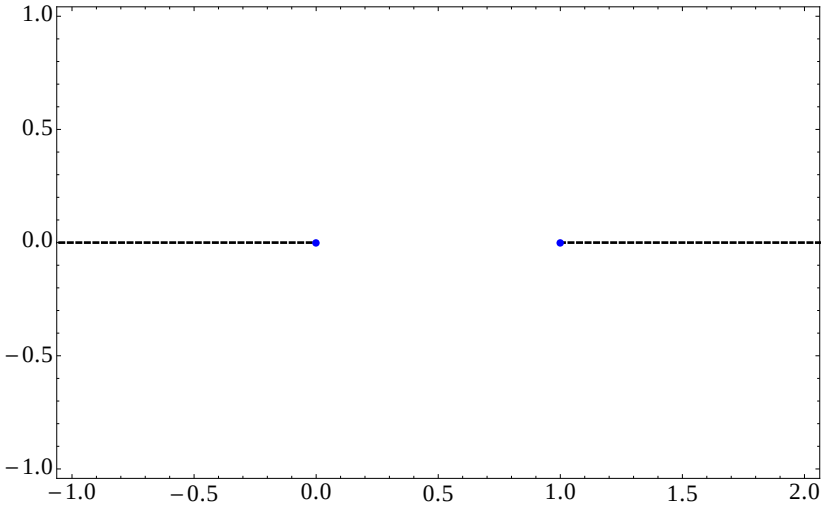


Figure 5.5: Continuing to complex $z$, our blocks have one branch cut from $-\infty$ to 0 and another from 1 to $\infty$. This differs from higher-dimensional blocks which are analytic on $\mathbb{C} \setminus (1, \infty)$. As an example, we may multiply two $SL(2;\mathbb{R})$ blocks to get an $SL(2;\mathbb{C})$ block. This causes the left cut to cancel and the right cut to double.

Unlike in higher dimensions, there is only one cross-ratio on which 1D conformal blocks can depend. We take this to be $z = \frac{x_{12}x_{34}}{x_{13}x_{24}}$. The explicit functions

$$g_{\mathcal{O}}(z) = z^{\Delta}{}_2F_1(\Delta - \Delta_{12}, \Delta + \Delta_{34}, 2\Delta; z) \ , \ x_1 < x_2 < x_3 < x_4 \tag{5.27}$$

were found in [288, 289]. Because the region of validity does not cover all of $\mathcal{R}$, we will need

$$\tilde{g}_{\mathcal{O}}(z) = \left(\frac{z}{z-1}\right)^{\Delta} {}_2F_1\left(\Delta+\Delta_{12}, \Delta+\Delta_{34}, 2\Delta; \frac{z}{z-1}\right) \ , \ x_2 < x_1 < x_3 < x_4 \tag{5.28}$$

as well. Using (5.27) for $z \in (0, \frac{1}{2})$ and (5.28) for $z \in (-1, 0)$ leads to six regions. These correspond to the six possible orderings of $x_1, x_2, x_3$ after fixing $x_4 = \infty$.[7] Putting back kinematic factors, we have

$$\begin{aligned} \frac{\mathrm{d}\lambda_{ijk}}{\mathrm{d}g} &= \sum_{\mathcal{O}} (\lambda_{i\hat{\mathcal{O}}\mathcal{O}}\lambda_{jk\mathcal{O}} I_1 + \lambda_{\hat{\mathcal{O}}i\mathcal{O}}\lambda_{jk\mathcal{O}} I_2) + \text{perms} \\ I_1 &= \int_0^{\frac{1}{2}} \mathrm{d}z \frac{g_{\mathcal{O}}(z)}{z^{\Delta_i+1}} \\ I_2 &= \int_{-1}^{0} \mathrm{d}z \frac{\tilde{g}_{\mathcal{O}}(z)(1-z)^{\Delta_k-\Delta_j}}{(-z)^{\Delta_i+1}} \ . \end{aligned} \tag{5.29}$$

A straightforward calculation yields

$$\begin{aligned} I_1 &= \frac{z^{\Delta-\Delta_i}}{\Delta-\Delta_i} {}_2F_1(\Delta-\Delta_i, \Delta+\Delta_j-\Delta_k, 2\Delta, z)\Big|_0^{\frac{1}{2}} \\ &\to \frac{2^{\Delta_i-\Delta}}{\Delta-\Delta_i} {}_2F_1\left(\Delta-\Delta_i, \Delta+\Delta_j-\Delta_k, 2\Delta, \frac{1}{2}\right) \end{aligned} \tag{5.30}$$

where we have dropped finitely many terms in the last step. This amounts to renormalization as the negative powers of $z$ are precisely the divergences from $\Delta < \Delta_i$ operators in $\mathcal{O}_i \times \hat{\mathcal{O}}$. These are implicitly assumed to be subtracted in the naive integrals (5.29).

To proceed further, we will need some identities, namely the two Pfaff transformations which combine to give an Euler transformation.

$$\begin{aligned} {}_2F_1(a,b,c,z) &= (1-z)^{-a} {}_2F_1\left(a, c-b, c; \frac{z}{z-1}\right) \\ &= (1-z)^{-b} {}_2F_1\left(c-a, b, c; \frac{z}{z-1}\right) \\ &= (1-z)^{c-a-b} {}_2F_1(c-a, c-b, c; z) \end{aligned} \tag{5.31}$$

[7] This phenomenon of the s-channel splitting into two pieces occurs because there is no continuous way to move one operator around another. One consequence of this is that only cyclic permutations of $(i,j,k)$ leave $\lambda_{ijk}$ invariant [116].

Using these on the second integral,

$$I_2 = \int_{-1}^{0} \mathrm{d}z (-z)^{\Delta-\Delta_i-1} {}_2F_1(\Delta-\Delta_i+1, \Delta+\Delta_j-\Delta_k, 2\Delta; z) \,. \tag{5.32}$$

We now renormalize and use a Pfaff transformation to send the argument $-1$ back to $\frac{1}{2}$.

$$I_2 \to \frac{2^{\Delta_i-\Delta}}{\Delta-\Delta_i} {}_2F_1\left(\Delta-\Delta_i, \Delta-\Delta_j+\Delta_k, 2\Delta; \frac{1}{2}\right) \tag{5.33}$$

We might have expected this form because the switch $(x_1, \Delta_1) \leftrightarrow (x_2, \Delta_2)$ is the same as $(x_3, \Delta_3) \leftrightarrow (x_4, \Delta_4)$. We arrive at our full coupled system by permuting labels in the results above.

$$\begin{aligned}
\frac{\mathrm{d}\Delta_i}{\mathrm{d}g} &= -2\lambda_{ii\hat{\mathcal{O}}} \\
\frac{\mathrm{d}\lambda_{ijk}}{\mathrm{d}g} &= \sum_{\mathcal{O}} \frac{2^{\Delta_i-\Delta}}{\Delta-\Delta_i}\left[\lambda_{i\hat{\mathcal{O}}\mathcal{O}}\lambda_{jk\mathcal{O}} {}_2F_1\left(\begin{matrix}\Delta-\Delta_i, \Delta+\Delta_{jk} \\ 2\Delta\end{matrix}; \frac{1}{2}\right) + \lambda_{\hat{\mathcal{O}}i\mathcal{O}}\lambda_{jk\mathcal{O}} {}_2F_1\left(\begin{matrix}\Delta-\Delta_i, \Delta+\Delta_{kj} \\ 2\Delta\end{matrix}; \frac{1}{2}\right)\right] \\
&\quad + \sum_{\mathcal{O}} \frac{2^{\Delta_j-\Delta}}{\Delta-\Delta_j}\left[\lambda_{j\hat{\mathcal{O}}\mathcal{O}}\lambda_{ik\mathcal{O}} {}_2F_1\left(\begin{matrix}\Delta-\Delta_j, \Delta+\Delta_{ik} \\ 2\Delta\end{matrix}; \frac{1}{2}\right) + \lambda_{\hat{\mathcal{O}}j\mathcal{O}}\lambda_{ik\mathcal{O}} {}_2F_1\left(\begin{matrix}\Delta-\Delta_j, \Delta+\Delta_{ki} \\ 2\Delta\end{matrix}; \frac{1}{2}\right)\right] \\
&\quad + \sum_{\mathcal{O}} \frac{2^{\Delta_k-\Delta}}{\Delta-\Delta_k}\left[\lambda_{k\hat{\mathcal{O}}\mathcal{O}}\lambda_{ij\mathcal{O}} {}_2F_1\left(\begin{matrix}\Delta-\Delta_k, \Delta+\Delta_{ij} \\ 2\Delta\end{matrix}; \frac{1}{2}\right) + \lambda_{\hat{\mathcal{O}}k\mathcal{O}}\lambda_{ij\mathcal{O}} {}_2F_1\left(\begin{matrix}\Delta-\Delta_k, \Delta+\Delta_{ji} \\ 2\Delta\end{matrix}; \frac{1}{2}\right)\right]
\end{aligned} \tag{5.34}$$

When $\Delta = \Delta_i$ is exchanged, it is helpful to use the formula

$$\frac{\partial}{\partial\gamma} 2^{-\gamma} {}_2F_1\left(\begin{matrix}\gamma, \Delta+\Delta_{jk} \\ 2\Delta\end{matrix}; \frac{1}{2}\right)\Bigg|_{\gamma=0} = -\log(2) + \frac{\Delta+\Delta_{jk}}{4\Delta} {}_3F_2\left(\begin{matrix}1, 1, \Delta+\Delta_{jk}+1 \\ 2, 2\Delta+1\end{matrix}; \frac{1}{2}\right) \,. \tag{5.35}$$

There are two pertinent comments to be made about these equations. The first is that, as with the sum rule, we have made a choice for how to remove power-law divergences associated with individual conformal blocks. Our previous discussion, regarding Figure 5.3 and Figure 5.4, is therefore applicable to the ODE system as well. We could, in principle, find other expressions to replace (5.34) that are just as correct. The predictions of these equations would only differ from those of (5.34) if they were used to evolve an initial condition that did not correspond to a CFT with an exactly marginal coupling.

The second is that we have not yet assumed invariance under parity. As there is no other dimension, we could just as well call it time-reversal. In a 1D parity-violating theory, it is often said that the dynamical part of the four-point correlator is not only a function of the cross-ratio $z$ [290]. This means that even for identical operators, $\langle \mathcal{O}(x_1)\mathcal{O}(x_2)\mathcal{O}(x_3)\mathcal{O}(x_4)\rangle$

with the points sent to $(0, z, 1, \infty)$ need not have any kinematical relation to the same correlator with the points sent to $(z, 0, 1, \infty)$. In our derivation above, when we wrote each integrand in terms of the position of $\hat{\mathcal{O}}$, we did not assume that these could be glued together in a parity-preserving way. Doing so would amount to a restriction on the OPE coefficients. Consider a partial wave in the expansion of $\langle \mathcal{O}_1(x_1)\mathcal{O}_2(x_2)\mathcal{O}_3(x_3)\mathcal{O}_4(x_4)\rangle$:

$$\lambda_{12\mathcal{O}}\lambda_{34\mathcal{O}} z^{\Delta-\Delta_1-\Delta_2}{}_2F_1(\Delta-\Delta_1+\Delta_2, \Delta+\Delta_3-\Delta_4; 2\Delta; z)\ . \tag{5.36}$$

Under $(12)(34)$, $z$ maps to itself but (5.36) maps to

$$\lambda_{21\mathcal{O}}\lambda_{43\mathcal{O}} z^{\Delta-\Delta_1-\Delta_2}(1-z)^{\Delta_1-\Delta_2-\Delta_3+\Delta_4}{}_2F_1(\Delta+\Delta_1-\Delta_2, \Delta-\Delta_3+\Delta_4; 2\Delta; z)\ . \tag{5.37}$$

which suggests the Euler transformation. We see that (5.37) is only the same function if $\lambda_{ijk}$ and $\lambda_{jik}$ differ at most by a sign. More generally, parity-preserving four-point functions must be invariant under $\{(), (12)(34), (13)(24), (14)(23)\} = \mathbb{Z}_2 \times \mathbb{Z}_2$ — the set of transformations that stabilize $z$. This reflects the fact that there are 6 channels, but 24 configurations of four points. A non-trivial check is that, when OPE coefficients are restricted as above, our differential equation for $\lambda_{ijk}$ has the $S_4/(\mathbb{Z}_2 \times \mathbb{Z}_2) = S_3$ symmetry befitting three operators that can couple to the parity-even $\hat{\mathcal{O}}$. Parity symmetry is common in defect CFTs, for example, because it is inherited from the parent theory.

### 5.2.2 Avoided level crossing

Even if one does not have a concrete model of a non-trivial conformal manifold in one dimension, a general prediction that can be distilled from (5.34) is a strong preference against nearly degenerate operators. Consider two primaries $\mathcal{O}_1$ and $\mathcal{O}_2$ where, for some value of the coupling $g_0$, $\Delta_1 - \Delta_2$ is parametrically small. We take it to be positive without loss of generality. By the von Neumann-Wigner non-crossing rule, we expect it to stay positive for $g > g_0$. For a demonstration of this occuring in maximally supersymmetric Yang-Mills theory, see [33]. Also, [291] discussed this in the context of the $\frac{1}{N}$ expansion where the "distance of closest approach" is determined by the mixing matrix between planar and non-

planar eigenstates. Taking the second derivative of one of the dimensions,

$$\begin{aligned}\frac{\mathrm{d}^2\Delta_1}{\mathrm{d}g^2} &= -2\frac{\mathrm{d}\lambda_{11\hat{\mathcal{O}}}}{\mathrm{d}g}\\ &= -4\sum_{\mathcal{O}}\frac{2^{\Delta_1-\Delta}}{\Delta-\Delta_1}\lambda^2_{1\hat{\mathcal{O}}\mathcal{O}^2}F_1\left(\begin{array}{c}\Delta-\Delta_1,\Delta+\Delta_1-1\\ 2\Delta\end{array};\frac{1}{2}\right)\\ &-4\sum_{\mathcal{O}}\frac{2^{\Delta_1-\Delta}}{\Delta-\Delta_1}\lambda_{\hat{\mathcal{O}}1\mathcal{O}}\lambda_{1\hat{\mathcal{O}}\mathcal{O}^2}F_1\left(\begin{array}{c}\Delta-\Delta_1,\Delta-\Delta_1+1\\ 2\Delta\end{array};\frac{1}{2}\right)\\ &-4\sum_{\mathcal{O}}\frac{2^{1-\Delta}}{\Delta-1}\lambda_{\hat{\mathcal{O}}\hat{\mathcal{O}}\mathcal{O}}\lambda_{11\mathcal{O}_2}F_1\left(\begin{array}{c}\Delta-1,\Delta\\ 2\Delta\end{array};\frac{1}{2}\right)\,. \end{aligned}\tag{5.38}$$

Our ability to quickly take the second derivative is only guaranteed because we are considering a manifold that has only one marginal operator and therefore a flat connection [272, 273]. Three values of $\Delta$ lead to small denominators in (5.38) but the only one that can dominate the sum is $\Delta=\Delta_2$. Indeed, $\Delta_1$ and 1 yield divergences whose renormalized versions are $O(1)$ numbers in view of (5.35). Knowing this, we can approximate the differential equation as

$$\begin{aligned}\frac{\mathrm{d}^2\Delta_1}{\mathrm{d}g^2} &\approx 4\frac{\lambda^2_{12\hat{\mathcal{O}}}2^{\Delta_1-\Delta_2}}{\Delta_1-\Delta_2}\left[{}_2F_1\left(\begin{array}{c}-\Delta_{12},\Delta_2+\Delta_1-1\\ 2\Delta_2\end{array};\frac{1}{2}\right)+{}_2F_1\left(\begin{array}{c}-\Delta_{12},\Delta_2-\Delta_1+1\\ 2\Delta_2\end{array};\frac{1}{2}\right)\right]\\ &\approx \frac{8\lambda^2_{12\hat{\mathcal{O}}}}{\Delta_1-\Delta_2}\,. \end{aligned}\tag{5.39}$$

In the first step, we have assumed that our theory has a parity symmetry. Since operators with different quantum numbers are allowed to cross, we are interested in $\mathcal{O}_1$ and $\mathcal{O}_2$ which have the same parity. This means that $\lambda_{11\hat{\mathcal{O}}}$, $\lambda_{22\hat{\mathcal{O}}}$ and $\lambda_{12\hat{\mathcal{O}}}$ all exist and are independent of the label ordering. After switching the labels to find $\frac{\mathrm{d}^2\Delta_2}{\mathrm{d}g^2}$, the differential equation for $y\equiv\Delta_1-\Delta_2$ is

$$\frac{\mathrm{d}^2 y}{\mathrm{d}g^2}=\frac{16\lambda^2_{12\hat{\mathcal{O}}}}{y}\,.\tag{5.40}$$

It is not necessarily true that $\lambda_{12\hat{\mathcal{O}}}$ is slowly varrying compared to $y$. Therefore we will compute its variation by going back to (5.34).

$$\begin{aligned}\frac{\mathrm{d}\lambda_{12\hat{\mathcal{O}}}}{\mathrm{d}g} &\approx \frac{2}{\Delta_2-\Delta_1}\lambda_{12\hat{\mathcal{O}}}\lambda_{22\hat{\mathcal{O}}}+\frac{2}{\Delta_1-\Delta_2}\lambda_{12\hat{\mathcal{O}}}\lambda_{11\hat{\mathcal{O}}}\\ &= \frac{2\lambda_{12\hat{\mathcal{O}}}}{y}(\lambda_{11\hat{\mathcal{O}}}-\lambda_{22\hat{\mathcal{O}}})\\ &= -\frac{\lambda_{12\hat{\mathcal{O}}}}{y}\frac{\mathrm{d}y}{\mathrm{d}g}\,. \end{aligned}\tag{5.41}$$

Solving this separable equation yields

$$\frac{\mathrm{d}^2 y}{\mathrm{d}g^2} = \frac{2c}{y^3} \tag{5.42}$$

where $c$ is a positive constant. The right-hand side is $-\frac{\mathrm{d}}{\mathrm{d}y}U(y)$ for the potential function $U(y) = \frac{c}{y^2}$. Having turned this into a 1D classical scattering problem, we see that $U(y)$ is always a repulsive potential. In particular, $U(0) = +\infty$ means that a shrinking $y$ will always reach a turning point.

This argument appears not to rely on one dimension. The crucial feature we have used is that $\frac{\mathrm{d}\lambda_{ijk}}{\mathrm{d}g}$ contains a $\frac{1}{\Delta-\Delta_i}$ singularity for each dimension $\Delta$ primary in $\mathcal{O}_i \times \hat{\mathcal{O}}$. To see this appearing more generally, consider the regulated integral

$$\int_{B(r)} \mathrm{d}^d x \left\langle \mathcal{O}_i(0)\hat{\mathcal{O}}(x)\mathcal{O}_j(\hat{e})\mathcal{O}_k(\infty)\right\rangle \tag{5.43}$$

where $r \ll 1$. Even if we cannot evaluate (5.43) exactly, we know that one term of it will come from inserting the pair of states $|\mathcal{O}\rangle\langle\mathcal{O}|$. It can then be argued that operators with $\Delta \to \Delta_i$ will dominate over all other choices. In the all-scalar case for instance, the $\mathcal{O}$ term of the integral becomes

$$\int_{B(r)} \mathrm{d}^d x \frac{\lambda_{i\hat{\mathcal{O}}\mathcal{O}}\lambda_{jk\mathcal{O}}}{|x|^{d+\Delta_i-\Delta}} \tag{5.44}$$

which leads to $\frac{r^{\Delta-\Delta_i}}{\Delta-\Delta_i}$. Depending on the sign of $\Delta-\Delta_i$, the boundary term is either manifestly zero, or zero as a result of our regulating procedure.

Besides demonstrating agreement with [291], lack of level crossing may be seen as a consistency check of the equations we have been using. If operator pairs with $\Delta_1 \approx \Delta_2$ could occur throughout the conformal manifold, the differential equation for $\lambda_{11\hat{\mathcal{O}}}$ would contain terms that are large — possibly large enough to combat the suppression by powers of $g$ in conformal perturbation theory. From this point of view, it is encouraging that our system abhors the regime $y \ll 1$.

### 5.2.3 The compact free boson

Despite our success in the previous calculation, the question of whether evolution equations can be used to solve a conformal manifold is still open. We are therefore asking whether (5.24) contains a full description of the operator algebra, including non-perturbative dynamics. As a first indication that this is plausible, we will show that the compact free boson satisfies the desired ODE system exactly.

If the free boson theory is written in terms of a fundamental field $\phi(z,\bar{z})$, we may use the equation of motion to split it into holomorphic and anti-holomorphic parts; $\phi(z,\bar{z}) = X(z) + \bar{X}(\bar{z})$. When the fields take values on a circle of radius $r$, this leads to the on-shell

action

$$S = -\frac{1}{\pi}\int \mathrm{d}z\mathrm{d}\bar{z}\;\partial X\bar{\partial}\bar{X} \quad , \quad X \sim X + 2\pi r\;. \tag{5.45}$$

The prefactor is chosen so that the $U(1)$ current, $J(z) \equiv i\partial X(z)$, is unit normalized. We have already seen that the marginal operator in this model is $\hat{\mathcal{O}} = J\bar{J}$. Since this is proportional to the Lagrangian density,

$$S + \delta g \int \mathrm{d}z\mathrm{d}\bar{z}\;\hat{\mathcal{O}} = (1 + \pi\delta g)S\;. \tag{5.46}$$

To get back to the original action, we must rescale $X$ and $\bar{X}$ by $\sqrt{1+\pi\delta g}$. This shifts the compactification radius by $\delta r = \frac{1}{2}\pi r\delta g$, allowing us to solve

$$r = r_0 e^{\frac{\pi}{2}g}\;. \tag{5.47}$$

It is enough to check that (5.24) is satisfied for the $U(1)$ primaries. These are the $V_{q,\bar{q}}(z,\bar{z}) =: e^{i\sqrt{2}qX(z)}e^{i\sqrt{2}\bar{q}\bar{X}(\bar{z})}:$ vertex operators. By periodicity and single-valuedness, the charges are specified by two integers [292]

$$(\sqrt{2}q, \sqrt{2}\bar{q}) \in \Gamma = \left\{ \left(\frac{n}{r} + \frac{mr}{2}, \frac{n}{r} - \frac{mr}{2}\right) \;\middle|\; m,n \in \mathbb{Z} \right\}\;. \tag{5.48}$$

Combining (5.47) with (5.48), we find

$$\begin{aligned} \frac{\mathrm{d}\Delta_{(m,n)}}{\mathrm{d}g} &= \frac{\mathrm{d}}{\mathrm{d}g}\left(q^2 + \bar{q}^2\right) \\ &= -\pi\left(\frac{n^2}{r^2} - \frac{m^2r^2}{4}\right)\;. \end{aligned} \tag{5.49}$$

To see if our equations predict this, we must evaluate $\left\langle \hat{\mathcal{O}}(z,\bar{z})V_{(m,n)}(z_1,\bar{z}_1)V^*_{(m,n)}(z_2,\bar{z}_2)\right\rangle$. This is simple because the Virasoro primary $\hat{\mathcal{O}}$ is in the identity multiplet of $U(1)$. Using the fact that $J = a_{-1}I$, the Ward identities

$$\begin{aligned} J(z)V_{q,\bar{q}}(w,\bar{w}) &= \frac{q}{z-w}V_{q,\bar{q}}(w,\bar{w}) + \ldots \\ \bar{J}(\bar{z})V_{q,\bar{q}}(w,\bar{w}) &= \frac{\bar{q}}{\bar{z}-\bar{w}}V_{q,\bar{q}}(w,\bar{w}) + \ldots \end{aligned} \tag{5.50}$$

are easy to derive. This leads to the OPE coefficient

$$\begin{aligned}\lambda_{(m,n)(m,n)\hat{\mathcal{O}}} &= q\bar{q} \\ &= \frac{1}{2}\left(\frac{n^2}{r^2} - \frac{m^2 r^2}{4}\right) .\end{aligned} \tag{5.51}$$

The first equation in (5.24) is therefore verified.

Turning to the second equation, the left-hand side vanishes by the well known OPE of vertex operators:

$$\lambda_{(m_1,n_1)(m_2,n_2)(m_3,n_3)} = \delta_{q_1+q_2+q_3,0}\delta_{\bar{q}_1+\bar{q}_2+\bar{q}_3,0} . \tag{5.52}$$

The right-hand side, while daunting for a general 2D theory, may be evaluated for the free boson without the conformal block expansion. This is possible because of the Ward identity and the formula

$$\int \mathrm{d}^2 z \frac{1}{z-z_i}\frac{1}{\bar{z}-\bar{z}_j}\bigg|_{\mathrm{reg}} = \begin{cases} 2\pi \log|z_{ij}| & i \neq j \\ 0 & i = j \end{cases} \tag{5.53}$$

understood as a principal value.[8] We now follow the method of [293] to show that a first-order insertion of $\hat{\mathcal{O}}$ produces no shift in the highest-weight OPE coefficients.

$$\begin{aligned} & \int \mathrm{d}^2 z \left\langle J(z)\bar{J}(\bar{z}) V_{q_1,\bar{q}_1}(z_1,\bar{z}_1) V_{q_2,\bar{q}_2}(z_2,\bar{z}_2) V_{q_3,\bar{q}_3}(z_3,\bar{z}_3)\right\rangle \Big|_{\mathrm{reg}} \\ = & \int \mathrm{d}^2 z \left(\frac{q_1}{z-z_1}+\frac{q_2}{z-z_2}+\frac{q_3}{z-z_3}\right)\left(\frac{\bar{q}_1}{\bar{z}-\bar{z}_1}+\frac{\bar{q}_2}{\bar{z}-\bar{z}_2}+\frac{\bar{q}_3}{\bar{z}-\bar{z}_3}\right)\Big|_{\mathrm{reg}} \\ & \langle V_{q_1,\bar{q}_1}(z_1,\bar{z}_1) V_{q_2,\bar{q}_2}(z_2,\bar{z}_2) V_{q_3,\bar{q}_3}(z_3,\bar{z}_3)\rangle \\ = & 2\pi[(q_1\bar{q}_2+q_2\bar{q}_1)\log|z_{12}| - (2q_1\bar{q}_1+q_1\bar{q}_2+q_2\bar{q}_1)\log|z_{13}| - (2q_2\bar{q}_2+q_1\bar{q}_2+q_2\bar{q}_1)\log|z_{23}|] \\ & \langle V_{q_1,\bar{q}_1}(z_1,\bar{z}_1) V_{q_2,\bar{q}_2}(z_2,\bar{z}_2) V_{q_3,\bar{q}_3}(z_3,\bar{z}_3)\rangle \end{aligned} \tag{5.54}$$

In the last step, we have used the fact that $q_3$ is a shorthand for $-(q_1+q_2)$ and similarly for $\bar{q}_3$. This prefactor, with its $\log|z_{ij}|$ terms, is precisely what we would find if we applied $\frac{\mathrm{d}}{\mathrm{d}g}$ to the three-point function and allowed it to act on the charge lattice alone.

The derivation in [293] applies not only to the free boson, but to all WZW models deformed by current-current terms. When the currents are non-abelian, the terms that generate the Cartan subalgebra stay exactly marginal. In other words, the conformal manifold is multi-dimensional. As this is an interesting topic for the future, it is likely that the work done on WZW models can serve as a guide for finding the appropriate generalization of (5.24).

[8] One way to see that (5.53) holds is to check that both sides are Green's functions of the operators $\partial_i\bar{\partial}_i$ and $\partial_j\bar{\partial}_j$.

## 5.3 Proving a bootstrap bound

Some first steps toward using the sum rule (5.8) with asymptotic results were given in [283]. As usual, we separate the identity, which is always present, from the other operators whose dimensions should be constrained.

$$\sum_{\mathcal{O}\neq I}\lambda^2_{\hat{\mathcal{O}}\hat{\mathcal{O}}\mathcal{O}}\int_{\mathcal{R}}\mathrm{d}^d x|x|^{-2d}G_{\mathcal{O}}(u,v)\Big|_{\text{reg}}=-\int_{\mathcal{R}}\mathrm{d}^d x|x|^{-2d}\Big|_{\text{reg}} \tag{5.55}$$

The idea is to cut off the left-hand side at some value $\Delta_*$ and replace the rest of the sum with

$$\Sigma(\Delta_*)\equiv\int_{\mathcal{R}}\mathrm{d}^d x|x|^{-2d}\frac{(2\Delta_*)^{4d}}{\Gamma(4d+1)}|\rho(x\cdot\hat{e}+i|x-(x\cdot\hat{e})\hat{e}|)|^{\Delta_*} \tag{5.56}$$

from (4.66), assuming that the known asymptotics have "kicked-in" by this point. By choosing a $\Delta_*$ which makes $\Sigma(\Delta_*)$ less than the right-hand side of (5.55), we may conclude that at least one $\Delta<\Delta_*$ primary with a positive integrated block must exist in $\hat{\mathcal{O}}\times\hat{\mathcal{O}}$. Setting $d=4$, [283] found that this happens for $\Delta_*\approx 16.3$ in their scheme, suggesting the presence of a spin 0, 4, 8 or 12 operator of lesser dimension.

Although such a bound is non-rigorous, it could potentially be improved by the results of [42]. The problem with this bound in its current state is that even CFTs with *classically* marginal $\hat{\mathcal{O}}$ already obey stronger ones from crossing symmetry and unitarity. Taking $\ell=4$ for example, we already expect $\Delta\leq 12$, saturated by the generalized free field, to come from the numerical bootstrap. Despite the fairly slow convergence compared to Figure 4.13, it is easy to confirm this. A natural next step is to re-derive numerical bounds by inputting (5.55) as a crossing equation in its own right. This means searching for functionals that are positive on $N$ component vectors where the first component is an integrated conformal block and the other $N-1$ components are derivatives of a convolved conformal block.[9] These functionals give rigorous bounds when they exist.

In all dimensions $d\geq 2$, we have found that the bounds arising this way are the same as the ones from the usual numerical bootstrap — imposing the marginality sum rule does nothing.[10] On the other hand, $d=1$ shows drastic improvement. The $\Delta\leq 3$ bound, saturated by the generalized free fermion, comes down to $\Delta\leq 2$ which we may associate with the generalized free boson. It is worth reminding ourselves at this point that (5.8) does not necessarily single out conformal manifolds that are interesting. Although the linear term in

$$S=\int \mathrm{d}x\phi\partial^{-1}\phi+g\phi \tag{5.57}$$

[9] This requires some massaging for `SDPB` which accepts rational functions multiplied by $r_*^\Delta$ where $r_*=3-2\sqrt{2}$. After taking the appropriate integral of a conformal block, we also have $R_*^\Delta$ where $R_*=2-\sqrt{3}$. This is solved by writing $R_*^\Delta=r_*^\Delta\sum_{n=0}^\infty\frac{1}{n!}\left(\Delta\log\frac{R_*}{r_*}\right)^n$ and cutting off the sum.

[10] We should not assume that this will still be the case with superconformal blocks.

is simply a field redefinition, it counts as a marginal operator with a vanishing beta function according to everything we have described so far. As such, the above setup cannot hope to do better than (5.57) which has $\Delta_\phi = 1$ and $\Delta_{\phi^2} = 2$. The rest of this section will explain why (5.57) is not just allowed but extremal.

### 5.3.1 Polyakov blocks

Much of the work will be done if we can switch to a basis which cancels the finite part from the regulated integral of the identity block. The main candidates we are aware of are exchange Witten diagrams. Since these are manifestly crossing symmetric, it is clear that the counterterm subtractions, shown in Figure 5.3, do not have to be split among infinitely many multiplets. In particular, the identity block is

$$W_0(z) = 1 + \left(\frac{1}{1-z}\right)^{2\Delta_\phi} + z^{2\Delta_\phi} , \tag{5.58}$$

which vanishes after we multiply by the kinematic prefactor and subtract the disconnected four-point function. The validity of (5.58) is easy to see from the $AdS_2$ perspective, where the diagram is built solely from boundary-to-boundary propagators. As we will see, expressions become quite non-trivial once the bulk is involved.

This approach has a long and unfinished history with crossing symmetric blocks first being proposed by Polyakov in [10]. It was only pointed out in later reviews [294, 295] that Polyakov and Witten had both discovered very similar functions. Mellin space versions of these functions were successfully used in [143, 296, 297] to predict $O(\varepsilon^3)$ anomalous dimensions and OPE coefficients of all broken currents in the Wilson-Fisher fixed-point. The central claim made in these papers is that a certain set of crossing symmetric $\tilde{W}_{\Delta,\ell}$ functions is not just a basis, but a basis that can be used with the same OPE coefficients.

$$G(z,\bar{z}) = \sum_{\mathcal{O}} \lambda_{12\mathcal{O}}\lambda_{34\mathcal{O}} g_{\mathcal{O}}^{\Delta_{12},\Delta_{34}}(z,\bar{z}) \sum_{\mathcal{O}} \lambda_{12\mathcal{O}}\lambda_{34\mathcal{O}} \tilde{W}_{\mathcal{O}}(z,\bar{z}) \tag{5.59}$$

The problem of constructing these functions in $d \geq 2$ is still open and it is remarkable that such progress in the epsilon expansion was possible with functions that violate (5.59) at some high order [298]. Indeed, the Witten blocks defined in AdS, the blocks used in [10, 143, 294–297], and the true "Polyakov blocks" satisfying (5.59) are all different. When expressed in Mellin space, they differ in their entire part which is a polynomial.[11] What this means in

[11] The fact that there is no canonical vertex for coupling spinning fields in a Witten diagram is also sometimes called a polynomial ambiguity. The ambiguity for how a Witten diagram needs to be modified (in any one of these conventions) is completely separate and present for scalar fields as well.

position space is that we may take

$$W_\Delta(z) = \sum_{j=0}^{\infty} \left[\alpha_j(\Delta) g_{2\Delta_\phi+2j}(z) + \beta_j(\Delta)\partial g_{2\Delta_\phi+2j}(z)\right] \tag{5.60}$$

and shift the double-twist coefficients arbitrarily as long as these shifts are mild enough so as not to introduce a branch cut. Here $\partial g_\Delta(z)$ denotes differentiation with respect to $\Delta$.

We know the values of $\alpha(0)$ and $\beta(0)$ from the solution of the generalized free boson. However, the special thing about 1D CFT is that the known analytic functionals dual to the crossing equation allow us to solve for $\alpha(\Delta)$ and $\beta(\Delta)$ in full generality [118]. The orthogonality relations

$$\begin{aligned}
\omega_j'\left[F^-_{2\Delta_\phi+2k}\right] &= \delta_{jk} \text{ for } j,k \geq 1 \quad , \quad \omega_j\left[F^-_{2\Delta_\phi+2k}\right] = 0 \text{ for } j \geq 1, k \geq 0 \\
\hat{\omega}_j\left[F^-_{2\Delta_\phi+2k}\right] &= \delta_{jk} \text{ for } j,k \geq 0 \quad , \quad \hat{\omega}_j'\left[F^-_{2\Delta_\phi+2k}\right] = 0 \text{ for } j \geq 0, k \geq 1
\end{aligned} \tag{5.61}$$

make it clear that

$$\begin{aligned}
\alpha_j(\Delta) &= -\hat{\omega}_j\left[F^-_\Delta\right] - \beta_1(\Delta)\hat{\omega}_j'\left[F^-_{2\Delta_\phi}\right] \text{ for } j \geq 0 \\
\beta_j(\Delta) &= -\omega_j\left[F^-_\Delta\right] - \beta_1(\Delta)\omega_j'\left[F^-_{2\Delta_\phi}\right] \text{ for } j \geq 1\,.
\end{aligned} \tag{5.62}$$

As shown in [118], we must subtract the last term in order to make the double-twist blocks cancel out when $W_\Delta(z)$ is summed over a physical spectrum. In other words,

$$\begin{aligned}
\tilde{W}_\Delta(z) &= W_\Delta(z) - \beta_1(\Delta)\partial g_{2\Delta_\phi}(z) \\
&+ \beta_1(\Delta)\sum_{j=1}^{\infty}\omega_j'\left[F^-_{2\Delta_\phi}\right]\partial g_{2\Delta_\phi+2j}(z) + \beta_1(\Delta)\sum_{j=0}^{\infty}\hat{\omega}_j'\left[F^-_{2\Delta_\phi}\right] g_{2\Delta_\phi+2j}(z) \\
&= g_\Delta(z) - \sum_{j=0}^{\infty}\hat{\omega}_j\left[F^-_\Delta\right] g_{2\Delta_\phi+2j}(z) - \sum_{j=1}^{\infty}\omega_j\left[F^-_\Delta\right]\partial g_{2\Delta_\phi+2j}(z)
\end{aligned} \tag{5.63}$$

is a valid Polyakov block. Completeness of (5.61) guarantees crossing symmetry while the swapping property [120] establishes (5.59).

We are now interested in the sum rule for 1D Polyakov blocks with $\Delta_\phi = 1$.

$$\sum_{\mathcal{O}} \lambda^2_{\hat{\mathcal{O}}\hat{\mathcal{O}}\mathcal{O}} \int_{\mathcal{R}} \mathrm{d}x |x|^{-2} \tilde{W}_{\mathcal{O}}(z)\Big|_{\text{reg}} = 0 \tag{5.64}$$

Before specifying the action of each functional, the important properties are determined by (5.61) and the behaviour in Figure 5.2. By inspection, the general term in (5.64) has

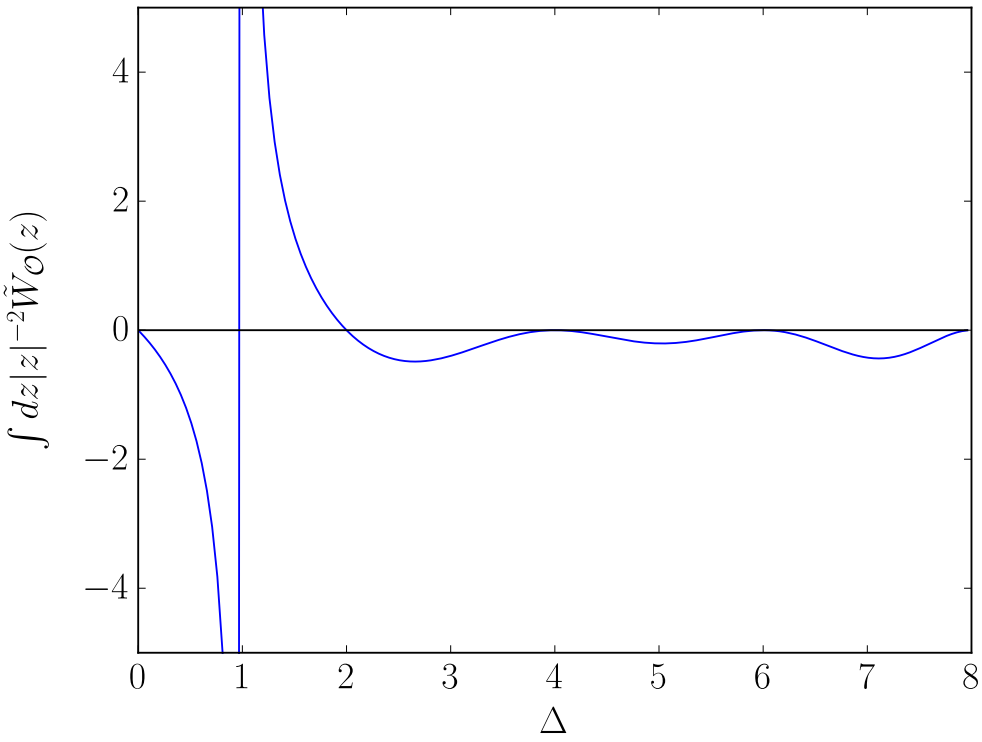


Figure 5.6: The regulated integral of a Polyakov block as a function of $\Delta$ for $\Delta_\phi = 1$. Due to the zeros at double-twist dimensions, which are mostly second-order, this function has exactly the same form as the action of an extremal functional for the gap $\Delta = 2$. It would be interesting to check that the numerical bootstrap is returning this functional multiplied by $-1$.

zeros at all $\Delta$ values that are even integers — the spectrum of the generalized free boson. Moreover, the only first-order zero, apart from the identity, occurs at $\Delta = 2$ — the gap picked out by the numerics. The proof of this bound now follows the logic of the extremal functional method which states that any perturbation to this spectrum with a larger gap would necessarily produce a functional which turns the sum rule into a contradiction. To fully convince ourselves, we should plot the integrated Polyakov block, which we have done in Figure 5.6. This has been done by evaluating the integral

$$\omega\left[F_\Delta^-\right] = 2\sin^2\left[\frac{\pi}{2}(\Delta - 2\Delta_\phi)\right]\int_0^1 \mathrm{d}z g(z) z^{-2\Delta_\phi} g_\Delta^{0,0}(z) \tag{5.65}$$

using techniques similar to those in [299]. The kernel for the first type of functional satisfying

(5.61) is given by

$$g_j(z) = -\frac{2\Gamma(2j+2)^2}{\pi^2\Gamma(4j+3)}\left[P_{2j+1}(1-2z) + P_{2j+1}\left(\frac{z-2}{z}\right) - P_1(1-2z) - P_1\left(\frac{z-2}{z}\right)\right]. \tag{5.66}$$

The $P_1$ Legendre polynomials have been subtracted in order to satisfy swapping. The second type of kernel is more involved but it can again be computed using the methods of [117].

$$\begin{aligned}\hat{g}_j(z) &= \frac{2\Gamma(2j+2)^2}{\pi^2\Gamma(4j+3)}\left[\hat{p}_{2j+2}(z) + \hat{p}_{2j+2}\left(\frac{1}{z}\right) - \frac{\Gamma(2j+2)^2}{\Gamma(4j+4)}g^{0,0}_{2j+2}(1-z)\right] \\ &+ \left[H(2j+1) - H\left(2j+\frac{1}{2}\right) - 2\log(2)\right]g_j(z)\end{aligned} \tag{5.67}$$

Here, we have defined

$$\hat{p}_n(z) = \sum_{k=0}^{n-1}\frac{(n)_k(1-n)_k}{(k!)^2}\left[2H(k) - 2H(n+k-1) - \log(z)\right]z^k \tag{5.68}$$

with $H(x)$ denoting the harmonic number.

### 5.3.2 Superconformal line defects

Our previous use of Polyakov blocks was motivated by the fact that, in such a basis, the identity block yields a vanishing contribution to the two-loop beta function. An immediate consequence was that this also holds for any operator with a double-twist scaling dimension. These operators clearly make an appearance in the free theory but it is also possible to see them in interacting theories with supersymmetry. Protected operators that are fixed at these dimensions occur in superconformal line defects that have exactly marginal operators [300]. The conformal manifolds obtained in this way are again trivial, in the sense that the scaling dimensions and OPE coefficients are constants, but it is no longer possible to solve for these constants explicitly.

We will discuss the theory in [301] which can be obtained from a Wilson-Maldacena line of $\mathcal{N} = 4$ super Yang-Mills. Its integrability properties were subsequently studied in [302–304]. This theory has $\mathfrak{osp}(4^*|4)$ symmetry whose bosonic part consists of the $\mathfrak{so}(2,1)$ conformal group and an $\mathfrak{so}(3) \times \mathfrak{sp}(4)$ R-symmetry. The $\mathfrak{so}(3)$ describes the three *spatial* directions transverse to the line, while the remaining R-symmetry is what gives rise to marginal operators. It can be seen as a remnant of the $\mathfrak{su}(4) \simeq \mathfrak{so}(6)$ R-symmetry of the parent theory. Once a scalar coupling to the line has been chosen, there is an $\mathfrak{so}(5) \simeq \mathfrak{sp}(4)$ worth of *internal* directions which are transverse. The multiplet of short primaries that deform this internal space is exactly marginal. The displacement operator, associated with deformations in the physical space, is a descendant at level one.

OPEs with a universal form were studied from the abstract point of view in [238] which described three important types of exchanged multiplets.

1. Short operators $\mathcal{B}_k$ with dimension $k$ and R-symmetry Dynkin labels of $[0,k]$.
2. Semi-short operators $\mathcal{C}_{[a,b]}$ with dimension $a+b$ and R-symmetry Dynkin labels of $[a,b]$.
3. Long operators that are constrained to be $\mathfrak{so}(3)$ singlets but otherwise unprotected.

The displacement OPE is $\mathcal{B}_1 \times \mathcal{B}_1$ — it contains $\mathcal{B}_2$, $\mathcal{C}_{[2,0]}$ and infinitely many long operators with $\Delta \geq 1$. Notice that $\Delta_{\mathcal{B}_2} = 2\Delta_{\mathcal{B}_1}$ which means that the short exchanged primary is a double-twist. We are therefore well on our way towards showing that the beta function is insensitive to this operator. If the superconformal block for $\mathcal{B}_1$ contains only conformal blocks with $2\Delta_{\mathcal{B}_1}+2n$ and not $2\Delta_{\mathcal{B}_1}+2n+1$, regulated integrals will vanish once we promote them to Polyakov blocks.

To see that this is the case, we may again follow [238] and contract the $\mathcal{B}_1$ operators with $y_i$ polarization vectors to avoid writing indices in the fundamental of $\mathfrak{so}(5)$. The four-point function is then expressed in terms of three cross-ratios

$$\begin{aligned}
&\langle \mathcal{B}_1\mathcal{B}_1\mathcal{B}_1\mathcal{B}_1\rangle = \frac{y_{12}^2 y_{34}^2}{x_{12}^2 x_{34}^2}\mathcal{G}(\chi,\zeta_1,\zeta_2) \\
&\chi = \frac{x_{12}x_{34}}{x_{13}x_{24}}\ ,\ \zeta_1\zeta_2 = \frac{y_{12}^2 y_{34}^2}{y_{13}^2 y_{24}^2}\ ,\ (1-\zeta_1)(1-\zeta_2) = \frac{y_{14}^2 y_{23}^2}{y_{13}^2 y_{24}^2}\ .
\end{aligned} \tag{5.69}$$

The Ward identity that must be imposed on $\mathcal{G}(\chi,\zeta_1,\zeta_2)$ is

$$\left(\frac{\partial\mathcal{G}}{\partial\zeta_1}+\frac{1}{2}\frac{\partial\mathcal{G}}{\partial\chi}\right)\Big|_{\zeta_1=\chi} = \left(\frac{\partial\mathcal{G}}{\partial\zeta_2}+\frac{1}{2}\frac{\partial\mathcal{G}}{\partial\chi}\right)\Big|_{\zeta_2=\chi} = 0 \tag{5.70}$$

and its solutions are identified with the superconformal blocks. There is a special solution with only three terms in its $\mathfrak{sl}(2)$ block expansion and the right asymptotics to correspond to $\mathcal{B}_2$. Stripping off the distances in position space, we find

$$\begin{aligned}
y_{12}^2 y_{34}^2 \mathcal{G}_{\mathcal{B}_2}(\chi,\zeta_1,\zeta_2) &= y_{12}^2 y_{34}^2\left[\frac{1}{10}\left(1-\frac{1}{\zeta_1}-\frac{1}{\zeta_2}\right)g_3(\chi)+\frac{3}{350}g_4(\chi)\right. \\
&\qquad \left.+\left(\frac{3}{10}-\frac{1}{2\zeta_1}-\frac{1}{2\zeta_2}+\frac{1}{\zeta_1\zeta_2}\right)g_2(\chi)\right] \\
&= \frac{1}{10}\left[-2y_{12}^2y_{34}^2+5y_{13}^2y_{24}^2+5y_{14}^2y_{23}^2\right]g_2(\chi) \\
&+ \frac{1}{10}\left[y_{14}^2y_{23}^2-y_{13}^2y_{24}^2\right]g_3(\chi)+\frac{3}{350}y_{12}^2y_{34}^2g_4(\chi)\ .
\end{aligned} \tag{5.71}$$

We now see that the $g_3(\chi)$ block is absent when the $y_i$ polarization vectors are all the same. This is certainly the case when we focus on the beta function of a single linear combination of

the five marginal operators. Different $y_i$ vectors, leading to the appearance of $g_3(\chi)$, appear in mixed correlators that are relevant for anomalous dimensions.

So far, we have only discussed $\mathfrak{osp}(4^*|4)$ as the blocks in the displacement OPE have already been derived. Recently, a similar bootstrap problem was setup for $\mathfrak{osp}(4^*|2)$, corresponding to a line defect in an $\mathcal{N} = 2$ SCFT [305]. It would be interesting to repeat this analysis for the six other instances of a 1D superconformal algebra, one of which contains a free parameter [306, 307].

# Chapter 6

# Conclusion

We have uncovered new facts about the space of conformal field theories with a focus on continuous families. Our results have relied heavily on conformal perturbation theory. In one case it was combined with numerical bootstrap data in order to estimate critical exponents. In another, it was used as a stepping stone to what is very likely a non-perturbative result. Overall we are excited about conformal perturbation theory and its ability to translate a wide range of conjectures into testable statements about CFT data.

The theory that has been studied most thoroughly in this thesis is the long-range Ising model (LRI). Our compelling picture for understanding the crossover has taught us that it involves not only the short-range Ising model (SRI) but a decoupled Gaussian field as well. Flowing away from the decoupled limit, we advanced the quantitative study of LRI critical exponents. An infrared duality between two flows, which we dubbed $\phi^4$ and $\sigma\chi$, was what made this progress possible. Other infrared dualities are expected to arise by the same basic mechanism — they lead to a non-renormalization theorem called the *shadow relation*, summarized in our case by $\Delta_\sigma + \Delta_\chi = d$.

After developing our duality, we saw that the shadow relation leads to a wealth of information about OPE coefficients and infinitely many protected double-trace operators. The result provides a tantalizing analogy with the superconformal bootstrap wherein conformal blocks can be packaged together in known ways. Leveraging this fact and varrying $\Delta_T$, the dimension of the leading spin-2 operator, we produced a number of rigorous bounds on the 3D LRI from a six correlator system. The allowed regions contain lobes with distinguished points near the edge that exhibit various properties expected of the LRI. These can be located with the help of the extremal functional method [90, 242].

## 6.1 Future directions

For interested readers, we list open problems relating to both the duality and the bootstrap exploration of the LRI.

- It would be interesting to establish a sharper connection with nonlocal theories that live on a boundary. When the parent theory is defined in a fixed AdS background, the boundary theory is necessarily conformal. A holographic dual of the long-range Ising model would be most welcome.

- A description of the crossover for one dimension was neglected in this work. The appearance of second-order phase transitions in one dimension was in fact one of the original motivations for studying the LRI [186]. The ability to apply our result here is doubtful since the order parameter for the "1D critical Ising model" should formally be treated as a $\Delta_\sigma = 0$ field yielding a $\sigma\chi$ deformation that does nothing. The situation could perhaps be improved if we could go above one dimension but the appropriate framework for CFTs in $1 < d < 2$ appears to be poorly understood.

- Problems with the $d \to 1$ limit not commuting with the crossover limit are mirrored in another context. To perform the $\sigma\chi$ flow at large $N$, we need to include $\frac{1}{N}$ corrections first. This could be worth pursuing since the vector generalization of the LRI is exactly solvable at large $N$. Checking that we get the right one-loop exact anomalous dimensions would yield a proof of our duality in this case.

- It would be interesting to return to the 2D bootstrap where we argued that the interesting part of the bound stays the same as more scalar correlators are added. A possible remedy is adding external (non-conserved) spin-2 operators to the system that we have used for the LRI [308]. If this works, it could be used to resolve discrepancies in the Monte Carlo community [200, 201].

- If external spin-2 operators are successful in the 2D case, the constraints that follow from them might be worth exploring in 3D as well [279, 280]. Although this is a much more demanding problem, it appears to be our best hope for finding kinks or islands close to $s = s_*$.

- A minibootstrap (familiar from the supersymmetric examples [309]) will be possible if we can solve for the OPE coefficient of a protected operator $\mathcal{O} = [\sigma\chi]_{n,\ell}$. For integer spin, $\lambda_{\sigma\chi\mathcal{O}}$ takes an indeterminate form. Analytically continuing the spin in this expression gives us a point of contact with recent work on light-ray operators [310].

The part of our work with the greatest potential for future development is probably the section on conformal manifolds. We have only scratched the surface of this borderline case between two halves of the bootstrap community — isolated fixed points versus RG flows. First, we have a two-loop equation coming from $\beta(g) = 0$ which is ripe for use in the numerical bootstrap. We have argued that this sum rule is best formulated in terms of Polyakov blocks and pointed to superconformal line defects as a suitable playground. There are bound to be many others if the Polyakov blocks can be worked out in higher dimensions. Second, the existence of a single perturbation that preserves conformal invariance implies

an infinite system of coupled ODEs which can be used to evolve observables from one value of the coupling to another. An important open problem is generalizing this to a system of PDEs that can handle more realistic conformal manifolds with curvature. Another important problem is using these equations to evolve the open string spectrum in a system with a D-brane moduli space [311, 312]. These conformal manifolds are guaranteed to be nonlocal but the challenges posed by local theories are more serious — free points are an infinite Zamolodchikov distance away from interacting points.

On the one hand, it is physically clear from how we derived these equations that their solutions must describe a conformal manifold. On the other hand, it is not mathematically clear how such simple equations can know about the remarkable subtleties of an operator algebra with a marginal coupling. We will close with a discussion of this tension which provides a humbling perspective on why quantum field theory as a whole, despite our best efforts, is still non-rigorous.

Clearly, the expression for $\partial\lambda_{ijk}/\partial g$ can be written in many different ways by changing the renormalization scheme. Indeed an invariant right-hand side would be wrong as the coupling itself is unphysical. We cannot have scheme-independent equations because even the solutions are scheme-dependent until we suitably reparameterize $g$. A proof of scheme-independence up to a diffeomorphism would be most welcome but, like crossing symmetry, it should only emerge from the equations when they are used to evolve very specific initial conditions. A random initial condition should permit highly unphysical behaviour since a generic choice for $\Delta_i$ and $\lambda_{ijk}$ is not a conformal manifold or even a conformal field theory. A very similar problem arises when using the Callan-Symanzik equation to compute anomalous dimensions in isolated fixed points. Usually one chooses the simplest correlation function that allows access to the operator of interest. But going rogue, there are infinitely many complicated correlation functions that can be used, yielding increasingly useless identities for renormalized integrals that most often look very difficult to prove with the mathematical literature. This appears to echo Hadamard's satement that "the shortest path between two truths in the real domain passes through the complex domain". Whether computing dimensions with the Callan-Symanzik equation or the conformal manifold system, we arrive at a great number of truths found by passing through the domain of operator valued distributions.

# Appendix A

# Correlators on the two-sheeted cover

Twisted sector four-point functions in orbifolds of the compact free boson are traditionally expressed as an infinite sum. We will evaluate several of them and find economical expressions at $R^2 = 2^M$ due to the doubling identities

$$\begin{aligned}
\vartheta_2(2\tau) &= \sqrt{\frac{\vartheta_3(\tau)^2 - \vartheta_4(\tau)^2}{2}} \quad \vartheta_2\left(\frac{1}{2}\tau\right) = \sqrt{2\vartheta_2(\tau)\vartheta_3(\tau)} \\
\vartheta_3(2\tau) &= \sqrt{\frac{\vartheta_3(\tau)^2 + \vartheta_4(\tau)^2}{2}} \quad \vartheta_3\left(\frac{1}{2}\tau\right) = \sqrt{\vartheta_3(\tau)^2 + \vartheta_2(\tau)^2} \\
\vartheta_4(2\tau) &= \sqrt{\vartheta_3(\tau)\vartheta_4(\tau)} \quad \vartheta_4\left(\frac{1}{2}\tau\right) = \sqrt{\vartheta_3(\tau)^2 - \vartheta_2(\tau)^2}
\end{aligned} \tag{A.1}$$

which preserve the homogeneity of $K(z)$ in (2.110).

We will start with the middle row of Table 2.5 where the sums describe correlators in the $R = \sqrt{2}$ theory. The first of these is evaluated in [55].

$$\begin{aligned}
\sum_{m,n} q^{\frac{1}{2}\left(m+\frac{n}{2}\right)^2} \bar{q}^{\frac{1}{2}\left(m-\frac{n}{2}\right)^2} &= \sum_{m,n} \left[ q^{\frac{1}{2}(n+m)^2} \bar{q}^{\frac{1}{2}(n-m)^2} + q^{\frac{1}{2}\left(n+m+\frac{1}{2}\right)^2} \bar{q}^{\frac{1}{2}\left(n-m+\frac{1}{2}\right)^2} \right] \\
&= \sum_{m,n} \left[ q^{\frac{1}{2}m^2} \bar{q}^{\frac{1}{2}n^2} + q^{\frac{1}{2}\left(m+\frac{1}{2}\right)^2} \bar{q}^{\frac{1}{2}\left(n+\frac{1}{2}\right)^2} \right] \frac{1 + (-1)^{m+n}}{2} \\
&= \frac{1}{2}\left( |\vartheta_2(\tau)|^2 + |\vartheta_3(\tau)|^2 + |\vartheta_4(\tau)|^2 \right)
\end{aligned} \tag{A.2}$$

In the first step, the sum that includes all $\frac{n}{2}$ has been split into one sum over $\mathbb{Z}$ and another over $\mathbb{Z} + \frac{1}{2}$. In the second step, we have recognized that as $m$ and $n$ vary, $(n+m, n-m)$ runs over all pairs of integers whose sum is even. We can get the related sums through

straightforward modifications of the trick in [55].

$$\begin{aligned}\sum_{m,n} q^{\frac{1}{2}\left(m+\frac{n}{2}+\frac{1}{2}\right)^2}\bar{q}^{\frac{1}{2}\left(m-\frac{n}{2}+\frac{1}{2}\right)^2} &= \sum_{m,n}\left[q^{\frac{1}{2}\left(n+m+\frac{1}{2}\right)^2}\bar{q}^{\frac{1}{2}\left(n-m-\frac{1}{2}\right)^2}+q^{\frac{1}{2}(n+m+1)^2}\bar{q}^{\frac{1}{2}(n-m)^2}\right]\\ &= \sum_{m,n}\left[q^{\frac{1}{2}\left(m-\frac{1}{2}\right)^2}\bar{q}^{\frac{1}{2}\left(n-\frac{1}{2}\right)^2}+q^{\frac{1}{2}m^2}\bar{q}^{\frac{1}{2}n^2}\right]\frac{1-(-1)^{m+n}}{2}\\ &= \frac{1}{2}\left(|\vartheta_2(\tau)|^2+|\vartheta_3(\tau)|^2-|\vartheta_4(\tau)|^2\right) \end{aligned} \tag{A.3}$$

Inserting factors of $(-1)^n$ has the effect of changing the sign between the $\mathbb{Z}$ and $\mathbb{Z}+\frac{1}{2}$ sums. Working this out, we find

$$\begin{aligned}\sum_{m,n}(-1)^n q^{\frac{1}{2}\left(m+\frac{n}{2}\right)^2}\bar{q}^{\frac{1}{2}\left(m-\frac{n}{2}\right)^2} &= \sum_{m,n}\left[q^{\frac{1}{2}m^2}\bar{q}^{\frac{1}{2}n^2}-q^{\frac{1}{2}\left(m+\frac{1}{2}\right)^2}\bar{q}^{\frac{1}{2}\left(n+\frac{1}{2}\right)^2}\right]\frac{1+(-1)^{m+n}}{2}\\ &= \frac{1}{2}\left(-|\vartheta_2(\tau)|^2+|\vartheta_3(\tau)|^2+|\vartheta_4(\tau)|^2\right) \end{aligned} \tag{A.4}$$

and

$$\begin{aligned}\sum_{m,n}(-1)^n q^{\frac{1}{2}\left(m+\frac{n}{2}+\frac{1}{2}\right)^2}\bar{q}^{\frac{1}{2}\left(m-\frac{n}{2}+\frac{1}{2}\right)^2} &= \sum_{m,n}\left[q^{\frac{1}{2}\left(m-\frac{1}{2}\right)^2}\bar{q}^{\frac{1}{2}\left(n-\frac{1}{2}\right)^2}-q^{\frac{1}{2}m^2}\bar{q}^{\frac{1}{2}n^2}\right]\frac{1-(-1)^{m+n}}{2}\\ &= \frac{1}{2}\left(|\vartheta_2(\tau)|^2-|\vartheta_3(\tau)|^2+|\vartheta_4(\tau)|^2\right)\ . \end{aligned} \tag{A.5}$$

Moving on to $R=2$, the first sum we need is even easier to obtain.

$$\begin{aligned}\sum_{m,n} q^{\frac{1}{4}(m+n)^2}\bar{q}^{\frac{1}{4}(m-n)^2} &= \frac{1}{2}\left(\left|\vartheta_3\left(\frac{1}{2}\tau\right)\right|^2+\left|\vartheta_4\left(\frac{1}{2}\tau\right)\right|^2\right)\\ &= \frac{1}{2}\left(|\vartheta_3(\tau)^2+\vartheta_2(\tau)^2|+|\vartheta_3(\tau)^2-\vartheta_2(\tau)^2|\right)\\ &= \frac{1}{2}\left(|\vartheta_3(\tau)^2+\vartheta_4(\tau)^2|+|\vartheta_3(\tau)^2-\vartheta_4(\tau)^2|\right) \end{aligned} \tag{A.6}$$

We have used the doubling identities in the second step and modular invariance in the third. Going to half-integers similarly gives

$$\sum_{m,n} q^{\frac{1}{4}\left(m+n+\frac{1}{2}\right)^2}\bar{q}^{\frac{1}{4}\left(m-n+\frac{1}{2}\right)^2} = \frac{1}{2}\left|\vartheta_2\left(\frac{1}{2}\tau\right)\right|^2 = |\vartheta_2(\tau)\vartheta_3(\tau)|\ . \tag{A.7}$$

The alternating version of (A.6) is

$$\begin{aligned}\sum_{m,n}(-1)^n q^{\frac{1}{4}(m+n)^2}\bar{q}^{\frac{1}{4}(m-n)^2} &= \sum_{m,n}\left[q^{\frac{1}{4}(2n+m)^2}\bar{q}^{\frac{1}{4}(2n-m)^2} - q^{\frac{1}{4}(2n+1+m)^2}\bar{q}^{\frac{1}{4}(2n+1-m)^2}\right]\\ &= \sum_{m,n}\left[q^{\left(n+\frac{m}{2}\right)^2}\bar{q}^{\left(n-\frac{m}{2}\right)^2} - q^{\left(n+\frac{m}{2}+\frac{1}{2}\right)^2}\bar{q}^{\left(n-\frac{m}{2}+\frac{1}{2}\right)^2}\right]\\ &= |\vartheta_4(2\tau)|^2 = |\vartheta_3(\tau)\vartheta_4(\tau)|\,. \end{aligned} \tag{A.8}$$

For the alternating version of (A.7), we need some new machinery. Recall that the Jacobi triple product reads $\prod_{n=1}^{\infty}(1-q^n)(1+q^{n-\frac{1}{2}}x)(1+q^{n+\frac{1}{2}}x^{-1}) = \sum_n q^{\frac{1}{2}n^2}x^n$. We will be interested in applying this with $q \mapsto q^2$ and $x \mapsto \pm q^{\frac{1}{2}}$. Guided by our expectations for what the next sum should be, we will start with product representations for the theta functions. While none of $|\vartheta_2|^2$, $|\vartheta_3|^2$ or $|\vartheta_4|^2$ are perfect squares on their own, we conveniently get perfect squares once we multiply them.

$$\begin{aligned}|\vartheta_2(\tau)\vartheta_3(\tau)| &= \sqrt{2}q^{\frac{1}{16}}\prod_{n=1}^{\infty}(1-q^{2n})\left(1+q^{n-\frac{1}{2}}\right)\times(q\leftrightarrow\bar{q})\\ &= \sqrt{2}q^{\frac{1}{16}}\prod_{n=1}^{\infty}(1-q^{2n})\left(1+q^{2n-\frac{1}{2}}\right)\left(1+q^{2n-\frac{3}{2}}\right)\times(q\leftrightarrow\bar{q})\\ &= \sqrt{2}q^{\frac{1}{16}}\prod_{n=1}^{\infty}[1-(q^2)^n]\left[1+(q^2)^{n-\frac{1}{2}}q^{\frac{1}{2}}\right]\left[1+(q^2)^{n-\frac{1}{2}}q^{-\frac{1}{2}}\right]\times(q\leftrightarrow\bar{q})\\ &= 2(q\bar{q})^{\frac{1}{16}}\sum_{m,n}(q^2)^{\frac{1}{2}m^2}(\bar{q}^2)^{\frac{1}{2}n^2}q^{\frac{1}{2}m}\bar{q}^{\frac{1}{2}n}\\ &= 2\sum_{m,n}q^{\left(m+\frac{1}{4}\right)^2}\bar{q}^{\left(n+\frac{1}{4}\right)^2}\\ |\vartheta_2(\tau)\vartheta_4(\tau)| &= \sqrt{2}q^{\frac{1}{16}}\prod_{n=1}^{\infty}(1-q^{2n})\left(1-q^{n-\frac{1}{2}}\right)\times(q\leftrightarrow\bar{q})\\ &= \sqrt{2}q^{\frac{1}{16}}\prod_{n=1}^{\infty}(1-q^{2n})\left(1-q^{2n-\frac{1}{2}}\right)\left(1-q^{2n-\frac{3}{2}}\right)\times(q\leftrightarrow\bar{q})\\ &= \sqrt{2}q^{\frac{1}{16}}\prod_{n=1}^{\infty}[1-(q^2)^n]\left[1-(q^2)^{n-\frac{1}{2}}q^{\frac{1}{2}}\right]\left[1-(q^2)^{n-\frac{1}{2}}q^{-\frac{1}{2}}\right]\times(q\leftrightarrow\bar{q})\\ &= 2(q\bar{q})^{\frac{1}{16}}\sum_{m,n}(-1)^{m+n}(q^2)^{\frac{1}{2}m^2}(\bar{q}^2)^{\frac{1}{2}n^2}q^{\frac{1}{2}m}\bar{q}^{\frac{1}{2}n}\\ &= 2\sum_{m,n}(-1)^{m+n}q^{\left(m+\frac{1}{4}\right)^2}\bar{q}^{\left(n+\frac{1}{4}\right)^2}\end{aligned}$$

By writing one product over $n$ as a product over even and odd $n$, we have found an expression for the sum that comes up next.

$$\begin{aligned}\sum_{m,n}(-1)^n q^{\frac{1}{4}\left(m+n+\frac{1}{2}\right)^2}\bar{q}^{\frac{1}{4}\left(m-n+\frac{1}{2}\right)^2} &= \sum_{m,n}\left[q^{\frac{1}{4}\left(2n+m+\frac{1}{2}\right)^2}\bar{q}^{\frac{1}{4}\left(2n-m-\frac{1}{2}\right)^2} - q^{\frac{1}{4}\left(2n+m+\frac{3}{2}\right)^2}\bar{q}^{\frac{1}{4}\left(2n-m+\frac{1}{2}\right)^2}\right] \\ &= \sum_{m,n}\left[q^{\left(n+\frac{m}{2}+\frac{1}{4}\right)^2}\bar{q}^{\left(n-\frac{m}{2}-\frac{1}{4}\right)^2} - q^{\left(n+\frac{m}{2}+\frac{3}{4}\right)^2}\bar{q}^{\left(n-\frac{m}{2}+\frac{1}{4}\right)^2}\right] \\ &= 2\sum_{m,n}\left[q^{\left(m+n+\frac{1}{4}\right)^2}\bar{q}^{\left(m-n+\frac{1}{4}\right)^2} - q^{\left(m+n+\frac{3}{4}\right)^2}\bar{q}^{\left(m-n-\frac{1}{4}\right)^2}\right] \\ &= 2\sum_{m,n} q^{\left(m+\frac{1}{4}\right)^2}\bar{q}^{\left(n+\frac{1}{4}\right)^2}\left[\frac{1+(-1)^{m+n}}{2} - \frac{1-(-1)^{m+n}}{2}\right] \\ &= 2\sum_{m,n}(-1)^{m+n} q^{\left(m+\frac{1}{4}\right)^2}\bar{q}^{\left(n+\frac{1}{4}\right)^2} = |\vartheta_2(\tau)\vartheta_4(\tau)| \end{aligned} \tag{A.9}$$

We have repeatedly used the fact that there is no difference between an exponent shifted by $\frac{1}{4}$ and an exponent shifted by $\frac{3}{4}$. This follows from reindexing.

As we have written Table 2.5, the same information about $R = 2$ correlators is contained in another set of sums which should give linear combinations of the four above. Fortunately, our formula derived from the Jacobi triple product continues to be applicable. Going through them quickly, the first is

$$\begin{aligned}\sum_{m,n} q^{\left(m+\frac{n}{4}\right)^2}\bar{q}^{\left(m-\frac{n}{4}\right)^2} &= \sum_{m,n}\left[q^{(n+m)^2}\bar{q}^{(n-m)^2} + q^{\left(n+m+\frac{1}{2}\right)^2}\bar{q}^{\left(n-m+\frac{1}{2}\right)^2} + 2q^{\left(n+m+\frac{1}{4}\right)^2}\bar{q}^{\left(n-m+\frac{1}{4}\right)^2}\right] \\ &= \frac{1}{2}\left(|\vartheta_2(2\tau)|^2 + |\vartheta_3(2\tau)|^2 + |\vartheta_4(2\tau)|^2 + |\vartheta_2(\tau)\vartheta_3(\tau)| + |\vartheta_2(\tau)\vartheta_4(\tau)|\right) \\ &= \frac{1}{2}\left(|\vartheta_2(\tau)\vartheta_3(\tau)| + |\vartheta_2(\tau)\vartheta_4(\tau)| + |\vartheta_3(\tau)\vartheta_4(\tau)|\right) \\ &+ \frac{1}{4}\left(|\vartheta_3(\tau)^2 + \vartheta_4(\tau)^2| + |\vartheta_3(\tau)^2 - \vartheta_4(\tau)^2|\right) \ , \end{aligned} \tag{A.10}$$

the second is

$$\begin{aligned}\sum_{m,n} q^{\left(m+\frac{n}{4}+\frac{1}{2}\right)^2}\bar{q}^{\left(m-\frac{n}{4}+\frac{1}{2}\right)^2} &= \sum_{m,n}\left[q^{(n+m+\frac{1}{2})^2}\bar{q}^{(n-m-\frac{1}{2})^2} + q^{(n+m+1)^2}\bar{q}^{(n-m)^2} + 2q^{\left(n+m+\frac{3}{4}\right)^2}\bar{q}^{\left(n-m-\frac{1}{4}\right)^2}\right] \\ &= \frac{1}{2}\left(|\vartheta_2(2\tau)|^2 + |\vartheta_3(2\tau)|^2 - |\vartheta_4(2\tau)|^2 + |\vartheta_2(\tau)\vartheta_3(\tau)| - |\vartheta_2(\tau)\vartheta_4(\tau)|\right) \\ &= \frac{1}{2}\left(|\vartheta_2(\tau)\vartheta_3(\tau)| - |\vartheta_2(\tau)\vartheta_4(\tau)| - |\vartheta_3(\tau)\vartheta_4(\tau)|\right) \\ &+ \frac{1}{4}\left(|\vartheta_3(\tau)^2 + \vartheta_4(\tau)^2| + |\vartheta_3(\tau)^2 - \vartheta_4(\tau)^2|\right) \ , \end{aligned} \tag{A.11}$$

the third is

$$\begin{aligned}\sum_{m,n}(-1)^n q^{\left(m+\frac{n}{4}\right)^2}\bar{q}^{\left(m-\frac{n}{4}\right)^2} &= \sum_{m,n}\left[q^{(n+m)^2}\bar{q}^{(n-m)^2}+q^{\left(n+m+\frac{1}{2}\right)^2}\bar{q}^{\left(n-m+\frac{1}{2}\right)^2}-2q^{\left(n+m+\frac{1}{4}\right)^2}\bar{q}^{\left(n-m+\frac{1}{4}\right)^2}\right]\\ &= \frac{1}{2}\left(|\vartheta_2(2\tau)|^2+|\vartheta_3(2\tau)|^2+|\vartheta_4(2\tau)|^2-|\vartheta_2(\tau)\vartheta_3(\tau)|-|\vartheta_2(\tau)\vartheta_4(\tau)|\right)\\ &= \frac{1}{2}\left(-|\vartheta_2(\tau)\vartheta_3(\tau)|-|\vartheta_2(\tau)\vartheta_4(\tau)|+|\vartheta_3(\tau)\vartheta_4(\tau)|\right)\\ &+\frac{1}{4}\left(|\vartheta_3(\tau)^2+\vartheta_4(\tau)^2|+|\vartheta_3(\tau)^2-\vartheta_4(\tau)^2|\right) \qquad (A.12)\end{aligned}$$

and the fourth is

$$\begin{aligned}\sum_{m,n}(-1)^n q^{\left(m+\frac{n}{4}+\frac{1}{2}\right)^2}\bar{q}^{\left(m-\frac{n}{4}+\frac{1}{2}\right)^2} &= \sum_{m,n}\left[q^{(n+m+\frac{1}{2})^2}\bar{q}^{(n-m-\frac{1}{2})^2}+q^{(n+m+1)^2}\bar{q}^{(n-m)^2}-2q^{\left(n+m+\frac{3}{4}\right)^2}\bar{q}^{\left(n-m-\frac{1}{4}\right)^2}\right]\\ &= \frac{1}{2}\left(|\vartheta_2(2\tau)|^2+|\vartheta_3(2\tau)|^2-|\vartheta_4(2\tau)|^2-|\vartheta_2(\tau)\vartheta_3(\tau)|+|\vartheta_2(\tau)\vartheta_4(\tau)|\right)\\ &= \frac{1}{2}\left(-|\vartheta_2(\tau)\vartheta_3(\tau)|+|\vartheta_2(\tau)\vartheta_4(\tau)|-|\vartheta_3(\tau)\vartheta_4(\tau)|\right)\\ &+\frac{1}{4}\left(|\vartheta_3(\tau)^2+\vartheta_4(\tau)^2|+|\vartheta_3(\tau)^2-\vartheta_4(\tau)^2|\right)\ . \qquad (A.13)\end{aligned}$$

There is one more set of calculations that yields to the brute force tools we have seen. These are the ones at $R=2\sqrt{2}$ — the "blue sums" in the row that has both red and blue. The first actually coincides with the very first sum in this section.

$$\sum_{m,n} q^{\frac{1}{2}\left(m+\frac{n}{2}\right)^2}\bar{q}^{\frac{1}{2}\left(m-\frac{n}{2}\right)^2} = \frac{1}{2}\left(|\vartheta_2(\tau)|^2+|\vartheta_3(\tau)|^2+|\vartheta_4(\tau)|^2\right) \qquad (A.14)$$

The next two require the boxed formula from the Jacobi triple product. They are

$$\begin{aligned}\sum_{m,n} q^{\frac{1}{2}\left(m+\frac{n}{2}+\frac{1}{4}\right)^2}\bar{q}^{\frac{1}{2}\left(m-\frac{n}{2}-\frac{1}{4}\right)^2} &= \sum_{m,n}\left[q^{\frac{1}{2}\left(n+m+\frac{1}{4}\right)^2}\bar{q}^{\frac{1}{2}\left(n-m+\frac{1}{4}\right)^2}+q^{\frac{1}{2}\left(n+m+\frac{3}{4}\right)^2}\bar{q}^{\frac{1}{2}\left(n-m+\frac{3}{4}\right)^2}\right]\\ &= 2\sum_{m,n} q^{\frac{1}{2}\left(m+\frac{1}{4}\right)^2}\bar{q}^{\frac{1}{2}\left(n+\frac{1}{4}\right)^2}\left[\frac{1+(-1)^{m+n}}{2}\right]\\ &= \frac{1}{2}\left(\left|\vartheta_2\left(\frac{1}{2}\tau\right)\vartheta_4\left(\frac{1}{2}\tau\right)\right|+\left|\vartheta_2\left(\frac{1}{2}\tau\right)\vartheta_4\left(\frac{1}{2}\tau\right)\right|\right) \qquad (A.15)\\ &= \left|\frac{1}{2}\vartheta_2(\tau)\vartheta_3(\tau)[\vartheta_3(\tau)^2+\vartheta_2(\tau)^2]\right|^{\frac{1}{2}}+\left|\frac{1}{2}\vartheta_2(\tau)\vartheta_3(\tau)[\vartheta_3(\tau)^2-\vartheta_2(\tau)^2]\right|^{\frac{1}{2}}\end{aligned}$$

and

$$\begin{aligned}\sum_{m,n}(-1)^m q^{\frac{1}{2}\left(m+\frac{n}{2}\right)^2}\bar{q}^{\frac{1}{2}\left(m-\frac{n}{2}\right)^2} &= \sum_{m,n}(-1)^m\left[q^{\frac{1}{2}(n+m)^2}\bar{q}^{\frac{1}{2}(n-m)^2}+q^{\frac{1}{2}\left(n+m+\frac{1}{2}\right)^2}\bar{q}^{\frac{1}{2}\left(n-m+\frac{1}{2}\right)^2}\right]\\ &= |\vartheta_4(4\tau)|^2+|\vartheta_2(2\tau)\vartheta_4(2\tau)| \qquad \text{(A.16)}\\ &= \left|\frac{1}{2}\vartheta_3(\tau)\vartheta_4(\tau)[\vartheta_3(\tau)^2+\vartheta_4(\tau)^2]\right|^{\frac{1}{2}}+\left|\frac{1}{2}\vartheta_3(\tau)\vartheta_4(\tau)[\vartheta_3(\tau)^2-\vartheta_4(\tau)^2]\right|^{\frac{1}{2}}.\end{aligned}$$

This last sum might be the only one where we have to relate it to the others by modular transformation instead of computing it directly.

$$\begin{aligned}\sum_{m,n}(-1)^m q^{\frac{1}{2}\left(m+\frac{n}{2}+\frac{1}{4}\right)^2}\bar{q}^{\frac{1}{2}\left(m-\frac{n}{2}-\frac{1}{4}\right)^2} &= \left|\frac{1}{2}\vartheta_2(\tau)\vartheta_4(\tau)[\vartheta_2(\tau)^2+\vartheta_4(\tau)^2]\right|^{\frac{1}{2}}\\ &\quad+\left|\frac{1}{2}\vartheta_2(\tau)\vartheta_4(\tau)[\vartheta_2(\tau)^2-\vartheta_4(\tau)^2]\right|^{\frac{1}{2}} \qquad \text{(A.17)}\end{aligned}$$

# Appendix B

# Linear difference equations

Asymptotic analysis of sequences obeying three term recurrence relations such as (3.22) and (3.43) is a well understood subject, going by the name Birkhoff-Trjitzinsky theory. The following theorem summarizes a number of results from it [313].

**Theorem 1.** *Let $y_1(n)$ and $y_2(n)$ be the two linearly independent solutions of the difference equation*

$$y(n+2) + a(n)y(n+1) + b(n)y(n) = 0 \tag{B.1}$$

*where the coefficients have asymptotic expansions $a(n) \sim \sum_{s=0}^{\infty} \frac{a_s}{n^s}$ and $b(n) \sim \sum_{s=0}^{\infty} \frac{b_s}{n^s}$.*

1. *If the characteristic equation $\rho^2 + a_0\rho + b_0 = 0$ has two distinct roots $\rho_1$ and $\rho_2$, the solutions satisfy $y_j(n) \sim \rho_j^n n^{\alpha_j} \sum_{s=0}^{\infty} \frac{c_{s,j}}{n^s}$ where $\alpha_j = \frac{a_1\rho_j + b_1}{a_0\rho_j + 2b_0}$.*

2. *Otherwise, consider the double root $\rho$. If the auxiliary equation $a_1\rho + b_1 = 0$ is not satisfied, the solutions satisfy $y_j(n) \sim \rho^n e^{(-1)^j\beta\sqrt{n}} n^{\alpha} \sum_{s=0}^{\infty} (-1)^{js} \frac{c_s}{n^{s/2}}$ where $\alpha = \frac{1}{4} + \frac{b_1}{2b_0}$ and $\beta = 2\sqrt{\frac{a_0 a_1 - 2b_1}{2b_0}}$.*

3. *Otherwise, consider the roots $\alpha_1$ and $\alpha_2$ of the indicial equation $\alpha(\alpha-1)\rho^2 + (a_1\alpha + a_2)\rho + b_2 = 0$, ordered according to $\Re\alpha_2 \geq \Re\alpha_1$. If $\alpha_2 - \alpha_1 \notin \mathbb{Z}_{\geq 0}$, the solutions satisfy $y_j(n) \sim \rho^n n^{\alpha_j} \sum_{s=0}^{\infty} \frac{c_{s,j}}{n^s}$.*

4. *Otherwise, let $m = \alpha_2 - \alpha_1$. The asymptotic expansion for the first solution is unchanged from the previous case but for the second solution we must use $y_2(n) \sim \rho^n n^{\alpha_2} \left(\sum_{s=0}^{\infty} \frac{d_s}{n^s} - \frac{d_m}{n^m}\right) + c\log(n)y_1(n)$.*

Taking (B.1) to be the recurrence relation for Wilson polynomials, we find the roots $\rho = 1$, $\alpha_1 = -2(a+x)$ and $\alpha_2 = -2(a-x)$ in the third case of the theorem. Each coefficient in (3.42) can then be written as a linear combination of two functions asymptotic to power-laws. As seen in Table B.1, all of them decay to zero. When comparing to the results of [40, 41], one

| Coefficient | Leading rates |
|---|---|
| $c_{2n}^{\sigma\sigma(1,1)\sigma\sigma}$ | $n^{-\frac{8+2\Delta_\sigma}{3}}$ and $n^{2\Delta_\sigma-2}$ |
| $c_{2n}^{\sigma\sigma(1,3)\sigma\sigma}$ | $n^{-\frac{5+8\Delta_\sigma}{3}}$ and $n^{-1}$ |

Table B.1: Decay rates of the fundamental solutions that comprise two of our main results. We have not included the prefactors in (3.42). These will make the convergence much faster, namely $(1/16)^n$, which can be predicted from the growth rate of $K_{2n}(1)$.

must remember that $c_{2n}^{\sigma\sigma(1,1)\sigma\sigma}$ and $c_{2n}^{\sigma\sigma(1,3)\sigma\sigma}$ include many squared OPE coefficients due to the increasing amount of degeneracy at each level of a Verma module.

Our main claim about $c_{2n}^{\sigma\sigma(1,1)\sigma\sigma}$ and $c_{2n}^{\sigma\sigma(1,3)\sigma\sigma}$ — that they are positive for finite $n$ — cannot be proven with asymptotics. Instead, we will use a theorem from [314] which bounds the ratio between neighbouring terms in a sequence.

**Theorem 2.** *Let $x(n)$ be a solution of*

$$x(n) \geq \frac{a(n)}{b(n)}x(n-1) - \frac{c(n)}{d(n)}x(n-2) \tag{B.2}$$

*where $a(n)$, $b(n)$, $c(n)$ and $d(n)$ are degree-$k$ polynomials with positive leading terms. Also define $f(n) = a(n+1)d(n+1) - \frac{2b_k}{a_k}b(n+1)c(n+1) - \frac{a_k}{2b_k}b(n+1)d(n+1)$. Finally, let $m$ be an integer large enough to guarantee that $b(n)$, $c(n)$, $d(n)$ and $f(n)$ have positive values for $n \geq m$. If $\frac{x(m)}{x(m-1)} > \frac{a_k}{2b_k}$ then $\frac{x(n)}{x(n-1)} > \frac{a_k}{2b_k}$ for $n \geq m$.*

**Proposition 1.** *The sequences $y_1(n) = P_n\left(\frac{7-2\Delta_\sigma}{6}, \frac{4-2\Delta_\sigma}{6}, -\frac{1-2\Delta_\sigma}{6}, \frac{5+2\Delta_\sigma}{6}; \frac{1+4\Delta_\sigma}{6}\right)$ and $y_2(n) = P_n\left(\frac{2+2\Delta_\sigma}{3}, \frac{1}{2}, -\frac{1}{2}, -\frac{1}{2}; \frac{1+4\Delta_\sigma}{6}\right)$ of Wilson polynomials are positive for $\frac{1}{8} \leq \Delta_\sigma \leq \frac{1}{2}$.*

*Proof.* The theorem above is more effective at identifying increasing sequences than ruling out changes of sign directly. Therefore, we will work with $x_1(n) = n^2 y_1(n)$ and $x_2(n) = n^2 y_2(n)$ — expressions that have been guided by the asymptotics in Table B.1.

Looking at the more difficult case first, $x_1(n)$ satisfies (B.2) with

$$\begin{aligned} b(n) &= (n-1)^2(n+1)(2n+1)(4n-3)(6n-4\Delta_\sigma+5) \\ c(n) &= n(n-1)(2n-1)(2n-3)(4n+1)(3n+2\Delta_\sigma-4) \\ d(n) &= (n-2)^2(n+1)(2n+1)(4n-3)(6n-4\Delta_\sigma+5)\,. \end{aligned} \tag{B.3}$$

These are clearly positive for $n > 2$. Also, by writing out the polynomial for $a(n)$, we find a leading coefficient of $a_6 = 2b_6 = 96$. It remains to check $f(n)$ or equivalently $(n+2)^{-1}(2n+3)^{-1}(4n+1)^{-1}(6n-4\Delta_\sigma+11)^{-1}f(n)$. This is a sixth degree polynomial in which $64\Delta_\sigma(\Delta_\sigma+1)n^6$ is followed immediately by negative coefficients. From this we see that the critical value of $n$, beyond which $f(n) > 0$, increases without bound as $\Delta_\sigma \to 0$. This reflects

the fact that the $n^2$ we introduced is only able to overpower $n^{2\Delta_\sigma-2}$ for strictly positive $\Delta_\sigma$. Fortunately, the smallest value of $\Delta_\sigma$ that we consider is $\frac{1}{8}$ leading to a critical value of $n = 44$. Since $x_1(44) > x_1(43)$, we establish positivity of the entire sequence $x_1(n)$ by checking its first 44 terms.

Things will be easier for $x_2(n)$ which satisfies (B.2) for

$$\begin{aligned} b(n) &= (n-1)^2(6n+4\Delta_\sigma-11)(6n+4\Delta_\sigma-5)^2(6n+4\Delta_\sigma+1)(12n+4\Delta_\sigma-23) \\ c(n) &= 1296n^2(n-1)(n-3)(12n+4\Delta_\sigma-11) \\ d(n) &= (6n+4\Delta_\sigma-11)(6n+4\Delta_\sigma-5)^2(6n+4\Delta_\sigma+1)(12n+4\Delta_\sigma-23)\ . \end{aligned} \tag{B.4}$$

Additionally, we find $a_6 = 2b_6 = 31104$ and an $f(n)$ proportional to $(6n+4\Delta_\sigma-5)(6n+4\Delta_\sigma+1)^2(6n+4\Delta_\sigma+7)(12n+4\Delta_\sigma-11)$. The non-trivial factor of $f(n)$ begins with $41472(\Delta_\sigma-\frac{1}{8})n^5$ which is potentially problematic, but the next coefficient that follows it is positive for all real $\Delta_\sigma$. As a result, $f(n)$ is positive for $n > 3$ just like the polynomials above. Checking that $x_2(3) > x_2(2) > x_2(1) > 0$, positivity of $x_2(n)$ has been proven as well. □

Although we do not have closed-form solutions for them, it is possible that $c_{2n}^{\epsilon\epsilon(1,1)\epsilon\epsilon}$, $c_{2n}^{\epsilon\epsilon(1,3)\epsilon\epsilon}$ and $c_{2n}^{\epsilon\epsilon(1,5)\epsilon\epsilon}$ are positive as well. The main hint of this, which we now prove, is that the Virasoro blocks containing them have positive Taylor coefficients around $z = 0$. The fact that this is a necessary condition follows trivially from expanding $g(z) = \sum_{n=0}^{\infty} c_{2n}K_{r+2n}(z)$. The analogous statement in higher dimensions was proven in [315].

**Proposition 2.** *Let $b_k$ be a sequence starting at $b_0 = 1$ with the rest of the terms given by (3.47). If $\Delta_\epsilon > 1$, the sequence monotonically increases.*

*Proof.* Defining $K = k + r$ for brevity, we have

$$\begin{aligned} &[4K^3+8(1-\Delta_\epsilon)K^2+(3\Delta_\epsilon^2-14\Delta_\epsilon+4)K+3\Delta_\epsilon(\Delta_\epsilon-2)]b_{k+1} = \\ &[12K^2-4(5\Delta_\epsilon+1)K+6\Delta_\epsilon^2]Kb_k \\ &-[12K^3-16(\Delta_\epsilon+2)K^2+2(\Delta_\epsilon^2+12\Delta_\epsilon+14)K+2(\Delta_\epsilon-2)(\Delta_\epsilon+1)(\Delta_\epsilon+2)]b_{k-1} \\ &+[4K^3-4(\Delta_\epsilon+5)K^2-(\Delta_\epsilon^2-10\Delta_\epsilon-32)K+(\Delta_\epsilon-2)(\Delta_\epsilon+2)(\Delta_\epsilon+4)]b_{k-2}\ . \end{aligned} \tag{B.5}$$

Although this has four terms, we will convert it to a simpler recursion having only three. We do this by assuming that the piece with $b_{k-1}$ and $b_{k-2}$ is bounded by some function of $b_k$ and $b_{k-1}$. Our ansatz for this function is $[4K^2-12(\Delta_\epsilon+1)K+M]Kb_k+4K^3b_{k-1}$. In other words, we need to show that

$$\begin{aligned} &[4K^2-12(\Delta_\epsilon+1)K+M]Kb_k > \\ &[8K^3-16(\Delta_\epsilon+2)K^2+2(\Delta_\epsilon^2+12\Delta_\epsilon+14)K+2(\Delta_\epsilon-2)(\Delta_\epsilon+1)(\Delta_\epsilon+2)]b_{k-1} \\ &-[4K^3-4(\Delta_\epsilon+5)K^2-(\Delta_\epsilon^2-10\Delta_\epsilon-32)K+(\Delta_\epsilon-2)(\Delta_\epsilon+2)(\Delta_\epsilon+4)]b_{k-2}\ . \end{aligned} \tag{B.6}$$

Using (B.6) in (B.5), we find an expression of the form $R_+(K)b_{k+1} > R_0(K)b_k + R_-(K)b_{k-1}$. We will perform a rescaling to instead write this as

$$\begin{aligned} S_+(K)b_{k+1} &> S_0(K)b_k + S_-(K)b_{k-1} \\ S_i(K) &\equiv [4(K+1)^2 - 12(\Delta_\epsilon + 1)(K+1) + M](K+1)R_+(K)^{-1}R_i(K) \ . \end{aligned} \tag{B.7}$$

For our assumption to be true, the fractional coefficients in (B.7) must exceed the $K \mapsto K+1$ versions of the ones in (B.6). These two conditions each give one side of an inequality for $M$. The result is $10\Delta_\epsilon^2 + 20\Delta_\epsilon + 4 < M < 10\Delta_\epsilon^2 + 29\Delta_\epsilon + 4$ which may be satisfied for any $\Delta_\epsilon > 0$. Having chosen $M$ appropriately, we have moved the problem into the domain of the theorem above. The monotonicity proof for $b_k$ is now identical to the one for $n^2 c_{2n}^{\sigma\sigma(1,1)\sigma\sigma}$ and $n^2 c_{2n}^{\sigma\sigma(1,3)\sigma\sigma}$. □

# Appendix C

# Spinor formalism

In chapter 3, we employ a useful framework for studying fractional $d$ gamma matrices given in [173]. The main idea is to realize the Clifford algebra by treating the matrices as free fermionic fields themselves. Writing an antisymmetrized combination as

$$\Gamma_{\mu_1\ldots\mu_n} = \frac{\delta}{\delta a^{\mu_1}}\ldots\frac{\delta}{\delta a^{\mu_n}}\exp\left(a_\mu\psi^\mu\right)\Big|_{a=0}, \tag{C.1}$$

the product of many such matrices can again be written as a differential operator acting on an exponential via the Baker-Campbell-Hausdorff formula. By moving derivatives until all contracted pairs appear beside eachother, we may show that the coefficients in

$$\begin{aligned}\Gamma_{A_1}\ldots\Gamma_{A_N}\Gamma_B\Gamma_{A_{s(1)}}\ldots\Gamma_{A_{s(N)}} &= R\Gamma_B\\ \Gamma_{A_1}\ldots\Gamma_{A_N}\otimes\Gamma_{A_{s(1)}}\ldots\Gamma_{A_{s(N)}} &= \sum_{m=0}^{\infty}\frac{1}{m!}R_m\Gamma_C\otimes\Gamma_C\end{aligned} \tag{C.2}$$

contain the signs

$$R\propto\eta(-1)^{m(n_1+\cdots+n_N)}(-1)^{\binom{n_1}{2}+\cdots+\binom{n_N}{2}},\ R_m\propto\eta(-1)^{\binom{n_1}{2}+\cdots+\binom{n_N}{2}}. \tag{C.3}$$

Here, $\eta$ is the part that depends on the specific permutation given in (C.2). A contracted pair of derivatives is then written as

$$\left(\frac{\delta}{\delta a^\mu}\frac{\delta}{\delta a^\dagger_\mu}\right)^{n_i} = \partial_{x_i}^{n_i}\exp\left(x_i\frac{\delta}{\delta a^\mu}\frac{\delta}{\delta a^\dagger_\mu}\right)\Big|_{x=0} \tag{C.4}$$

so that $R$ and $R_m$ both take the form of derivatives with respect to $x_i$. Specifically,

$$\begin{aligned} R &= \eta(-1)^{m(n_1+\cdots+n_N)}(-1)^{\binom{n_1}{2}+\cdots+\binom{n_N}{2}}\partial_{x_1}^{n_1}\ldots\partial_{x_N}^{n_N}\left[(\mathcal{A}+\mathcal{B})^{d-m}(\mathcal{A}-\mathcal{B})^m\right]_{x=0} \\ R_m &= \eta(-1)^{\binom{n_1}{2}+\cdots+\binom{n_N}{2}}\partial_{x_1}^{n_1}\ldots\partial_{x_N}^{n_N}\left[\mathcal{A}^{d-m}\mathcal{B}^m\right]_{x=0} \end{aligned} \tag{C.5}$$

in terms of expectation values

$$\begin{aligned} \mathcal{A} &= \left\langle \exp\left[-\sum_{i<j} a_i a_j + a^\dagger_{s(i)}a^\dagger_{s(j)}\right]\right\rangle \\ \mathcal{B} &= -\left\langle \exp\left[-\sum_{i<j} a_i a_j + a^\dagger_{s(i)}a^\dagger_{s(j)}\right]\sum_{i,j} a_i a^\dagger_{s(j)}\right\rangle . \end{aligned} \tag{C.6}$$

that are computed with $\left\langle a_i a_i^\dagger\right\rangle = -x_i$. This leads to Table C.1 for $N=3$ which is the highest value we need in the present analysis. We have corrected two typos in [173].

| $(s(1),s(2),s(3))$ | $\eta$ | $\mathcal{A}$ | $\mathcal{B}$ |
|---|---|---|---|
| $(3,2,1)$ | $1$ | $1+x_1x_2+x_1x_3+x_2x_3$ | $x_1+x_2+x_3+x_1x_2x_3$ |
| $(1,2,3)$ | $(-1)^{n_1n_2+n_1n_3+n_2n_3}$ | $1-x_1x_2-x_1x_3-x_2x_3$ | $x_1+x_2+x_3-x_1x_2x_3$ |
| $(2,1,3)$ | $(-1)^{n_1n_3+n_2n_3}$ | $1+x_1x_2-x_1x_3-x_2x_3$ | $x_1+x_2+x_3+x_1x_2x_3$ |
| $(1,3,2)$ | $(-1)^{n_1n_2+n_1n_3}$ | $1-x_1x_2-x_1x_3+x_2x_3$ | $x_1+x_2+x_3+x_1x_2x_3$ |
| $(3,1,2)$ | $(-1)^{n_1n_2}$ | $1-x_1x_2+x_1x_3+x_2x_3$ | $x_1+x_2+x_3-x_1x_2x_3$ |
| $(2,3,1)$ | $(-1)^{n_2n_3}$ | $1+x_1x_2+x_1x_3-x_2x_3$ | $x_1+x_2+x_3-x_1x_2x_3$ |

Table C.1: Data for computing the $N=3$ cases of (C.2). If $N=1$ and $N=2$ are desired, they can be obtained by the appropriate substitutions of $n_i=0$.

One application of this approach is to show that the coefficients in

$$\left(\Gamma_B^{(n)}\right)^\alpha{}_\beta\left(\Gamma_B^{(n)}\right)^\gamma{}_\delta = \sum_{p=0}^{\infty}\Omega_{np}(0)\left(\Gamma_C^{(p)}\right)^\alpha{}_\delta\left(\Gamma_C^{(p)}\right)^\gamma{}_\beta \tag{C.7}$$

may be obtained from

$$\Omega_{np}(x) = \frac{(-1)^{np+\binom{n}{2}+\binom{p}{2}}}{\mathrm{Tr}(\mathbf{1})p!}\partial_x^n\left[(1+x)^{d-p}(1-x)^p\right] . \tag{C.8}$$

We have repeatedly referred to (C.7) as the Fierz identity. This term is also sometimes used for more specialized identities that follow from (C.7) when the fermions in question are identical. An example of this is the equivalence of all 2D Thirring models for $N=1$ — a

statement that can be read off from the eigenvectors of $\Omega$. The naive expression for $\Omega(0)^2$ involves a divergent sum [169, 316]. Therefore, the right condition to impose is that $\Omega(x)\Omega(y)$ have a continuation which yields the identity at $x = y = 0$. Performing this computation, we find

$$\begin{aligned}\Omega_{nm}(x)\Omega_{mk}(y) &= \mathrm{Tr}(\mathbf{1})^{-2}\sum_{m=0}^{\infty}\frac{(-1)^{m(n+k)+\binom{n}{2}+\binom{k}{2}}}{m!k!}\partial_x^n[(1+x)^{d-m}(1-x)^m]\partial_y^m[(1+y)^{d-k}(1-y)^k] \\ &= \mathrm{Tr}(\mathbf{1})^{-2}\frac{\Gamma(d+1-k)}{\Gamma(d+1)\Gamma(k+1)}(-1)^{\binom{n}{2}+\binom{k}{2}} \\ &\quad \partial_x^n\partial_y^k\left[(1+x)^d(1+y)^d\left(1+(-1)^{n+k}\frac{1-x}{1+x}\frac{1-y}{1+y}\right)\right] . \end{aligned} \tag{C.9}$$

For $n+k$ even, the derivative is $\partial_x^n\partial_y^k(2+2xy)^d\big|_{x=y=0} = 2^d\frac{\Gamma(d+1)\Gamma(k+1)}{\Gamma(d+1-k)}\delta_{nk}$. This has the right form for any $d$. For $n+k$ odd, on the other hand, we need $\partial_x^n\partial_y^k(2x+2y)^d\big|_{x=y=0}$ to vanish. This happens whenever $n+k \neq d$ which is to say that it always happens unless $d$ is an odd integer. The conclusion is that $\mathrm{Tr}(\mathbf{1}) = 2^{\frac{d}{2}}$ holds almost everywhere with only the odd dimensions being special.

# Appendix D

# Nilpotent invariant tensors

Here we show that (3.99) has only the trivial solution. This requires much more than a counting argument since it is a nonlinear system for arbitrarily many variables. The first line, which we call the nilpotence condition, guarantees that two Feynman diagrams are identically zero. The second line, which we call the closure condition, asserts that the other two Feynman diagrams generate the same type of vertex that is already being considered. We will actually analyze a more general system where the nilpotence and closure conditions are

$$S(p)^{ik}{}_{ab}S(q)^{ab}{}_{jl} = S(p)^{ib}{}_{al}S(q)^{ak}{}_{jb} = 0\ ,\ 1 \leq p, q \leq Q \tag{D.1}$$

and

$$S(p)^{ik}{}_{jl} = c_{p,0}S(p)^{ia}{}_{jb}S(p)^{bk}{}_{al} + \sum_{q=1}^{Q} c_{p,q}\left(S(q)^{ia}{}_{bj}S(p)^{bk}{}_{al} + S(p)^{ai}{}_{bj}S(q)^{kb}{}_{al}\right) \tag{D.2}$$

respectively. The result we have used in chapter 3 follows from setting $Q = 1$.

To derive a cubic constraint, we should plug (D.2) into $S(p)^{ik}{}_{jl}S(p)^{lm}{}_{kn}$ in two different ways. Setting the left substitution equal to the right substitution, we have

$$\sum_{q=1}^{Q} c_{p,q}S(q)^{ia}{}_{bj}S(p)^{bk}{}_{al}S(p)^{lm}{}_{kn} = \sum_{q=1}^{Q} c_{p,q}S(p)^{ia}{}_{jb}S(p)^{bk}{}_{al}S(q)^{ml}{}_{kn} \tag{D.3}$$

where the $c_{p,0}$ terms have cancelled. Next, we will take $\sum_{q=1}^{Q} c_{p,q}S(q)^{ja}{}_{bi}S(p)^{ik}{}_{jl}S(r)^{lm}{}_{nk}$ and use (D.2) to expand the middle tensor. This expansion consists of a single term, rather than

$Q+1$ terms, due to the nilpotence relation (D.1).

$$\begin{aligned}\sum_{q=1}^{Q} c_{p,q} S(q)^{ja}{}_{bi} S(p)^{ik}{}_{jl} S(r)^{lm}{}_{nk} &= c_{p,0} \sum_{q=1}^{Q} c_{p,q} S(q)^{ja}{}_{bi} S(p)^{is}{}_{jt} S(p)^{tk}{}_{sl} S(r)^{lm}{}_{nk} \\ &= c_{p,0} \sum_{q=1}^{Q} c_{p,q} S(p)^{ja}{}_{ib} S(p)^{is}{}_{jt} S(q)^{kt}{}_{sl} S(r)^{lm}{}_{nk} \\ &= 0 \end{aligned} \tag{D.4}$$

After applying (D.3) to reorder the factors, we have again used (D.1) to see that the whole expression vanishes. We may also write

$$\sum_{r=1}^{Q} c_{p,r} S(q)^{ja}{}_{bi} S(p)^{ik}{}_{jl} S(r)^{lm}{}_{nk} = 0 \ , \tag{D.5}$$

as the same procedure clearly works when the sum runs over $r$ instead of $q$.

We now have enough information to make sense of two contractions other than $S(p)^{ik}{}_{jl} S(p)^{lm}{}_{kn}$. The first one is

$$S(p)^{ik}{}_{jl} S(q)^{lm}{}_{nk} = c_{p,0} S(p)^{ia}{}_{jb} S(p)^{bk}{}_{al} S(q)^{lm}{}_{nk} \ . \tag{D.6}$$

To ensure vanishing of the higher $c_{p,q}$ terms, we have combined (D.1) with (D.4). Similarly,

$$S(q)^{ik}{}_{lj} S(p)^{lm}{}_{kn} = c_{p,0} S(q)^{ik}{}_{lj} S(p)^{la}{}_{kb} S(p)^{bm}{}_{an} \tag{D.7}$$

after combining (D.1) with (D.5). Notice that after summing (D.6) and (D.7) over $q$, we arrive at

$$\sum_{q=1}^{Q} c_{p,q} S(p)^{ik}{}_{jl} S(q)^{lm}{}_{nk} = \sum_{q=1}^{Q} c_{p,q} S(q)^{ik}{}_{lj} S(p)^{lm}{}_{kn} \tag{D.8}$$

as a consequence of (D.3).

We will now define powers of our rank-4 tensors by

$$[S(p)^n]^{ik}{}_{jl} \equiv S(p)^{ia_1}{}_{jb_1} S(p)^{b_1 a_2}{}_{a_1 b_2} \dots S(p)^{b_{n-2} a_{n-1}}{}_{a_{n-2} b_{n-1}} S(p)^{b_{n-1} k}{}_{a_{n-1} l} \ . \tag{D.9}$$

With this notation, it is helpful to contract (D.2) with $S(p)^{n-2}$ and take traces as follows.

$$\begin{aligned} c_{p,0} [S(p)^n]^{ik}{}_{ki} &= [S(p)^{n-1}]^{ik}{}_{ki} - 2 \sum_{q=1}^{Q} c_{p,q} S(q)^{ia}{}_{bk} [S(p)^{n-1}]^{bk}{}_{ai} \\ c_{p,0} S(q)^{ia}{}_{bk} [S(p)^n]^{bk}{}_{ai} &= S(q)^{ia}{}_{bk} [S(p)^{n-1}]^{bk}{}_{ai} \end{aligned} \tag{D.10}$$

We have used (D.8) to move all factors of $S(p)$ to one side of $S(q)$. Starting with $S(p)^{ik}{}_{ki} =$

$S(q)^{ia}_{\ bk} S(p)^{bk}_{\ ai} = 0$, it follows that the equations in (D.10) all vanish by induction. In particular, our set of traceless matrices includes all powers of $\tilde{S}(p)$, defined by $\tilde{S}(p)^{(ij)}_{\ \ (lk)} \equiv S(p)^{ik}_{\ \ jl}$. This implies that $\tilde{S}(p)$ is nilpotent.

Given $\tilde{S}(p)^{(ij)}_{\ \ (lk)}$, we can regard it as a linear map that acts on the right vector $v^{(lk)} \equiv S(r)^{lm}_{\ \ nk}$ for fixed $(mn)$. By (D.5),

$$\tilde{S}(p)^{(ij)}_{\ \ (lk)} v^{(lk)} = c_{p,0} \tilde{S}(p)^{(ij)}_{\ \ (ab)} \tilde{S}(p)^{(ab)}_{\ \ (lk)} v^{(lk)} \ . \tag{D.11}$$

A similar statement with $v$ playing the role of a left vector would follow from (D.4). If $\tilde{S}(p)v$ were non-zero, (D.11) would tell us that $\tilde{S}(p)$ has an eigenvalue of $c_{p,0}^{-1}$, contradicting the fact that it is nilpotent. Therefore,

$$S(p)^{ik}_{\ \ jl} S(r)^{lm}_{\ \ nk} = 0 \tag{D.12}$$

which kills all $Q$ terms of the sum we have been using. Looking at (D.2) one more time, we find $\tilde{S}(p) = c_{p,0} \tilde{S}(p)^2$. The tensor structures now have to vanish as only the zero matrix is both nilpotent and idempotent.

# Appendix E

# Numerical details

In this appendix, we list the crossing equations that are relevant to our numerical study of the long-range Ising model in chapter 4. We also discuss some issues related to the effective superblocks that arise in the LRI and other nonlocal theories with a shadow relation.

## E.1 Crossing equations

Here, we write the statement of crossing symmetry that can be used to find kinks. Clearly, $\langle\sigma\sigma\sigma\sigma\rangle$, $\langle\epsilon\epsilon\epsilon\epsilon\rangle$ and $\langle\chi\chi\chi\chi\rangle$ each have one crossing equation. By repeating the analysis of [78], one sees that the mixed correlators $\langle\sigma\sigma\epsilon\epsilon\rangle$, $\langle\sigma\sigma\chi\chi\rangle$ and $\langle\epsilon\epsilon\chi\chi\rangle$ each have three. The full system is

$$\sum_{\mathcal{O}^+_{2|\ell}} \left(\lambda_{\sigma\sigma\mathcal{O}}\ \lambda_{\epsilon\epsilon\mathcal{O}}\ \lambda_{\chi\chi\mathcal{O}}\right) V^{(0)}_{\Delta,\ell} \begin{pmatrix} \lambda_{\sigma\sigma\mathcal{O}} \\ \lambda_{\epsilon\epsilon\mathcal{O}} \\ \lambda_{\chi\chi\mathcal{O}} \end{pmatrix} + \sum_{\mathcal{O}^-} \lambda^2_{\sigma\epsilon\mathcal{O}} V^{(1)}_{\Delta,\ell} + \lambda^2_{\epsilon\chi\mathcal{O}} V^{(3)}_{\Delta,\ell} + \sum_{\mathcal{O}^+} \lambda^2_{\sigma\chi\mathcal{O}} V^{(2)}_{\Delta,\ell} = 0 \quad \text{(E.1)}$$

where each vector has twelve components. We first write these components for the sums with no restriction on spin.

$$V^{(1)}_{\Delta,\ell} = \begin{bmatrix} 0 \\ 0 \\ 0 \\ F^{\sigma\epsilon;\sigma\epsilon}_{-,\Delta,\ell} \\ 0 \\ 0 \\ (-1)^\ell F^{\epsilon\sigma;\sigma\epsilon}_{-,\Delta,\ell} \\ -(-1)^\ell F^{\epsilon\sigma;\sigma\epsilon}_{+,\Delta,\ell} \\ 0 \\ 0 \\ 0 \\ 0 \end{bmatrix}, V^{(2)}_{\Delta,\ell} = \begin{bmatrix} 0 \\ 0 \\ 0 \\ 0 \\ F^{\sigma\chi;\sigma\chi}_{-,\Delta,\ell} \\ 0 \\ 0 \\ 0 \\ (-1)^\ell F^{\chi\sigma;\sigma\chi}_{-,\Delta,\ell} \\ -(-1)^\ell F^{\chi\sigma;\sigma\chi}_{+,\Delta,\ell} \\ 0 \\ 0 \end{bmatrix}, V^{(3)}_{\Delta,\ell} = \begin{bmatrix} 0 \\ 0 \\ 0 \\ 0 \\ 0 \\ F^{\epsilon\chi;\epsilon\chi}_{-,\Delta,\ell} \\ 0 \\ 0 \\ 0 \\ 0 \\ (-1)^\ell F^{\chi\epsilon;\epsilon\chi}_{-,\Delta,\ell} \\ -(-1)^\ell F^{\chi\epsilon;\epsilon\chi}_{+,\Delta,\ell} \end{bmatrix} \tag{E.2}$$

The first sum, whose operators must have even spin, involves components that are $3 \times 3$ matrices. We write them individually as

$$\begin{aligned} V^{(0)}_1 &= \begin{pmatrix} F^{\sigma\sigma;\sigma\sigma}_{-,\Delta,\ell} & 0 & 0 \\ 0 & 0 & 0 \\ 0 & 0 & 0 \end{pmatrix}, \quad V^{(0)}_{7,8} = \begin{pmatrix} 0 & \frac{1}{2}F^{\sigma\sigma;\epsilon\epsilon}_{\mp,\Delta,\ell} & 0 \\ \frac{1}{2}F^{\sigma\sigma;\epsilon\epsilon}_{\mp,\Delta,\ell} & 0 & 0 \\ 0 & 0 & 0 \end{pmatrix} \\ V^{(0)}_2 &= \begin{pmatrix} 0 & 0 & 0 \\ 0 & F^{\epsilon\epsilon;\epsilon\epsilon}_{-,\Delta,\ell} & 0 \\ 0 & 0 & 0 \end{pmatrix}, \quad V^{(0)}_{9,10} = \begin{pmatrix} 0 & 0 & \frac{1}{2}F^{\sigma\sigma;\chi\chi}_{\mp,\Delta,\ell} \\ 0 & 0 & 0 \\ \frac{1}{2}F^{\sigma\sigma;\chi\chi}_{\mp,\Delta,\ell} & 0 & 0 \end{pmatrix} \\ V^{(0)}_3 &= \begin{pmatrix} 0 & 0 & 0 \\ 0 & 0 & 0 \\ 0 & 0 & F^{\chi\chi;\chi\chi}_{-,\Delta,\ell} \end{pmatrix}, \quad V^{(0)}_{11,12} = \begin{pmatrix} 0 & 0 & 0 \\ 0 & 0 & \frac{1}{2}F^{\epsilon\epsilon;\chi\chi}_{\mp,\Delta,\ell} \\ 0 & \frac{1}{2}F^{\epsilon\epsilon;\chi\chi}_{\mp,\Delta,\ell} & 0 \end{pmatrix} \end{aligned} \tag{E.3}$$

with the rest being zero.

As we have already mentioned, these crossing equations do not account for the correlators $\langle\sigma\sigma\sigma\chi\rangle$, $\langle\chi\chi\chi\sigma\rangle$ and $\langle\epsilon\epsilon\sigma\chi\rangle$. Even though (E.1) is enough to impose both constraints from the nonlocal equation of motion, the more general system makes it clear that we do not need

multiple sums for operators in the same representation. The sum rule

$$\sum_{\mathcal{O}^+_{2|\ell}} (\lambda_{\sigma\sigma\mathcal{O}}\ \lambda_{\epsilon\epsilon\mathcal{O}}\ \lambda_{\chi\chi\mathcal{O}}\ \lambda_{\sigma\chi\mathcal{O}})\, \tilde{V}^{(0)}_{\Delta,\ell} \begin{pmatrix} \lambda_{\sigma\sigma\mathcal{O}} \\ \lambda_{\epsilon\epsilon\mathcal{O}} \\ \lambda_{\chi\chi\mathcal{O}} \\ \lambda_{\sigma\chi\mathcal{O}} \end{pmatrix}$$
$$+ \sum_{\mathcal{O}^-} (\lambda_{\sigma\epsilon\mathcal{O}}\ \lambda_{\epsilon\chi\mathcal{O}})\, \tilde{V}^{(1)}_{\Delta,\ell} \begin{pmatrix} \lambda_{\sigma\epsilon\mathcal{O}} \\ \lambda_{\epsilon\chi\mathcal{O}} \end{pmatrix} + \sum_{\mathcal{O}^+_{2\nmid\ell}} \lambda^2_{\sigma\chi\mathcal{O}} \tilde{V}^{(2)}_{\Delta,\ell} = 0 \tag{E.4}$$

now has sixteen rows. It is trivial to determine the first twelve by demanding that the equations of (E.1) are captured in (E.4). Therefore, we will simply write

$$\tilde{V}^{(0)}_{13} = \begin{pmatrix} 0 & 0 & 0 & \frac{1}{2}F^{\sigma\sigma;\sigma\chi}_{-,\Delta,\ell} \\ 0 & 0 & 0 & 0 \\ 0 & 0 & 0 & 0 \\ \frac{1}{2}F^{\sigma\sigma;\sigma\chi}_{-,\Delta,\ell} & 0 & 0 & 0 \end{pmatrix}, \tilde{V}^{(0)}_{14} = \begin{pmatrix} 0 & 0 & 0 & 0 \\ 0 & 0 & 0 & 0 \\ 0 & 0 & 0 & \frac{1}{2}F^{\chi\chi;\sigma\chi}_{-,\Delta,\ell} \\ 0 & 0 & \frac{1}{2}F^{\chi\chi;\sigma\chi}_{-,\Delta,\ell} & 0 \end{pmatrix}$$
$$\tilde{V}^{(0)}_{15} = \begin{pmatrix} 0 & 0 & 0 & 0 \\ 0 & 0 & 0 & \frac{1}{2}F^{\epsilon\epsilon;\sigma\chi}_{-,\Delta,\ell} \\ 0 & 0 & 0 & 0 \\ 0 & \frac{1}{2}F^{\epsilon\epsilon;\sigma\chi}_{-,\Delta,\ell} & 0 & 0 \end{pmatrix}, \tilde{V}^{(0)}_{16} = \begin{pmatrix} 0 & 0 & 0 & 0 \\ 0 & 0 & 0 & \frac{1}{2}F^{\epsilon\epsilon;\sigma\chi}_{+,\Delta,\ell} \\ 0 & 0 & 0 & 0 \\ 0 & \frac{1}{2}F^{\epsilon\epsilon;\sigma\chi}_{+,\Delta,\ell} & 0 & 0 \end{pmatrix} \tag{E.5}$$

for $\mathcal{O}^+_{2|\ell}$,

$$\tilde{V}^{(1)}_{13,14} = \begin{pmatrix} 0 & 0 \\ 0 & 0 \end{pmatrix}, \quad \tilde{V}^{(1)}_{15,16} = \begin{pmatrix} 0 & \frac{1}{2}F^{\sigma\epsilon;\epsilon\chi}_{\mp,\Delta,\ell} \\ \frac{1}{2}F^{\sigma\epsilon;\epsilon\chi}_{\mp,\Delta,\ell} & 0 \end{pmatrix} \tag{E.6}$$

for $\mathcal{O}^-$ and $\tilde{V}^{(2)}_{13,14,15,16} = 0$ for $\mathcal{O}^+_{2\nmid\ell}$. The presence of extra equations and larger matrices certainly increases the computation time when using the full system (E.4). However, the main impact on performance comes from the fact that conformal blocks with vanishing and non-vanishing dimension differences can now be found in the same matrix. In simpler problems, the former blocks can be approximated with rational functions of a much lower degree, owing to the fact that their residues vanish for half of the poles in the Table 2.3. In the present case, this advantage is lost as all entries of the $4 \times 4$ matrix need to be accompanied by a common denominator.

After trying a few examples, the bounds from (E.4) appear indistinguishable from those obtained with (E.1). This is consistent with a piece of lore stating that additional four-point functions only help if they increase the number of gaps / OPE constraints that can be imposed. An earlier example of this was noticed in [78] which first studied the 3D Ising model using three correlators. Without a constraint on the number of relevant $\mathbb{Z}_2$-odd operators, the allowed region turned out to be the same as what was already known from a single correlator.

## E.2 Implementing the superblocks

If we wish to combine conformal blocks according to (4.158), the correct rational approximations will include extra poles apart from those captured in Table 2.3. The coefficient $R(\Delta,\ell)$ in the superblock

$$\mathcal{G}_{\Delta,\ell}(u,v) = g^{0,0}_{\Delta,\ell}(u,v) + R(\Delta,\ell)v^{\Delta_\sigma-\frac{d}{2}}g^{\Delta_{\chi\sigma},\Delta_{\sigma\chi}}_{\Delta,\ell}(u,v) \tag{E.7}$$

can be written as an infinite product since the numerator and denominator of (4.143) have the same sum of gamma function arguments.[1]

$$R(\Delta,\ell) = \prod_{k=0}^{\infty}\frac{(\Delta+\ell+2k)^2(\Delta-2\Delta_\sigma-\ell-2k)(\Delta+2\Delta_\sigma-2d-\ell-2k)}{(\Delta-d-\ell-2k)^2(\Delta-2\Delta_\sigma+d+\ell+2k)(\Delta+2\Delta_\sigma-d+\ell+2k)} \tag{E.8}$$

| | Step size | Number of points |
|---|---|---|
| $\ell=0$ | 0.01 | 1700 |
| $\ell=2$ | 0.01 | 1550 |
| $2\nmid\ell$ | 2 | 10 |

Table E.1: The grid spacing $\Delta_{N+1}-\Delta_N$ and number of points used for operators in $\sigma\times\chi$ once all consequences of the shadow relation are imposed. After the last point, we use rational approximation to demand positivity on individual sum rule vectors in a continuum. In other words, we no longer impose the shadow relation after a high enough cutoff in $\Delta$.

To rule out solutions to crossing, we use the semidefinite program solver `SDPB` [77]. This requires a "positive-times-polynomial" expression for the derivative of each conformal block, or more precisely, convolved conformal block (4.155) as these are what enter in crossing equations. The existence of a positive prefactor for each polynomial is usually attributed to the fact that poles in Table 2.3 are below the unitarity bound. For the superblocks here, we have poles on the whole real line coming from (E.8). This time, positivity is a consequence of the fact that every pole above the unitarity bound is a double pole. Although this seems forunate, numerical stability is an additional obstacle to using the rational approximation (E.8).

For normal operation of `SDPB`, the user constructs a measure out of a given block's poles and then uses it to compute a basis of orthogonal polynomials [77]. These polynomials only exist for the ordinary blocks because our superblocks are singular above the unitarity bound. In other words, the double poles do not interfere with positivity but they lead to a measure

[1]Since these poles are completely different from those of homogeneous, or even inhomogeneous conformal blocks, the degrees of the rational approximations used here are two times those of the simple ten correlator system and four times those of the simple six correlator system. This is the first of two slowdowns caused by superblocks that we will encounter.

that is not normalizable. Because of this, we have been unable to complete a full run of `SDPB` by applying $k_{\text{max}} = 40$ to the rational approximation (E.8). Instead, Figure 4.22 was produced by evaluating superblocks on a discrete $\Delta$ grid which allows us to use the exact gamma functions. It would be interesting to see if alternative solvers are able to remove this complication. Table E.1 shows our discretization choices for odd-spin operators (which are protected) and even-spin operators (which should approximate a continuum) when using the information in (4.157).

This results in file sizes of about 1GB. We have checked that shrinking the step size and including superblocks for $\ell = 4$ does not lead to a significant change in the allowed region of Figure 4.22.

# Appendix F

# Checks of the OPE coefficient ratio

In this appendix, we study the scalar version of the OPE coefficient ratios

$$R_{12} \equiv \frac{\lambda_{12\phi}}{\lambda_{12\phi^3}} = \lambda \frac{\Gamma(\frac{\Delta_\phi+\Delta_{12}}{2})\Gamma(\frac{\Delta_\phi-\Delta_{12}}{2})}{\Gamma(\frac{\Delta_{\phi^3}+\Delta_{12}}{2})\Gamma(\frac{\Delta_{\phi^3}-\Delta_{12}}{2})} A(\lambda) \tag{F.1}$$

and

$$R_{12} \equiv \frac{\lambda_{12\chi}}{\lambda_{12\sigma}} = g \frac{\Gamma(\frac{\Delta_\chi+\Delta_{12}}{2})\Gamma(\frac{\Delta_\chi-\Delta_{12}}{2})}{\Gamma(\frac{\Delta_\sigma+\Delta_{12}}{2})\Gamma(\frac{\Delta_\sigma-\Delta_{12}}{2})} \tilde{A}(g) \tag{F.2}$$

derived in chapter 4. While it would be hard to check all of the predictions that they encode, we provide several non-trivial checks that the two flows ($\phi^4$ and $\sigma\chi$ or "old and new" respectively) are compatible.

## F.1 Old flow

Scalar conformal primaries of the mean field theory schematically have the form:

$$\mathcal{O} \sim \partial^{2k}\phi^n, \tag{F.3}$$

where derivatives have to be distributed and contracted to get a primary. We take two primaries of this form, assuming $n_1 \geq n_2$ without loss of generality. To get a possibility for a nonzero three-point function, we assume that $n_1 - n_2$ is odd.

Genericaly (F.1) predicts $R_{12} = O(\lambda)$. However, there are exceptions if

1. $n_1 = n_2 + 1$, $k_1 \geq k_2$
2. $n_1 = n_2 + 3$, $k_1 \geq k_2$

In case 1 (2), the second gamma function in the numerator (denominator) is near a pole. Assuming that $\mathcal{O}_1$ and $\mathcal{O}_2$ get unequal anomalous dimensions $O(\lambda)$ we expect $\Gamma \sim 1/\lambda$. This

predicts

$$\text{case 1: } R_{12} = O(1), \qquad \text{case 2: } R_{12} = O(\lambda^2)\,. \tag{F.4}$$

We would like to check, in several simple examples, how this agrees with the perturbation theory.

First consider $k_1 = k_2 = 0$. Let us start with $\mathcal{O}_1 = \phi^{n+1}$, $\mathcal{O}_2 = \phi^n$ (case 1). In perturbation theory, the three-point functions $\langle\phi\phi^{n+1}\phi^n\rangle$ and $\langle\phi^3\phi^{n+1}\phi^n\rangle$ exist already in the mean-field theory. Thus $R_{12} = O(1)$, in agreement with the above prediction.

Next let us examine $\mathcal{O}_1 = \phi^{n+3}$, $\mathcal{O}_2 = \phi^n$ (case 2). In perturbation theory, the three-point function $\langle\phi^3\phi^{n+3}\phi^n\rangle$ appears at $O(1)$, while $\langle\phi\phi^{n+3}\phi^n\rangle$ needs one coupling insertion. Moreover, the integral over the position of this insertion gives an extra $O(\varepsilon)$ suppression, thanks to the formula:

$$\int \frac{\mathrm{d}x}{|x+y|^{2a}|x|^{2b}} \sim \frac{1}{\Gamma(d-a-b)}\,, \tag{F.5}$$

where in the considered case $a+b = d+O(\varepsilon)$.[1] So all in all we have $R_{12} = O(\varepsilon\lambda) = O(\lambda^2)$, in agreement with (F.4).

Now let us consider $\mathcal{O}_2 = \phi^n$, $\mathcal{O}_1 = \phi^{n+5+2r}$. In perturbation theory, both three-point functions require coupling insertions:

$$\langle\phi\mathcal{O}_1\mathcal{O}_2\rangle_\lambda = O(\lambda^{r+2}), \qquad \langle\phi^3\mathcal{O}_1\mathcal{O}_2\rangle_\lambda = O(\lambda^{r+1})\,. \tag{F.6}$$

Both have just one power of $\varepsilon$ suppression so $R_{12} = O(\lambda)$ as expected for the generic case.

Let us now examine a more complicated example. We would like to understand the origin of the restriction $k_1 \geq k_2$. We will only study $n_1 = n_2 + 1$ but $k_1, k_2$ general. The three-point function $\langle\phi\mathcal{O}_1\mathcal{O}_2\rangle$ is nonzero in the mean field theory if and only if $\mathcal{O}_1$ occurs in the OPE $\phi(x)\times\mathcal{O}_2(0)$. To pick up terms with $n_1 = n_2+1$ copies of $\phi$ in the OPE, we are not allowed to take any Wick contractions, only to expand $\phi(x)$ around $x = 0$. This will produce terms with a non-negative number of derivatives acting on $\phi$, *i.e.* all $\mathcal{O}_1$ operators of this type have $k_1 \geq k_2$. Analogously it is easy to see that $\mathcal{O}_1 \subset \phi^3\times\mathcal{O}_2$ is only possible if $k_1 \geq k_2$.

Hence, we get the following picture. If $k_1 \geq k_2$, then both three-point functions $\langle\phi\mathcal{O}_1\mathcal{O}_2\rangle$, $\langle\phi^3\mathcal{O}_1\mathcal{O}_2\rangle$ exist in the mean-field theory. We thus expect $R_{12} = O(1)$ and this is what (F.4) predicts in this case. On the other hand if $k_1 < k_2$, then we need coupling insertions to generate the three-point functions. Generically we expect $\langle\phi^3\mathcal{O}_1\mathcal{O}_2\rangle_\lambda = O(\lambda)$. On the other hand, $\langle\phi\mathcal{O}_1\mathcal{O}_2\rangle_\lambda = O(\lambda^2)$, since the diagrams with just one coupling insertions will vanish, being proportional to a vanishing mean-field correlator. So we indeed expect $R_{12} = O(\lambda)$, consistently with (F.4).

[1] The physical reason for this suppression is that the integral becomes conformal for $\varepsilon = 0$, and can be interpreted as the leading correction to the two-point function $\langle\phi\phi^3\rangle$, so it must vanish for $\varepsilon = 0$ since conformal invariance forbids nonzero two-point functions of operators of unequal dimension.

## F.2 New flow

For generic $\mathcal{O}_1$ and $\mathcal{O}_2$, the $\chi$ OPE coefficient is suppressed by a power of $g$, reflecting the factorization of the theory into the product of the SRI and of the Gaussian $\chi$ model as $s \to s_*$. As we will see, there are however interesting cases where one of the gamma functions develops a pole, corresponding to a non-vanishing $\chi$ correlator in the factorized theory (if the pole is in one of the numerator gamma functions) or to a further suppression of the $\chi$ correlator in conformal perturbation theory (if the pole is in one of the denominator gamma functions).

Let $\{\mathcal{O}^{\rm SRI}_{\Delta_i,\ell_i,\alpha_i}\}$ be the conformal primary operators of the SRI, where $\Delta_i$ and $\ell_i$ are their conformal dimensions and spins, and $\alpha_i = \pm 1$ their $\mathbb{Z}_2$ quantum numbers. The general scalar primary of the factorized theory at $s = s_*$ takes the schematic form

$$\partial^{\ell+2k}[\mathcal{O}^{\rm SRI}_{\Delta,\ell,\alpha}\chi^n]\,, \tag{F.7}$$

where the derivatives are contracted to give a scalar and distributed in such a way to give a primary. The $\chi$ parity $\beta = (-1)^n$ is an exact $\mathbb{Z}_2$ symmetry in the factorized theory. The interaction preserves the diagonal $\mathbb{Z}_2$ symmetry, whose quantum number we denote by $\nu = \alpha\cdot\beta$. As we turn on $g$, two operators with different $\mathcal{O}^{\rm SRI}$ and different numbers of $\chi$'s can *a priori* mix, provided that they have the same conformal dimension and that $\alpha_1\beta_1 = \alpha_2\beta_2$. In such a case, the correct dilation eigenstates will be linear combinations of states of the form (F.7). This is however a very rare and perhaps impossible phenomenon, which we will discuss at the end. In the bulk of the analysis, we will assume that both $\mathcal{O}_1$ and $\mathcal{O}_2$ take the form (F.7),[2]

$$\mathcal{O}_1 = \partial^{\ell_1+2k_1}[\mathcal{O}^{\rm SRI}_{\Delta_1,\ell_1,\alpha_1}\chi^{n_1}]\,, \quad \mathcal{O}_2 = \partial^{\ell_2+2k_2}[\mathcal{O}^{\rm SRI}_{\Delta_2,\ell_2,\alpha_2}\chi^{n_2}]\,. \tag{F.8}$$

In order for the three-point functions $\langle\mathcal{O}_1\mathcal{O}_2\sigma\rangle$ and $\langle\mathcal{O}_1\mathcal{O}_2\chi\rangle$ to have a chance of being non-zero, the diagonal $\mathbb{Z}_2$'s of $\mathcal{O}_1$ and $\mathcal{O}_2$ must be opposite, $\nu_1 = -\nu_2$, and we will assume that this is always the case.

In the factorized theory at $s = s_*$, $\sigma$ and $\chi$ have different $\mathbb{Z}_2\times\mathbb{Z}_2$ quantum numbers, respectively $(-,+)$ and $(+,-)$, so if $\langle\mathcal{O}_1\mathcal{O}_2\sigma\rangle$ is nonzero, $\langle\mathcal{O}_1\mathcal{O}_2\chi\rangle$ is zero, and *vice versa*. We then expect the ratio (F.2) to be either zero or infinite as $g \to 0$.

With no loss of generality, we will assume that $n_1 \geq n_2$. Let us enumerate the various cases:

1. $n_1 = n_2$

   In this case, the scaling in $g$ as $g \to 0$ expected from $\mathbb{Z}_2\times\mathbb{Z}_2$ selection rules is given, generically, by[3]

   $$\langle\mathcal{O}_1\mathcal{O}_2\sigma\rangle_g = O(1)\,, \quad \langle\mathcal{O}_1\mathcal{O}_2\chi\rangle_g = O(g)\,. \tag{F.9}$$

[2] A common phenomenon is the mixing of states of the form (F.7) with the same $\mathcal{O}^{\rm SRI}$ and the same $n$, $k$ and $\ell$, but different ways to distribute the derivatives.

[3] One exceptional case is $\mathcal{O}_1 = \mathcal{O}_1^{\rm SRI}\mathcal{O}_1^{\chi}$ and $\mathcal{O}_2 = \mathcal{O}_2^{\rm SRI}\mathcal{O}_2^{\chi}$ with $\mathcal{O}_1^{\chi}$ and $\mathcal{O}_2^{\chi}$ two different $\chi$ theory

Indeed $\alpha_1 = -\alpha_2$, making $\langle \mathcal{O}_1^{\rm SRI} \mathcal{O}_2^{\rm SRI} \sigma \rangle \neq 0$ in the SRI. While $\langle \mathcal{O}_1 \mathcal{O}_2 \sigma \rangle$ is already nonzero at $g = 0$, a nonzero $\langle \mathcal{O}_1 \mathcal{O}_2 \chi \rangle$ requires one insertion of the interaction $g\sigma\chi$. We have $\Delta_{12} = \Delta_1^{\rm SRI} - \Delta_2^{\rm SRI} + 2k_1 - 2k_2$ at $g = 0$. In the generic case, there are no poles coming from the gamma functions of (F.2), and the $O(g)$ behavior of the ratio expected from conformal perturbation theory is correctly reproduced. We have checked in simple examples that the numerical coefficients are also correctly reproduced.

No two operators in the SRI have dimensions differing by $\Delta_\chi$ plus an integer, so for $n_1 = n_2$ there are never poles from the numerator gamma functions. It is possible however to have a pole from the denominator gamma functions, resulting in a zero in $R_{12}$, if $\Delta_{12} = \Delta_\sigma + 2k_1 - 2k_2$ with $k_1 \geq k_2$, or $\Delta_{12} = -\Delta_\sigma + 2k_1 - 2k_2$ with $k_1 \leq k_2$. Given that operators with given $\mathbb{Z}_2 \times \mathbb{Z}_2$ quantum numbers acquire an $O(g^2)$ anomalous dimension, this zero should be interpreted as an additional factor of $g^2$, so all in all $R_{12} = O(g^3)$ in these cases. Let us see in an example how this can be compatible with conformal perturbation theory. Take

$$\mathcal{O}_1 = \sigma\chi^n\,, \quad \mathcal{O}_2 = \chi^n\,. \tag{F.10}$$

We still have $\langle \mathcal{O}_1 \mathcal{O}_2 \sigma \rangle_g = O(1)$, but we are going to argue that $\langle \mathcal{O}_1 \mathcal{O}_2 \chi \rangle_g = O(g^3)$. Indeed, the $O(g)$ contribution to $\langle \mathcal{O}_1 \mathcal{O}_2 \chi \rangle_g$ arises from the integral

$$g \int \langle \sigma\chi^n(x_1)\, \chi^n(x_2)\, \chi(x_3)\, \sigma\chi(y) \rangle_0 {\rm d}y\,, \tag{F.11}$$

which needs to be regulated and renormalized. We claim that the renormalized integral is actually $O(\delta)$, so that the net contribution is $O(g\delta) = O(g^3)$. A quick and dirty way to see this is to evaluate the integral in dimensional regularization, using (F.5). Proving this for examples more complicated than (F.10) requires a version of (F.5) with an extra $(x+z)^{2c}$ in the numerator.

2. $n_1 = n_2 + 1$

   Since we require $\nu_1 = -\nu_2$, in this case we have $\alpha_1 = \alpha_2$. In the generic case, $\mathcal{O}_1^{\rm SRI}$ and $\mathcal{O}_2^{\rm SRI}$ are two *different* operators with the same short-range $\mathbb{Z}_2$ quantum number, and then

   $$\langle \mathcal{O}_1 \mathcal{O}_2 \sigma \rangle_g = O(g)\,, \quad \langle \mathcal{O}_1 \mathcal{O}_2 \chi \rangle_g = O(g^2)\,. \tag{F.12}$$

   Indeed, for the first correlator one needs a single insertion of the interaction, while the second correlator vanishes at $g = 0$ (because $\mathcal{O}_1^{\rm SRI} \neq \mathcal{O}_2^{\rm SRI}$) and then selection rules force the insertion of *two* interactions. We observe again the generic behavior $O(g)$ for the ratio of OPE coefficients, in agreement with (F.2).

primaries which contain $\chi$ the same number of times. In this case $\langle \mathcal{O}_1 \mathcal{O}_2 \sigma \rangle$ vanishes in the factorized theory, and the analysis needs to be modified.

The more interesting case is when $\mathcal{O}_1^{\rm SRI} = \mathcal{O}_2^{\rm SRI}$. Then selection rules would predict

$$\langle \mathcal{O}_1 \mathcal{O}_2 \sigma \rangle_g = O(g)\,, \quad \langle \mathcal{O}_1 \mathcal{O}_2 \chi \rangle_g = O(1)\,. \tag{F.13}$$

In this case, $\Delta_{12} = \Delta_\chi + 2k_1 - 2k_2$ for $g = 0$. If $k_1 \geq k_2$, we encounter in a pole from the second gamma function in the numerator of (F.2). Operators with definite $\mathbb{Z}_2 \times \mathbb{Z}_2$ quantum numbers acquire anomalous dimension at order $O(g^2)$, so for small $g$ the pole is regulated to $\frac{1}{g^2}$, and $R_{12} \sim \frac{1}{g}$, in agreement with (F.13). On the other hand, if $k_1 < k_2$, we seem to have a problem. There is *no* pole in the gamma function, so (F.2) predicts $R_{12} \sim O(g)$, in contradiction with (F.13).

To understand the resolution of this puzzle, we consider the following example. Let

$$\mathcal{O}_1 = \sigma\chi^3\,, \quad \mathcal{O}_2^A = \sigma(\partial_\mu\chi\partial^\mu\chi + a\chi\Box\chi)\,, \quad \mathcal{O}_2^B = \partial_\mu\sigma\partial_\mu\chi\chi + b\Box\sigma\chi^2\,, \tag{F.14}$$

where the coefficients $a$ and $b$ are fixed such that $\mathcal{O}_2^A$ and $\mathcal{O}_2^B$ are conformal primaries. It is important to realize that $\mathcal{O}_2^A$ and $\mathcal{O}_2^B$ mix in conformal perturbation theory, indeed the $O(g^2)$ correction to the dilation operator contains an off-diagonal term arising from the non-vanishing correlator $\langle \mathcal{O}_2^A\, \mathcal{O}_2^B\, \sigma\chi\sigma\chi\rangle_0$. The eigenstates of the dilation operator take the form

$$\mathcal{O}_2^I = \mathcal{O}_2^A + c\mathcal{O}_2^B \quad \mathcal{O}_2^{II} = \mathcal{O}_2^A + d\mathcal{O}_2^B\,, \tag{F.15}$$

where the coefficients $c$ and $d$ have no $g$ dependence. We claim that

$$\langle \mathcal{O}_1 \mathcal{O}_2 \sigma \rangle = O(g)\,, \quad \langle \mathcal{O}_1 \mathcal{O}_2 \chi \rangle = O(g^2)\,, \tag{F.16}$$

where $\mathcal{O}_2$ is either one of the dilation eigenstates in (F.15), so that $R_{12} = O(g)$ in agreement with (F.2). Indeed

$$\langle \mathcal{O}_1(x_1)\mathcal{O}_2(x_2)\chi(x_3)\rangle_0 \sim \langle \chi(x_1)\chi(x_3)\rangle_0\, \langle \sigma\chi^2(x_1)\mathcal{O}_2(x_2)\rangle_0 = 0\,, \tag{F.17}$$

where in the last step we have used orthogonality of conformal primaries of different dimension. We then need to go to $O(g^2)$ to find a non-zero contribution to $\langle \mathcal{O}_1\mathcal{O}_2\chi\rangle_g$. On the other hand,

$$\langle \mathcal{O}_1(x_1)\mathcal{O}_2(x_2)\sigma(x_3)\sigma\chi(x_4)\rangle_0 \sim \langle \chi(x_1)\chi(x_4)\rangle_0\, \langle \sigma\chi^2(x_1)\mathcal{O}_2(x_2)\sigma(x_3)\sigma(x_4)\rangle_0 \neq 0\,, \tag{F.18}$$

so $\langle \mathcal{O}_1\mathcal{O}_2\sigma\rangle_g = O(g)$. It is essential that the dilation eigenstate $\mathcal{O}_2 \neq \mathcal{O}_2^A$, *i.e.* that it does *not* factorize into $\sigma$ times a primary of the $\chi$ theory, otherwise the correlator (F.18) would vanish.

3. $n_1 = n_2 + 2m$, $m \geq 1$ We must have $\alpha_1 = -\alpha_2$. Selection rules and the requirement

that we have enough $\chi$ insertions would naively give

$$\langle \mathcal{O}_1 \mathcal{O}_2 \sigma \rangle_g = O(g^{2m}) \,, \quad \langle \mathcal{O}_1 \mathcal{O}_2 \chi \rangle_g = O(g^{2m-1}) \,, \tag{F.19}$$

but the actual behavior is

$$\langle \mathcal{O}_1 \mathcal{O}_2 \sigma \rangle_g = O(g^{2m}) \,, \quad \langle \mathcal{O}_1 \mathcal{O}_2 \chi \rangle_g = O(g^{2m+1}) \,. \tag{F.20}$$

One can convince oneself in examples that the $O(g^{2m-1})$ contribution to $\langle \mathcal{O}_1 \mathcal{O}_2 \chi \rangle_g$ vanishes – the corresponding renormalized correlator turns out to be $O(\delta)$, a phenomenon we already encountered in (F.11). It would be nice to find a general argument. Conformal perturbation theory is then consistent with the generic behavior $R_{12} = O(g)$ predicted by (F.2).

4. $n_1 = n_2 + 2m + 1$, $m \geq 1$ Now $\alpha_1 = \alpha_2$. The naive scaling is

$$\langle \mathcal{O}_1 \mathcal{O}_2 \sigma \rangle_g = O(g^{2m+1}) \,, \quad \langle \mathcal{O}_1 \mathcal{O}_2 \chi \rangle_g = O(g^{2m}) \,, \tag{F.21}$$

and the correct one

$$\langle \mathcal{O}_1 \mathcal{O}_2 \sigma \rangle_g = O(g^{2m+1}) \,, \quad \langle \mathcal{O}_1 \mathcal{O}_2 \chi \rangle_g = O(g^{2m+2}) \,, \tag{F.22}$$

for the same reason as the previous case. Again, we find agreement with (F.2).

Finally, let us consider the possibility of mixing of states of the form (F.7) with different $\mathbb{Z}_2 \times \mathbb{Z}_2$ quantum numbers. This requires a conspiracy of quantum numbers that is hard to arrange. A naive candidate is the following. Take $d = 2$ and consider

$$\mathcal{O}_A = (\partial_\mu \chi \partial_\mu \chi + a \, \chi \Box \chi) \chi^{n-2} \,, \quad \mathcal{O}_B = \sigma \chi^{n+1} \,, \tag{F.23}$$

where the coefficient $a$ is fixed to make $\mathcal{O}_A$ a conformal primary. Since $\Delta_\chi + \Delta_\sigma = 2$, both states have dimension $2 + n\Delta_\chi$. At first sight, it might seem that the dilation operator has an off-diagonal component at $O(g)$ arising from

$$g \int \langle \mathcal{O}_A(x_1) \mathcal{O}_B(x_2) \, \chi\sigma(y) \rangle \mathrm{d}y \,. \tag{F.24}$$

However, this correlator is $O(\delta)$ for the same reason as the correlator in (F.17). An off-diagonal component would arise at $O(g^3)$, but there are diagonal anomalous dimensions already at $O(g^2)$, which presumably lift the degeneracy between $\mathcal{O}_A$ and $\mathcal{O}_B$. So it appears that there is no mixing after all, barring some coincidence. It would be nice to decide this one way or another by a detailed computation.

Let us consider the power counting in the scenario that the two states (F.24) *do* mix to leading order (since maybe a more intricate example would actually work along these lines).

Let $\mathcal{O}_1$ be one of the two dilation eigenstates, of the form

$$\mathcal{O}_1 = \mathcal{O}_A + b\,\mathcal{O}_B \tag{F.25}$$

for some coefficient $b = O(1)$, and choose

$$\mathcal{O}_2 = \chi^n \sigma\,. \tag{F.26}$$

Then we have

$$\langle \mathcal{O}_1 \mathcal{O}_2 \sigma \rangle_g = O(1)\,, \quad \langle \mathcal{O}_1 \mathcal{O}_2 \chi \rangle_g = O(1)\,, \tag{F.27}$$

so $R_{12}$ would be finite in the $g \to 0$ limit in this scenario. Note that $\Delta_{12} = \Delta_\chi$ for $g = 0$, which gives rise to a pole in (F.2). Now however the anomalous dimension of $\mathcal{O}_1$ is of order $O(g)$. The pole is regulated to $\frac{1}{g}$ and (F.2) predicts $R_{12} = O(1)$. So we win again.

# Bibliography


[1] H. D. Politzer, "Reliable perturbative results for strong interactions," *Phys. Rev. Lett.* **30** (1973) 1346–1349.

[2] D. J. Gross and F. Wilczek, "Ultraviolet behavior of non-abelian gauge theories," *Phys. Rev. Lett.* **30** (1973) 1343–1346.

[3] S. J. Parke and T. R. Taylor, "Amplitude for $n$-gluon scattering," *Phys. Rev. Lett.* **56** (1986) 2459–2460.

[4] G. Chew, "S-matrix theory of strong interactions without elementary particles," *Rev. Mod. Phys.* **34** (1962) 394–401.

[5] M. F. Paulos, J. Penedones, J. Toledo, B. C. van Rees and P. Vieira, "The S-matrix bootstrap I: QFT in AdS," *JHEP* **11** (2017) 133, 1607.06109.

[6] M. F. Paulos, J. Penedones, J. Toledo, B. C. van Rees and P. Vieira, "The S-matrix bootstrap II: Two dimensional amplitudes," *JHEP* **11** (2017) 143, 1607.06110.

[7] M. F. Paulos, J. Penedones, J. Toledo, B. C. van Rees and P. Vieira, "The S-matrix bootstrap III: Higher dimensional amplitudes," 1708.06765.

[8] A. Homrich, J. Penedones, J. Toledo, B. C. van Rees and P. Vieira, "The S-matrix bootstrap IV: Multiple amplitudes," 1905.06905.

[9] S. Ferrara, A. F. Grillo and R. Gatto, "Tensor representations of conformal algebra and conformally covariant operator product expansion," *Annals Phys.* **76** (1973) 161–188.

[10] A. M. Polyakov, "Nonhamiltonian approach to conformal quantum field theory," *Zh. Eksp. Teor. Fiz.* **66** (1974) 23–42.

[11] A. Dymarsky, Z. Komargodski, A. Schwimmer and S. Theisen, "On scale and conformal invariance in four dimensions," 1309.2921.

[12] A. A. Belavin, A. M. Polyakov and A. B. Zamolodchikov, "Infinite conformal symmetry in two-dimensional quantum field theory," *Nucl. Phys.* **B241** (1984) 333–380.

[13] S. Rychkov, "EPFL lectures on conformal field theory in $D \geq 3$ dimensions," in *Briefs in Physics*. Springer, 2016. 1601.05000.

[14] D. Simmons-Duffin, "The conformal bootstrap," in *Theoretical Advanced Study Institute in Elementary Particle Physics: New Frontiers in Fields and Strings: Boulder, CO, USA, June 1–26*. 2015. 1602.07982.

[15] D. Poland, S. Rychkov and A. Vichi, "The conformal bootstrap: Theory, numerical techniques and applications," 1805.04405.

[16] R. Rattazzi, S. Rychkov, E. Tonni and A. Vichi, "Bounding scalar operator dimensions in 4D CFT," *JHEP* **12** (2008) 031, 0807.0004.

[17] J. Maldacena, "The large-N limit of superconformal field theories and supergravity," *Int. J. Theor. Phys.* **38** (1998) 1113–1133, 9711.200.

[18] S. Rychkov and A. Vichi, "Universal constraints on conformal operator dimensions," *Phys. Rev.* **D80** (2009) 045006, 0905.2211.

[19] F. Caracciolo and S. Rychkov, "Rigorous limits on the interaction strength in quantum field theory," *Phys. Rev.* **D81** (2010) 085037, 0912.2726.

[20] R. Rattazzi, S. Rychkov and A. Vichi, "Central charge bounds in 4D conformal field theory," *Phys. Rev.* **D83** (2011) 046011, 1009.2725.

[21] R. Rattazzi, S. Rychkov and A. Vichi, "Bounds in 4D conformal field theories with global symmetry," *J. Phys. A: Math. Theor.* **44** (2011) 035402, 1009.5985.

[22] A. Vichi, "Improved bounds for CFTs with global symmetries," *JHEP* **1** (2012) 162, 1106.4037.

[23] S. El-Showk, M. F. Paulos, D. Poland, S. Rychkov, D. Simmons-Duffin and A. Vichi, "Solving the 3D Ising model with the conformal bootstrap," *Phys. Rev.* **D86** (2012) 025002, 1203.6064.

[24] F. Kos, D. Poland and D. Simmons-Duffin, "Bootstrapping the $O(N)$ vector models," *JHEP* **06** (2014) 091, 1307.6856.

[25] S. El-Showk, M. F. Paulos, D. Poland, S. Rychkov, D. Simmons-Duffin and A. Vichi, "Solving the 3D Ising model with the conformal bootstrap II: c-minimization and precise critical exponents," *J. Stat. Phys.* **157** (2014) 869–914, 1403.4545.

[26] Y. Nakayama and T. Ohtsuki, "Approaching conformal window of $O(n) \times O(m)$ symmetric Landau-Ginzburg models from conformal bootstrap," *Phys. Rev.* **D89** (2014) 126009, 1404.0489.

[27] Y. Nakayama and T. Ohtsuki, "Five dimensional $O(N)$ symmetric CFTs from conformal bootstrap," *Physics Letters B* **734** (2014) 193–197, 1404.5201.

[28] Y. Nakayama and T. Ohtsuki, "Bootstrapping phase transitions in QCD and frustrated spin systems," *Phys. Rev.* **D91** (2015) 021901, 1407.6195.

[29] J. B. Bae and S. J. Rey, "Conformal bootstrap approach to $O(N)$ fixed points in five dimensions," 1412.6549.

[30] S. M. Chester, S. S. Pufu and R. Yacoby, "Bootstrapping $O(N)$ vector models in $4 < d < 6$," *Phys. Rev.* **D91** (2015) 086014, 1412.7746.

[31] D. Poland and D. Simmons-Duffin, "Bounds on 4D conformal and superconformal field theories," *JHEP* **5** (2010) 017, 1009.2087.

[32] D. Poland, D. Simmons-Duffin and A. Vichi, "Carving out the space of 4D CFTs," *JHEP* **5** (2012) 110, 1109.5176.

[33] C. Beem, L. Rastelli and B. C. van Rees, "The $\mathcal{N} = 4$ superconformal bootstrap," *Phys. Rev. Lett.* **111** (2013) 071601, 1304.1803.

[34] S. M. Chester, J. Lee, S. S. Pufu and R. Yacoby, "The $\mathcal{N} = 8$ superconformal bootstrap in three dimensions," *JHEP* **9** (2014) 143, 1406.4814.

[35] C. Beem, M. Lemos, P. Liendo, L. Rastelli and B. C. van Rees, "The $\mathcal{N} = 2$ superconformal bootstrap," *JHEP* **3** (2016) 183, 1412.7541.

[36] A. L. Fitzpatrick, J. Kaplan, D. Poland and D. Simmons-Duffin, "The analytic bootstrap and AdS superhorizon locality," *JHEP* **12** (2013) 004, 1212.3616.

[37] Z. Komargodski and A. Zhiboedov, "Convexity and liberation at large spin," *JHEP* **11** (2013) 140, 1212.4103.

[38] L. F. Alday, "Large spin perturbation theory," *Phys. Rev. Lett.* **119** (2017) 111601, 1611.01500.

[39] S. Caron-Huot, "Analyticity in spin in conformal theories," *JHEP* **09** (2017) 078, 1703.00278.

[40] D. Pappadopulo, S. Rychkov, J. Espin and R. Rattazzi, "OPE convergence in conformal field theory," *Phys. Rev.* **D86** (2012) 105043, 1208.6449.

[41] S. Rychkov and P. Yvernay, "Remarks on the convergence properties of the conformal block expansion," *Physics Letters B* **753** (2015) 682–686, 1510.08486.

[42] B. Mukhametzhanov and A. Zhiboedov, "Analytic Euclidean bootstrap," 1808.03212.

[43] B. Mukhametzhanov and A. Zhiboedov, "Modular invariance, tauberian theorems and microcanonical entropy," 1904.06359.

[44] M. S. Costa, V. Goncalves and J. Penedones, "Conformal Regge theory," *JHEP* **12** (2012) 091, 1209.4355.

[45] L. F. Alday, A. Bissi and E. Perlmutter, "Holographic reconstruction of AdS exchanges from crossing symmetry," *JHEP* **08** (2017) 147, 1705.02318.

[46] M. Kulaxizi, A. Parnachev and A. Zhiboedov, "Bulk phase shift, CFT Regge limit and Einstein gravity," *JHEP* **06** (2018) 121, 1705.02934.

[47] D. Li, D. Meltzer and D. Poland, "Conformal bootstrap in the Regge limit," *JHEP* **12** (2017) 13, 1705.03453.

[48] M. S. Costa, T. Hansen and J. Penedones, "Bounds for OPE coefficients on the Regge trajectory," *JHEP* **10** (2017) 197, 1707.07689.

[49] S. Coleman and J. Mandula, "All possible symmetries of the S-matrix," *Phys. Rev.* **159** (1967) 1251.

[50] J. Maldacena and A. Zhiboedov, "Constraining conformal field theories with a higher-spin symmetry," *J. Phys. A: Math. Theor.* **46** (2013) 214011, 1112.1016.

[51] J. Polchinski, "Scale and conformal invariance in quantum field theory," *Nucl. Phys.* **B303** (1988) 226–236.

[52] M. A. Rajabpour, "Conformal symmetry in non-local field theories," *JHEP* **06** (2011) 076, 1103.3625.

[53] W. E. Caswell, "Asymptotic behavior of non-abelian gauge theories to two-loop order," *Phys. Rev. Lett.* **33** (1974) 244–246.

[54] T. Banks and A. Zaks, "On the phase structure of vector-like gauge theories with massless fermions," *Nucl. Phys.* **B196** (1982) 189–204.

[55] P. Ginsparg, "Applied conformal field theory," in *Fields, strings and critical phenomena (Les Houches, Session XLIX)*, J. Z. J. E. Brézin, ed. 1988. hep-th/9108028.

[56] G. Moore and N. Seiberg, "Classical and quantum conformal field theory," *Commun. Math. Phys.* **123** (1989) 177–254.

[57] C. Beem, M. Lemos, P. Liendo, W. Peelaers, L. Rastelli and B. C. van Rees, "Infinite chiral symmetry in four dimensions," *Commun. Math. Phys.* **336** no. 3, (2015) 1359–1433, 1312.5344.

[58] M. Hogervorst, M. Paulos and A. Vichi, "The ABC (in any D) of logarithmic CFT," *JHEP* **10** (2017) 201, 1605.03959.

[59] H. Osborn, "N = 1 superconformal symmetry in four dimensional quantum field theory," *Annals Phys.* **272** (1999) 243–294, hep-th/9808041.

[60] W. Nahm, "Supersymmetries and their representations," *Nucl. Phys.* **B135** (1978) 149–166.

[61] N. Arkani-Hamed, Y.-t. Huang and S.-H. Shao, "On the positive geometry of conformal field theory," *JHEP* **06** (2019) 124, 1812.07739.

[62] K. Sen, A. Sinha and A. Zahed, "Positive geometry in the diagonal limit of the conformal bootstrap," 1906.07202.

[63] J.-F. Fortin and W. Skiba, "A recipie for conformal blocks," 1905.00036.

[64] J.-F. Fortin and W. Skiba, "New methods for conformal correlation functions," 1905.00434.

[65] B. Czech, L. Lamprou, S. McCandish, B. Mosk and J. Sully, "A stereoscopic look into the bulk," *JHEP* **07** (2016) 129, 1604.03110.

[66] F. A. Dolan and H. Osborn, "Conformal four point functions and the operator product expansion," *Nucl. Phys.* **B599** (2001) 459–496, hep-th/0011040.

[67] K. Sen and M. Yamazaki, "Pology of superconformal blocks," 1810.01264.

[68] M. Gillioz, "Momentum space conformal blocks on the light cone," *JHEP* **10** (2018) 125, 1807.07003.

[69] M. Isachenkov and V. Schomerus, "Superintegrability of $d$-dimensional conformal blocks," *Phys. Rev. Lett.* **117** (2016) 071602, 1602.01858.

[70] M. Isachenkov, P. Liendo, Y. Linke and V. Schomerus, "Calgero-Sutherland approach to defect blocks," *JHEP* **10** (2018) 204, 1806.09703.

[71] P. Linedo, Y. Linke, V. Schomerus, "A Lorentzian inversion formula for defect CFT," 1903.05222.

[72] E. Hijano, P. Kraus, E. Perlmutter and R. Snively, "Witten diagrams revisited: The AdS geometry of conformal blocks," *JHEP* **01** (2016) 146, 1508.00501.

[73] E. Hijano, P. Kraus, E. Perlmutter and R. Snively, "Semiclassical Virasoro blocks from $AdS_3$ gravity," *JHEP* **12** (2015) 077, 1508.04987.

[74] S. El-Showk and K. Papadodimas, "Emergent spacetime and holographic CFTs," *JHEP* **10** (2012) 106, 1101.4163.

[75] X. Zhou, "Recursion relations in Witten diagrams and conformal partial waves," *JHEP* **05** (2019) 006, 1812.01006.

[76] M. F. Paulos, "JuliBootS: A hands-on guide to the conformal bootstrap," 1412.4127.

[77] D. Simmons-Duffin, "A semidefinite program solver for the conformal bootstrap," *JHEP* **06** (2015) 174, 1502.02033.

[78] F. Kos, D. Poland and D. Simmons-Duffin, "Bootstrapping mixed correlators in the 3D Ising model," *JHEP* **11** (2014) 109, 1406.4858.

[79] C. Behan, "PyCFTBoot: A flexible interface for the conformal bootstrap," *Commun. Comput. Phys.* **22** (2017) 1–38, 1602.02810.

[80] Y. Nakayama and T. Ohtsuki, "Conformal bootstrap dashing hopes of emergent symmetry," *Phys. Rev. Lett.* **117** (2016) 131601, 1602.07295.

[81] M. Go and Y. Tachikawa, "Autoboot: A generator of bootstrap equations with global symmetry," 1903.01522.

[82] N. Bao and J. Liu, "Quantum algorithms for conformal bootstrap," *Nucl. Phys.* **B946** (2019) 114702, 1811.05676.

[83] F. A. Dolan and H. Osborn, "Conformal partial waves and the operator product expansion," *Nucl. Phys.* **B678** (2004) 491–507, hep-th/0309180.

[84] M. Hogervorst and S. Rychkov, "Radial coordinates for conformal blocks," *Phys. Rev.* **D87** (2013) 106004, 1303.1111.

[85] I. Esterlis, A. L. Fitzpatrick and D. Ramirez, "Closure of the operator product expansion in the non-unitary bootstrap," *JHEP* **11** (2016) 30, 1606.07458.

[86] D. Karateev, P. Kravchuk, M. Serone and A. Vichi, "Fermion conformal bootstrap in 4d," 1902.05969.

[87] J. Penedones, E. Trevisani and M. Yamazaki, "Recursion relations for conformal blocks," *JHEP* **9** (2016) 70, 1509.00428.

[88] R. Dijkgraaf, J. Maldacena, G. Moore and E. Verlinde, "A black hole Farey tail," hep-th/0005003.

[89] M. Hogervorst, H. Osborn and S. Rychkov, "Diagonal limit for conformal blocks in d dimensions," *JHEP* **08** (2013) 014, 1305.1321.

[90] S. El-Showk and M. F. Paulos, "Bootstrapping conformal field theories with the extremal functional method," *Phys. Rev. Lett.* **111** (2013) 241601, 1211.2810.

[91] D. Karateev, P. Kravchuk and D. Simmons-Duffin, "Weight shifting operators and conformal blocks," *JHEP* **02** (2018) 081, 1706.07813.

[92] P. Kravchuk, "Casimir recursion relations for general conformal blocks," *JHEP* **02** (2018) 011, 1709.05347.

[93] R. S. Erramilli, L. V. Iliesiu, P. Kravcuk, "Recursion relation for general 3d blocks," 1907.11247.

[94] D. Simmons-Duffin, "The lightcone bootstrap and the spectrum of the 3D Ising CFT," *JHEP* **03** (2017) 086, 1612.08471.

[95] S. El-Showk, M. F. Paulos, D. Poland, S. Rychkov, D. Simmons-Duffin and A. Vichi, "Solving the 3D Ising model with the conformal bootstrap II: c-minimization and precise critical exponents," *J. Stat. Phys.* **157** (2014) 869–914, 1403.4545.

[96] A. C. Echeverri, B. von Harling and M. Serone, "The effective bootstrap," *JHEP* **9** (2016) 97, 1606.02771.

[97] W. Li, "New method for conformal bootstrap with OPE truncations," 1711.09075.

[98] C. Behan, "The unitary subsector of generalized minimal models," *Phys. Rev.* **D97** (2018) 094020, 1712.06622.

[99] Z. Komargodski and D. Simmons-Duffin, "The random-bond Ising model in 2.01 and 3 dimensions," *J. Phys. A: Math. Theor.* **50** (2017) 154001, 1603.04444.

[100] S. Rychkov, D. Simmons-Duffin and B. Zan, "Non-gaussianity of the critical 3d Ising model," *SciPost. Phys.* **2** (2017) 1, 1612.02436.

[101] P. Bowcock, "Quasi-primary fields and associativity of chiral algebras," *Nucl. Phys.* **B356** (1991) 367–386.

[102] A. B. Zamolodchikov, "Infinite additional symmetries in two-dimensional conformal quantum field theory," *Teor. Mat. Phys.* **65** (1985) 347–359.

[103] V. Kac, "Contravariant form for infinite dimensional Lie alebras and superalgebras," *Lecture Notes in Physics* **94** (1979) 441–445.

[104] D. Friedan, Z. Qiu and S. Shenker, "Conformal invariance, unitarity, and critical exponents in two dimensions," *Phys. Rev. Lett.* **52** no. 18, (1984) 1575–1578.

[105] D. Friedan, Z. Qiu and S. Shenker, "Details of the non-unitarity proof for highest weight representations of the Virasoro algebra," *Commun. Math. Phys.* **107** (1986) 535–542.

[106] N. Afkhami-Jeddi, K. Colville, T. Hartman, A. Maloney and E. Perlmutter, "Constraints on higher spin $CFT_2$," *JHEP* **05** (2018) 092, 1707.07717.

[107] V. S. Dotsenko and V. A. Fateev, "Conformal algebra and multipoint correlation functions in 2D statistical models," *Nucl. Phys.* **B240** (1984) 312–348.

[108] V. S. Dotsenko and V. A. Fateev, "Four point correlation functions and the operator algebra in the two-dimensional conformal invariant theories with central charge $c \leq 1$," *Nucl. Phys.* **B251** (1985) 691–734.

[109] V. S. Dotsenko and V. A. Fateev, "Operator algebra of two-dimensional conformal theories with central charge $c \leq 1$," *Physics Letters B* **154** (1985) 291–295.

[110] I. Runkel and G. M. T. Watts, "A non-rational CFT with $c = 1$ as a limit of minimal models," *JHEP* **09** (2001) 006, hep-th/0107118.

[111] E. T. Whittaker; G. N. Watson, *A course of modern analysis*. Cambridge University Press, 1927.

[112] L. Dixon, D. Friedan, E. Martinec and S. Shenker, "The conformal field theory of orbifolds," *Nucl. Phys.* **B282** (1987) 13–73.

[113] N. Shiba, "The Aharonov-Bohm effect on entanglement entropy in conformal field theory," *Phys. Rev.* **D96** (2017) 065016, 1701.00688.

[114] N. de Sousa, *Open descendants at $c = 1$*. PhD thesis, Dutch National Institute for Nuclear and High-Energy Physics, 2003. hep-th/0505090.

[115] R. Dijkgraaf, E. Verlinde and H. Verlinde, "$c = 1$ conformal field theories on Riemann surfaces," *Commun. Math. Phys.* **115** (1988) 649–690.

[116] D. Mazáč, "Analytic bounds and emergence of $AdS_2$ physics from the conformal bootstrap," *JHEP* **04** (2017) 146, 1611.10060.

[117] D. Mazáč and M. Paulos, "The analytic functional bootstrap I: 1D CFTs and 2D S-matrices," *JHEP* **02** (2019) 162, 1803.10233.

[118] D. Mazáč and M. Paulos, "The analytic functional bootstrap II: Natural bases for the crossing equation," *JHEP* **02** (2019) 163, 1811.10646.

[119] D. Gaiotto, D. Mazac and M. F. Paulos, "Bootstrapping the 3D Ising twist defect," *JHEP* **3** (2014) 100, 1310.5078.

[120] J. Qiao and S. Rychkov, "Cut-touching linear functionals in the conformal bootstrap," *JHEP* **06** (2017) 076, 1705.01357.

[121] S. El-Showk, M. F. Paulos, D. Poland, S. Rychkov, D. Simmons-Duffin and A. Vichi, "Conformal field theories in fractional dimensions," *Phys. Rev. Lett.* **112** (2014) 141601, 1309.5089.

[122] N. Bobev, S. El-Showk, D. Mazáč, "Bootstrapping SCFTs with four supercharges," *JHEP* **08** (2015) 142, 1503.02081.

[123] S. M. Chester, L. V. Iliesiu, S. S. Pufu and R. Yacoby, "Bootstrapping $O(N)$ vector models with four supercharges in $3 \leq d \leq 4$," *JHEP* **5** (2016) 103, 1511.07552.

[124] A. Cappelli, L. Maffi and S. Okuda, "Critical Ising model in varrying dimension by conformal bootstrap," *JHEP* **01** (2019) 161, 1811.07751.

[125] M. Hogervorst, S. Rychkov and B. C. van Rees, "Unitarity violation at the Wilson-Fisher fixed point," *Phys. Rev.* **D93** (2016) 125025, 1512.00013.

[126] P. Goddard, A. Kent and D. Olive, "Virasoro algebras and coset space models," *Physics Letters B* **152** no. 88, (1985) .

[127] P. Goddard, A. Kent and D. Olive, "Unitary representations of the Virasor and super-Virasoro algebras," *Communications in Mathematical Physics* **103** (1986) 105–119.

[128] P. Liendo, L. Rastelli and B. C. van Rees, "The bootstrap program for boundary CFT$_d$," *JHEP* **7** (2013) 113, 1210.4258.

[129] F. Kos, D. Poland, D. Simmons-Duffin and A. Vichi, "Precision islands in the Ising and $O(N)$ models," *JHEP* **08** (2016) 036, 1603.04436.

[130] Al. B. Zamolodchikov, "Three-point function in the minimal Liouville gravity," *Theoretical and Mathematical Physics* **142** no. 2, (2005) 183–196.

[131] A. A. Belavin and A. B. Zamolodchikov, "Moduli integrals and ground ring in minimal Liouville gravity," *JETP Lett.* **82** no. 1, (2005) 7–13.

[132] S. Ribault, "Conformal field theory on the plane," 1406.4290.

[133] P. Desrosiers, L. Lapointe and P. Mathieu, "Superconformal field theory and Jack superpolynomials," *JHEP* **9** (2012) 37, 1205.0784.

[134] A. A. Belavin, M. A. Bershtein and G. M. Tarnopolsky, "Bases in coset conformal field theory from AGT correspondence and Macdonald polynomials at the roots of unity," *JHEP* **3** (2013) 19, 1211.2788.

[135] L. Alarie-Vezina, P. Desrosiers and P. Mathieu, "Ramond singular vectors and Jack superpolynomials," *J. Phys. A: Math. Theor.* **47** (2013) 035202, 1309.7965.

[136] M. Hogervorst and B. C. van Rees, "Crossing symmetry in alpha space," *JHEP* **11** (2017) 193, 1702.08471.

[137] M. Hogervorst, "Crossing kernels for boundary and crosscap CFTs," 1703.08159.

[138] F. Gliozzi, "Constraints on conformal field theories in diverse dimensions from the bootstrap mechanism," *Phys. Rev. Lett.* **111** (2013) 161602, 1307.3111.

[139] F. Gliozzi and A. Rago, "Critical exponents of the 3d Ising and related models from the conformal bootstrap," *JHEP* **10** (2014) 42, 1403.6003.

[140] F. Gliozzi, P. Liendo, M. Meineri and A. Rago, "Boundary and interface CFTs from the conformal bootstrap," *JHEP* **5** (2015) 36, 1502.07217.

[141] A. Vichi, *A new method to explore conformal field theories in any dimension*. PhD thesis, École Polytechnique Fédérale de Lausanne, 2011.

[142] R. Koekoek and R. F. Swarttouw, "The Askey-scheme of hypergeometric orthogonal polynomials and its q-analogue," *Reports of the Faculty of Technical Mathematics and Informatics* **94** no. 5, (1996) . math/9602214.

[143] R. Gopakumar, A. Kaviraj, K. Sen and A. Sinha, "A Mellin space approach to the conformal bootstrap," *JHEP* **5** (2017) 27, 1611.08407.

[144] W. Chu, "Analytical formulae for extended ${}_3F_2$-series of Watson-Whipple-Dixon with two extra integer parameters," *Mathematics of Computation* **81** no. 277, (2012) 467–479.

[145] J. A. Wilson, "Three term contiguous relations and some new orthogonal polynomials," in *Pade and Rational Approximations*, R. V. E. Saff, ed., pp. 227–232. Academic Press, 1977.

[146] P. Suchanek, *Recursive methods of determination of 4-point blocks in $N = 1$ superconformal field theories*. PhD thesis, Jagiellonian University, 2009.

[147] P. Furlan, A. C. Ganchev and V. B. Petkova, "Fusion matrices and $c < 1$ (quasi) local conformal theories," *Int. J. Mod. Phys.* **A5** no. 14, (1990) 2721–2735.

[148] M. Pawelkiewicz, V. Schomerus and P. Suchanek, "The universal Racah-Wigner symbol for $U_q(OSp(1|2))$," *JHEP* **4** (2014) 79, 1307.6866.

[149] S. Ribault, "On 2d CFTs that interpolate between minimal models," *SciPost. Phys.* **6** (2019) 075, 1809.03722.

[150] S. El-Showk and M. F. Paulos, "Extremal bootstrapping: Go with the flow," 1605.08087.

[151] C.-M. Chang and Y.-H. Lin, "Carving out the end of the world or (superconformal bootstrap in six dimensions)," *JHEP* **8** (2017) 128, 1705.05392.

[152] C.-M. Chang, M. Fluder, Y.-H. Lin and Y. Wang, "Spheres, charges, instantons and bootstrap: A five-dimensional odyssey," 1710.08418.

[153] M. Cornagliotto, M. Lemos and P. Liendo, "Bootstrapping the $(A_1, A_2)$ Argyres-Douglas theory," *JHEP* **3** (2018) 33, 1711.00016.

[154] S. Collier, P. Kravchuk, Y.-H. Lin and X. Yin, "Bootstrapping the spectral function: On the uniqueness of Liouville theory and the universality of BPZ," 1702.00423.

[155] Y. H. Lin, S. H. Shao, D. Simmons-Duffin, Y. Wang and X. Yin, "N=4 superconformal bootstrap of the K3 CFT," *JHEP* **5** (2017) 126, 1511.04065.

[156] Y.-H. Lin, S.-H Shao, Y. Wang and X. Yin, "$(2, 2)$ superconformal bootstrap in two dimensions," *JHEP* **5** (2017) 112, 1610.05371.

[157] M. Cornagliotto, M. Lemos and V. Schomerus, "Long multiplet bootstrap," *JHEP* **10** (2017) 119, 1702.05101.

[158] M. F. Paulos, S. Rychkov, B. C. van Rees and B. Zan, "Conformal invariance in the long-range Ising model," *Nucl. Phys.* **B902** (2016) 246–291, 1509.00008.

[159] C. Behan, L. Rastelli, S. Rychkov and B. Zan, "A scaling theory for the long-range to short-range crossover and an infrared duality," *J. Phys. A: Math. Theor.* **50** (2017) 354002, 1703.05325.

[160] C. Behan, L. Rastelli, S. Rychkov and B. Zan, "Long-range critical exponents near the short-range crossover," *Phys. Rev. Lett.* **118** (2017) 241601, 1703.03430.

[161] M. Hogervorst, S. Rychkov and B. C. van Rees, "Univarity violation at Wilson-Fisher fixed point in 4-epsilon dimensions," *Phys. Rev.* **D93** (2016) 125025, 1512.00013.

[162] E. Dyer, A. L. Fitzpatrick and Y. Xin, "Constraints on flavored 2d CFT partition functions," *JHEP* **2** (2018) 148, 1709.01533.

[163] S. Rychkov, "Conformal bootstrap in three dimensions?," 1111.2115.

[164] Z. Li and N. Su, "3D CFT archipelago from single correlator bootstrap," 1706.06960.

[165] D. Friedan, Z. Qiu and S. Shenker, "Superconformal invariance in two dimensions and the tricritical Ising model," *Physics Letters B* **151** (1985) 37–43.

[166] Z. Qiu, "Supersymmetry, two-dimensional critical phenomena and the tricritical Ising model," *Nucl. Phys.* **B270** (1986) 205–234.

[167] D. Poland, D. Simmons-Duffin and A. Vichi, "Carving out the space of 4D CFTs," *JHEP* **5** (2012) 110, 1109.5176.

[168] Y. Ji and M. Kelly, "Unitarity violation in non-integer dimensional Gross-Neveu-Yukawa model," *Phys. Rev.* **D97** (2018) 105004, 1802.03222.

[169] Y. Ji and A. N. Manashov, "On operator mixing in fermionic CFTs in non-integer dimensions," *Phys. Rev.* **D98** (2018) 105001, 1809.00021.

[170] D. J. Gross and A. Neveu, "Dynamical symmetry breaking in asymptotically free field theories," *Phys. Rev.* **D10** (1974) 3235–3253.

[171] A. Bondi, G. Curci, G. Paffuti and P. Rossi, "Ultraviolet properties of the generalized Thirring model with $U(N)$ symmetry," *Phys. Lett.* **B216** (1989) 345–348.

[172] A. Bondi, G. Curci, G. Paffuti and P. Rossi, "Metric and central charge in the perturbative approach to two dimensional fermionic models," *Annals. Phys.* **199** (1990) 268–339.

[173] A. N. Vasiliev, S. É. Derkachev and N. A. Kivel, "A technique for calculating the $\gamma$-matrix structures of the diagrams of a toal four-fermion interaction with infinite number of vertices in $d = 2 + \epsilon$ dimensional regularization," *Theor. Math. Phys.* **103** (1995) 487–495.

[174] A. N. Vasiliev, M. I. Vyazovskii, S. É. Derkachev and N. A. Kivel, "On the equivalence of renormalizations in standard and dimensional regularizations of 2D four-fermion interactions," *Theor. Math. Phys.* **107** (1996) 441–455.

[175] A. N. Vasiliev, M. I. Vyazovskii, S. É. Derkachev and N. A. Kivel, "Three-loop calculation of the anomalous field dimension in the full four-fermion $U_N$-symmetric model," *Theor. Math. Phys.* **107** (1996) 710–719.

[176] A. N. Vasiliev and M. I. Vyazovskii, "Proof of the absence of multiplicative renormalizability of the Gross-Neveu model in the dimensional regularization $d = 2 + \epsilon$," *Theor. Math. Phys* **113** (1997) 1277–1288.

[177] J. A. Gracey, T. Luthe and Y. Schröder, "Four loop renormalization of the Gross-Neveu model," *Phys. Rev.* **D94** (2016) 125028, 1609.05071.

[178] L. Fei, S. Giombi, I. R. Klebanov and G. Tarnopolsky, "Yukawa CFTs and emergent supersymmetry," 1607.05316.

[179] A. J. Buras and P. H. Weisz, "QCD nonleading corrections to weak decays in dimensional regularization and 't Hooft-Veltman schemes," *Nucl. Phys.* **B333** (1990) 66–99.

[180] M. J. Dugan and B. Grinstein, "On the vanishing of evanescent operators," *Phys. Lett.* **B256** (1991) 239–244.

[181] L. Di Pietro and E. Stamou, "Operator mixing in $\varepsilon$-expansion: Scheme and evanescent (in)dependence," *Phys. Rev.* **D97** (2018) 065007, 1708.03739.

[182] H. Osborn and A. Stergiou, "Seeking fixed points in multiple coupling scalar theories in the $\varepsilon$ expansion," *JHEP* **5** (2018) 051, 1707.06165.

[183] S. Rychkov and A. Stergiou, "General properties of multiscalar RG flows in $d = 4 - \varepsilon$," *SciPost. Phys.* **6** (2019) 008, 1810.10541.

[184] L. Onsager, "Crystal statistics I: A two-dimension model with an order-disorder transition," *Phys. Rev.* **65** (1944) 117.

[185] S. El-Showk, M. F. Paulos, D. Poland, S. Rychkov, D. Simmons-Duffin and A. Vichi, "Solving the 3D Ising model with the conformal bootstrap," *Phys. Rev.* **D86** (2012) 025022, 1203.6064.

[186] F. J. Dyson, "Existence of a phase-transition in a one-dimensional Ising ferromagnet," *Commun. Math. Phys.* **12** (1969) 91–107.

[187] A. Schwarz, "Axiomatic conformal theory in dimensions $> 2$ and AdS / CT correspondence," *Lett. Math. Phys.* **106** (2016) 1181–1197, 1509.08064.

[188] M. E. Fisher, S.-K. Ma and B. G. Nickel, "Critical exponents for long-range interactions," *Phys. Rev. Lett.* **29** (1972) 917–920.

[189] A. N. Vasiliev, *The field theoretic renormalization group in critical behavior theory and stochastic dynamics*. CRC Press, 2004.

[190] J. C. Collins, *Renormalization*. Cambridge University Press, 1986.

[191] K. Symanzik, "On calculations in conformal invariant field theories," *Lett. Nuovo. Cim.* **3** (1972) 734–738.

[192] E. Boos and A. I. Davydychev, "A method of evaluating massive feynman integrals," *Theor. Math. Phys.* **89** (1991) 1052–1063.

[193] L. Caffarelli and L. Silvestre, "An extension problem related to the fractional Laplacian," *Commun. Part. Diff. Eq.* **32** (2007) 1245–1260, arXiv:math/0608640.

[194] J. Sak, "Recursion relations and fixed points for ferromagnets with long-range interactions," *Phys. Rev.* **B8** (1973) 281–285.

[195] J. Sak, "Low-temperature renormalization group for ferromagnets with long-range interactions," *Phys. Rev.* **B15** (1977) 4344–4347.

[196] J. L. Cardy, *Scaling and renormalization in statistical physics*. Cambridge University Press, 1996.

[197] C. P. Herzog and I. Shamir, "On marginal operators in boundary conformal field theory," 1906.11281.

[198] D. Larson, H. G. Katzgraber, M. A. Moore and A. P. Young, "Numerical studies of a one-dimensional 3-spin spin-glass model with long-range interactions," *Phys. Rev.* **B81** (2010) 064415, 0908.2224.

[199] R. A. Baños, L. A. Fernandez, V. Martin-Mayor and A. P. Young, "The correspondence between long-range and short-range spin glasses," *Phys. Rev.* **B86** (2012) 134416, 1207.7014.

[200] T. Blanchard, M. Picco and M. A. Rajapbour, "Influence of long-range interactions on the critical behavior of the Ising model," *EPL* **101** (2013) 56003, 1211.6758.

[201] M. C. Angelini, G. Parisi and F. Ricci-Tersenghi, "Relations between short range and long range Ising models," *Phys. Rev.* **E89** (2014) 062120, 1401.6805.

[202] M. Lohmann, G. Slade and B. C. Wallace, "Critical two-point function for long-range $O(n)$ models below the upper critical dimension," *J. Stat. Phys.* **169** (2017) 1132–1161, 1705.08540.

[203] M. Aizenman and R. Fernández, "Critical exponents for long-range interactions," *Lett. Math. Phys.* **16** (1988) 39–49.

[204] S. Rychkov and Z. M. Tan, "The epsilon-expansion from conformal field theory," *J. Phys. A: Math. Theor.* **48** (2015) 29FT01, 1505.00963.

[205] N. Seiberg, "Electric-magnetic duality in supersymmetric nonabelian gauge theories," *Nucl. Phys.* **B435** (1995) 129–146, arXiv:hep-th/9411149 [hep-th].

[206] M. E. Peskin, "Mandelstam-'t Hooft duality in abelian lattice models," *Annals Phys.* **113** (1978) 122–152.

[207] C. Dasgupta and B. I. Halperin, "Phase transition in a lattice model of superconductivity," *Phys. Rev. Lett.* **47** (1981) 1556–1560.

[208] E. Brezin, G. Parisi and F. Ricci-Tersenghi, "The crossover region between long-range and short-range interactions for the critical exponents," *J. Stat. Phys.* **157** (2014) 855–868, 1407.3358.

[209] A. B. Zamolodchikov, "Renormalization group and perturbation theory near fixed points in two-dimensional field theory," *Sov. J. Nucl. Phys.* **46** (1987) 1090.

[210] J. Cardy, "Conformal field theory and statistical Mechanics," in *Fields, Strings and Critical Phenomena (Les Houches, Session XLIX)*, E. Brézin and J. Zinn-Justin, ed. 1989.

[211] A. Cappelli, J. I. Latorre and X. Vilasis-Cardona, "Renormalization group patterns and C theorem in more than two-dimensions," *Nucl. Phys.* **B376** (1992) 510–538, arXiv:hep-th/9109041 [hep-th].

[212] M. R. Gaberdiel, A. Konechny and C. Schmidt-Colinet, "Conformal perturbation theory beyond the leading order," *J. Phys. A: Math. Theor.* **42** (2009) 105402, arXiv:0811.3149 [hep-th].

[213] R. Poghossian, "Two dimensional renormalization group flows in next to leading order," *JHEP* **01** (2014) 167, arXiv:1303.3015 [hep-th].

[214] M. S. Costa, T. Hansen, J. Penedones and E. Trevisani, "Radial expansion for spinning conformal blocks," *JHEP* **07** (2016) 057, arXiv:1603.05552 [hep-th].

[215] M. P. Mattis, "Correlations in two-dimensional critical theories," *Nucl. Phys.* **B285** (1987) 671–686.

[216] E. D. Skvortsov, "On (un)broken higher-spin symmetry in vector models," in *International Workshop on Higher Spin Gauge Theories: Singapore, November 4-6, 2015*, pp. 103–137. 2017. arXiv:1512.05994 [hep-th].

[217] S. Giombi and B. Kirilin, "Anmalous dimensions in CFT with weakly broken higher spin symmetry," *JHEP* **11** (2016) 068, 1601.01310.

[218] K. Roumpedakis, "Leading order anomalous dimensions at the Wilson-Fisher fixed point from CFT," *JHEP* **07** (2017) 109, 1612.08115.

[219] H. Osborn and A. Petkos, "Implications of conformal invariance in field theories for general dimensions," *Annals Phys.* **231** (1994) 311–362.

[220] C. Behan, "Bootstrapping the long-range ising model in three dimensions," *J. Phys. A: Math. Theor.* **52** (2019) 075401, arXiv:1810.07199.

[221] A. L. Fitzpatrick and J. Kaplan, "Unitarity and the holographic S-matrix," *JHEP* **10** (2012) 032, 1112.4845.

[222] O. Aharony, L. F. Alday, A. Bissi and E. Perlmutter, "Loops in AdS from conformal field theory," *JHEP* **7** (2017) 036, 1612.03891.

[223] P. A. Dirac, "Wave equations in conformal space," *Annals Math.* **37** (1936) 429–442.

[224] M. S. Costa, J. Penedones, D. Poland and S. Rychkov, "Spinning conformal correlators," *JHEP* **11** (2011) 071, 1107.3554.

[225] M. S. Costa, J. Penedones, D. Poland and S. Rychkov, "Spinning conformal blocks," *JHEP* **11** (2011) 154, 1109.6321.

[226] D. Simmons-Duffin, "Projectors, shadows and conformal blocks," *JHEP* **04** (2014) 146, 1204.3894.

[227] K. Sen and Y. Tachikawa, "First-order conformal perturbation theory by marginal operators," 1711.05947.

[228] M. S. Costa and T. Hansen, "Conformal correlators of mixed-symmetry tensors," *JHEP* **02** (2015) 151, 1411.7351.

[229] F. A. Dolan and H. Osborn, "Superconformal symmetry, correlation functions and the operator product expansion," *Nucl. Phys.* **B629** (2002) 3–73, hep-th/0112251.

[230] Z. Li and N. Su, "The most general 4D $\mathcal{N} = 1$ superconformal blocks for scalar operators," *JHEP* **05** (2016) 163, 1602.07097.

[231] E. Luijten and H. W. J. Blöte, "The boundary between long-range and short-range critical behavior," *Phys. Rev. Lett.* **89** (2002) 025703, cond-math/0112472.

[232] M. Picco, "Critical behavior of the Ising model with long range interactions," 1207.1018.

[233] T. Horita, H. Suwa and S. Todo, "Upper and lower critical decay exponents of Ising ferromagnets with long-range interaction," *Phys. Rev.* **E95** (2017) 012143, 1605.09496.

[234] F. Kos, D. Poland, D. Simmons-Duffin and A. Vichi, "Bootstrapping the $O(N)$ archipelago," *JHEP* **11** (2015) 106, 1504.07997.

[235] M. Lemos and P. Liendo, "Bootstrapping $\mathcal{N} = 2$ chiral correlators," *JHEP* **01** (2016) 025, 1510.03866.

[236] Z. Li and N. Su, "Bootstrapping mixed correlators in the five dimensional critical $O(N)$ models," *JHEP* **04** (2017) 098, 1607.07077.

[237] D. Li, D. Meltzer and A. Stergiou, "Bootstrapping mixed correlators in 4D $\mathcal{N} = 1$ SCFTs," *JHEP* **07** (2017) 029, 1702.00404.

[238] P. Liendo, C. Meneghelli and V. Mitev, "Bootstrapping the half-BPS line defect," *JHEP* **10** (2018) 077, 1806.01862.

[239] M. Baggio, N. Bobev, S. M. Chester, E. Lauria and S. S. Pufu, "Decoding a three-dimensional conformal manifold," *JHEP* **02** (2018) 062, 1712.02698.

[240] J. Rong and N. Su, "Bootstrapping the minimal $\mathcal{N} = 1$ superconformal theory in three dimensions," 1807.04434.

[241] A. Atanasov, A. Hillman and D. Poland, "Bootstrapping the minimal 3D SCFT," 1807.05702.

[242] D. Poland and D. Simmons-Duffin, "Bounds on 4D conformal and superconformal field theories," *JHEP* **05** (2011) 017, 1009.2087.

[243] R. Wong and M. Wyman, "A generalization of Watson's lemma," *Can. J. Math.* **24** (1972) 185–208.

[244] J. P. McClure and R. Wong, "Asymptotic expansion of a quadruple integral involving a Bessel function," *J. Comput. Appl. Math.* **33** (1990) 199–215.

[245] W. P. Wolf, "The Ising model and real magnetic materials," *Braz. J. Phys.* **30** (2000) .

[246] D. Dantchev and J. Rudnick, "Subleading long-range interactions and violations of finite size scaling," *Eur. Phys. J. B* **21** (2001) 251–268, cond-mat/0010478.

[247] S. Reynal, *Phase transitions in long-range spin models: The power of generalized ensembles*. PhD thesis, Cergy-Pontoise University, 2005.

[248] T. J. Williams, A. E. Taylor, A. D. Christianson, S. E. Hahn, R. S. Fishman, D. S. Parker, M. A. McGuire, B. C. Sales and M. D. Lumsden, "Extended magnetic exchange interactions in the high-temperature ferromagnet MnBi," *Appl. Phys. Lett.* **108** (2016) 192403, 1603.02750.

[249] S. T. Bramwell, M. J. Harris, B. C. den Hertog, M. J. P. Gingras, J. S. Gardner, D. F. McMorrow, A. R. Wildes, A. L. Cornelius, J. D. M. Champion, R. G. Meiko and T. Fennell, "Spin correlations in $Ho_2Ti_2O_7$: A dipolar spin ice system," *Phys. Rev. Lett.* **87** (2001) 047205, cond-mat/0101114.

[250] K. De'Bell, A. B. MacIsaac and J. P. Whitehead, "Dipolar effects in magnetic thin films and quasi-two-dimensional systems," *Rev. Mod. Phys.* **72** (2000) 225–257.

[251] J. W. Britton, B. C. Sawyer, A. C. Keith, C.-C. J. Wang, J. K. Freericks, H. Uys, M. J. Biercuk and J. J. Bollinger, "Engineered, two-dimensional Ising interations in a trapped-ion quantum simulator with hundreds of spins," *Nature* **484** (2012) 489–492.

[252] J. G. Bohnet, B. C. Sawyer, J. W. Britton, M. L. Wall, A. M. Rey, M. Foss-Feig and J. J. Bollinger, "Quantum spin dynamics and entanglement generation with hundreds of trapped ions," *Science* **352** (2016) 1297–1301.

[253] R. Landing, L. Hruby, N. Dogra, M. Landini, R. Mottl, T. Donner and T. Esslinger, "Quantum phases from competing short and long-range interactions in an optical lattice," *Nature* **532** (2016) 476–479.

[254] C.-L. Hung, A. González-Tudela, J. I. Cirac and H. J. Kimble, "Quantum spin dynamics with pairwise-tunable long-range interactions," *PNAS* **113** (2016) E4946–E4955.

[255] L. Ilesiu, M. Kologlu, R. Mahajan, E. Perlmutter and D. Simmons-Duffin, "The conformal bootstrap at finite temperature," 1802.10266.

[256] Y. Gobeil, A. Maloney, G. S. Ng and J.-Q. Wu, "Thermal conformal blocks," 1802.10537.

[257] A. C. Petkou and A. Stergiou, "Dynamics of finite-temperature CFTs from OPE inversion formulas," *Phys. Rev. Lett.* **121** (2018) 071602, 1806.02340.

[258] A. Manenti, "Thermal CFTs in momentum space," 1905.01355.

[259] L. Pauling, "The application of the quantum mechanics to the structure of the hydrogen molecule and hydrogen molecule-ion and to related problems," *Chem. Rev.* **5** (1928) 173–213.

[260] A. C. Ipsen and K. Splittorff, "The van der Waals interaction in one, two and three dimensions," *Am. J. Phys.* **85** (2015) 150, 1401.8141.

[261] S. J. Gates Jr, M. T. Grisaru, M. Rocek and W. Siegel, *Superspace, or one thousand and one lessons in supersymmetry*. Frontiers in Physics, 1983.

[262] N. Seiberg, "Supersymmetry and non-peturbative beta functions," *Physics Letters B* **206** (1988) 75–80.

[263] R. G. Leigh and M. J. Strassler, "Exactly marginal operators and duality in four dimensional N=1 supersymmetric gauge theory," *Nucl. Phys.* **B447** (1995) 95–136, hep-th/9503121.

[264] M. J. Strassler, "On renormalization group flows and exactly marginal operators in three dimensions," hep-th/9810223.

[265] C.-M. Chang and X. Yin, "Families of conformal fixed points on N=2 Chern-Simons matter theories," *JHEP* **5** (2010) 108, 1002.0568.

[266] D. Green, Z. Komargodski, N. Seiberg, Y. Tachikawa and B. Wecht, "Exactly marginal deformations and global symmetries," *JHEP* **6** (2010) 106, 1005.3545.

[267] J. Gomis, P.-S. Hsin, Z. Komargodski, A. Schwimmer, N. Seiberg and S. Theisen, "Anomalies, conformal manifolds and spheres," *JHEP* **3** (2016) 22, 1509.08511.

[268] J. Gomis, Z. Komargodski, H. Ooguri, N. Seiberg and Y. Wang, "Shortening anomalies in supersymmetric theories," *JHEP* **1** (2017) 67, 1611.03101.

[269] M. Buican, "Compact conformal manifolds," *JHEP* **1** (2015) 112, 1410.3006.

[270] C. Cordova, T. T. Dumitrescu and K. Intriligator, "Multiplets of superconformal symmetry in diverse dimensions," 1612.00809.

[271] C. Behan, "Conformal manifolds: ODEs from OPEs," *JHEP* **03** (2017) 127, 1709.03967.

[272] K. Ranganathan, H. Sonoda and B. Zwiebach, "Connections on the state space over conformal field theories," *Nucl. Phys.* **B414** (1994) 405–460, hep-th/9304053.

[273] M. Baggio, V. Niarchos and K. Papadodimas, "Aspects of Berry phase in QFT," *JHEP* **4** (2017) 62, 1701.05587.

[274] D. Li, D. Meltzer and D. Poland, "Conformal collider physics from the lightcone bootstrap," *JHEP* **2** (2016) 143, 1511.08025.

[275] T. Hartman, S. Jain and S. Kundu, "A new spin on causality constraints," *JHEP* **10** (2016) 141, 1601.07904.

[276] D. M. Hofman, D. Li, D. Meltzer, D. Poland and F. Rejon-Barrera, "A proof of the conformal collider bounds," *JHEP* **6** (2016) 11, 1603.03711.

[277] L. Iliesiu, F. Kos, D. Poland, S. S. Pufu, D. Simmons-Duffin and R. Yacoby, "Bootstrapping 3D fermions," *JHEP* **3** (2016) 120, 1508.00012.

[278] L. Iliesiu, F. Kos, D. Poland, S. S. Pufu and D. Simmons-Duffin, "Bootstrapping 3D fermions with global symmetries," *JHEP* **1** (2017) 036, 1705.03484.

[279] A. Dymarsky, J. Penedones, E. Trevisani and A. Vichi, "Charting the space of 3D CFTs with a continuous global symmetry," 1705.04278.

[280] A. Dymarsky, F. Kos, P. Kravchuk, D. Poland and D. Simmons-Duffin, "The 3d stress-tensor bootstrap," *JHEP* **02** (2018) 164, 1708.05718.

[281] D. Berenstein and A. Miller, "Conformal perturbation theory, dimensional regularization and AdS / CFT correspondence," *Phys. Rev.* **D90** (2014) 086011, 1406.4142.

[282] D. Berenstein and A. Miller, "Logarithmic enhancements in conformal perturbation theory and their real time interpretation," 1607.01922.

[283] V. Bashmakov, M. Bertolini and H. Raj, "On non-supersymmetric conformal manifolds: field theory and holography," *JHEP* **11** (2017) 167, 1709.01749.

[284] J. L. Cardy, "Continuously varrying exponents and the value of the central charge," *J. Phys. A: Math. Theor.* **20** (1987) 891–896.

[285] N. J. A. Sloane, "The online encyclopedia of integer sequences,". http://oeis.org.

[286] Y. Tachikawa, "N=2 supersymmetric dynamics for pedestrians," *Lecture Notes in Physics* **890** (2014) , 1312.2684.

[287] Z. U. Khandker, D. Li, D. Poland and D. Simmons-Duffin, "$\mathcal{N} = 1$ superconformal blocks for general scalar operators," *JHEP* **8** (2014) 49, 1404.5300.

[288] F. A. Dolan and H. Osborn, "Conformal partial waves: Further mathematical results," 1108.6194.

[289] R. Jackiw and S.-Y. Pi, "Conformal blocks for the 4-point function in conformal quantum mechanics," *Phys. Rev.* **D86** (2012) 045017, 1205.0443.

[290] K. Bulycheva, "A note on the SYK model with complex fermions," 1706.07411.

[291] G. P. Korchemsky, "On level crossing in conformal field theories," *JHEP* **3** (2016) 212, 1512.05362.

[292] P. Bouwknegt and K. Schoutens, "W-symmetry in conformal field theory," *Physics Reports* **223** (1993) 183–276, hep-th/9210010.

[293] S. Förste and D. Roggenkamp, "Current-current deformations of conformal field theories, and WZW models," *JHEP* **5** (2003) 71, hep-th/0304234.

[294] K. Sen and A. Sinha, "On critical exponents without Feynman diagrams," *J. Phys. A: Math. Theor.* **49** no. 44, (2016) , 1510.07770.

[295] H. Isono, T. Noumi and G. Shiu, "Momentum space approach to crossing symmetric CFT correlators," *JHEP* **07** (2018) 136, 1805.11107.

[296] R. Gopakumar, A. Kaviraj, K. Sen and A. Sinha, "Conformal bootstrap in Mellin space," *Phys. Rev.* **D118** (2017) 081601, 1609.00572.

[297] P. Dey, A. Kaviraj and A. Sinha, "Mellin space bootstrap for global symmetry," *JHEP* **07** (2017) 019, 1612.05032.

[298] P. Dey, K. Ghosh and A. Sinha, "Simplifying large spin bootstrap in Mellin space," *JHEP* **01** (2018) 152, 1709.06110.

[299] M. F. Paulos and B. Zan, "A functional approach to the numerical conformal bootstrap," 1904.03193.

[300] P. Liendo and C. Meneghelli, "Bootstrap equations for $\mathcal{N} = 4$ SYM with defects," *JHEP* **01** (2017) 122, 1608.05126.

[301] S. Giombi, R. Roiban and A. A. Tseytlin, "Half-BPS Wilson loop and $AdS_2/CFT_1$," *Nucl. Phys.* **B922** (2017) 499–527, 1706.00756.

[302] S. Giombi and S. Komatsu, "Exact correlators on the Wilson loop in $\mathcal{N} = 4$ SYM: Localization, defect CFT and integrability," *JHEP* **05** (2018) 109, 1802.05201.

[303] S. Giombi and S. Komatsu, "More exact results in the Wilson loop defect CFT: Bulk-defect OPE, nonplanar corrections and quantum spectral curve," *J. Phys. A: Math. Theor.* **52** (2019) 125401, 1811.02369.

[304] N. Kiryu and S. Komatsu, "Correlation functions on the half-BPS Wilson loop: Perturbation and hexagonalization," *JHEP* **02** (2019) 090, 1812.04593.

[305] A. Gimenez-Grau and P. Liendo, "Bootstrapping line defects in $\mathcal{N} = 2$ theories," 1907.04345.

[306] O. Nachtmann, "Positivity constraints for anomalous dimensions," *Nucl. Phys.* **B63** (1973) 237–247.

[307] A. Van Proeyen, "Tools for supersymmetry," hep-th/9910030.

[308] H. Osborn, "Conformal blocks for arbitrary spin in two dimensions," *Phys. Lett.* **B718** (2012) 169–172, 1205.1941.

[309] C. Beem, L. Rastelli and B. C. van Rees, "W symmetry in six dimensions," *JHEP* **05** (2015) 017, 1404.1079.

[310] P. Kravchuk and D. Simmons-Duffin, "Light-ray operators in conformal field theory," *JHEP* **11** (2018) 102, 1805.00098.

[311] C. G. Callan, I. R. Klebanov, A. W. W. Ludwig and J. M. Maldacena, "Exact solution of a boundary conformal field theory," *Nucl. Phys.* **B422** (1994) 417–448, hep-th/9402113.

[312] J. Polchinski and L. Thorlacius, "Free fermion representation of a boundary conformal field theory," *Phys. Rev.* **D50** (1994) R622–R626, hep-th/9404008.

[313] R. Wong, "Five lectures on asymptotic theory," in *Differential equations and asymptotic theory in mathematical physics*, R. W. Z. Hua, ed., pp. 189–263. World Scientific, 2004.

[314] E. X. W. Xia and X. M. Yao, "The signs of three-term recurrence sequences," *Discrete Applied Mathematics* **159** (2011) 2290–2296.

[315] T. Hartman, S. Jain and S. Kundu, "Causality constraints in conformal field theory," *JHEP* **5** (2016) 99, 1509.00014.

[316] L. V. Avdeev, "Fierz identities in spaces of nonintegral dimension," *Theor. Math. Phys.* **58** (1984) 203–207.